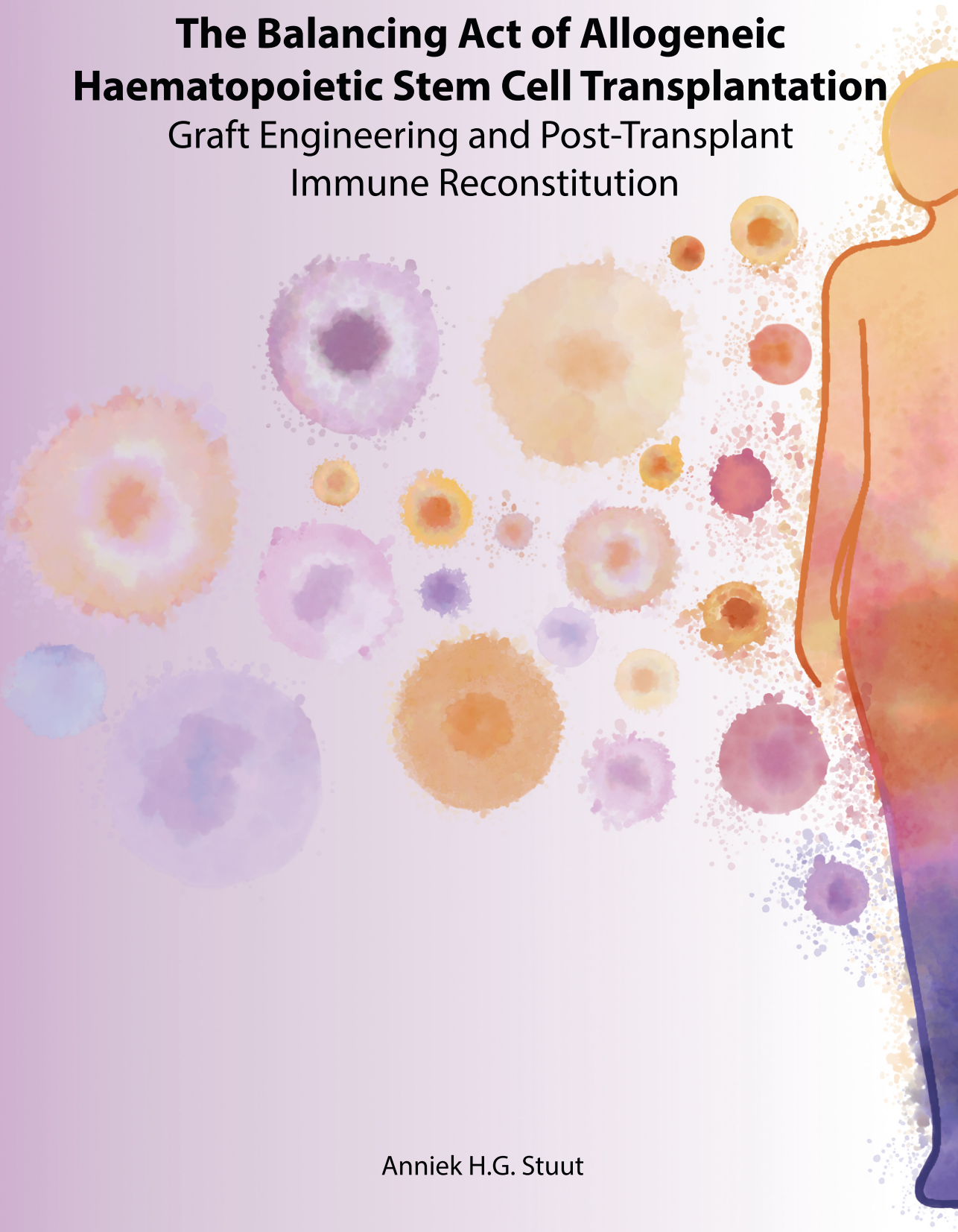
The Balancing Act of Allogeneic Haematopoietic Stem Cell Transplantation

Graft Engineering and Post-Transplant Immune Reconstitution



Anniek H.G. Stuut

The Balancing Act of Allogeneic Haematopoietic Stem Cell Transplantation:

Graft Engineering and Post-Transplant Immune Reconstitution

Anniek Henderika Geertruida Stuut

ISBN: 978-90-393-8062-8
DOI: https://doi.org/10.33540/3584

Cover design: Anniek Stuut
Layout & Printing: ProefschriftMaken | proefschriftmaken.nl

Copyright © Anniek Stuut 2026
All rights reserved. No part of this publication may be reproduced, stored in a retrieval system, or transmitted in any form or by any means, electronic, mechanical, by photocopying, or otherwise, without the prior permission of the author. The copyrights of published articles have been transferred to the respective journals.

Printing of this thesis was financially supported by UMC Utrecht, Fonds Wetenschappelijk Onderzoek of the MPN Stichting, and PhD program Infection & Immunity Utrecht

The Balancing Act of Allogeneic Haematopoietic Stem Cell Transplantation

Graft Engineering and Post-Transplant Immune Reconstitution

De balans na allogene hematopoëtische stamceltransplantatie:

Transplantaatbewerking en herstel van het immuunsysteem
(met een samenvatting in het Nederlands)

Proefschrift

ter verkrijging van de graad van doctor aan de
Universiteit Utrecht
op gezag van de
rector magnificus, prof. dr. ir. W. Hazeleger,
ingevolge het besluit van het College voor Promoties
in het openbaar te verdedigen op
vrijdag 10 juli 2026 des middags te 12.15 uur

door

Anniek Henderika Geertruida Stuut
geboren op 6 september 1995
te Stadskanaal

Promotor:

Prof. dr. J.H.E. Kuball

Copromotoren:

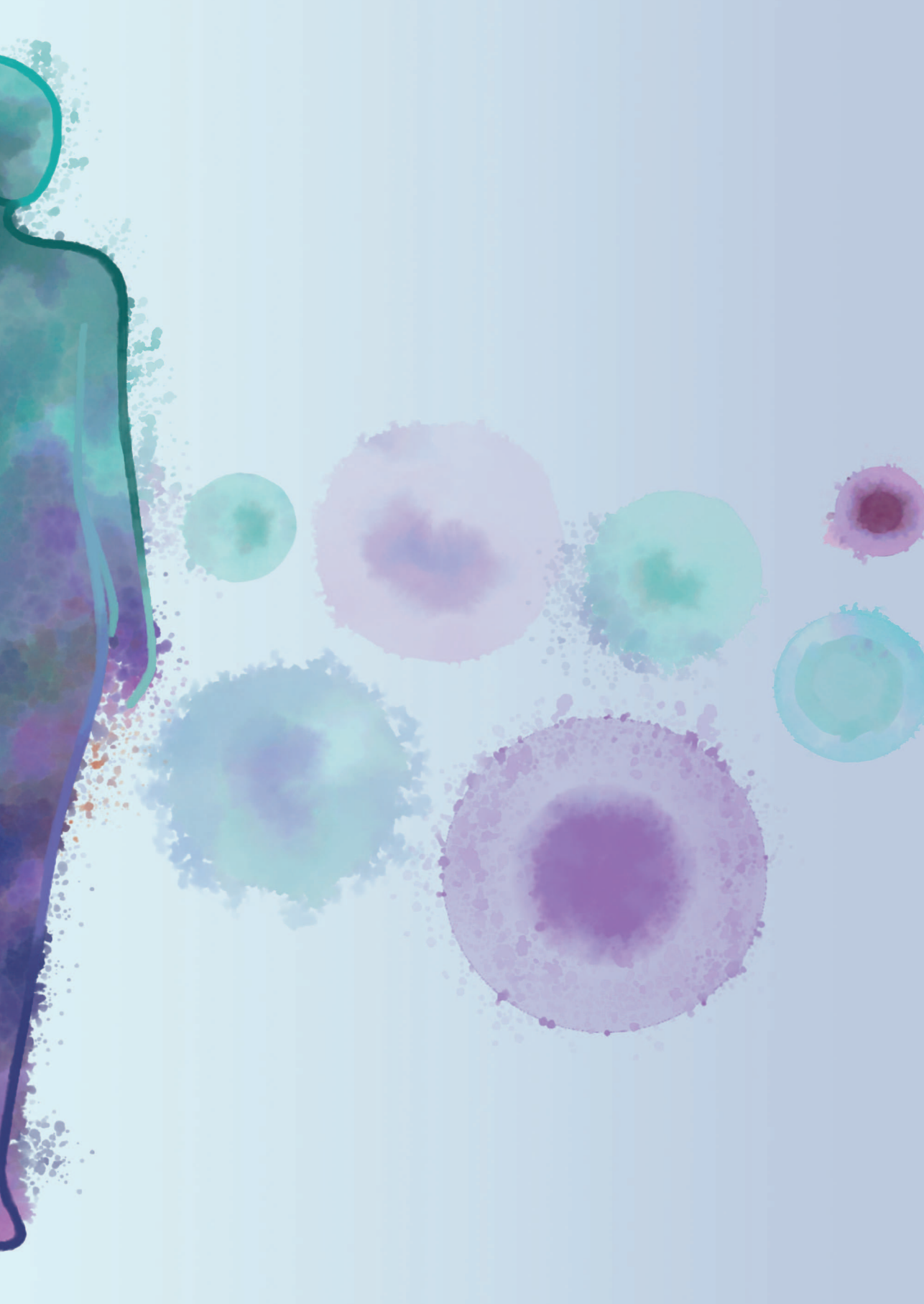
Dr. M.A. de Witte
Dr. Z. Sebestyen

Beoordelingscommissie:

Prof. dr. J.A.M. Borghans
Prof. dr. M. Heemskerk
Prof. dr. H.L. Leavis (voorzitter)
Prof. dr. M.C. Minnema
Dr. S. Nierkens

TABLE OF CONTENTS

Chapter 1	General Introduction	7
Part 1	**Clinical outcomes after αβT-cell-depleted allogeneic HSCT**	23
Chapter 2	Improved GVHD-free and relapse-free survival after ex vivo αβTCR and CD19 depleted allogeneic HSCT compared to T cell replete HSCT *Published in Bone Marrow Transplantation, 2025*	25
Chapter 3	Graft engineering: how long can you wait, how low can you go, and pandemic readiness *Published in Bone Marrow Transplantation, 2023*	51
Chapter 4	Peri-transplant ruxolitinib enhances survival in myelofibrosis patients undergoing αβTCR and CD19-depleted stem cell transplantation *Revised version submitted*	65
Part 2	**Immune reconstitution after αβT-cell-depleted allogeneic HSCT**	87
Chapter 5	Short-Term Post-Transplant Proteomics in Myeloid Malignancies *Manuscript in preparation*	89
Chapter 6	Platform-Imprinted Transcriptional and Clonal Remodeling of αβ and γδT Cells After Allogeneic Transplantation *Revised version submitted*	111
Chapter 7	Summarising Discussion	161
Chapter 8	Appendices	179
	Nederlandse samenvatting	181
	Acknowledgements/Dankwoord	184
	List of publications	190
	Curriculum Vitae	191



1

General Introduction

Allogeneic haematopoietic stem cell transplantation (allo-HSCT) is the only curative treatment option for various haematologic malignancies. In this complex procedure, a recipient first undergoes conditioning to prepare for the infusion of hematopoietic stem cells from a healthy donor, after which the donor cells replace the recipient's entire hematopoietic system. Allo-HSCT was first performed in humans in the 1950s[1]. In the first decades, allo-HSCT procedures were complicated by lethal immunological reactions of the graft against the host, now known as graft-versus-host disease (GVHD)[2]. Despite these initial setbacks, the identification of human leukocyte antigens (HLA) enabled better matching of recipient-donor pairs[3]. This led to the first successful transplants being performed in the 1970[2,4], with two major publications reporting powerful graft-versus-leukaemia (GVL) effect[5,6].

Over the years, the success of allo-HSCT has risen dramatically. As of 2020, nearly 1.5 million allo-HSCT procedures had been performed in more than 1,500 centres, underscoring the importance of this procedure[7]. Nevertheless, there is still a high risk of mortality and morbidity after allo-HSCT. In a European registry cohort, 1-year non-relapse mortality after allo-HSCT remains substantial (~12% in 2010-2016), and clinically relevant GVHD is still common (extensive chronic GVHD ~14% at 1-year)[8]. Thus, even after all these years, the main challenge of allo-HSCT remains preventing GVHD without sacrificing GVL effects, while minimising additional toxicities. The first part of this thesis examines how an allo-HSCT platform combining myeloablative conditioning with *ex vivo* αβT-cell depletion affects clinical outcomes. The second part of this thesis focuses on how the immune system, especially T cells, recovers after allo-HSCT and on the factors that shape this recovery.

PART I: FACTORS INFLUENCING CLINICAL OUTCOMES AFTER ALLO-HSCT

Conditioning Regimens

One of the key determinants of the balance between GVL and toxicity is the conditioning regimen administered before transplantation. The role of a conditioning regimen in haematologic malignancies is dual: to reduce the number of patient T cells to prevent graft rejection and to decrease the number of malignant cells. Conditioning-induced tissue injury and tumour cell death can also shape the early inflammatory environment and antigen exposure, which, in turn, influence the post-transplant immune response[9]. Total body irradiation (TBI) was the only conditioning regimen used in the early days of allo-HSCT, as it is both myeloablative and immunosuppressive[3]. Later, effective drug-based conditioning regimens were discovered[10]. Due to the high toxicity of myeloablative conditioning regimens in older patients and patients with comorbidities, reduced-intensity regimens were developed in the late 1990s[3,11,12]. These reduced-intensity regimens depend on the graft to eradicate the cancer, leading to higher relapse rates in advanced haematologic

malignancies[13]. However, they have also led to the broader application of allo-HSCT, especially in elderly patients and/or those with comorbidities[3]. While these conditioning regimens can influence toxicities and thereby non-relapse mortality, GVHD risk depends mainly on donor immune cells and their regulation. Thus, if we seek to further modulate the balance between GVHD and GVL, we must look beyond conditioning regimens.

T cell depletion and graft engineering strategies

Because GVHD arises primarily from donor αβT cells, decades of work have focused on graft-engineering strategies to decouple GVHD from GVL activity, for example, by depleting T cells from the allograft. Clinically, these approaches aim to reduce GVHD while maintaining disease control and acceptable infectious risk. While early efforts were less successful due to increased relapse risk[14], there has recently been increased interest in both *in vivo* and *ex vivo* depletion or selection of immune cells. *In vivo* strategies to deplete T cells include anti-thymocyte globulin (ATG), Alemtuzumab, and post-transplantation cyclophosphamide (PT-Cy)[15]. ATG is an infusion of antibodies against human T cells, typically administered pre-transplant, and broadly reduces T-cell numbers. Alemtuzumab is an anti-CD52 monoclonal antibody that can be administered directly to the patient or added to the allograft product ('in the bag') shortly before infusion, resulting in broad lymphocyte depletion. In contrast, PT-Cy is given after graft infusion and is thought to preferentially target rapidly proliferating alloreactive T cells early after transplantation.

Ex vivo depletion, also known as graft engineering, is increasingly used in Europe[16]. Several options are available; the most stringent is $CD34^+$ selection[17,18]. Among *ex vivo* depletion options, most patients in Europe are treated with an αβT-cell-depleted allograft[16]. αβT-cell-depleted allo-HSCT was first pioneered in children and in a haploidentical setting[19-22], and later introduced in adults with 9/10- or 10/10-HLA-matched related or unrelated donors[23]. To reduce the risk of Epstein-Barr virus (EBV) reactivation, CD19 depletion was subsequently added to this procedure[22,24]. These *in vivo* and *ex vivo* depletion strategies can shape post-transplant immune recovery, often reflecting a clinical trade-off: lowering GVHD by limiting early αβT-cell alloreactivity, while potentially altering viral control. Accordingly, their downstream effects on immune-reconstitution trajectories are discussed in more detail in **Part II.**

Beyond the choice of graft engineering method, transplant outcomes may also be influenced by graft composition, including the dose of $CD34^+$ hematopoietic stem cells, as well as by implementation factors such as cryopreservation[25]. These considerations became particularly relevant during the COVID-19 pandemic, when logistics and donor availability increased the use of cryopreserved products in many centres. Beyond these graft-related variables, additional peri-transplant interventions further shape outcomes and immune recovery.

GVHD prophylaxis and peri-transplant immunomodulation

Peri-transplant immunomodulation is a third modifiable component that directly shapes GVHD risk and may influence immune recovery. GVHD prophylaxis strategies differ across centres and are closely linked to the transplantation platform (T-cell-depleted or non-T-cell-depleted/T-cell-replete). In our αβT-cell-depleted platform, a short-term course of mycophenolate mofetil (MMF) is used as GVHD prophylaxis. In contrast, T-cell-replete platforms generally require more intensive GVHD prophylaxis regimens[7]. Because these approaches differentially suppress or deplete T cells early after transplantation, they are likely to contribute to platform-specific patterns of immune reconstitution.

Beyond standard prophylaxis, targeted peri-transplant immunomodulation may be considered in selected patient groups. For example, ruxolitinib, established as a treatment option for glucocorticoid-refractory GVHD[26], has been explored peri-transplant in patients with myelofibrosis[27,28], a group with a high inflammatory burden and increased GVHD susceptibility. This strategy and its clinical impact are examined in **Chapter 4.** Together, these platform- and disease-tailored choices help set the conditions for immune reconstitution after allo-HSCT.

PART II: IMMUNE RECONSTITUTION AFTER ALLO-HSCT

Immune reconstitution of all immune subsets partly determines the success of stem cell transplantation, as it plays a central role in balancing the GVL effect, preventing infections, and minimising the risk of GVHD[29]. Because transplantation platforms differ in the extent to which donor T cells are infused and/or pharmacologically suppressed, they can generate distinct post-transplant immune trajectories, with potential consequences for clinical outcomes.

Overall timeline of immune recovery

Generally, immune reconstitution occurs in two distinct waves: the innate system reconstitutes early after allo-HSCT, whereas the adaptive system reconstitutes more slowly[29,30] (**Figure 1**). Reconstitution of the innate immune system generally takes weeks to a few months. Neutrophils and monocytes are the first cells to recover, typically within 20 days and a few weeks, respectively, with the absolute neutrophil count being used as an early indicator of engraftment[31-33]. Of the lymphocyte population, NK cells are the first to recover to normal numbers, a process that can take up to four months. On the other hand, complete recovery of the adaptive immune system can take months to years, as this process is more complex. Moreover, for adaptive cells, both the quantity and the diversity of the repertoire are essential.

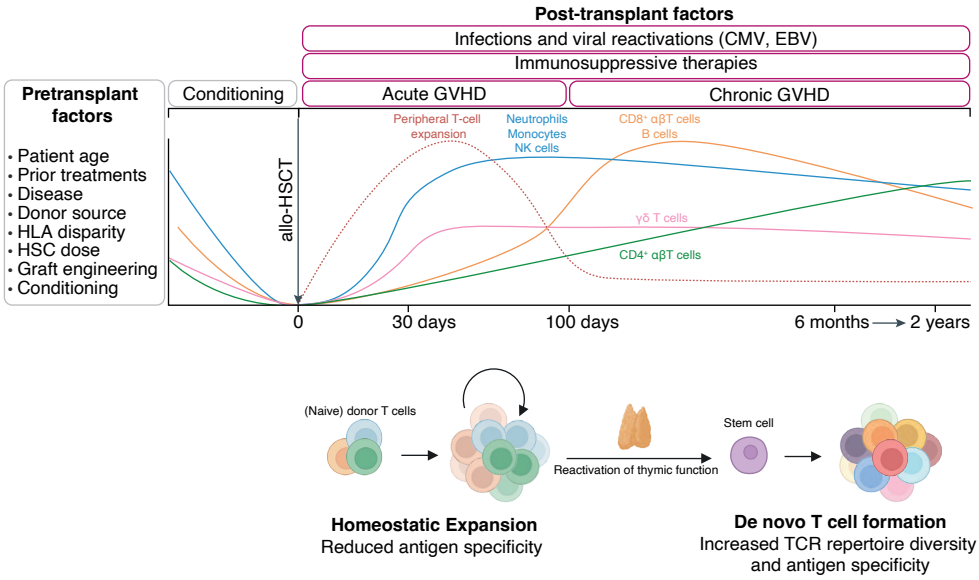


Figure 1. Overview of dynamics and influences on immune reconstitution after allogeneic hematopoietic stem cell transplantation. *Schematic overview of factors influencing immune reconstitution and the kinetics of lymphocyte recovery after allogeneic haematopoietic stem cell transplantation (allo-HSCT). Top panel: Innate cells recover relatively early, while adaptive cells take longer to recover. Early T-cell recovery results from peripheral T-cell expansion. Pre-transplant and post-transplant factors can modulate immune reconstitution. Bottom panel: Two distinct mechanisms contribute to T-cell reconstitution: (1) homeostatic expansion of (naïve) donor T cells transferred with the graft and (2) de novo T-cell formation through reactivation of thymic function, generating new T cells from donor stem cells with increased T cell receptor (TCR) repertoire diversity and antigen specificity. Adapted from Velardi et al*[34]

Across these waves, a few cell types dominate early clinical risk: neutrophils and monocytes provide the first barrier against bacterial and fungal infections, NK cells expand early and can contribute to anti-leukemic activity, and adaptive lymphocytes, particularly T cells, shape the balance between GVL, viral control, and GVHD. In this thesis, T cells are central because both the desired (GVL) and undesired (GVHD) effects are primarily T-cell-mediated[35-37]. Accordingly, T-cell reconstitution is a major predictor of clinical outcome[29,38]. Importantly, the kinetics and phenotype of these recovering cells are strongly shaped by the early post-transplant environment.

Early after allo-HSCT, conditioning-related tissue injury, lymphodepletion, and microbial translocation can trigger systemic inflammation and strong cytokine signals. This inflammatory milieu shapes antigen exposure and cytokine availability, thereby influencing the expansion and differentiation of emerging immune subsets[9]. In parallel, viral reactivations, particularly cytomegalovirus (CMV), can exert strong selective pressure on the post-transplant lymphocyte pool.

T cell subsets and repertoire diversity

Against this background, we next outline how T-cell subsets and TCR repertoire diversity recover, because these qualitative features can shift the balance between GVHD, GVL, and viral control even when overall lymphocyte counts appear similar. In addition to conventional αβT cells, we also consider γδT cells, because they can reconstitute early after allo-HSCT and have been implicated in anti-leukaemic and antiviral responses.

Here, 'diversity' refers to the number and distribution of unique TCR clonotypes, as captured by sequencing-based repertoire analyses. TCR diversity is generated by somatic recombination of the V-J (for α and γ) and V-D-J (for β and δ) gene segments, resulting in different amino acid sequences and antigen specificity. The cleavage of hairpin loops, the addition of P-nucleotides, and the random addition and subtraction of N-nucleotides further increase this diversity, leading to around 10^{20} αβTCR possibilities[39]. The theoretical diversity of the γδTCR repertoire is lower than that of αβTCRs because fewer distinct V-D-J segments are available for recombination. However, multiple D gene segments can be incorporated into the δ chain during recombination, leading to an estimated theoretical diversity of 10^{18} γδTCRs[40-43].

γδT cells in humans can be subdivided into two main subsets based on their Vδ gene segment: $V\delta2^{pos}$ and $V\delta2^{neg}$ γδT cells (**Table 1**). The majority of γδT cells in healthy donors are $V\delta2^{pos}$ and express a $V\gamma9^{pos}$ γ chain. These $V\gamma9V\delta2^{pos}$ γδT cells are semi-invariant, thus having lower diversity than expected. Moreover, it has been found that individuals can share identical $V\gamma9V\delta2^{pos}$ γδTCR sequences, termed 'public' TCRs[44]. $V\gamma9V\delta2^{pos}$ γδT cells are described as innate-like and respond to phosphorylated antigens in an MHC-independent manner, which are increased in infected and tumorous cells. In contrast, $V\delta2^{neg}$ γδT cells are described as adaptive-like and share phenotypic and functional characteristics with $CD8^{+}$ αβT cells[45-47]. Furthermore, $V\delta2^{neg}$ γδTCRs are 'private', even in highly expanded clonotypes[45,48,49]. This private repertoire complicates ligand identification. While several ligands have been described for $V\delta2^{neg}$ γδTCRs, ranging from MHC and MHC-like molecules to MHC-unrelated proteins, most remain unknown[49,50].

Table 1. Overview of two main γδT cell subsets

$V\delta2^{pos}$ γδT cells	$V\delta2^{neg}$ γδT cells
1-5% of peripheral CD3+ T cells	up to 50% of tissue CD3+ T cells
anti-tumour reactivity	anti-tumour reactivity
anti-EBV reactivity	anti-CMV reactivity
innate-like	adaptive-like

EBV, Epstein-Barr Virus; CMV, cytomegalovirus

Whereas the αβTCR repertoire in healthy donors is highly diverse, the Vδ2^{pos} γδTCR repertoire is more oligoclonal, with relatively large TCR clonotypes already present in the foetal stage of development[51-54]. In contrast, studies of cord blood have shown that the Vδ2^{neg} TCR repertoire is diverse before birth, whereas sequencing adult peripheral blood has revealed more focused repertoires with a limited number of highly expanded clones[45,46].

T cell reconstitution in allo-HSCT

After this general overview of repertoire concepts, we focus on the mechanisms and subset-specific kinetics of T-cell recovery after allo-HSCT. T cell reconstitution is influenced by multiple pre- and post-transplant factors, including the conditioning regimen, recipient and donor age, infections, and graft engineering[55-60]. Reconstitution of T cells consists of two mechanisms in distinct waves: peripheral expansion and thymopoiesis (**Figure 1**). Peripheral expansion is the first wave, in which donor T cells in the graft expand and proliferate in response to cytokine exposure and/or TCR stimulation[55,56,59,61]. The second wave is thymopoiesis, the $^{de\ novo}$ generation of T cells from donor-derived haematopoietic stem cells in the thymus. Thymopoiesis yields novel, phenotypically naïve T cells with increased TCR diversity[59,62-66].

However, there is variation between the recovery of several T cell subsets (**Figure 1**). The 'unconventional' γδT cell population is one of the earliest to recover post-HSCT. γδT cell reconstitution is thought to mainly derive from homeostatic peripheral expansion during the first year post-allo-HSCT[57-59,67]. Considering αβT cells, CD8$^+$ αβT cells can reconstitute to normal levels within 10 months after allo-HSCT[58,68,69]. On the other hand, CD4$^+$ αβT cells generally reconstitute slowly, remaining low for 2 to 5 years after transplantation, even in the T-cell-replete setting[70]. This slow recovery of CD4$^+$ αβT cells suggests that they may be more dependent on thymopoiesis. After prolonged follow-up of over 5 years, CD4$^+$ αβT cells can recover to near-normal levels in T-cell-replete allo-HSCT[71]. For both CD4$^+$ and CD8$^+$ αβT cells, the recovery of the naïve pool is delayed. This delay is more pronounced in adults than in children due to thymic involution, which is likely to affect TCR repertoire diversity[72].

TCR repertoire dynamics in allo-HSCT

Beyond cell counts, the diversity of the TCR repertoire is increasingly associated with better clinical outcomes[62-65]. Using next-generation sequencing (NGS) methods, several studies have found that αβTCR repertoire diversity remains diminished after allo-HSCT compared to healthy donor repertoires[73-76]. Clinical factors such as donor type, conditioning regimen, and the use of ATG have been shown to affect αβTCR repertoire diversity[76,77]. However, there is conflicting evidence on whether αβTCR repertoire diversity is correlated with or predictive of clinical outcomes, such as acute GVHD and relapse[73-77]. By comparison, the γδTCR repertoire has been less extensively studied after allo-HSCT. However, one

sequencing study in a T-cell-replete setting reported that γδT-cell reconstitution was accompanied by a γδTCR repertoire diversity similar to that of healthy donors[48].

Impact of viral reactivations on αβ and γδTCR repertoires

Among the factors shaping post-transplant αβ and γδTCR repertoire dynamics are viral reactivations. A significant force shaping post-transplant diversity in both the αβ and γδTCR repertoires is CMV reactivation. CMV reactivation is associated with many changes in the T cell repertoire, including skewing of both $CD8^+$ αβT cells and $V\delta2^{neg}$ γδT cells towards effector phenotypes, and causing a shift from a predominant $V\delta2^{pos}$ γδTCR repertoire to a $V\delta2^{neg}$ repertoire[78-81]. Specifically, CMV reactivation induces clonal expansion of CMV-specific $CD8^+$ αβT cells and $V\delta2^{neg}$ γδT cells, resulting in reduced diversity of the TCR repertoire[48,75,79]. This process is called "memory inflation" and is thought to lead to significant defects in the $CD8^+$ αβTCR repertoire. Moreover, this effect on the TCR repertoire may be very long-lasting, with CMV-specific clones found 5 years after allo-HSCT[82]. However, little is known about the combined impact of T cell depletion in allo-HSCT settings and CMV reactivation on the TCR repertoire.

THESIS OUTLINE

Despite the increasing use of *in vivo* and *ex vivo* T-cell depletion strategies, the effects of these strategies on immune reconstitution and the balance between GVHD, relapse, and infectious complications remain incompletely understood. Therefore, this thesis aims to characterise clinical outcomes and immune reconstitution after αβT-cell-depleted allo-HSCT, and to examine how CMV reactivation influences these processes. In the first part of this thesis, we focus on patient outcomes after αβT-cell-depleted allo-HSCT in different contexts. In the second part of this thesis, we focus on post-transplant dynamics of T cells and immune-related proteins.

Chapter 2 is a retrospective single-centre analysis in which we studied the outcomes of patients who received a myeloablative conditioning regimen including ATG with an αβT-cell-depleted allograft compared with two cohorts that received T-cell-replete allo-HSCT with or without ATG. In **Chapter 3**, we retrospectively analysed whether patient outcomes after receiving αβT-cell-depleted allografts were influenced by lower graft $CD34^+$ cell counts ($< 4\times10^6$/kg), delayed graft infusion after apheresis (≥48hrs), or graft freezing. **Chapter 4** focuses on patients with myelofibrosis. Here, we retrospectively analysed whether the addition of peri-transplant ruxolitinib to a myeloablative conditioning regimen, with T-cell depletion, could improve outcomes in these patients.

To further investigate immune reconstitution after allo-HSCT, we employed several techniques. In **Chapter 5**, we investigate short-term changes in immune-related proteins following αβT-cell-depleted allo-HSCT using Olink proteomics. We included patients with AML, myelodysplastic syndrome (MDS), and myelofibrosis, where the patients with myelofibrosis received peri-transplant ruxolitinib. In **Chapter 6,** we studied the reconstitution of T cells after both αβT-cell-depleted allo-HSCT and T-cell-replete allo-HSCT. Using mixed-effect linear modelling, we investigated the influence of CMV reactivation on the numerical reconstitution of αβ and γδT cells. Moreover, we used next-generation bulk TCR sequencing and single-cell RNA and TCR sequencing to investigate how patient T cells differ from their stem cell donors and to examine the impact of CMV and the allo-HSCT platform on T cell repertoire dynamics.

REFERENCES

1. Thomas ED, Lochte HL, Jr., Lu WC, Ferrebee JW. Intravenous infusion of bone marrow in patients receiving radiation and chemotherapy. *N Engl J Med*. 1957;257(11):491-496.
2. Thomas E, Storb R, Clift RA, et al. Bone-marrow transplantation (first of two parts). *N Engl J Med*. 1975;292(16):832-843.
3. Copelan EA. Hematopoietic stem-cell transplantation. *N Engl J Med*. 2006;354(17):1813-1826.
4. Thomas ED, Storb R, Clift RA, et al. Bone-marrow transplantation (second of two parts). *N Engl J Med*. 1975;292(17):895-902.
5. Weiden PL, Flournoy N, Thomas ED, et al. Antileukemic effect of graft-versus-host disease in human recipients of allogeneic-marrow grafts. *N Engl J Med*. 1979;300(19):1068-1073.
6. Weiden PL, Sullivan KM, Flournoy N, Storb R, Thomas ED, Seattle Marrow Transplant T. Antileukemic effect of chronic graft-versus-host disease: contribution to improved survival after allogeneic marrow transplantation. *N Engl J Med*. 1981;304(25):1529-1533.
7. Granot N, Storb R. History of hematopoietic cell transplantation: challenges and progress. *Haematologica*. 2020;105(12):2716-2729.
8. Penack O, Peczynski C, Mohty M, et al. How much has allogeneic stem cell transplant-related mortality improved since the 1980s? A retrospective analysis from the EBMT. *Blood Adv*. 2020;4(24):6283-6290.
9. Lake RA, Robinson BW. Immunotherapy and chemotherapy--a practical partnership. *Nat Rev Cancer*. 2005;5(5):397-405.
10. Santos GW, Tutschka PJ, Brookmeyer R, et al. Marrow transplantation for acute nonlymphocytic leukemia after treatment with busulfan and cyclophosphamide. *N Engl J Med*. 1983;309(22):1347-1353.
11. McSweeney PA, Niederwieser D, Shizuru JA, et al. Hematopoietic cell transplantation in older patients with hematologic malignancies: replacing high-dose cytotoxic therapy with graft-versus-tumor effects. *Blood*. 2001;97(11):3390-3400.
12. Storb R, Sandmaier BM. Nonmyeloablative allogeneic hematopoietic cell transplantation. *Haematologica*. 2016;101(5):521-530.
13. Levine JE, Uberti JP, Ayash L, et al. Lowered-intensity preparative regimen for allogeneic stem cell transplantation delays acute graft-versus-host disease but does not improve outcome for advanced hematologic malignancy. *Biol Blood Marrow Transplant*. 2003;9(3):189-197.
14. Goldman JM, Gale RP, Horowitz MM, et al. Bone marrow transplantation for chronic myelogenous leukemia in chronic phase. Increased risk for relapse associated with T-cell depletion. *Ann Intern Med*. 1988;108(6):806-814.
15. de Witte M, Daenen LGM, van der Wagen L, et al. Allogeneic Stem Cell Transplantation Platforms With Ex Vivo and In Vivo Immune Manipulations: Count and Adjust. *Hemasphere*. 2021;5(6):e580.
16. de Witte MA, Mooyaart JE, Hoogenboom JD, et al. Activity of ex vivo graft and DLI Engineering within the last decade increases, a survey from the EBMT Cellular Therapy & Immunobiology Working Party. *Bone Marrow Transplant*. 2023.
17. Pasquini MC, Devine S, Mendizabal A, et al. Comparative outcomes of donor graft CD34+ selection and immune suppressive therapy as graft-versus-host disease prophylaxis for patients with acute myeloid leukemia in complete remission undergoing HLA-matched sibling allogeneic hematopoietic cell transplantation. *J Clin Oncol*. 2012;30(26):3194-3201.
18. Barba P, Hilden P, Devlin SM, et al. Ex Vivo CD34(+)-Selected T Cell-Depleted

Peripheral Blood Stem Cell Grafts for Allogeneic Hematopoietic Stem Cell Transplantation in Acute Leukemia and Myelodysplastic Syndrome Is Associated with Low Incidence of Acute and Chronic Graft-versus-Host Disease and High Treatment Response. *Biol Blood Marrow Transplant*. 2017;23(3):452-458.

19. Bertaina A, Romano M, Rutella S, et al. HLA Haploidentical Stem Cell Transplantation After Removal of αβ+ T Lymphocytes and B Lymphocytes Is an Effective Treatment for Children with Life-Threatening, Non-Malignant Disorders. *Blood*. 2012;120(21):2018-2018.
20. Maschan M, Shelikhova L, Ilushina M, et al. TCR-alpha/beta and CD19 depletion and treosulfan-based conditioning regimen in unrelated and haploidentical transplantation in children with acute myeloid leukemia. *Bone Marrow Transplant*. 2016;51(5):668-674.
21. Locatelli F, Bauquet A, Palumbo G, Moretta F, Bertaina A. Negative depletion of alpha/beta+ T cells and of CD19+ B lymphocytes: a novel frontier to optimize the effect of innate immunity in HLA-mismatched hematopoietic stem cell transplantation. *Immunol Lett*. 2013;155(1-2):21-23.
22. Locatelli F, Merli P, Pagliara D, et al. Outcome of children with acute leukemia given HLA-haploidentical HSCT after alphabeta T-cell and B-cell depletion. *Blood*. 2017;130(5):677-685.
23. de Witte MA, Janssen A, Nijssen K, et al. alphabeta T-cell graft depletion for allogeneic HSCT in adults with hematological malignancies. *Blood Adv*. 2021;5(1):240-249.
24. Bethge WA, Eyrich M, Mielke S, et al. Results of a multicenter phase I/II trial of TCRalphabeta and CD19-depleted haploidentical hematopoietic stem cell transplantation for adult and pediatric patients. *Bone Marrow Transplant*. 2022;57(3):423-430.
25. Dholaria B, Malki MMA, Artz A, Savani BN. Securing the graft during pandemic: are we ready for cryopreservation for all? *Biol Blood Marrow Transplant*. 2020;26(7):e145-e146.
26. Zeiser R, von Bubnoff N, Butler J, et al. Ruxolitinib for Glucocorticoid-Refractory Acute Graft-versus-Host Disease. *N Engl J Med*. 2020;382(19):1800-1810.
27. Wall SA, Tamari R, DeFilipp Z, Hobbs GS. Optimization of allogeneic hematopoietic cell transplantation for patients with myelofibrosis treated with ruxolitinib: eligibility, best practices, and improving transplant outcomes. *Ann Hematol*. 2025;104(4):2125-2141.
28. Kroger N, Shahnaz Syed Abd Kadir S, Zabelina T, et al. Peritransplantation Ruxolitinib Prevents Acute Graft-versus-Host Disease in Patients with Myelofibrosis Undergoing Allogenic Stem Cell Transplantation. *Biol Blood Marrow Transplant*. 2018;24(10):2152-2156.
29. Hammoudi T, Nucera S, Troullioud Lucas AG, et al. Harmonized immune recovery monitoring after HCT: evidence and practical guidance from the Westhafen Intercontinental Group. *Blood Adv*. 2025;9(23):6141-6157.
30. Fu W, Chen J, Hu X. Immune reconstitution following allogeneic hematopoietic cell transplantation and CAR-T therapy: dynamics, determinants, and directions. *Best Pract Res Clin Haematol*. 2025;38(2):101634.
31. Bensinger WI, Clift R, Martin P, et al. Allogeneic peripheral blood stem cell transplantation in patients with advanced hematologic malignancies: a retrospective comparison with marrow transplantation. *Blood*. 1996;88(7):2794-2800.
32. de Koning C, Plantinga M, Besseling P, Boelens JJ, Nierkens S. Immune Reconstitution after Allogeneic Hematopoietic Cell Transplantation in Children. *Biol Blood Marrow Transplant*. 2016;22(2):195-206.

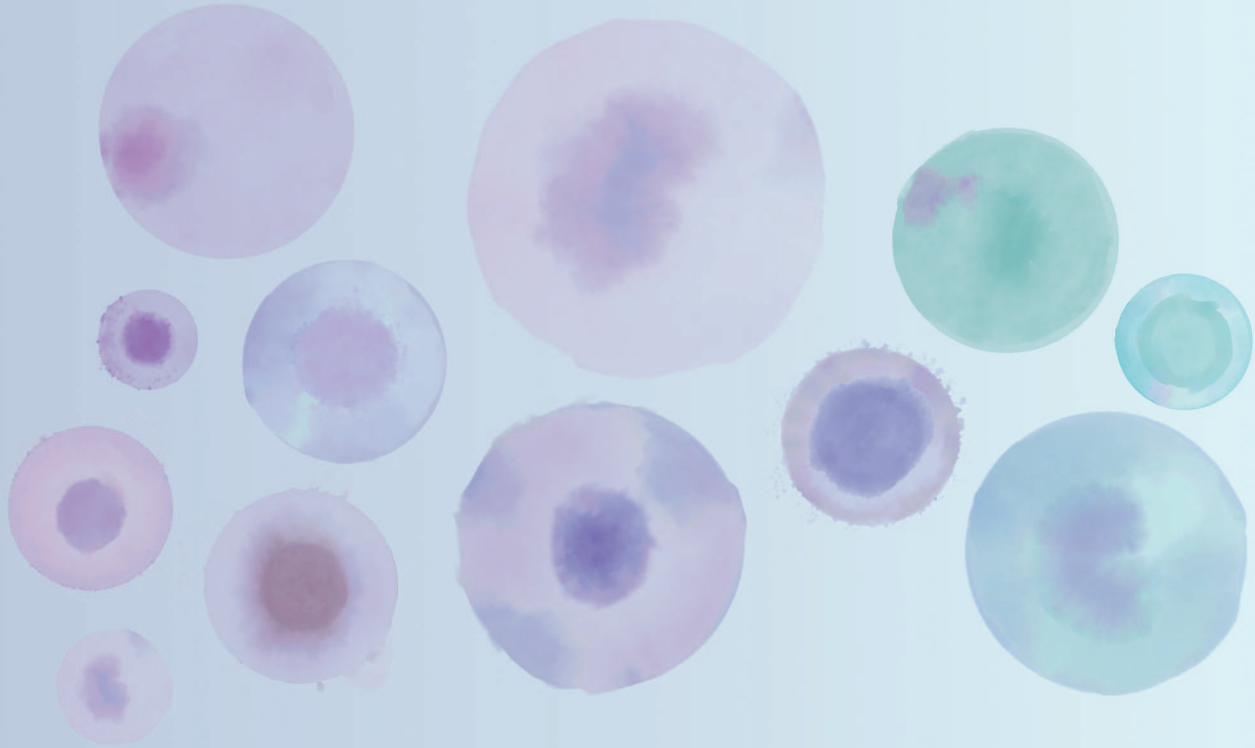
33. de Koning C, Langenhorst J, van Kesteren C, et al. Innate Immune Recovery Predicts CD4(+) T Cell Reconstitution after Hematopoietic Cell Transplantation. *Biol Blood Marrow Transplant*. 2019;25(4):819-826.
34. Velardi E, Tsai JJ, van den Brink MRM. T cell regeneration after immunological injury. *Nat Rev Immunol*. 2021;21(5):277-291.
35. van Besien K. Allogeneic transplantation for AML and MDS: GVL versus GVHD and disease recurrence. *Hematology Am Soc Hematol Educ Program*. 2013;2013:56-62.
36. Gustafsson Jernberg A, Remberger M, Rinyδen O, Winiarski J. Graft-versus-leukaemia effect in children: chronic GVHD has a significant impact on relapse and survival. *Bone Marrow Transplant*. 2003;31(3):175-181.
37. Ferrara JL, Levine JE, Reddy P, Holler E. Graft-versus-host disease. *Lancet*. 2009;373(9674):1550-1561.
38. Goldberg JD, Zheng J, Ratan R, et al. Early recovery of T-cell function predicts improved survival after T-cell depleted allogeneic transplant. *Leuk Lymphoma*. 2017;58(8):1859-1871.
39. Zarnitsyna VI, Evavold BD, Schoettle LN, Blattman JN, Antia R. Estimating the diversity, completeness, and cross-reactivity of the T cell repertoire. *Front Immunol*. 2013;4:485.
40. Elliott JF, Rock EP, Patten PA, Davis MM, Chien YH. The adult T-cell receptor delta-chain is diverse and distinct from that of fetal thymocytes. *Nature*. 1988;331(6157):627-631.
41. Kazen AR, Adams EJ. Evolution of the V, D, and J gene segments used in the primate gammadelta T-cell receptor reveals a dichotomy of conservation and diversity. *Proc Natl Acad Sci U S A*. 2011;108(29):E332-340.
42. Legut M, Cole DK, Sewell AK. The promise of gammadelta T cells and the gammadelta T cell receptor for cancer immunotherapy. *Cell Mol Immunol*. 2015;12(6):656-668.
43. Fichtner AS, Ravens S, Prinz I. Human gammadelta TCR Repertoires in Health and Disease. *Cells*. 2020;9(4).
44. Vyborova A, Janssen A, Gatti L, et al. γ9δ2 T-Cell Expansion and Phenotypic Profile Are Reflected in the CDR3δ Repertoire of Healthy Adults. *Frontiers in Immunology*. 2022;13.
45. Davey MS, Willcox CR, Joyce SP, et al. Clonal selection in the human Vdelta1 T cell repertoire indicates gammadelta TCR-dependent adaptive immune surveillance. *Nat Commun*. 2017;8:14760.
46. Davey MS, Willcox CR, Baker AT, Hunter S, Willcox BE. Recasting Human Vdelta1 Lymphocytes in an Adaptive Role. *Trends Immunol*. 2018;39(6):446-459.
47. McMurray JL, von Borstel A, Taher TE, et al. Transcriptional profiling of human Vdelta1 T cells reveals a pathogen-driven adaptive differentiation program. *Cell Rep*. 2022;39(8):110858.
48. Ravens S, Schultze-Florey C, Raha S, et al. Human gammadelta T cells are quickly reconstituted after stem-cell transplantation and show adaptive clonal expansion in response to viral infection. *Nat Immunol*. 2017;18(4):393-401.
49. Willcox BE, Willcox CR. gammadelta TCR ligands: the quest to solve a 500-million-year-old mystery. *Nat Immunol*. 2019;20(2):121-128.
50. Beringer DX, Straetemans T, Minguet S, et al. Disrupting the balance between activating and inhibitory receptors of gammadeltaT cells for effective cancer immunotherapy. *Nat Rev Cancer*. 2025.
51. Sherwood AM, Desmarais C, Livingston RJ, et al. Deep sequencing of the human TCRgamma and TCRbeta repertoires suggests that TCRbeta rearranges after alphabeta and gammadelta T cell commitment. *Sci Transl Med*. 2011;3(90):90ra61.
52. Cairo C, Armstrong CL, Cummings JS, et al. Impact of age, gender, and race on circulating gammadelta T cells. *Hum Immunol*. 2010;71(10):968-975.

53. Cairo C, Sagnia B, Cappelli G, et al. Human cord blood gammadelta T cells expressing public Vgamma2 chains dominate the response to bisphosphonate plus interleukin-15. *Immunology*. 2013;138(4):346-360.
54. Dimova T, Brouwer M, Gosselin F, et al. Effector Vgamma9Vdelta2 T cells dominate the human fetal gammadelta T-cell repertoire. *Proc Natl Acad Sci U S A*. 2015;112(6):E556-565.
55. Williams KM, Hakim FT, Gress RE. T cell immune reconstitution following lymphodepletion. *Semin Immunol*. 2007;19(5):318-330.
56. Oshrine BR, Li Y, Teachey DT, Heimall J, Barrett DM, Bunin N. Immunologic recovery in children after alternative donor allogeneic transplantation for hematologic malignancies: comparison of recipients of partially T cell-depleted peripheral blood stem cells and umbilical cord blood. *Biol Blood Marrow Transplant*. 2013;19(11):1581-1589.
57. Airoldi I, Bertaina A, Prigione I, et al. gammadelta T-cell reconstitution after HLA-haploidentical hematopoietic transplantation depleted of TCR-alphabeta+/CD19+ lymphocytes. *Blood*. 2015;125(15):2349-2358.
58. Minculescu L, Marquart HV, Ryder LP, et al. Improved Overall Survival, Relapse-Free-Survival, and Less Graft-vs.-Host-Disease in Patients With High Immune Reconstitution of TCR Gamma Delta Cells 2 Months After Allogeneic Stem Cell Transplantation. *Front Immunol*. 2019;10:1997.
59. Dekker L, de Koning C, Lindemans C, Nierkens S. Reconstitution of T Cell Subsets Following Allogeneic Hematopoietic Cell Transplantation. *Cancers (Basel)*. 2020;12(7).
60. Pei XY, Huang XJ. The role of immune reconstitution in relapse after allogeneic hematopoietic stem cell transplantation. *Expert Rev Clin Immunol*. 2024;20(5):513-524.
61. Matsuoka K, Kim HT, McDonough S, et al. Altered regulatory T cell homeostasis in patients with CD4+ lymphopenia following allogeneic hematopoietic stem cell transplantation. *J Clin Invest*. 2010;120(5):1479-1493.
62. Talvensaari K, Clave E, Douay C, et al. A broad T-cell repertoire diversity and an efficient thymic function indicate a favorable long-term immune reconstitution after cord blood stem cell transplantation. *Blood*. 2002;99(4):1458-1464.
63. Li Y, Xu L. Evaluation of TCR repertoire diversity in patients after hematopoietic stem cell transplantation. *Stem Cell Investig*. 2015;2:17.
64. Clave E, Lisini D, Douay C, et al. Thymic function recovery after unrelated donor cord blood or T-cell depleted HLA-haploidentical stem cell transplantation correlates with leukemia relapse. *Front Immunol*. 2013;4:54.
65. Gkazi AS, Margetts BK, Attenborough T, et al. Clinical T Cell Receptor Repertoire Deep Sequencing and Analysis: An Application to Monitor Immune Reconstitution Following Cord Blood Transplantation. *Front Immunol*. 2018;9:2547.
66. Klein AK, Patel DD, Gooding ME, et al. T-Cell recovery in adults and children following umbilical cord blood transplantation. *Biol Blood Marrow Transplant*. 2001;7(8):454-466.
67. Suessmuth Y, Mukherjee R, Watkins B, et al. CMV reactivation drives posttransplant T-cell reconstitution and results in defects in the underlying TCRbeta repertoire. *Blood*. 2015;125(25):3835-3850.
68. Bosch M, Dhadda M, Hoegh-Petersen M, et al. Immune reconstitution after anti-thymocyte globulin-conditioned hematopoietic cell transplantation. *Cytotherapy*. 2012;14(10):1258-1275.
69. Alho AC, Kim HT, Chammas MJ, et al. Unbalanced recovery of regulatory and effector T cells after allogeneic stem cell transplantation contributes to chronic GVHD. *Blood*. 2016;127(5):646-657.

70. Storek J, Gooley T, Witherspoon RP, Sullivan KM, Storb R. Infectious morbidity in long-term survivors of allogeneic marrow transplantation is associated with low CD4 T cell counts. *American Journal of Hematology*. 1997;54(2):131-138.
71. Storek J, Joseph A, Espino G, et al. Immunity of patients surviving 20 to 30 years after allogeneic or syngeneic bone marrow transplantation. *Blood*. 2001;98(13):3505-3512.
72. Storek J. Immunological reconstitution after hematopoietic cell transplantation - its relation to the contents of the graft. *Expert Opin Biol Ther*. 2008;8(5):583-597.
73. Yew PY, Alachkar H, Yamaguchi R, et al. Quantitative characterization of T-cell repertoire in allogeneic hematopoietic stem cell transplant recipients. *Bone Marrow Transplant*. 2015;50(9):1227-1234.
74. Link-Rachner CS, Eugster A, Rucker-Braun E, et al. T-cell receptor-alpha repertoire of CD8+ T cells following allogeneic stem cell transplantation using next-generation sequencing. *Haematologica*. 2019;104(3):622-631.
75. Buhler S, Bettens F, Dantin C, et al. Genetic T-cell receptor diversity at 1 year following allogeneic hematopoietic stem cell transplantation. *Leukemia*. 2020;34(5):1422-1432.
76. Leick M, Gittelman RM, Yusko E, et al. T Cell Clonal Dynamics Determined by High-Resolution TCR-beta Sequencing in Recipients after Allogeneic Hematopoietic Cell Transplantation. *Biol Blood Marrow Transplant*. 2020;26(9):1567-1574.
77. Goel M, Eugster A, Schetelig J, Bonifacio E, Bornhauser M, Link-Rachner CS. Potential of TCR sequencing in graft-versus-host disease. *Bone Marrow Transplant*. 2022.
78. Khairallah C, Dechanet-Merville J, Capone M. gammadelta T Cell-Mediated Immunity to Cytomegalovirus Infection. *Front Immunol*. 2017;8:105.
79. Gaballa A, Alagrafi F, Uhlin M, Stikvoort A. Revisiting the Role of gammadelta T Cells in Anti-CMV Immune Response after Transplantation. *Viruses*. 2021;13(6).
80. Knight A, Madrigal AJ, Grace S, et al. The role of Vdelta2-negative gammadelta T cells during cytomegalovirus reactivation in recipients of allogeneic stem cell transplantation. *Blood*. 2010;116(12):2164-2172.
81. Scheper W, Van Dorp S, Kersting S, et al. γδT cells elicited by CMV reactivation after allo-SCT cross-recognize CMV and leukemia. *Leukemia*. 2013;27(6):1328-1338.
82. Calderin Sollet Z, Schafer A, Ferrari-Lacraz S, et al. CMV serostatus and T-cell repertoire diversity 5 years after allogeneic hematopoietic stem cell transplantation. *Leukemia*. 2023;37(4):948-951.

Part 1

Clinical outcomes after αβT-cell-depleted allogeneic HSCT



2

Improved GVHD-free and relapse-free survival after *ex vivo* αβTCR and CD19 depleted allogeneic HSCT compared to T cell replete HSCT

A.H.G. Stuut[1]*, C. Nijssen[2]*, L. van der Wagen[2], A. van Rhenen[2], L.G.M. Daenen[2], A. Janssen[2], F.A. Verheij[2], I. Brinkman[2], F.M. Verduyn Lunel[3], H. Koene[4], R. Fijnheer[5], H.J. Prins[6], K. Westinga[6], J. Drylewicz[1], J. Kuball^[1, 2], M.A. de Witte^[#1,2]

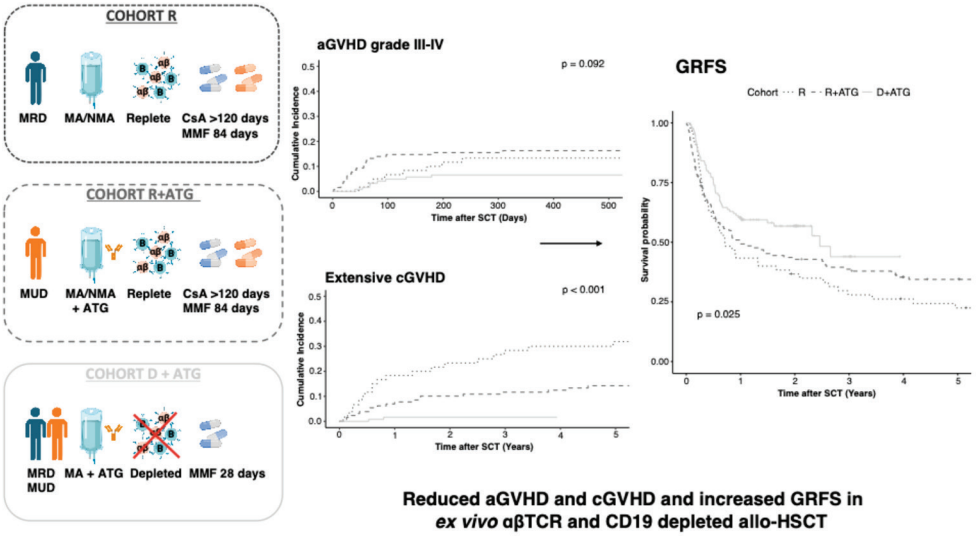
1 Center for Translational Immunology, University Medical Center Utrecht, The Netherlands
2 Department of Hematology, University Medical Center Utrecht, The Netherlands
3 Department of Medical Microbiology, University Medical Center Utrecht, The Netherlands
4 Department of Internal Medicine, Antonius Ziekenhuis, Nieuwegein, The Netherlands.
5 Department of Internal Medicine, Meander Medisch Centrum, Amersfoort, The Netherlands
6 Cell Therapy Facility, University Medical Center Utrecht, The Netherlands
* Shared first author
^ Shared senior author
# Corresponding author

Bone Marrow Transplant 2025; 60 (5):673-81

ABSTRACT

Allogeneic hematopoietic stem cell transplantation (allo-HSCT) aims to cure patients without inducing severe graft-versus-host disease (GVHD) or relapse. In prospective studies of mostly pediatric patients with haploidentical donors, ex vivo αβTCR/CD19 depletion has shown low incidences of GVHD, but data for adults with matched related (MRD) or unrelated donors (MUD) remain limited. We analyzed the outcomes of recipients who received a myeloablative regimen plus ATG, followed by an αβTCR/CD19 depleted allograft (cohort D+ATG (n = 122)), and compared outcomes to T cell replete cohorts (cohort R (N=60); without ATG; R+ATG = with ATG (N=129) in a single centre retrospective analysis. In D+ATG, the incidence of aGVHD grade III-IV was 7%, compared to 13% in R and 16% in R+ATG (p=0.09). Extensive cGVHD was reduced from 23% in R and 10% in R+ATG to 2% in D+ATG (p<0.001). The reduced incidence of cGVHD led to a superior GVHD-relapse free survival (GRFS) of 56.7% in D+ATG versus 36.7% in R and and 42.8% in R+ATG (p=0.03) at 2 years. In conclusion, the combination of myeloablative conditioning, ATG and *ex vivo* αβTCR/CD19 depletion appears to be a promising approach to enhance GRFS in adult patients up to 75 years of age undergoing allo-HSCT.

GRAPHICAL ABSTRACT



Reduced aGVHD and cGVHD and increased GRFS in *ex vivo* αβTCR and CD19 depleted allo-HSCT

INTRODUCTION

Allogeneic hematopoietic stem cell transplantation (allo-HSCT) is the only curative treatment option for various high-risk hematological malignancies. A major factor jeopardizing allo-HSCT is the development of graft-versus-host-disease GVHD. αβT cells play an important role in the pathology of GVHD[1,2]. Consequently, T cell depletion is recommended by the European Society for Blood and Marrow Transplantation (EBMT) as GHVD prophylaxis[3]. *In vivo* strategies of depleting T cells include anti-thymocyte globulins (ATG)[4-9], posttransplant cyclophosphamide (PTCy)[9-15] and alemtuzumab[16]. *Ex vivo* graft engineering strategies have advanced during the last decades and various strategies are available, with combined αβT cell and $CD19^+$ B cell depletion (later referred to as αβTCR/CD19 depletion), "Campath-in-the-bag", and $CD34^+$ selection being among the most frequently used within EBMT centers[17]. Furthermore, it has been shown that *ex vivo* engineered allografts can also be frozen in order to allow administration during pandemic events[18].

The combination of αβTCR/CD19 depletion was first used in haplo-identical allo-HSCT for children with non-malignant disorders[19], and has subsequently shown favorable outcomes in children and adults with hematological malignancies[20,21]. More recently, αβTCR/CD19 depletion has been shown to be safe and effective in allo-HSCT with 10/10 and 9/10 HLA-matched unrelated donors (MUD) in children[22]. We previously reported on the outcome of adults with hematological malignancies undergoing αβTCR depleted allo-HSCT without B-cell depletion, transplanted with matched related donors (MRD) and MUD[23]. In this αβTCR depletion study severe cGVHD appeared to be higher as compared to outcomes of combined αβTCR/CD19 depletion[20,21], therefore, and in order to reduce the risk of Epstein-Barr virus (EBV) reactivation, CD19 depletion was added to our standard allo-HSCT protocol. As comparisons between αβTCR/CD19 depleted allo-HSCT and other transplantation platforms are limited, we performed a single center analysis comparing outcomes of adult patients who underwent an αβTCR/CD19 depleted allo-HSCT from MRD and MUD to recipients of full (T cell replete) allografts, either with or without ATG. To our knowledge, we are the first to show a beneficial effect of αβTCR/CD19 depletion on GVHD-relapse free survival (GRFS) compared to patients receiving non-depleted allografts in MRD and MUD in adults with hematological malignancies.

PATIENTS AND METHODS

Clinical cohort

All adults with hematological malignancies who received an allo-HSCT between October 2011 and August 2021 in the University Medical Center Utrecht (UMCU) were considered to be included in this retrospective analysis. Patients that received αβT cell depleted allo-

HSCT without CD19 depletion, patients with a mismatched related donor, and patients not in complete remission (CR) that received a sequential regimen of chemotherapy and reduced intensity conditioning regimen ('FLAMSA-RIC[24]), or second/third allo-HSCT were excluded. Clinical data were extracted from the EBMT registry. All patients provided written informed consent indicating their agreement to allow data to be sent to EBMT. The informed consent form was approved by the local ethical committee (METC nr 21-322) at the UMCU in accordance with the Helsinki Declaration.

Donor selection and graft processing

9/10 or 10/10 HLA-matched related donors (MRD) or matched unrelated donors (MUD) were selected according to local guidelines. Peripheral blood mononuclear cells (PBMCs) were used as a stem cell source. *Ex vivo* αβTCR/CD19 depletion was performed using anti-αβTCR and anti-CD19 antibodies in combination with magnetic microbeads using the automated CliniMACS device (Miltenyi Biotec, Bergisch Gladbach, Germany), as described previously[25,26]. Data with regards to graft processing is provided in the supplemental material. Graft composition before and after αβTCR/CD19 depletion is shown in **supplementary figure S1**.

Transplantation regimen

Patients were divided into three cohorts. Patients that received a full (T cell replete) graft were included in cohort R or cohort R+ATG depending on whether they received ATG (Thymoglobulin) during conditioning. *Ex vivo* αβTCR+CD19 depletion was implemented in 2017. All patients transplanted with an αβTCR/CD19 depleted allograft (cohort D+ATG) received an uniform myeloablative conditioning consisting of ATG 1.5 mg/kg IV days -12 to -9, fludarabine IV 40 mg/m^2 days -5 to -2 and busulfan IV (Busilvex) days -5 to -2. Patients transplanted with T cell replete allografts (cohort R and R+ATG) received either a myeloablative (MA) or non-myeloablative (NMA) conditioning regimen[27]. Conditioning regimens are summarized in **table 1.** Prevention and treatment of infections is provided in the supplemental material.

Statistical analysis

Clinical endpoints were defined according to EBMT guidelines[28]. Overall survival (OS) was defined as time from transplantation to death from any cause, censoring at the last day of follow-up. Event-free survival (EFS) was defined as time from transplantation to relapse, graft failure or death, censoring at the last day of follow-up. GVHD-free, relapse-free survival (GRFS) was defined as time from transplantation to relapse, acute GVHD (aGVHD) grade III-IV, extensive chronic GVHD (cGVHD), or death, censoring at the last day of follow up. Acute GVHD was staged and graded according to the Glucksberg classification [29]. cGVHD was staged according to the revised Seattle criteria[30]. CMV reactivation was defined as a viral load of >250 IU/ml, EBV reactivation was defined as >1000 IU/ml as assessed by PCR. Primary graft failure was defined as ANC $<0.5 \times 10^9$/L and platelets

below <20 x 10^9/L by day +28 . Secondary graft failure was defined as ANC <0.5 × 10^9/L after initial engraftment not related to relapse infection, or drug toxicity and a loss of donor hematopoiesis < 5%[28]. Neutrophil recovery was defined as the first of 3 consecutive days with an absolute neutrophil count (ANC) greater than 0.5x10^9/L. Platelet recovery was defined as a platelet count greater than 50x10^9/L, without platelet transfusion in the preceding 7 days.

Categorical variables were compared between the three cohorts using a Chi squared test or Fisher's exact test, depending on group size. Kruskal-Wallis test was used to compare age and follow up time between the three cohorts. Kaplan-Meier curves of OS, RFS and GRFS were plotted by treatment with ATG and *ex vivo* αβTCR+CD19 depletion and compared using log-rank tests. Relapse, non-relapse mortality (NRM), aGVHD, cGVHD, CMV and EBV reactivation were calculated as cumulative incidence (CI) curves to adjust the estimates for competing risks. Fine and Gray's test was used to assess differences between cumulative incidences. Multivariate analysis of GRFS was performed using Cox model. Statistical analysis was performed using R version 4.2.3 using packages survival (3.5-7) and tidycmprsk (0.2.0.9001). P-values <0.05 were considered statistically significant.

Table 1. Overview of conditioning regimens

	Cohort R, N = 60	**Cohort R+ATG, N = 129**	**Cohort D+ATG, N = 122**
MA	**<u>TBI12/CY , N = 8 (13%)</u>** - Cyclophosphamide 60 mg/kg i.v. days -4 to -3 - TBI 6 Gy days -1 to 0 - MMF 15 mg/kg for 84 days - Cyclosporine 1.5 mg/kg i.v. or 4.5 mg/kg p.o. for 180 days	**<u>ATG/TBI12/CY, N = 10 (8%)</u>** - ATG (Thymoglobulin®) 2 mg/kg i.v. days -8 to -5 - Cyclophosphamide 60 mg/kg i.v. days -4 to -3 - TBI 6 Gy days -1 to 0 - MMF 15 mg/kg for 84 days - Cyclosporine 1.5 mg/kg i.v. or 4.5 mg/kg p.o. for 180 days **<u>ATG/BU(AUC90)/FLU, N = 9 (7%)</u>** - ATG (Thymoglobulin®) 2 mg/kg i.v. days -9 to -6 - Fludarabine 40 mg/m^2 i.v. days -5 to -2 - Busulfan (Busilvex®) AUC 90 i.v. days -5 to -2 - MMF 15 mg/kg for 84 days - Cyclosporine 1.5 mg/kg i.v. or 4.5 mg/kg p.o. for 180 days	**<u>ATG/BU(AUC90)/FLU + ABTCR/CD19 depletion, N = 122 (100%)</u>** - ATG (Thymoglobulin®) 1.5 mg/kg i.v. days -12 to -9 - Fludarabine 40 mg/m^2 i.v. days -5 to -2 - Busulfan (Busilvex®) AUC 90 i.v. days -5 to -2 - MMF 15 mg/kg for 84 days

Table 1. Overview of conditioning regimens (*continued*)

	Cohort R, N = 60	Cohort R+ATG, N = 129	Cohort D+ATG, N = 122
NMA	**TBI2/FLU, N = 48 (80%)** - Fludarabine 30 mg/m^2 days -3 to -1 - TBI 2Gy day 0 - MMF 15 mg/kg for 84 days - Cyclosporine 1.5 mg/kg i.v. or 4.5 mg/kg p.o. for 180 days	**ATG/TBI2/FLU, N = 97 (75%)** - ATG (Thymoglobulin®) i.v. 2 mg/kg days -7 to -4 - Fludarabine 30 mg/m^2 days -3 to -1 - TBI 2Gy day 0 - MMF 15 mg/kg for 84 days - Cyclosporine 1.5 mg/kg i.v. or 4.5 mg/kg p.o. for 180 days	
	TBI6/FLU, N = 4 (7%) - Fludarabine 30 mg/m^2 days -6 to -2 - TBI 6 Gy days -1 to 0 - MMF 15 mg/kg for 84 days	**ATG/TBI6/FLU, N = 13 (10%)** - ATG (Thymoglobulin®) i.v. 2 mg/kg days -9 to -7 - Fludarabine 30 mg/m^2 days -6 to -2 - TBI 6 Gy days -1 to 0 - MMF 15 mg/kg for 84 days	

Cohort R – no ex vivo depletion, no ATG; cohort R+ATG – no ex vivo depletion, with ATG; cohort D+ATG – ex vivo αβTCR/CD19 depletion; TBI, total body irradiation; CY, cyclosporine; ATG, anti-thymocyte globulin; BU, busulfan; AUC, area under the curve; FLU, fludarabine; MMF, mycophenolate mofetil

RESULTS

Patient characteristics

To assess clinical outcomes of different transplantation platforms, a total of 311 patients were included in the analysis, 60 in cohort R (replete, no ATG), 129 in cohort R+ATG (replete, with ATG), and 122 in cohort D+ATG (*ex vivo* αβTCR/CD19 depletion, with ATG) (**Table 1-2**). No significant age differences were observed between all cohorts, with a mean age ranging from 54 to 55. Different hematological malignancies were included, with the largest group in all cohorts being AML/MDS-EB2, representing 35-40% of the patients. Due to the nature of this retrospective study, conditioning regimens varied between cohorts. All patients in cohort D+ATG received myeloablative conditioning, whereas in cohort R and cohort R+ATG 87% and 85% of patients received non-myeloablative conditioning, respectively (**Table 1-2**) ($p < 0.001$).

aGVHD and cGVHD

The cumulative incidence of grade II-IV aGVHD was lowest after αβTCR/CD19 depletion, with 16% at day 100 in cohort D+ATG and 38% in the cohort R+ATG ($p = 0.004$, pairwise comparison D+ATG vs R+ATG $p < 0.001$; **Figure 1A**). In cohort R the cumulative incidence of aGVHD II-IV was also higher (25% at day 100), as compared to cohort D+ATG, but this did not reach the level of significance ($p = 0.093$). The cumulative incidence of grade III-IV aGVHD did not differ significantly between the three cohorts ($p = 0.09$; **Figure 1B**). Neither conditioning with ATG nor *ex vivo* T cell depletion impacted limited cGVHD, as

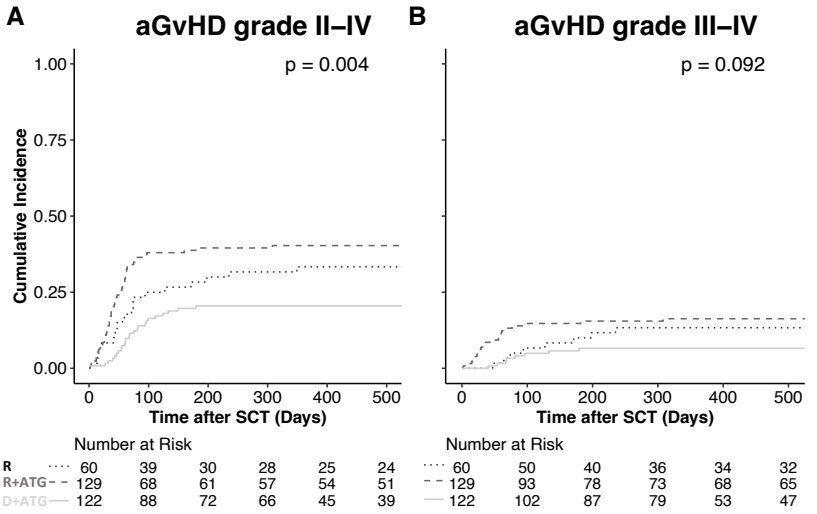
we found a two-year cumulative incidence of 15% in cohort R, 13% in cohort R+ATG and 16% in cohort D+ATG (p = 0.94; **Figure 1C**). This in contrast to the difference in extensive cGVHD, where the incidence was only 2% at two years in cohort D+ATG, compared to 23% in cohort R (p < 0.001) and 10% in cohort R+ATG (p = 0.007; **Figure 1D**). Since prophylactic donor lymphocyte infusions (DLIs) were standard in the D+ATG cohort, we evaluated the impact of DLI on GVHD incidence. In the D+ATG cohort, 58% (n = 71) received a prophylactic DLI, which was associated with lower rates of both acute and chronic GVHD compared to those who did not receive a DLI (**Supplementary table S1**).

Table 2. Baseline characteristics

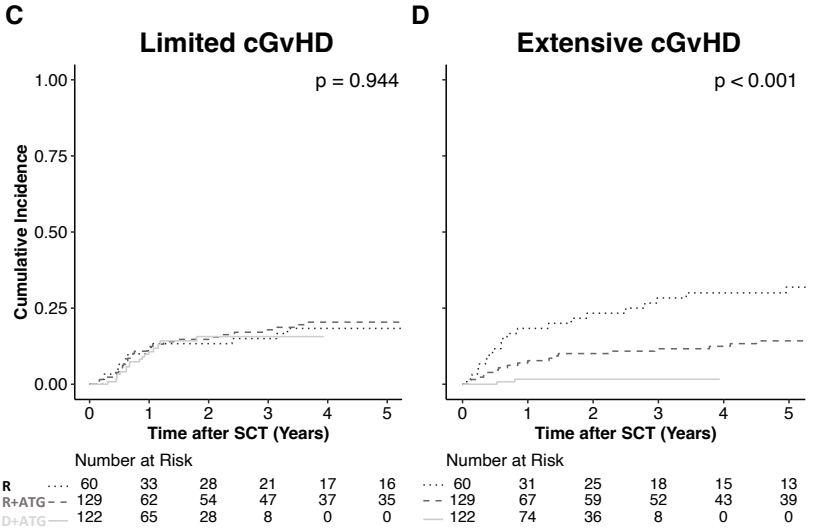
	Cohort R, N = 60	Cohort R+ATG, N = 129	Cohort D+ATG, N = 122	p-value
***Ex vivo* αβTCR/CD19 depletion (%)**	0 (0)	0 (0)	122 (100)	<0.001[1]
Myeloablative conditioning (%)	8 (13)	19 (15)	122 (100)	<0.001[1]
ATG (%)	0 (0)	129 (100)	122 (100)	<0.001[1]
Mean age, yrs (IQR)	54 (48, 64)	56 (51, 65)	55 (47, 66)	0.28[2]
Male (%)	35 (58)	85 (66)	67 (55)	0.20[1]
Median follow-up, months (IQR)	45 (11, 98)	48 (7, 100)	14 (11, 24)	<0.001[2]
Time period of SCT (%)				<0.001[1]
2011 - 2017	58 (97)	119 (92)	0 (0)	
2018 - 2022	2 (3)	10 (8)	122 (100)	
Disease (%)				0.055[1]
ALL	9 (15)	9 (7)	19 (16)	
AML/MDS-EB2	21 (35)	51 (40)	43 (35)	
LYMPHOMA	17 (28)	28 (22)	14 (11)	
MDS	4 (7)	13 (10)	9 (7)	
MF	4 (7)	14 (11)	14 (11)	
Other[3]	5 (8)	14 (11)	23 (19)	
Donor type (%)				<0.001
MRD 10/10	60 (100)	5(4)	23 (19)	
MUD 10/10	0 (0)	110 (85)	77 (63)	
MUD 9/10	0 (0)	14 (11)	22 (18)	
Number allo-HSCT (%)				
First	60 (100)	129 (100)	122 (100)	

TCR, T cell receptor; ATG, anti-thymocyte globulin; ALL, acute lymphatic leukemia; AML, acute myeloid leukemia; MDS, myelodysplastic syndrome; MF, myelofibrosis; MRD, matched related donor; MUD, matched unrelated donor; R – no ex vivo depletion, no ATG; R+ATG – no ex vivo depletion, with ATG; D+ATG – ex vivo αβTCR/CD19 depletion

[1] Pearson's Chi-squared test; [2] Kruskal-Wallis rank sum test; [3]Other: Bone marrow failure, chronic myeloid leukemia, MDS/myeloproliferative neoplasms, plasma cell leukemia, prolymphocytic leukemia



	100 days aGvHD grade II-IV % (95% CI)	2 year aGvHD grade II-IV % (95% CI)	100 days aGvHD grade III-IV % (95%)	2 year aGvHD grade III-IV % (95% CI)
R	25 (15 – 37)	33 (22 – 45)	7 (2 – 15)	13 (6 – 22)
R+ATG	38 (30 – 46)	40 (32 – 49)	15 (9 – 21)	16 (10 – 23)
D+ATG	16 (10 – 24)	20 (14 – 28)	5 (2 – 10)	7 (3 – 12)



	2 year limited cGvHD % (95% CI)	2 year extensive cGvHD % (95% CI)
R	13 (6 – 23)	23 (13 – 35)
R+ATG	15 (9 – 21)	10 (6 – 16)
D+ATG	16 (9 – 23)	2 (0 – 5)

Figure 1. Cumulative incidence of aGvHD and cGvHD. *The CI of GvHD is defined as time to onset of GvHD, with relapse and death as competing events. CI of aGVHD grade II-IV (A) and grade III-IV (B) with 100 days and 2 year CI reported in table. CI of limited cGvHD (C) and extensive cGVHD (D) with 2-year CI reported. Cohort R – no ex vivo depletion, no ATG; cohort R+ATG – no ex vivo depletion, with ATG; cohort D+ATG – ex vivo αβTCR-CD19 depletion. P-values shown calculated using Fine and Grey's test. Pairwise comparisons aGVHD II-IV D+ATG vs R p = 0.093, D+ATG vs R+ATG p < 0.001; extensive cGVHD D+ATG vs R p <0.001, D+ATG vs R+ATG p = 0.007*

According to international guidelines, patients with an unmanipulated allograft (R and R+ATG cohorts) did not receive ATG when transplanted with a MRD [28]. Furthermore, in the R and R+ATG cohorts, patients < 41 years with acute leukemia received MA conditioning, whereas most other patients underwent NMA conditioning. In contrast, the αβTCRCD19 depletion protocol included ATG and MA conditioning for all patients, creating imbalances in donor type, ATG use, and conditioning intensity across cohorts. To address these disparities and create more homogeneous groups, we analyzed patients as follows: MRD with NMA from the R cohort (NMA-no ATG-MRD), MUD with NMA from the R+ATG cohort (NMA-ATG-MUD), and MUD from the D+ATG cohort (MA-depletion+ATG-MUD). Also in these cohorts rates of aGVHD grade II-IV and extensive cGVHD in the MA-depletion+ATG-MUD cohort were significantly lower ($p = 0.036$ and $p < 0.001$, respectively; **Figure S2)**.

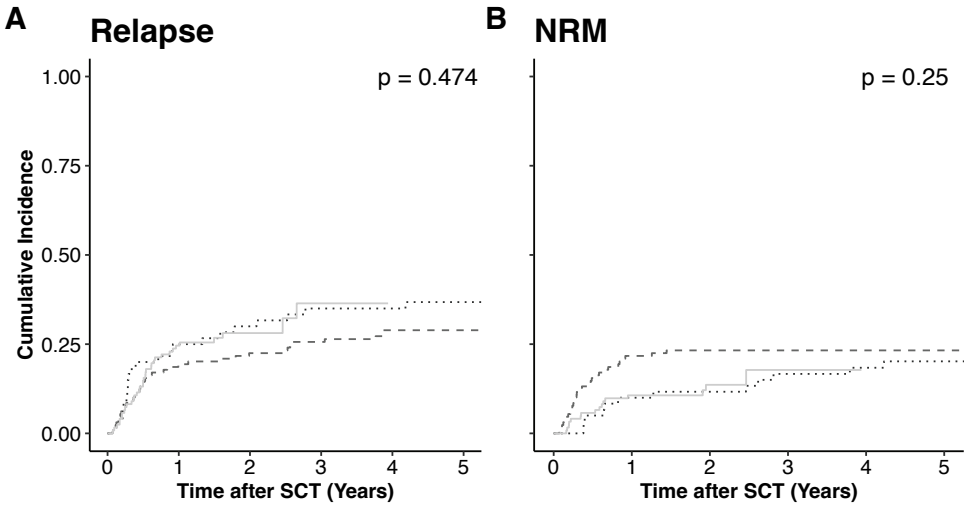
Viral reactivations

Viral reactivations of cytomegalovirus (CMV) and Epstein-Barr virus (EBV) after allo-HSCT are common and can cause severe complications[31,32]. As αβT cells are major drivers to control these infections we assessed frequencies of viral reactivations in the different cohorts. CMV serostatus was not significantly different between the three cohorts ($p = 0.44$) (**Supplementary table S2**). The incidence of CMV reactivation in seropositive patients was at one year was 50% in cohort R, compared to 58% in cohort R+ATG and 77% in cohort D+ATG ($p<0.001$; pairwise comparisons D+ATG vs R $p <0.001$; D+ATG vs R+ATG $p = 0.045$; R vs R+ATG $p = 0.022$) (**Figure S3A**).

In all cohorts, over 90% of patients were seropositive for EBV ($p = 0.21$; **Supplementary table S2**). Incidence of EBV reactivation did not differ significantly between cohorts ($p = 0.41$; **Figure S3B**). One-year incidence of EBV reactivation was 12% in cohort R, 20% in cohort R+ATG and 14% in cohort D+ATG. We conclude that both *in vivo* and *ex vivo* depletion of αβT cells increases the risk of CMV reactivation in seropositive patients, whereas EBV reactivation is not significantly affected when αβT cells and CD19 cells are *ex vivo* depleted.

Engraftment, relapse, NRM

We evaluated the impact of *ex vivo* graft engineering on engraftment, relapse, and NRM. Median neutrophil recovery was 15 days across all cohorts ($p = 0.81$), with primary/secondary graft failure rates of 0%/0% (R), 1%/3% (R+ATG), and 2%/5% (D+ATG) ($p = 0.50$; **Supplementary Table S3**). Two-year cumulative incidence of relapse was 30% in cohort R, 22% in cohort R+ATG and 28% in cohort D+ATG, which was not significantly different between the 3 cohorts ($p = 0.47$, **Figure 2A**). In addition, we found that the two-year cumulative incidence of NRM was lowest in cohort R (12%), however, this was not significantly different to two-year NRM in cohort R+ATG (23%) and cohort D+ATG (14%) ($p = 0.25$; **Figure 2B**). We conclude that relapse and NRM showed no significant differences between all cohorts.



	1-year relapse % (95% CI)	2-year relapse % (95 % CI)
R	25 (15 – 37)	30 (19 – 42)
R+ATG	19 (13 – 27)	22 (16 – 30)
D+ATG	25 (17 – 33)	28 (20 – 37)

	1-year NRM % (95% CI)	2-year NRM % (95 % CI)
R	10 (4 – 19)	12 (5 – 21)
R+ATG	22 (15 – 29)	23 (16 – 31)
D+ATG	11 (6 – 17)	14 (8 – 21)

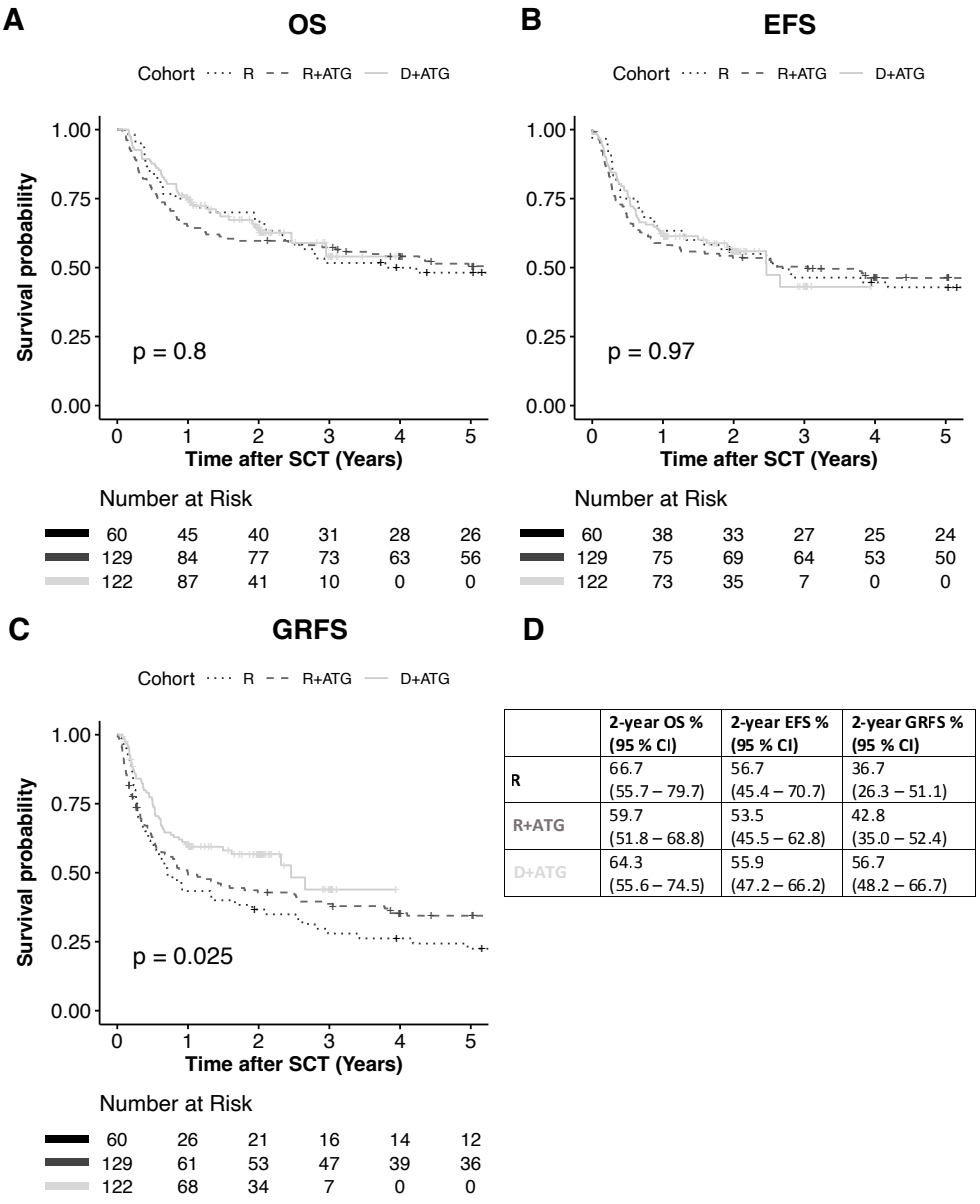
Figure 2. Relapse and NRM by ex vivo αβTCR/CD19 depletion and conditioning with ATG. *Cumulative incidence (CI) of relapse and NRM shown with a 5-year follow up. (A) The CI of relapse is defined as time to relapse, with death as a competing event. (B) NRM is defined as time to death without relapse or progression. 2-year cumulative incidences reported in table. Cohort R – no ex vivo depletion, no ATG; cohort R+ATG – no ex vivo depletion, with ATG; cohort D+ATG – ex vivo αβTCR/CD19 depletion. P-values shown calculated using Fine and Grey's test*

OS, EFS and GRFS

Finally, we addressed the impact of αβTCR/CD19 depletion on overall survival (OS), event-free survival (EFS) and GVHD-free, relapse-free survival (GRFS) at 2 years. With a median follow up of 14 months (range 2-47), OS was not different between all groups. In cohort D+ATG OS at two years was 64.3%, compared to 66.7% in cohort R and 59.7% in cohort R+ATG (p = 0.80; **Figure 3A**). EFS at two years was also comparable between the three cohorts, with 56.7% in cohort R, 53.5% in cohort R+ATG and 55.0% in cohort D+ATG (p = 0.97; **Figure 3B**). GRFS was significantly different between the three cohorts (p = 0.025; **Figure 3C**), with cohort D+ATG consistently showing the highest GRFS. At six months, GRFS in cohort D+ATG was superior (74.7%), compared to 60.0% and 62.2% in cohort R (p = 0.017) and cohort R+ATG (p = 0.047), respectively. The positive effect of *ex vivo* αβTCR/CD19 depletion was still evident at two years post allo-HSCT, as GRFS was 56.7% in cohort D+ATG, compared to 36.7% in cohort R, and 42.8% in cohort R+ATG **(Figure 3D)**.

After performing a multivariate Cox regression on GRFS, adjusted for sex, diagnosis, age, donor type and the use of ATG during conditioning, we found that *ex vivo* αβTCR/CD19 depletion positively impacted GRFS, with a hazard ratio (HR) of 0.64 (95%CI = 0.44 – 0.92; p = 0.017; **Table 3**). Considering the small number of patients in some disease groups, we pooled patients with AML and MDS-EB2 together and grouped patients with other malignancies as another group. After multivariate analysis, *ex vivo* αβTCR/CD19 depletion remained the only variable significantly impacting GRFS (HR = 0.65; 95%CI = 0.45 – 0.94; p = 0.024; **Supplementary Table S4**). Furthermore, we compared cohorts R+ATG with D+ATG, to exclude an interaction with ATG. This confirmed that *ex vivo* αβT cell and CD19 depletion significantly impacted GRFS (HR = 0.64; 95%CI= 0.44 – 0.92; p = 0.016; **Supplementary table S5**).

As we did for GVHD, we also aimed to categorize patients differently to account for differences in donor type, ATG administration, and conditioning intensity across cohorts: MRD with NMA conditioning from the R cohort (NMA-no ATG-MRD), MUD with NMA conditioning from the R+ATG cohort (NMA-ATG-MUD), and MUD from the D+ATG cohort (MA-depletion+ATG-MUD) (**Figure S4**). OS and EFS were not significantly different between the three cohorts (p = 0.61 and p = 0.79, respectively). However, GRFS was significantly improved in the MA-depletion+ATG-MUD group, compared to both the NMA-no ATG-MRD group and the NMA-ATG-MUD group (p = 0.018 and p = 0.039, respectively). Using a multivariate Cox regression analysis for GRFS, adjusted for sex, diagnosis, age and donor type, we observed that the combination of myeloablative conditioning and ex vivo αβTCR/CD19 depletion was associated with a significant improvement in GRFS (HR = 0.57; 95%CI= 0.37 – 0.89; p = 0.008; **Supplementary table S6**). Overall, our findings indicate that using a myeloablative conditioning regimen combined with ATG and *ex vivo* αβTCR/CD19 depletion significantly reduces the incidence of extensive cGVHD, leading to improved GRFS as compared to T cell replete cohorts.



	2-year OS % (95 % CI)	2-year EFS % (95 % CI)	2-year GRFS % (95 % CI)
R	66.7 (55.7 – 79.7)	56.7 (45.4 – 70.7)	36.7 (26.3 – 51.1)
R+ATG	59.7 (51.8 – 68.8)	53.5 (45.5 – 62.8)	42.8 (35.0 – 52.4)
D+ATG	64.3 (55.6 – 74.5)	55.9 (47.2 – 66.2)	56.7 (48.2 – 66.7)

Figure 3. OS, EFS and GRFS by ex vivo αβTCR/CD19 depletion and conditioning with ATG. *OS, EFS, and GRFS shown with a 5-year follow up. OS (A), EFS (B) and GRFS (C) were estimated by the Kaplan-Meier product. Log-rank test was used to determine p-values. Cohort R – no ex vivo depletion, no ATG; cohort R+ATG – no ex vivo depletion, with ATG; cohort D+ATG – ex vivo αβTCR/CD19 depletion. P-values shown calculated using the log-rank test. Pairwise comparisons GRFS D+ATG vs R p = 0.017; D+ATG vs R+ATG p = 0.047.*

Table 3. Multivariate analysis of risk factors for GRFS

Variable	HR	95% CI	P-value
Sex			
Male	*REF*	*REF*	*REF*
Female	1.16	0.86 – 1.57	0.3
Diagnosis			
AML/MDS-EB2	*REF*	*REF*	*REF*
ALL	0.75	0.43 – 1.32	0.3
Lymphoma	0.77	0.51 – 1.16	0.2
MDS	0.99	0.57 – 1.71	> 0.9
MF	1.30	0.78 – 2.16	0.3
Others	1.09	0.67 – 1.76	0.7
Age recipient			
Per 5 year increase	1.01	0.95 – 1.08	0.7
Donortype			
MRD 10/10	*REF*	*REF*	*REF*
MUD 10/10	0.69	0.40 – 1.18	0.2
MUD 9/10	0.69	0.34 – 1.37	0.3
Ex vivo graft depletion			
No depletion	*REF*	*REF*	*REF*
αβTCR/CD19 depletion	0.64	0.44 – 0.92	0.017
Conditioning with ATG			
Yes	*REF*	*REF*	*REF*
No	0.87	0.47 – 1.62	0.7

Cox model was used. AML, acute myeloid leukemia, MDS-EB2, myelodysplastic syndrome with excess blasts; ALL, acute lymphatic leukemia; MDS, myelodysplastic syndrome; MF, myelofibrosis; MRD, matched related donor; MUD, matched unrelated donor

DISCUSSION

Here we show that *ex vivo* αβTCR/CD19-depleted allo-HSCT, combined with ATG and a myeloablative conditioning, results in low incidences of acute and chronic GVHD. This translated into a GRFS of 57% at two years, outperforming the T cell-replete cohorts in this analysis (GRFS 38% and 41%). Notably, in T cell-replete HSCT of unrelated donors (cohort R+ATG) the incidence of aGHVD was increased, whereas in T cell-replete HSCT of related donors the incidence cGVHD was increased (cohort R). The protective impact of ATG on cGVHD is in line with was shown by Kröger et al, who also demonstrated that ATG mitigates severe cGVHD after allo-HSCT of HLA identical siblings[33]. The rate of extensive cGVHD of 2% in our study after the combination of ATG and αβTCR/CD19 depletion cohort is remarkably low, even in the context of ATG, and also lower when compared to our previous study in which we studied outcomes of αβTCR depletion alone[23]. These data

imply that the additional depletion of CD19$^+$ B cells may provide stronger protection against cGVHD development, however, comparative studies are warranted to support this hypothesis. Nevertheless, our current study as well as the study by Kröger et al. suggest that also for matched related donors a form of *in* or *ex vivo T cell* depletion should be provided as standard GVHD prophylaxis, as is already recommend by EBMT for matched unrelated donors[3]. Next to ATG and αβTCR/CD19 depletion, other *in vivo* (e.g. post transplantation cyclophosphamide (PT-Cy)) and *ex vivo* T cell depletion (e.g. CD34$^+$ selection, alemtuzumab) strategies are used to reduce severe GVHD[34]. Comparing these different platforms is challenging, as studies report on different patient and donor characteristics and comparative studies are missing. However multiple randomized controlled trials[15,35] and comparative registry-based retrospective studies[9,36] suggest improved GRFS after *in* or *ex vivo* depletion as compared to conventional T cell replete approaches with 'classical immune suppression' without any ATG or PT-Cy.

A downside of T cell depletion could be an increase in relapse and/or infections. Here, the incidence of CMV reactivations is mainly affected by ATG, with an additional impact of αβTCR/CD19 depletion (**Figure S2**). We assume that this risk will be significantly reduced by implementation of letermovir in the future[37-39]. The introduction of CD19$^+$ cell depletion to the *ex vivo* engineering platform reduced the risk of EBV reactivation, with incidence dropping from 44% in our previous study (αβT cell depletion alone) to 20% in the current study[23]. NRM was not increased in the *ex vivo* depleted allo-HSCT cohort compared to the cohorts receiving full grafts, despite the fact that all patients in the *ex vivo* depletion cohort received a myeloablative regimen, where in the T cell replete cohort > 80% received NMA conditioning regimens. Myeloablative conditioning is normally associated with higher NRM, especially in older patients[40], however, in our αβTCR/CD19 depleted allo-HSCT cohort myeloablative conditioning is well tolerated at all age groups. Relapse did not differ within cohorts, with a two-year incidence of 23-30%. Donor lymphocyte infusions (DLI) are increasingly implemented prophylactically or pre-emptively to increment the GvL effect of allo-HSCT[41]. As αβTCR/CD19 depletion requires only a very short course of systemic GVHD prophylaxis, a risk-based DLI strategy is a very plausible and powerful strategy to better control relapse.

In summary, we demonstrate that *ex vivo* αβTCR/CD19 depletion combined with a myeloablative conditioning regimen including ATG results in reduced GVHD and improved GRFS, when compared to two cohorts of patients receiving full grafts. Our data contribute to the accumulating evidence that allo-HSCT without any form of T cell depletion should be avoided, to increase the likelihood of reaching GRFS.

AUTHOR CONTRIBUTIONS

MdW and JK were responsible for the conception and design of the study. MdW and JK were funded for the study. LvdW, AvR, LvH, AJ, HK, RF, JK and MdW actively managed the patients. AS, CN, FV, IB, FVL, HK, RF, HJP and KW collected the data. AS, CN, IB and FV had full access to and verified the underlying data. AS, CN, JD, JK and MdW contributed to data analysis and interpretation. AS, CN, JD, JK and MdW wrote the original draft of the manuscript. AS and CN prepared the figures. AS and MdW were responsible for submission of the manuscript. All authors were responsible for critical revision of the manuscript and approved the final version of the manuscript.

DATA AVAILABILITY STATEMENT

The data that support the findings of this study are available from the EBMT registry, but restrictions apply to the availability of these data, which were used under license for the current study, and so are not publicly available. Data are, however, available from the authors upon reasonable request and with permission of the corresponding author.

REFERENCES

1. Korngold R, Sprent J. Lethal graft-versus-host disease after bone marrow transplantation across minor histocompatibility barriers in mice. Prevention by removing mature T cells from marrow. *J Exp Med*. 1978;148(6):1687-1698.
2. Shlomchik WD. Graft-versus-host disease. *Nat Rev Immunol*. 2007;7(5):340-352.
3. Penack O, Marchetti M, Aljurf M, et al. Prophylaxis and management of graft-versus-host disease after stem-cell transplantation for haematological malignancies: updated consensus recommendations of the European Society for Blood and Marrow Transplantation. *Lancet Haematol*. 2024.
4. Finke J, Bethge WA, Schmoor C, et al. Standard graft-versus-host disease prophylaxis with or without anti-T-cell globulin in haematopoietic cell transplantation from matched unrelated donors: a randomised, open-label, multicentre phase 3 trial. *Lancet Oncol*. 2009;10(9):855-864.
5. Mohty M, Labopin M, Balere ML, et al. Antithymocyte globulins and chronic graft-vs-host disease after myeloablative allogeneic stem cell transplantation from HLA-matched unrelated donors: a report from the Societe Francaise de Greffe de Moelle et de Therapie Cellulaire. *Leukemia*. 2010;24(11):1867-1874.
6. Pidala J, Tomblyn M, Nishihori T, et al. ATG prevents severe acute graft-versus-host disease in mismatched unrelated donor hematopoietic cell transplantation. *Biol Blood Marrow Transplant*. 2011;17(8):1237-1244.
7. Socie G, Schmoor C, Bethge WA, et al. Chronic graft-versus-host disease: long-term results from a randomized trial on graft-versus-host disease prophylaxis with or without anti-T-cell globulin ATG-Fresenius. *Blood*. 2011;117(23):6375-6382.
8. Bonifazi F, Rubio MT, Bacigalupo A, et al. Rabbit ATG/ATLG in preventing graft-versus-host disease after allogeneic stem cell transplantation: consensus-based recommendations by an international expert panel. *Bone Marrow Transplant*. 2020;55(6):1093-1102.
9. Penack O, Abouqateb M, Peczynski C, et al. ATG or post-transplant cyclophosphamide to prevent GVHD in matched unrelated stem cell transplantation? *Leukemia*. 2024;38(5):1156-1163.
10. Berger M, Lanino E, Cesaro S, et al. Feasibility and Outcome of Haploidentical Hematopoietic Stem Cell Transplantation with Post-Transplant High-Dose Cyclophosphamide for Children and Adolescents with Hematologic Malignancies: An AIEOP-GITMO Retrospective Multicenter Study. *Biol Blood Marrow Transplant*. 2016;22(5):902-909.
11. Mussetti A, Greco R, Peccatori J, Corradini P. Post-transplant cyclophosphamide, a promising anti-graft versus host disease prophylaxis: where do we stand? *Expert Rev Hematol*. 2017;10(5):479-492.
12. Uygun V, Karasu G, Daloglu H, et al. Haploidentical hematopoietic stem cell transplantation with post-transplant high-dose cyclophosphamide in high-risk children: A single-center study. *Pediatr Transplant*. 2019;23(7):e13546.
13. Sharma A, Rastogi N, Chatterjee G, Kapoor R, Nivargi S, Yadav SP. Haploidentical Stem Cell Transplantation With Post-transplant Cyclophosphamide for Pediatric Acute Leukemia is Safe and Effective. *J Pediatr Hematol Oncol*. 2021;43(7):e1033-e1036.
14. Broers AEC, de Jong CN, Bakunina K, et al. Posttransplant cyclophosphamide for prevention of graft-versus-host disease: results of the prospective randomized HOVON-96 trial. *Blood Adv*. 2022;6(11):3378-3385.

15. Bolanos-Meade J, Hamadani M, Wu J, et al. Post-Transplantation Cyclophosphamide-Based Graft-versus-Host Disease Prophylaxis. *N Engl J Med*. 2023;388(25):2338-2348.
16. Finazzi MC, Boschini C, Craddock C, Rambaldi A, Ward J, Malladi RK. Characteristics of graft-versus-host disease occurring after alemtuzumab-containing allogeneic stem cell transplants: incidence, organ involvement, risk factors and survival. *Br J Haematol*. 2020;188(4):550-559.
17. de Witte MA, Mooyaart JE, Hoogenboom JD, et al. Activity of ex vivo graft and DLI Engineering within the last decade increases, a survey from the EBMT Cellular Therapy & Immunobiology Working Party. *Bone Marrow Transplant*. 2023.
18. Nijssen K, Westinga K, Stuut A, et al. Graft engineering: how long can you wait, how low can you go, and pandemic readiness. *Bone Marrow Transplant*. 2023;58(7):820-822.
19. Bertaina A, Romano M, Rutella S, et al. HLA Haploidentical Stem Cell Transplantation After Removal of αβ+ T Lymphocytes and B Lymphocytes Is an Effective Treatment for Children with Life-Threatening, Non-Malignant Disorders. *Blood*. 2012;120(21):2018-2018.
20. Locatelli F, Merli P, Pagliara D, et al. Outcome of children with acute leukemia given HLA-haploidentical HSCT after alphabeta T-cell and B-cell depletion. *Blood*. 2017;130(5):677-685.
21. Bethge WA, Eyrich M, Mielke S, et al. Results of a multicenter phase I/II trial of TCRalphabeta and CD19-depleted haploidentical hematopoietic stem cell transplantation for adult and pediatric patients. *Bone Marrow Transplant*. 2022;57(3):423-430.
22. Leahy AB, Li Y, Talano JA, et al. Unrelated donor alpha/beta T cell- and B cell-depleted HSCT for the treatment of pediatric acute leukemia. *Blood Adv*. 2022;6(4):1175-1185.
23. de Witte MA, Janssen A, Nijssen K, et al. alphabeta T-cell graft depletion for allogeneic HSCT in adults with hematological malignancies. *Blood Adv*. 2021;5(1):240-249.
24. Schmid C, Schleuning M, Ledderose G, Tischer J, Kolb HJ. Sequential regimen of chemotherapy, reduced-intensity conditioning for allogeneic stem-cell transplantation, and prophylactic donor lymphocyte transfusion in high-risk acute myeloid leukemia and myelodysplastic syndrome. *J Clin Oncol*. 2005;23(24):5675-5687.
25. Chaleff S, Otto M, Barfield RC, et al. A large-scale method for the selective depletion of alphabeta T lymphocytes from PBSC for allogeneic transplantation. *Cytotherapy*. 2007;9(8):746-754.
26. Li Pira G, Malaspina D, Girolami E, et al. Selective Depletion of alphabeta T Cells and B Cells for Human Leukocyte Antigen-Haploidentical Hematopoietic Stem Cell Transplantation. A Three-Year Follow-Up of Procedure Efficiency. *Biol Blood Marrow Transplant*. 2016;22(11):2056-2064.
27. Bacigalupo A, Ballen K, Rizzo D, et al. Defining the intensity of conditioning regimens: working definitions. *Biol Blood Marrow Transplant*. 2009;15(12):1628-1633.
28. . In: Carreras E, Dufour C, Mohty M, Kroger N, eds. The EBMT Handbook: Hematopoietic Stem Cell Transplantation and Cellular Therapies. Cham (CH); 2019.
29. Przepiorka D, Weisdorf D, Martin P, et al. 1994 Consensus Conference on Acute GVHD Grading. *Bone Marrow Transplant*. 1995;15(6):825-828.
30. Lee SJ, Vogelsang G, Flowers ME. Chronic graft-versus-host disease. *Biol Blood Marrow Transplant*. 2003;9(4):215-233.
31. Teira P, Battiwalla M, Ramanathan M, et al. Early cytomegalovirus reactivation remains associated with increased transplant-related mortality in the current era: a CIBMTR analysis. *Blood*. 2016;127(20):2427-2438.

32. Fujimoto A, Suzuki R. Epstein-Barr Virus-Associated Post-Transplant Lymphoproliferative Disorders after Hematopoietic Stem Cell Transplantation: Pathogenesis, Risk Factors and Clinical Outcomes. *Cancers (Basel)*. 2020;12(2).
33. Kroger N, Solano C, Wolschke C, et al. Antilymphocyte Globulin for Prevention of Chronic Graft-versus-Host Disease. *N Engl J Med*. 2016;374(1):43-53.
34. de Witte M, Daenen LGM, van der Wagen L, et al. Allogeneic Stem Cell Transplantation Platforms With Ex Vivo and In Vivo Immune Manipulations: Count and Adjust. *Hemasphere*. 2021;5(6):e580.
35. Luznik L, Pasquini MC, Logan B, et al. Randomized Phase III BMT CTN Trial of Calcineurin Inhibitor-Free Chronic Graft-Versus-Host Disease Interventions in Myeloablative Hematopoietic Cell Transplantation for Hematologic Malignancies. *J Clin Oncol*. 2021:JCO2102293.
36. Lum SH, Albert MH, Gilbert P, et al. Outcomes of HLA-mismatched HSCT with TCRalphabeta/CD19 depletion or post-HSCT cyclophosphamide for inborn errors of immunity. *Blood*. 2024.
37. Marty FM, Ljungman P, Chemaly RF, et al. Letermovir Prophylaxis for Cytomegalovirus in Hematopoietic-Cell Transplantation. *N Engl J Med*. 2017;377(25):2433-2444.
38. Marzolini MAV, Mehra V, Thomson KJ, et al. Letermovir prophylaxis in T-cell-depleted transplants: breakthrough and rebound infections in the postmarketing setting. *Blood Adv*. 2021;5(21):4500-4503.
39. Russo D, Schmitt M, Pilorge S, et al. Efficacy and safety of extended duration letermovir prophylaxis in recipients of haematopoietic stem-cell transplantation at risk of cytomegalovirus infection: a multicentre, randomised, double-blind, placebo-controlled, phase 3 trial. *Lancet Haematol*. 2024;11(2):e127-e135.
40. Spyridonidis A, Labopin M, Savani BN, et al. Redefining and measuring transplant conditioning intensity in current era: a study in acute myeloid leukemia patients. *Bone Marrow Transplant*. 2020;55(6):1114-1125.
41. Pagliuca S, Schmid C, Santoro N, et al. Donor lymphocyte infusion after allogeneic haematopoietic cell transplantation for haematological malignancies: basic considerations and best practice recommendations from the EBMT. *Lancet Haematol*. 2024;11(6):e448-e458.

SUPPLEMENTARY MATERIAL

Supplementary Methods

Graft processing

The target cell number for collection was between 5-10 x 10^6 CD34+ cells and for infusion between 2-10 x 10^6 CD34+ cells/kg. For the αβTCR/CD19 depletion cohort, the graft was targeted to contain ≤25 × 10^3 TCRαβ+ T-cells/kg and 1 × 10^5 B cells/kg, respectively.

Prevention and treatment of infections

Selective decontamination consisting of e.g. anti-bacterial and antimycotic agents was administered according to local guidelines, which were not significantly changed during the timeframe of this study. Monitoring, prophylaxis and treatment of viral infections (like CMV and EBV) was performed according to local guidelines. Letermovir was not implemented as CMV prohylaxis. Pre-emptive therapy for CMV (Ganciclovir or Foscavir) was initiated after a positive CMV PCR (250 IU/ml) and continued until one negative result occurred after at least 14 days of treatment. Rituximab was initiated in cases of EBV DNA load > 5000 IU/ml, a detectable EBV DNA load on 2 subsequent measurements or at signs of EBV related disease. Rituximab was administered once a week for 4 consecutive weeks at 375 mg/m^2, but sometimes a reduced number of infusions were administered upon rapid decline of the viral load.

Supplementary table S1. Cumulative incidence of GVHD after prophylactic DLI

		Incidence aGVHD (95% CI)				Incidence cGVHD (95% CI)	
		100 days		1 year		2 years	
	N	Grade II-IV	Grade III-IV	Grade II-IV	Grade III-IV	Limited	Extensive
DLI	71	1 (0 – 7)	0 (-)	6 (2 – 13)	1 (0 – 7)	18 (9 – 28)	0 (-)
No DLI	51	37 (24 – 50)	12 (5 – 22)	41 (27 – 54)	14 (6 – 25)	12 (5 – 22)	4 (1 – 12)

DLI = donor lymphocyte infusion. Cumulative incidence of GVHD calculated with relapse and death as competing events. Patients were included in 'DLI' group if they received a DLI of 10^5 lymphocytes/kg in the first 3 months after ex vivo αβTCR/CD19 depleted allo-HSCT.

Supplementary table S2. CMV and EBV serostatus.

	Cohort R, N = 60	Cohort R+ATG, N = 129	Cohort D+ATG, N = 122	p-value[1]
CMV serostatus				0.44
R-/D	20 (33%)	42 (33%)	53 (43%)	
R-/D+	6 (10%)	15 (12%)	7 (6%)	
R+/D-	14 (23%)	24 (19%)	21 (17%)	
R+/D+	20 (33%)	48 (37%)	41 (34%)	

Supplementary table S2. CMV and EBV serostatus. (*continued*)

	Cohort R, N = 60	Cohort R+ATG, N = 129	Cohort D+ATG, N = 122	p-value[1]
EBV serostatus				0.21
R-/D-	0 (0%)	4 (3%)	1 (1%)	
R-/D+	2 (3%)	6 (5%)	4 (3%)	
R+/D-	3 (5%)	10 (8%)	12 (10%)	
R+/D+	53 (88%)	97 (75%)	100 (81%)	
Unknown	2 (3%)	12 (9%)	5 (4%)	

R – no ex vivo depletion, no ATG; R+ATG – no ex vivo depletion, with ATG; D+ATG – ex vivo αβTCR/CD19 depletion. CMV, cytomegalovirus; R, recipient; D, donor; EBV, Epstein-Barr virus

[1] *Pearson's Chi-Squared test*

Supplementary table S3. Overview of engraftment and graft failure

	Cohort R, N = 60	Cohort R+ATG, N = 129	Cohort D+ATG, N = 122	p-value
Neutrophil recovery in days, median (IQR)	15 (10 – 20)	15 (12 – 20)	15 (14 – 16)	0.76
Thrombocyte recovery in days, median (IQR)	3 (0 – 15)	13 (0 – 17)	14 (12 – 18)	< 0.001
Graft failure				
No graft failure (%)	60 (0)	125 (97)	115 (94)	0.50
Primary graft failure (%)	0 (0)	1 (1)	2 (2)	
Secondary graft failure (%)	0 (0)	3 (2)	5 (4)	

R – no ex vivo depletion, no ATG; R+ATG – no ex vivo depletion, with ATG; D+ATG – ex vivo αβTCR/CD19 depletion. P-values found using Kruskal-Wallis rank sum test for neutrophil and thrombocyte recovery, and Fisher's exact test for incidence of graft failure.

Supplementary Table S4. Multivariate analysis of risk factors for GRFS

Variable	HR	95% CI	P-value
Sex			
Male	*REF*	*REF*	*REF*
Female	1.13	0.84 – 1.53	0.4
Diagnosis			
AML/MDS EB2	*REF*	*REF*	*REF*
Other malignancies	0.92	0.68 – 1.25	0.6
Age recipient			
Per 5 year increase	1.03	0.97 – 1.09	0.4
Donortype			
MRD 10/10	*REF*	*REF*	*REF*
MUD 10/10	0.62	0.36 – 1.07	0.084
MUD 9/10	0.62	0.31 – 1.24	0.2

Supplementary Table S4. Multivariate analysis of risk factors for GRFS (*continued*)

Variable	HR	95% CI	P-value
Ex vivo graft depletion			
No depletion	*REF*	*REF*	*REF*
αβTCR/CD19 depletion	0.65	0.45 – 0.94	0.024
Conditioning with ATG			
Yes	*REF*	*REF*	*REF*
No	0.77	0.42 – 1.42	0.4

Cox model was used. AML, acute myeloid leukemia, MDS-EB2; myelodysplastic syndrome with excess blasts; MRD, matched related donor; MUD, matched unrelated donor

Supplementary Table S5. Multivariate analysis on risk factors for GRFS.

Variable	HR	95% CI	P-value
Sex			
Male	*REF*	*REF*	*REF*
Female	1.26	0.89 – 1.78	0.2
Diagnosis			
AML/MDS EB2	*REF*	*REF*	*REF*
Other	0.91	0.64 – 1.29	0.6
Age recipient			
Per 5 year increase	1.04	0.98 – 1.11	0.2
Donortype			
MRD 10/10	*REF*	*REF*	*REF*
MUD 10/10	0.64	0.37 – 1.09	0.10
MUD 9/10	0.64	0.32 – 1.26	0.2
Ex vivo graft depletion			
No depletion	*REF*	*REF*	*REF*
αβTCR/CD19 depletion	0.64	0.44 – 0.92	0.016

Patients without ATG in conditioning regimen (n = 60) excluded. Cox model was used. AML, acute myeloid leukemia, MDS EB2; myelodysplastic syndrome with excess blasts; MRD, matched related donor; MUD, matched unrelated donor

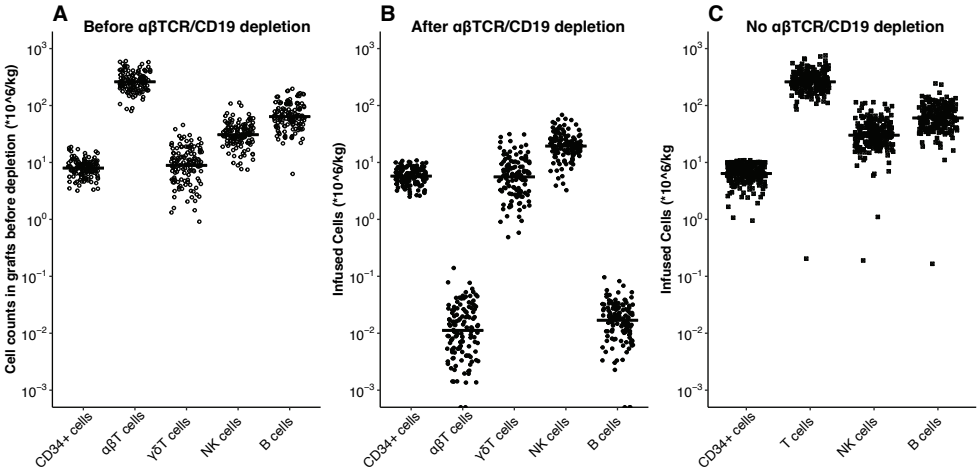
Supplementary Table S6. Multivariate analysis on risk factors for GRFS.

Variable	HR	95% CI	P-value
Sex			
Male	*REF*	*REF*	*REF*
Female	1.25	0.89 – 1.75	0.2

Supplementary Table S6. Multivariate analysis on risk factors for GRFS. (*continued*)

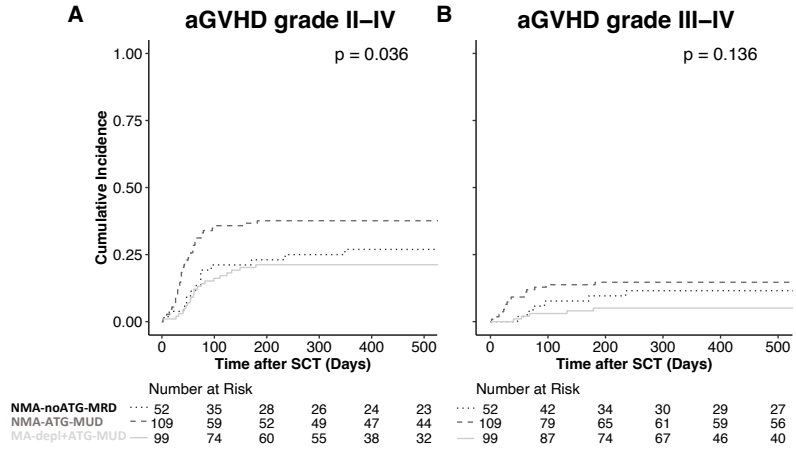
Variable	HR	95% CI	P-value
Diagnosis			
AML/MDS-EB2	*REF*	*REF*	*REF*
ALL	0.65	0.33 – 1.28	0.2
Lymphoma	0.67	0.43 – 1.03	0.068
MDS	0.94	0.52 – 1.69	0.8
MF	1.25	0.70 – 2.22	0.5
Others	1.22	0.71 – 2.10	0.5
Age recipient			
Per 5 year increase	0.98	0.91 – 1.06	0.7
Donortype			
MRD 10/10	*REF*	*REF*	*REF*
MUD 10/10	0.75	0.50 – 1.11	0.2
MUD 9/10	0.76	0.41 – 1.42	0.4
Conditioning type and depletion			
NMA-without depletion	*REF*	*REF*	*REF*
MA-with αβTCR/CD19 depletion	0.57	0.37 – 0.89	0.008

Cox model was used. Patients included from cohort NMA-no ATG-MRD – reduced intensity conditioning, no ex vivo depletion, no ATG, matched related donor (n = 52); cohort NMA-ATG-MUD – reduced intensity conditioning, no ex vivo depletion, with ATG, matched unrelated donor (n = 109); cohort MA-depletion+ATG-MUD – myeloablative conditioning, ex vivo αβTCR-CD19 depletion, with ATG, matched unrelated donors (n = 99). AML, acute myeloid leukemia; MDS-EB2, myelodysplastic syndrome with excess blasts; ALL, acute lymphatic leukemia; MDS, myelodysplastic syndrome; MF, myelofibrosis; MRD, matched related donor; MUD, matched unrelated donor; NMA, non-myeloablative conditioning; MA, myeloablative conditioning

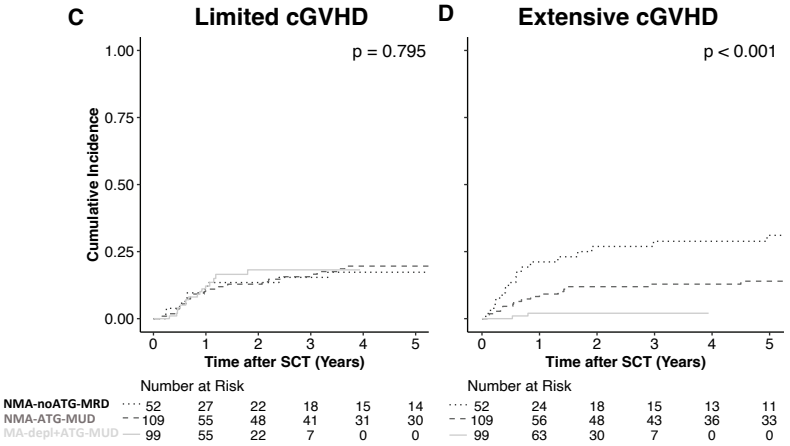


Supplementary Figure S1. Overview of graft composition.

Graft composition A) before αβTCR/CD19 depletion (n = 122) B) after αβTCR/CD19 depletion (n = 122) and C) without depletion (n = 182)



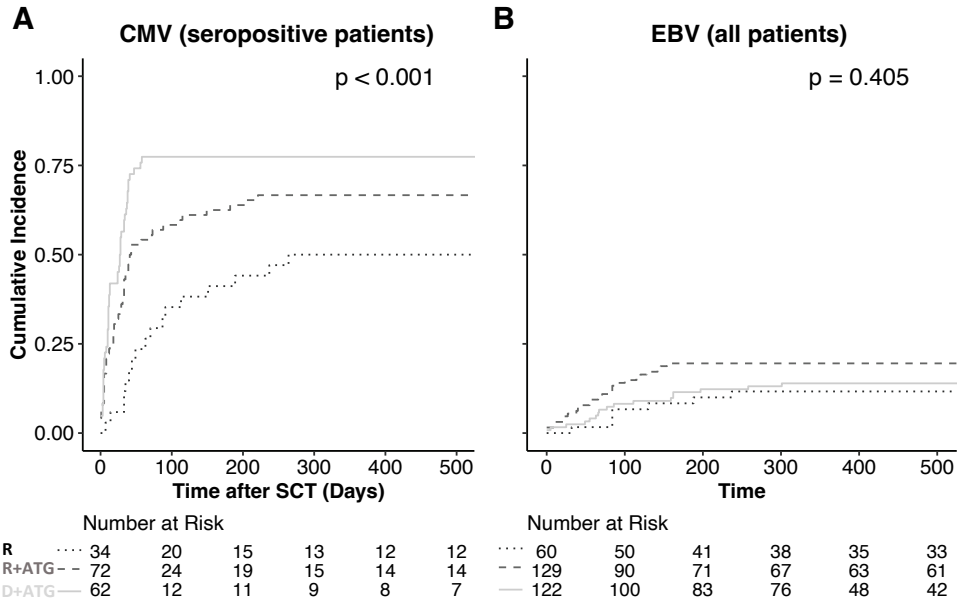
	100 days aGvHD grade II-IV % (95% CI)	2 year aGvHD grade II-IV % (95% CI)	100 days aGvHD grade III-IV % (95%)	2 year grade aGvHD grade III-IV % (95% CI)
NMA-noATG-MRD	25 (15 – 37)	33 (22 – 45)	7 (2 – 15)	13 (6 – 22)
NMA-ATG-MUD	38 (30 – 46)	40 (32 – 49)	15 (9 – 21)	16 (10 – 23)
MA-depl+ATG-MUD	16 (10 – 24)	20 (14 – 28)	5 (2 – 10)	7 (3 – 12)



	2 year limited cGvHD % (95% CI)	2 year extensive cGvHD % (95% CI)
NMA-noATG-MRD	13 (6 – 23)	23 (13 – 35)
NMA-ATG-MUD	15 (9 – 21)	10 (6 – 16)
MA-depl+ATG-MUD	16 (9 – 23)	2 (0 – 5)

Supplementary Figure S2. Cumulative incidence of aGvHD and cGvHD by *ex vivo* αβTCR/CD19 depletion and MA conditioning in MUD vs full graft and NMA conditioning with/without ATG in MUD and MRD

The CI of GvHD is defined as time to onset of GvHD, with relapse and death as competing events. CI of aGVHD grade II-IV (A) and grade III-IV (B) with 100 days and 2-year CI reported in table. CI of limited cGvHD (C) and extensive cGVHD (D) with 2-year CI reported. Cohort NMA-no ATG-MRD – reduced intensity conditioning, no ex vivo depletion, no ATG, matched related donor; cohort NMA-ATG-MUD – reduced intensity conditioning, no ex vivo depletion, with ATG, matched unrelated donor; cohort MA-depletion+ATG-MUD – myeloablative conditioning, ex vivo αβTCR+CD19 depletion, with ATG, matched unrelated donors. P-values shown calculated using Fine and Grey's test. Pairwise comparisons aGVHD II-IV MA depl+ATG MUD vs NMA no ATG MRD p = 0.6, MA depl+ATG MUD vs NMA ATG MUD p = 0.014; extensive cGVHD MA depl+ATG MUD vs NMA no ATG MRD p <0.001, MA depl+ATG MUD vs NMA ATG MUD p = 0.008

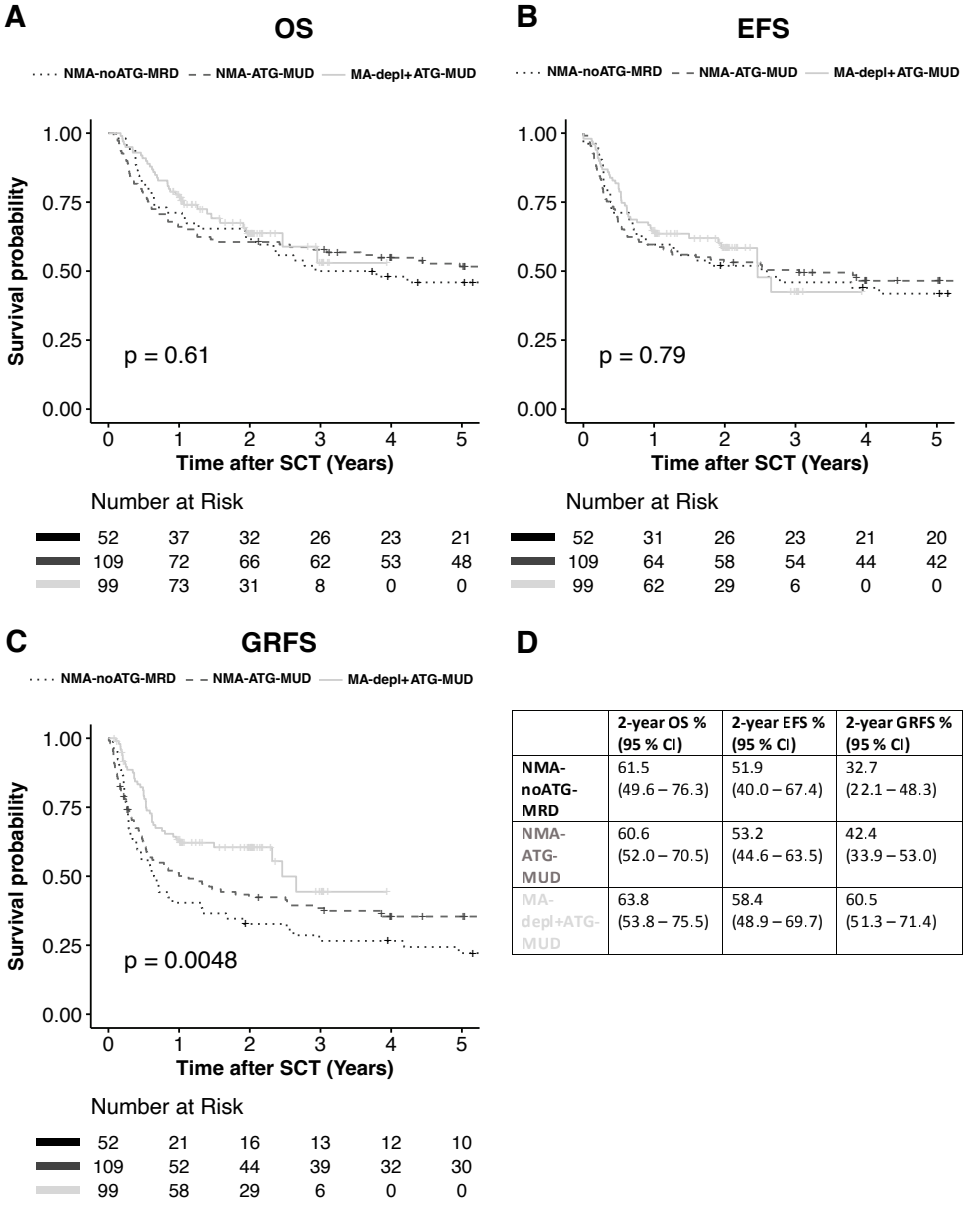


	100 days % CMV (95% CI)	100 days % CMV (95% CI)
R	35 (20 – 51)	50 (32 – 66)
R+ATG	58 (46 – 69)	67 (54 – 76)
D+ATG	77 (65 – 86)	77 (65 – 86)

	100 days % EBV (95% CI)	1 year % EBV (95% CI)
R	7 (2 – 15)	12 (5 – 21)
R+ATG	15 (9 – 22)	20 (13 – 27)
D+ATG	8 (4 – 14)	14 (9 – 21)

Supplementary Figure S3. Cumulative incidence of cytomegalovirus (CMV) in CMV seropositive patients and Epstein-Barr virus (EBV) in all patients

Cumulative incidence of CMV and EBV reactivations are calculated with relapse and death as competing events. CI of CMV (A) and EBV (B) with 100 days and 1-year CI reported in table. Patients with missing data for CMV reactivation (n = 46) or EBV reactivation (n = 37) were excluded. Cohort R – no ex vivo depletion, no ATG; cohort R+ATG – no ex vivo depletion, with ATG; cohort D+ATG – ex vivo αβTCR/CD19 depletion. P-values shown calculated using Fine and Grey's test. Pairwise comparisons CMV D+ATG vs R p <0.001; D+ATG vs R+ATG p = 0.045; R vs R+ATG p = 0.022

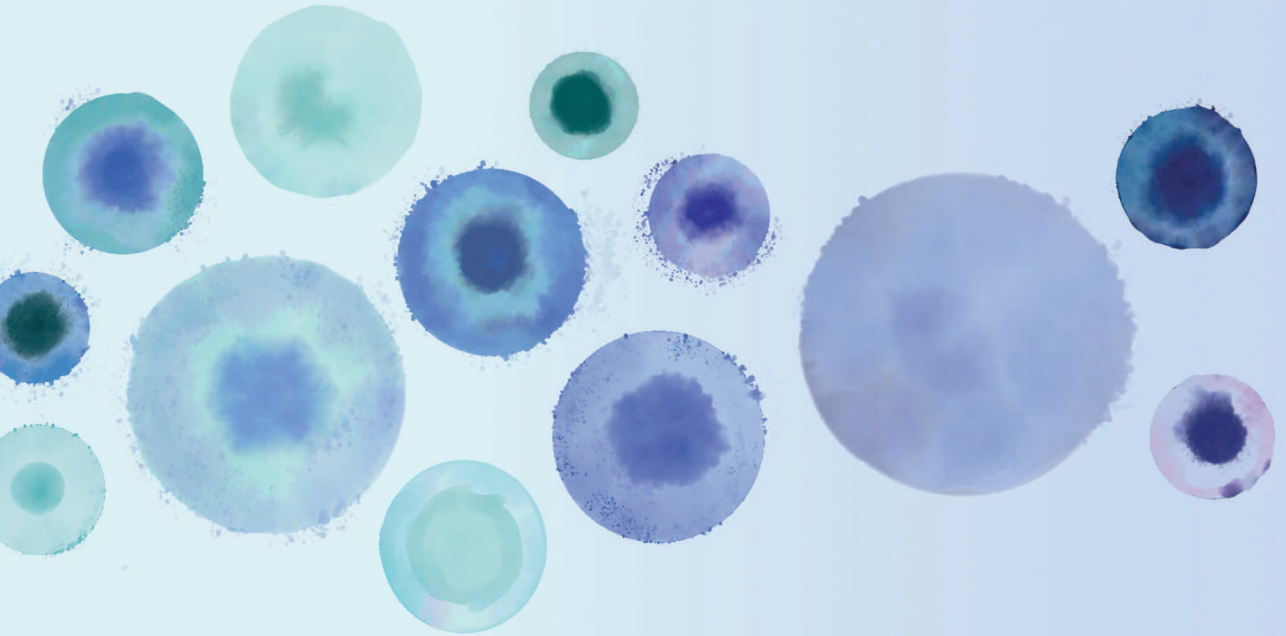


D

	2-year OS % (95 % CI)	2-year EFS % (95 % CI)	2-year GRFS % (95 % CI)
NMA-noATG-MRD	61.5 (49.6 – 76.3)	51.9 (40.0 – 67.4)	32.7 (22.1 – 48.3)
NMA-ATG-MUD	60.6 (52.0 – 70.5)	53.2 (44.6 – 63.5)	42.4 (33.9 – 53.0)
MA-depl+ATG-MUD	63.8 (53.8 – 75.5)	58.4 (48.9 – 69.7)	60.5 (51.3 – 71.4)

Supplementary Figure S4. OS, EFS and GRFS by *ex vivo* αβTCR/CD19 depletion and MA conditioning in MUD vs full graft with NMA conditioning with/without ATG in MUD and MRD

OS, EFS, and GRFS shown with a 5-year follow up. OS (A), EFS (B) and GRFS (C) were estimated by the Kaplan-Meier product. Log-rank test was used to determine p-values. Cohort NMA-no ATG-MRD – reduced intensity conditioning, no ex vivo depletion, no ATG, matched related donor; cohort NMA-ATG-MUD – reduced intensity conditioning, no ex vivo depletion, with ATG, matched unrelated donor; cohort MA-depletion+ATG-MUD – myeloablative conditioning, ex vivo αβTCR/CD19 depletion, with ATG, matched unrelated donors. P-values shown calculated using log-rank test. Pairwise comparisons GRFS MA depletion+ATG MUD vs NMA no ATG MRD p = 0.018; MA depletion+ATG MUD vs NMA ATG MUD p = 0.039.



3

Graft engineering: how long can you wait, how low can you go, and pandemic readiness

Klaartje Nijssen[1*], Kasper Westinga[2*], Anniek Stuut[3*], Anke Janssen[1,3], Anna van Rhenen[1], Lotte van der Wagen[1], Laura G M Daenen[1], Rimke Oostvogels[1], Moniek A de Witte[1,3#], Jürgen Kuball[1,3#+]

1 Department of Hematology, University Medical Center Utrecht, The Netherlands
2 Cell Therapy Facility, University Medical Center Utrecht, The Netherlands
3 Center for Translation Immunology
* These authors contributed equally to this work
# MdW, JK shared senior authors
+ Corresponding author

Bone Marrow Transplant 2023; 58(7): 820-822

Key points:

- Within the context of αβT cell depletion $1.7x10^6$ $CD34^+$ cells /kg infused within 68 hours are sufficient for engraftment

- Pandemic readiness of engineered grafts: Cryopreservation is feasible and does neither harm engraftment nor long-term overall survival.

Ex vivo graft engineering by means of αβT cell depletion is a promising platform to perform an allogeneic stem cell transplantation (allo-SCT), with low incidences of acute and chronic graft versus host disease (GVHD), for matched, mismatched,[1,2] and haploidentical donors[3,4]. Translation towards broader clinical implementation is facing graft-related variables with unknown impact. Firstly, additional laboratory procedures to perform graft engineering prolong the time from donation to infusion of the graft. Little information is available on how long grafts can be handled until infusion, or on how many $CD34^+$ cells must be harvested from a donor to attain a sufficient allograft resulting in profound engraftment. Graft engineering usually requires higher cell numbers, as the engineering process results in partial loss of cells. Finally, the option to cryopreserve an engineered graft remains essential during the time of an global pandemic[5], and more information is needed on whether the freezing procedure of an engineered allograft compromises outcome. Within this context we analyzed the questions "how long you can wait" until infusion, "how low can you go" with $CD34^+$ cell numbers, and whether cryopreservation puts patients at risk for primary graft failure.

All adults who received an αβT cell depleted allo-SCT product between 2013 and 2021 (n= 237) and have provided written informed consent in accordance with the JACIE guidelines and approved by the local ethical committee (METC nr 21-322) at the University Medical Center Utrecht (UMCU) were included in this retrospective analysis (baseline characteristics**, Supplementary Table S1**). Clinical data was reported to and extracted from the EBMT registry. All patients received a uniform myeloablative conditioning regimen[1]. αβT cell reduction was performed as previously reported[1]. In 2018, CD19 depletion was added to the graft engineering protocol[6]. Cryopreservation was performed in 24 patients before (n=3) or during (n=21) the COVID-19 pandemic, in line with EBMT and donor center guidelines[7]. Neutrophil recovery was defined as the first of 3 consecutive days with an absolute neutrophil count (ANC) greater than $0.5x10^9$/L. Platelet recovery was defined as a platelet count greater than $50x10^9$/L, without platelet transfusion in the preceding 7 days. Primary graft failure was defined as cytopenia and marrow hypoplasia at day 28. Secondary graft failure was characterized by loss of donor cells after initial engraftment and recurrent neutropenia and marrow hypoplasia. Poor graft function is defined as severe cytopenia of at least two cell lines in the presence of a hypoplastic bone marrow with full donor chimerism.

Graft composition of engineered products prior to infusion was analyzed by flow cytometry as part of their quality control. For fresh grafts, the median cell numbers were 5.8 x 10^6 $CD34^+$cells/kg (range 1.7-11.1), whereas the CD34+ cell number for frozen grafts, after thawing, was somewhat smaller (median $4.6x10^6$ $CD34^+$ cells/kg (range 2.6-11.3) (p=0.009). This is explained by a lower recovery of $CD34^+$ cells (**Supplementary table S2**). Consistent with this finding, the median number of infused $CD3^+$ T cells was also higher in fresh grafts as compared to frozen grafts after thawing; $5.9x10^6$ T cells (range 0.5-48.9)

vs 4.7x10^6 (range 0.6-13.3) (p=0.057) (**Supplementary table S2**). The median time to neutrophil recovery was 14 days in the fresh cohort (range 4-26), and 15 days in the frozen cohort (range 10- 29) (p=0.015). For platelets, the median time to recovery was also 14 days in the fresh cohort (range 9 - 440) and 15 days in the frozen cohort (range 11-110) (p=0.2) (**Supplementary table S2; Figure S1 A&B**). This is in line with a recent report for T cell replete grafts that freezing can impact platelet recovery[8].

Dutch guidelines advise for a maximum of 48 hours from apheresis to the time of infusion. For 60 of the 237 products (25%) out-of-spec (OOS) procedures were initiated, as they exceeded this recommended time frame. 85% (n=51) of all OOS were observed in the fresh cohort (**Supplementary table S3**). To assess the impact of time from apheresis to either infusion ('fresh cohort'), or time to cryopreservation ('frozen cohort') on primary engraftment, we compared outcomes in patients who received an allograft infused/cryopreserved within 48 hours after apheresis ('short') to outcomes of patients who received the allograft after 48 hours ('long'). Both for 'fresh' and 'frozen' grafts, we found no impact of time from apheresis to infusion on neutrophil or platelet engraftment (**Supplementary table S3; Figure S1A-B**). In addition, we observed no impact of prolonged time to infusion nor cryopreservation on the overall low incidence (3%) of graft failure or poor graft function (**Supplementary table S3**).

Graft engineering, as well as cryopreservation, can result in a partial loss of CD34$^+$cells. This anticipated loss is usually compensated by harvesting more stem cells from a donor. We ordered grafts of 10x10^{6}CD34$^+$cells/kg. 12% of the donors in our cohort underwent an additional day of collection (**Supplementary table S2**). Grafts of 7.8 x10^{6}CD34$^+$cells/kg (range 2.4-18.0) were received after collection. Median recovery of CD34$^+$cells after the completion of the depletion +/- cryopreservation procedure was 78% (fresh cohort) and 65% (frozen cohort) (**Supplementary table S2**). Within the EBMT, allografts of more than 4x10^6/kg CD34$^+$cells are recommended. We therefore compared outcomes of grafts with cell numbers lower than the recommended 4x10^6 CD34$^+$ cells/kg to allografts > 4x10^6 CD34$^+$ cells/kg. Here we show that for fresh, as well as for frozen allografts, infused CD34$^+$ cell numbers did not correlate with neutrophil engraftment (**Supplementary table S3, Supplementary figure S1C**). We did observe a significantly longer time to platelet engraftment in the recipients of smaller allograft in the fresh cohort (16 versus 14 days, p = 0.007) implying that lower CD34$^+$ cell number mainly affected thrombocyte recovery (**Supplementary table S3**). 7 cases of either graft failure or poor graft function were observed, all in recipients of fresh allografts of > 4x10^6/kg CD34$^+$ cells/kg (**Supplementary table S3**).

Finally, we analyzed long term outcome of patients receiving fresh versus frozen products, with different time to infusion and lower and higher cell numbers. We could not observe difference in overall survival when comparing outcome of patients receiving $CD34^+$ cell numbers below $4x10^6$ /kg (n=32) versus above (n = 205) (**Figure 1A**), neither between cohorts which had different times to infusion (<48h n= 177, >48 h n=60) (**Figure 1B**) nor between patients receiving a fresh (n = 213) or frozen allograft (n =24) (**Figure 1C**). Furthermore, there was no significant impact of any of these variables on acute or chronic GvHD (**Supplementary table S4**).

In summary, we show for the first time in an αβT cell depletion transplantation platform that infusing stem cell products until 68 hours after apheresis is feasible and does not impact long-term survival. Our data also challenge the currently recommended lowest number of $4x10^6CD34^+$cells/kg for allografts[9]. In line with guidelines for cryopreserved autologous stem cell grafts which advice $2x10^6CD34^+$cells/kg[9], we advocate that $2x10^6CD34^+$cells/kg are sufficient for both fresh and frozen allografts, which could prevent the need for an extra day of apheresis. Conflicting data have been reported on long-term outcomes with frozen products[10-12]. Long-term clinical outcomes after allo-SCT with a frozen product as a consequence of the COVID pandemic are only slowly emerging. Within this context our data add important information to the field by showing in a real-world data cohort with a reasonable follow up that cryopreservation of engineered grafts is a valid option.

DATA AVAILABILITY

The data that support the findings of this study are available from EBMT the registry, but restrictions apply to the availability of these data, which were used under license for the current study, and so are not publicly available. Data are however available from the authors upon reasonable request and with permission of the corresponding author.

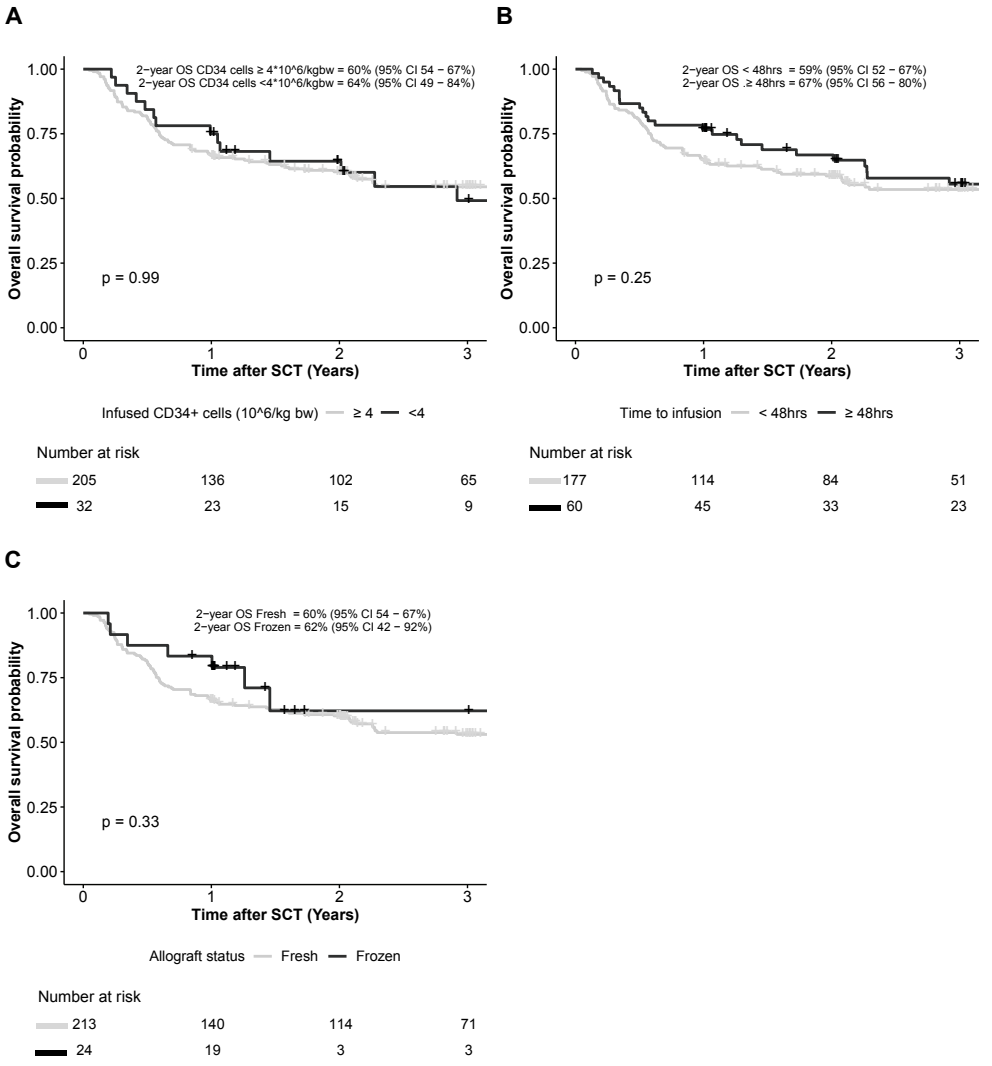


Figure 1: Impact of cryopreservation, time to infusion and cell numbers on overall survival.
Comparison of overall survival in (A) cohorts with cell number higher than (grey) or below (black) 4x10^6/kgCD34$^+$cells, (B) cohorts with time to infusion below (grey) and above (black) 48hrs, and (C) fresh (grey) versus frozen (black) cohort. Logrank test was used to assess differences between the groups. Bw = bodyweight

REFERENCES

1. de Witte MA, Janssen A, Nijssen K, et al. alphabeta T-cell graft depletion for allogeneic HSCT in adults with hematological malignancies. *Blood Adv*. 2021;5(1):240-249.
2. Laberko A, Sultanova E, Gutovskaya E, et al. Mismatched related vs matched unrelated donors in TCRalphabeta/CD19-depleted HSCT for primary immunodeficiencies. *Blood*. 2019;134(20):1755-1763.
3. Locatelli F, Merli P, Pagliara D, et al. Outcome of children with acute leukemia given HLA-haploidentical HSCT after alphabeta T-cell and B-cell depletion. *Blood*. 2017;130(5):677-685.
4. de Witte MAM, L.E.; Hoogeboom, J.D.; Chabannon; C., Malard; F. Ruggeri, A., Kuball, J. Activity of ex vivo graft and DLI Engineering within the last decade increases, a survey from the EBMT Cellular Therapy & Immunobiology Working Party *Bone Marrow Transplant*. 2023;in print
5. Dholaria B, Malki MMA, Artz A, Savani BN. Securing the graft during pandemic: are we ready for cryopreservation for all? *Biol Blood Marrow Transplant*. 2020;26(7):e145-e146.
6. Bethge WA, Eyrich M, Mielke S, et al. Results of a multicenter phase I/II trial of TCRalphabeta and CD19-depleted haploidentical hematopoietic stem cell transplantation for adult and pediatric patients. *Bone Marrow Transplant*. 2022;57(3):423-430.
7. Ljungman P, Mikulska M, de la Camara R, et al. The challenge of COVID-19 and hematopoietic cell transplantation; EBMT recommendations for management of hematopoietic cell transplant recipients, their donors, and patients undergoing CAR T-cell therapy. *Bone Marrow Transplant*. 2020;55(11):2071-2076.
8. Medd P, Nagra S, Hollyman D, Craddock C, Malladi R. Cryopreservation of allogeneic PBSC from related and unrelated donors is associated with delayed platelet engraftment but has no impact on survival. *Bone Marrow Transplant*. 2013;48(2):243-248.
9. Carreras E, Dufour C, Mohty M, Kroeger N. The EBMT Handbook. Hematopoietic Stem Cell Transplantation and Cellular Therapies; 2019.
10. Jacob RP, Flynn J, Devlin SM, et al. Universal Engraftment after Allogeneic Hematopoietic Cell Transplantation Using Cryopreserved CD34-Selected Grafts. *Transplant Cell Ther*. 2021.
11. Hsu JW, Farhadfar N, Murthy H, et al. The Effect of Donor Graft Cryopreservation on Allogeneic Hematopoietic Cell Transplantation Outcomes: A Center for International Blood and Marrow Transplant Research Analysis. Implications during the COVID-19 Pandemic. *Transplant Cell Ther*. 2021;27(6):507-516.
12. Hamadani M, Zhang MJ, Tang XY, et al. Graft Cryopreservation Does Not Impact Overall Survival after Allogeneic Hematopoietic Cell Transplantation Using Post-Transplantation Cyclophosphamide for Graft-versus-Host Disease Prophylaxis. *Biol Blood Marrow Transplant*. 2020;26(7):1312-1317.

SUPPLEMENTARY TABLES

Supplementary Table S1. Baseline characteristics of the cohort.

	Fresh, N = 213[1]	**Frozen**, N = 24[1]	**p-value**[2]
Patient Age	58.6 (19.2, 73.5)	51.9 (19.4, 69.4)	*0.3*
Median follow-up time (months)	24.2 (0.6, 87.3)	12.9 (2.3, 74.3)	*0.10*
Gender			*>0.9*
Female	79 (37%)	9 (38%)	
Male	134 (63%)	15 (62%)	
Diagnosis			*0.4*
Acute Leukemia (AML/ALL)	89 (42%)	12 (50%)	
Other malignancies	124 (58%)	12 (50%)	
Donor type			*0.3*
MRD	37 (17%)	7 (29%)	
MMRD	1 (0.5%)	0 (0%)	
MUD	136 (64%)	11 (46%)	
MMUD	39 (18%)	6 (25%)	

[1] *Median (Range); n (%)*

[2] *Wilcoxon rank sum test; Pearson's Chi-squared test; Fisher's exact test*

Other malignancies included lymphoma, myelodysplastic syndrome, myelofibrosis and multiple myeloma. Acute myeloid leukemia (AML); acute lymphatic leukemia (ALL); matched related donor (MRD), mismatched related donor (MMRD), matched unrelated donor (MUD), mismatched unrelated donor (MMUD).

Supplementary table S2. Graft characteristics and engraftment.

	Fresh, N = 213[1]	**Frozen**, N = 24[1]	**p-value**[2]
Second day of leukapheresis performed	25 (11.7%)	4 (16.7%)	*0.5*
Graft engineering			*<0.001*
αβ TCR depletion	144 (67.6%)	2 (9.1%)	
αβ TCR and CD19 depletion	69 (33.3%)	22 (91.7%)	
Time between apheresis and cryopreservation or infusion (hours)	46.1 (25.2, 68.8)	30.4 (24.5, 54.6)	*0.021*
Time between cryopreservation and infusion (days)		13.7 (2.8, 118.8)	
CD34$^+$ cells / kg (x 10^6) at collection	7.8 (2.4, 18.0)	7.3 (4.3, 14.3)	*0.8*
CD34$^+$ cells / kg (x 10^6) after depletion	5.8 (1.7, 16.8)	5.6 (3.1, 12.5)	*0.8*
CD34$^+$ cells / kg (x 10^6) in final product	5.8 (1.7, 11.1)	4.6 (2.6, 11.3)	*0.009*
CD34$^+$ recovery after depletion +/- cryopreservation (%)^	77.9 (30.7, 123.3)	65.2 (48.0, 92.6)	*<0.001*
CD3$^+$ T-cells / kg (x 10^6) before cryopreservation		6.2 (1.3, 16.0)	
CD3$^+$ T-cells / kg (x 10^6) in final product	5.9 (0.5, 48.9)	4.7 (0.6, 13.3)	*0.057*
Neutrophil recovery (>0.5 x 10^9 /L)			*0.2*
No	3 (1.4%)	0 (0%)	
Yes	210 (98.6%)	24 (100%)	
Platelet recovery (>50 x 10^9/L)			*0.2*
Never below	7 (3.3%)	2 (8.3%)	
No	10 (4.7%)	0 (0%)	
Yes	196 (92.0%)	22 (91.7%)	
Days to neutrophil recovery	14.0 (4.0, 26.0)	15.0 (10.0, 29.0)	*0.015*
Days to platelet recovery	14.0 (9.0, 440.0)	15.0 (11.0, 110.0)	*0.2*

[1]n (%); Median (Range) [2]Fisher's exact test; Pearson's Chi-squared test; Wilcoxon rank sum test

Patient characteristics, allograft characteristics and time to engraftment in freshly infused allografts and cryopreserved allografts.

^CD34$^+$ recovery was defined as viable CD34$^+$ cells after depletion with or without cryopreservation and was measured by flow cytometry with 7-AAD staining.

Supplementary table S3. Impact of time to infusion of grafts and CD34$^+$ cell number in grafts on engraftment for fresh and frozen grafts.

	Fresh grafts *Time to infusion*			**Frozen grafts** *Time to infusion*			**Fresh grafts** *Infused CD34+ cells/kg bw*			**Frozen grafts** *Infused CD34+ cells/kg bw*		
	Short (< 48 hrs) N = 162[1]	**Long (≥ 48 hrs)** N = 51[1]	**p-value**[2]	**Short (< 48 hrs)** N = 15[1]	**Long (≥ 48 hrs)** N = 9[1]	**p-value**[3]	**<4*10^6** N = 27[1]	**≥ 4*10^6** N = 186[1]	**p-value**[2]	**<4*10^6** N = 5[1]	**≥ 4*10^6** N = 19[1]	**p-value**[3]
Second day of leukapheresis performed	2 (1.2%)	23 (45%)	*<0.001*	1 (6.7%)	3 (33%)	*0.13*	12 (44%)	13 (7.0%)	*<0.001*	3 (60%)	1 (5.3%)	*0.018*
Graft engineering			*0.23*			*0.51*			*0.32*			*>0.99*
αβ TCR depletion	106 (65%)	38 (75%)		2 (13%)	0 (0%)		16 (59%)	128 (69%)		0 (0%)	2 (11%)	
αβ TCR and CD19 depletion	56 (35%)	13 (25%)		13 (87%)	9 (100%)		11 (41%)	58 (31%)		5 (100%)	17 (89%)	
Time between apheresis and cryopreservation or infusion (hours)	46 (25, 48)	52 (48, 69)	*<0.001*	28 (24, 44)	52 (48, 55)	*<0.001*	50 (30, 66)	46 (25, 69)	*0.015*	52 (27, 55)	29 (24, 53)	*0.036*
Time to neutrophil recovery (days)	14 (4, 26)	14 (8, 25)	*0.71*	15 (12, 24)	15 (10, 29)	*0.38*	14 (8, 25)	14 (4, 26)	0.83	15 (12, 29)	15 (10, 24)	*0.69*
Time to platelet recovery (days)	14 (9, 440)	14 (10, 47)	*0.46*	16 (11, 87)	15 (11, 110)	*0.81*	16 (12, 47)	14 (9, 440)	*0.007*	16 (15, 110)	15 (11, 87)	*0.22*
Primary graft failure	2 (1.2%)	1 (2.0%)	*0.56*	0 (0%)	0 (0%)		0 (0%)	3 (1.6%)	*>0.99*	0 (0%)	0 (0%)	
Secondary graft failure	1 (0.6%)	0 (0%)	*>0.99*	0 (0%)	0 (0%)		0 (0%)	1 (0.5%)	*>0.99*	0 (0%)	0 (0%)	
CD34 boost due to poor graft function	2 (1.2%)	1 (2.0%)	*0.56*	0 (0%)	0 (0%)		0 (0%)	3 (1.6%)	*>0.99*	0 (0%)	0 (0%)	

[1]n (%); Median (Range) [2]Fisher's exact test; Pearson's Chi-squared test; Wilcoxon rank sum test [3]Fisher's exact test; Wilcoxon rank sum exact test; Wilcoxon rank sum test
Bw = bodyweight.

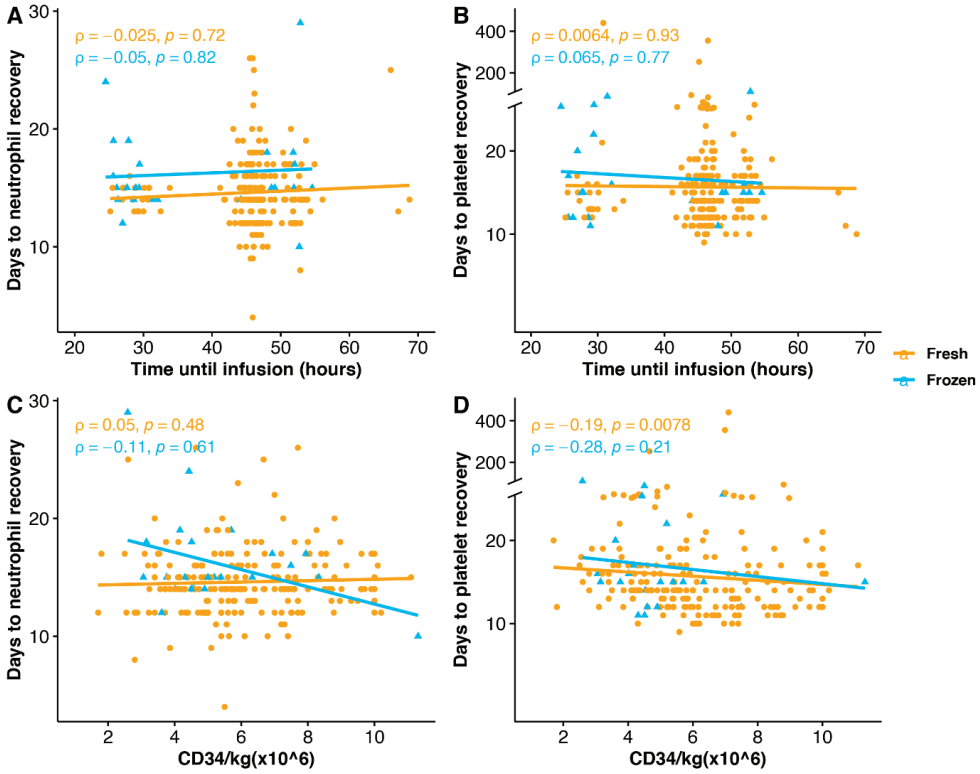
Supplementary table S4. Impact of CD34$^+$ cell numbers, time to infusion and cryopreservation of grafts on GvHD.

	<4*10^6 CD34+ cells/kg N = 32	≥4*10^6 CD34+ cells/kg N = 205	*p-value**	Time to infusion <48hrs N = 177	Time to infusion ≥ 48 hrs N = 60	*p-value**	Fresh grafts N = 213	Frozen grafts N = 24	*p-value**
aGvHD grade II-IV at 1 year^	21.9% (11.2, 42.6)	22.6% (17.5, 29.1)	*0.9*	24.4% (18.8, 31.7)	16.7% (9.4, 29.5)	*0.4*	22.6% (17.6, 29.1)	20.8% (9.4, 46.4)	*0.8*
aGvHD grade III-IV at 1 year^	9.4% (2.3, 23.0)	6.4% (3.6, 10.0)	*0.6*	7.4% (4.1, 12.0)	5.0% (1.3, 13.0)	*0.9*	6.6% (3.8, 10.0)	8.3% (1.4, 24)	*0.8*
Limited cGVHD at 2 years^	3.1% (0.22, 14.0)	14% (9.2, 19.0)	*0.1*	12% (7.8, 18.0)	12% (5.2, 22.0)	*0.7*	12.0% (8.0, 17.0)	13.0% (3.0, 29.0)	*0.8*
Extensive cGvHD at 2 years^	6.9% (1.1, 20.0)	4.5% (2.2, 8.1)	*>0.9*	3.5% (1.4, 7.1)	8.6% (3.1, 18)	*0.2*	4.3% (2.1, 7.7)	8.3% (1.4, 24.0)	*0.3*

*^ Cumulative incidence (95% Confidence Interval), *Gray's test*

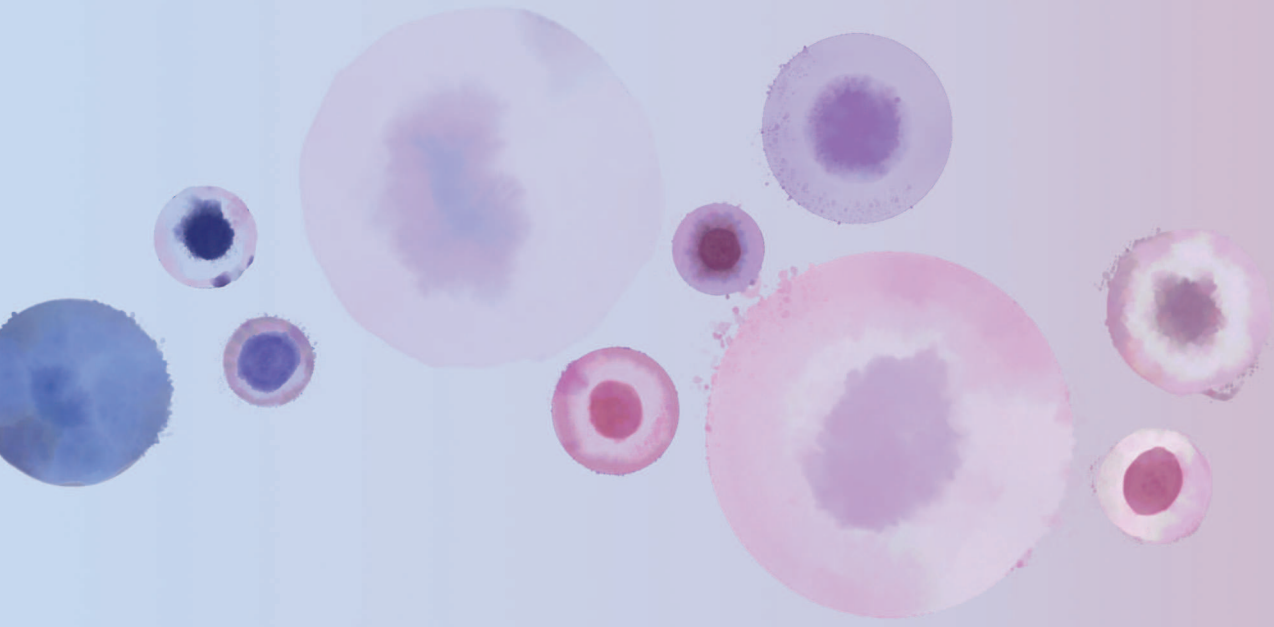
Acute graft versus host disease (aGvHD), chronic graft versus host disease (cGvHD)

SUPPLEMENTARY FIGURES



Supplementary figure S1: Impact of time until infusion and cell numbers on neutrophil and platelet engraftment with or without cryopreservation.

Correlation cryopreservation, number of CD34$^+$cells and time to infusion with neutrophil and platelet engraftment from fresh (circle) and frozen (triangle) products. Upper panels: time to neutrophil engraftment (A) and platelet engraftment (B) in cryopreserved allografts (blue) and fresh allografts (orange). Lower panels: Time to neutrophil engraftment (C) and platelet engraftment (D) based on infused number of CD34$^+$cells.



4

Peri-transplant ruxolitinib enhances survival in myelofibrosis patients undergoing αβTCR and CD19-depleted stem cell transplantation

Anniek Stuut[1*], Flores Weverling[1,2*], Anke Janssen[2], Frances Verheij[2], Iris Brinkman[2], Klaartje Nijssen[2], Pleun Schonewille[2], Christien Oudbier[2], Anna van Rhenen[2], Lotte van der Wagen[2], Laura Daenen[2], Reinier Raymakers[2], Kasper Westinga[3], Tim Hutten[4], Lisette van de Corput[4], Julia Drylewicz[1], Jurgen Kuball[1,2#], Moniek de Witte[1,2#]

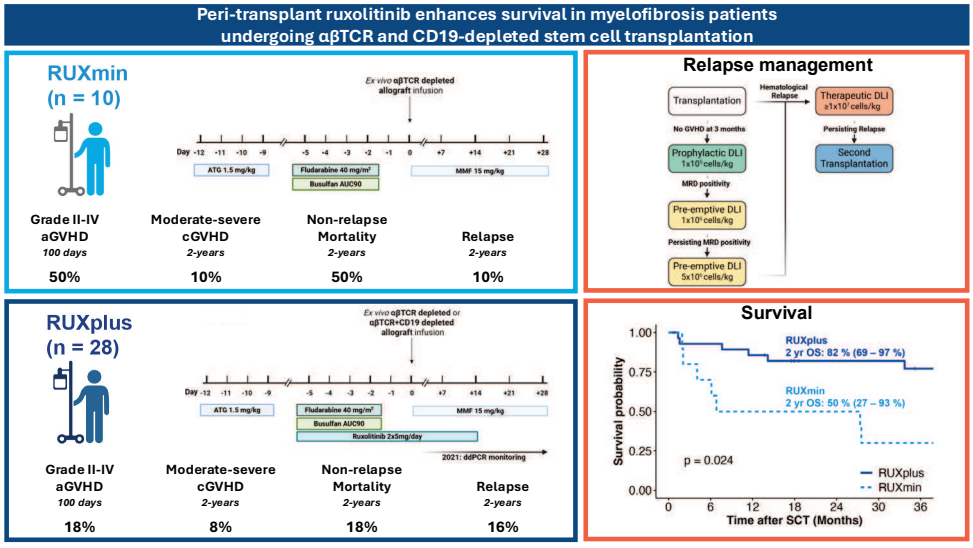
1. Center for Translational Immunology, University Medical Center Utrecht, Utrecht, The Netherlands
2. Department of Hematology, University Medical Center Utrecht, Utrecht, The Netherlands
3. Cell Therapy Facility, University Medical Center Utrecht, Utrecht, The Netherlands
4. Central Diagnostic Laboratory, University Medical Center Utrecht, Utrecht, The Netherlands

* Shared first authorship
\# Shared senior authorship

Revised version submitted

ABSTRACT

Allogeneic stem cell transplantation is the only curable therapy for myelofibrosis, but eligibility is complicated by advanced age and an increased risk of Graft-versus-Host Disease (GVHD). Although peri-transplant ruxolitinib and T cell depletion strategies have individually demonstrated potential in reducing GVHD, their combined use in myelofibrosis has not been studied. Moreover, the role of measurable residual disease (MRD)-guided donor lymphocyte infusions (DLI) in this setting remains undefined. To address this gap, we retrospectively analyzed 38 myelofibrosis patients (median age 65 years, range 33–72) who underwent myeloablative conditioning with ex vivo αβT cell-depleted grafts. Ten patients did not receive peri-transplant ruxolitinib, while 28 did, following a protocol change. Patients receiving peri-transplant ruxolitinib showed enhanced immune reconstitution. The incidence of acute GVHD grade III–IV at 100 days was lower with ruxolitinib (30% vs 4%, p = 0.065), while moderate–severe chronic GVHD was comparable (10 vs 8%). Two-year non-relapse mortality was lower in the ruxolitinib cohort (50% vs. 18%, p = 0.025), translating into improved overall survival (50% vs. 82%, p = 0.024). Hematological relapse rates were comparable (10% vs 16%). Among 13 patients with hematological or molecular relapse in the ruxolitinib cohort, six were successfully treated with DLI, while three patients underwent a second transplantation. In conclusion, myeloablative conditioning with αβTCR/CD19-depleted transplantation and peri-transplant ruxolitinib is a feasible strategy in patients with myelofibrosis. Our findings show a promising two-year overall survival and chronic GHVD rates and support further evaluation of MRD-guided DLI for relapse management.



INTRODUCTION

Myelofibrosis is a chronic myeloproliferative neoplasm marked by progressive bone marrow fibrosis, impaired blood cell production, and a significant symptom burden [1,2]. These symptoms commonly include cytopenia, splenomegaly, and constitutional symptoms such as fatigue, weight loss, and night sweats. Myelofibrosis is typically driven by somatic mutations in JAK2, CALR, or MPL genes, which lead to clonal expansion and chronic inflammation[3]. The disease may present as a primary disorder or evolve from other myeloproliferative neoplasms, including polycythemia vera and essential thrombocythemia. It primarily affects older adults and is associated with reduced quality of life and an increased risk of leukaemic transformation[4]. Given its progressive nature and high symptom burden, effective treatment of myelofibrosis is essential.

The only curative treatment option for myelofibrosis is allogeneic hematopoietic stem cell transplantation, but the outcomes of this treatment are influenced by both patient-related and treatment-related factors[5]. The average age and frailty of transplant patients are increasing[6,7], resulting in a shift towards reduced intensity conditioning regimens, as myeloablative conditioning regimens worsen non-relapse mortality in patients over 50 [5,6]. Nevertheless, significant challenges remain for myelofibrosis patients, including a high risk of non-relapse mortality and graft-versus-host disease (GVHD).

JAK inhibitors, such as ruxolitinib, can significantly improve symptoms and reduce splenomegaly in patients with high-risk myelofibrosis[8,9], but cannot cure myelofibrosis nor prevent leukemic transformation. In addition, ruxolitinib has also shown efficacy in treating steroid-resistant acute and chronic GVHD[10]. Ruxolitinib has been shown to reduce pro-inflammatory cytokines in both myelofibrosis and GVHD[11,12], with a reduction of regulatory T cells and pro-inflammatory T-helper cells type 1 and type 17[12]. Given these dual effects, ruxolitinib has been studied as a strategy to reduce GVHD incidence in patients with myelofibrosis after transplantation[13-16].

In parallel with treatments like ruxolitinib, researchers have also investigated graft-engineering approaches such as *ex vivo* T-cell depletion and $CD34^+$ selection to lower the risk of GVHD. We recently reported that removing αβT cells from the allograft significantly reduces GVHD incidence in patients with hematological malignancies, including myelofibrosis[17]. In agreement with this, another study showed that post-transplantation cyclophosphamide-mediated depletion of T cells reduces GVHD incidence in myelofibrosis patients[18]. However, the outcomes of combining T cell depletion and peri-transplantation ruxolitinib have not been investigated.

In this retrospective analysis, we evaluated outcomes of myelofibrosis patients after transplantation with a busulfan-based myeloablative conditioning and an αβTCR

+/- CD19-depleted allograft. This transplantation method resulted in favorable overall survival when combined with peri-transplantation ruxolitinib.

MATERIALS AND METHODS

Study Design and Data Sources

This retrospective cohort study included patients with myelofibrosis who underwent a hematopoietic stem cell transplantation with an αβT cell +/- CD19-depleted graft composition. Data were collected from electronic health records (HiX) and the European Society for Blood and Marrow Transplantation (EBMT) database. All patients provided informed consent for the use of their data for scientific purposes before transplantation. The informed consent was approved by the local ethical committee (METC nr 21-322) at the University Medical Centre Utrecht (UMCU) in accordance with the Declaration of Helsinki.

Patient Eligibility Criteria

Patients were eligible for inclusion if they underwent allogeneic stem cell transplantation for the treatment of myelofibrosis between July 2015 and October 2024. Patients who received melphalan-based conditioning were excluded. Eligibility for stem cell transplantation was based on local criteria, including Dynamic International Prognostic Score System (DIPSS) intermediate-1 with a high burden of constitutional symptoms, DIPSS intermediate-2 or high risk, or Mutation-Enhanced International Prognostic Score System (MIPSS70/MIPSS70+) high or very high risk[19]. Clinical-molecular myelofibrosis transplant scoring system (MTSS) was assessed before transplantation[20].

Donor selection and graft processing

Peripheral blood stem cells were collected from related or unrelated donors with a 9/10 or 10/10 human leukocyte antigen (HLA) match, following institutional donor selection guidelines. Grafts were processed by ex vivo depletion of αβT cell receptor (TCR) +/- $CD19^+$ B cells. CD19 depletion was added after a protocol change in 2021. *Ex vivo* depletion was performed using the automated CliniMACS® device (Miltenyi Biotec, Bergisch Gladbach, Germany). This procedure utilized magnetic microbeads conjugated with anti-αβTCR and, when applicable, anti-CD19 antibodies, as previously described[21,22].

Conditioning regimen

All patients received myeloablative conditioning consisting of antithymocyte globulin (ATG) 1.5 mg/kg IV on days −12 to−9, fludarabine 40 mg/m^2 IV on days −5 to−2, and busulfan (Busilvex®) AUC90 IV on days −5 to−2. For GVHD prophylaxis, patients received mycophenolate mofetil (Cellcept®) until day +28 post-transplantation. Patients who received a transplant before 2018 did not receive peri-transplant ruxolitinib (RUXmin),

while patients who received a transplant after 2018 received ruxolitinib at a dose of 5mg twice daily from day -5 to +14 (RUXplus; **Supplementary Figure S1**).

Clinical definitions

All time-to-event endpoints were measured from the date of stem cell infusion. Neutrophil recovery was defined as the first of three consecutive days with an absolute neutrophil count (ANC) greater than $0.5x10^9$/L. Platelet recovery was defined as a platelet count greater than $20x10^9$/L, without the need for platelet transfusions in the preceding seven days. Primary graft failure was defined as the absence of neutrophil recovery in the context of adequate graft infusion and in the absence of progressive disease or a marrow-compromising infection. Secondary graft failure was defined as the loss of donor-derived hematopoiesis following initial engraftment, also in the absence of disease progression or infection.

Acute GVHD (aGVHD) was graded using the Glucksberg classification, and chronic GVHD (cGVHD) was assessed according to the NIH consensus criteria for diagnosis and staging [23,24]. Hematological relapse was defined as the recurrence of clinical and/or hematologic features of myelofibrosis, such as cytopenia, splenomegaly, or increased bone marrow blasts.

Overall survival (OS) was defined as the time from transplantation to death from any cause. Event-free survival (EFS) was defined as the time from transplantation to the first occurrence of relapse, graft failure, or death. GVHD-free and relapse-free survival (GRFS) was defined as the time from transplantation to the first occurrence of relapse, graft failure, grade III–IV aGVHD or moderate-to-severe cGVHD. For all survival endpoints, patients were censored at their last day of follow-up if none of the defined events had occurred.

Molecular monitoring

In addition to clinical endpoints, minimal residual disease (MRD) was assessed through molecular monitoring. Digital droplet PCR (ddPCR) was introduced in 2021 for the detection of disease-defining mutations[25]. MRD positivity was defined as the reappearance of a previously identified molecular clone at levels exceeding 0.1% or as persistence at lower levels[26]. Donor lymphocyte infusion (DLI) was given starting 3 months post-transplant as follows: prophylactic at 3 months in the absence of GVHD, irrespective of MRD (1×10^5 $CD3^+$ cells/kg); pre-emptive for MRD positivity persisting/relapsing beyond this time point or at the physician's discretion (1×10^6-1×10^7 $CD3^+$ cells/kg); and therapeutic for hematologic relapse (1×10^7-1x10^8 $CD3^+$ cells/kg). Patients who progressed to hematologic relapse were further assessed for eligibility for a second allogeneic stem cell transplantation if therapeutic DLIs were ineffective.

Table 1: Baseline Characteristics

	RUXmin n = 10	RUXplus n = 28
Age at SCT, median (range)	62 (33 – 68)	65 (43 – 72)
Sex, n (%)		
Female	4 (40 %)	11 (39 %)
Prior JAK-inhibitor treatment, n (%)		
Yes	8 (80 %)	25 (89 %)
MPN subclass, n (%)		
Primary myelofibrosis	8 (80 %)	9 (32 %)
Post ET myelofibrosis	2 (20 %)	8 (29 %)
Post PV myelofibrosis	-	11 (39 %)
Donortype, n (%)		
10/10 MRD	1 (10 %)	5 (18 %)
9/10 MUD	-	3 (11 %)
10/10 MUD	9 (90 %)	20 (71 %)
Spleen size at SCT in cm[1], median (range)	2,5 (0 – 21)	2 (0 – 16)
≥ 5 cm[1], n (%)	4 (40 %)	11 (39 %)
≥ 15 cm[1], n (%)	2 (20 %)	2 (7 %)
DIPSS, n (%)		
Low	-	-
Intermediate-1	-	3 (11 %)
Intermediate-2	4 (40 %)	14 (50 %)
High	6 (60 %)	11 (39 %)
MIPSS 70 v2, n (%)		
Low	1 (10 %)	3 (11 %)
Intermediate	3 (30 %)	1 (4 %)
High	6 (60 %)	16 (57 %)
Very high	-	8 (29 %)
MTSS, n (%)		
Low	1 (10 %)	7 (25 %)
Intermediate	4 (40 %)	8 (29 %)
High	4 (40 %)	9 (32 %)
Very high	1 (10 %)	4 (14 %)
Conditioning scheme, n (%)		
ATG/Bu/Flu | αβTCR depleted	10 (100 %)	4 (14 %)
ATG/Bu/Flu | αβTCR & CD19 depleted	-	24 (86 %)
CD34x10^6/kg, median (range)	7,1 (3,2 – 9,5)	5,2 (3,1 – 9,2)
Median follow up (range); in months	17,1(1,9 – 110,5)	39,3(1,3– 85,8)
Year of SCT, n (%)		
2015 - 2017	10 (100 %)	-
2018 – 2023	-	28 (100 %)

[1] *In cm below the costal margin*

Statistical analysis

Data was analyzed using RStudio (R version 4.4.0). OS, EFS, and GRFS were calculated by Kaplan-Meier estimates and reported as percentages with 95% confidence intervals. Differences in survival were assessed using the log-rank test. Analyses were performed using the R package survival (version 3.8-3)[27]. Cumulative incidence functions were calculated to estimate the probability of acute or chronic GVHD, with death or relapse as competing risks. Additionally, cumulative incidence was also calculated for relapse (with death as competing risk), MRD positivity, and non-relapse mortality (NRM; with relapse as competing risk). Competing risk estimates were computed using the cuminc() function from the tidycmprsk package (version 1.1.0)[28]. Differences between cohorts were evaluated using Fine and Gray's subdistribution hazard model. Differences in cell counts were calculated using the Mann-Whitney U test. P-values <0.05 were considered statistically significant.

RESULTS

Patient Characteristics

Our analysis included 38 patients. Ten patients received an αβTCR-depleted transplant without ruxolitinib post-transplantation (RUXmin cohort), and 28 patients received an αβTCR +/- CD19-depleted transplant with two weeks of ruxolitinib (5 mg twice daily) post-transplantation (RUXplus cohort) (**Table 1**). In the RUXplus cohort, 86% of patients received an αβTCR- and CD19-depleted transplant. Median age was above 60 years for both cohorts. Over 80% of patients in both cohorts received prior JAK-inhibitor treatment.

Engraftment

To evaluate the impact of adding peri-transplantation ruxolitinib on engraftment, we compared the median time to engraftment of neutrophils and platelets, and the incidence of graft failure in both cohorts. Median time to neutrophil engraftment was 17 days in both the RUXmin and the RUXplus cohorts ($p = 0.87$) (**Table 2**). The median time to platelet engraftment was 34 days in the RUXmin cohort and 20 days in the RUXplus cohort ($p = 0.081$). There were two cases of graft failure: one case of primary graft failure in the RUXmin cohort and one case of secondary graft failure in the RUXplus cohort. Thus, we observed no significant differences in the incidence of graft failure.

Table 2: Overview of engraftment after transplantation

	RUXmin n = 10	RUXplus n = 28	p-value
Median engraftment, in days (IQR)			
Neutrophils	17 (14 – 22)	17 (12 – 25)	0.87
Platelets	34 (15 – 1114)	20 (14 – 57)	0.081
Graft failure, n (%)			0.46
Primary graft failure	1 (10 %)	0 (0 %)	
Secondary graft failure	0 (0 %)	1 (4 %)	

Immune Reconstitution

Since ruxolitinib has been shown to influence T cell numbers in myelofibrosis patients [12,14,29], we compared immune reconstitution between the RUXmin and RUXplus cohorts (**Figure 1**). We observed higher $CD8^+$ αβT cell counts in the RUXplus cohort at both one month and one-year post-transplant (median 27 vs 16 cells/μL, p = 0.05; 204 vs 67 cells/μL, p = 0.02). Moreover, $CD4^+$ αβT cell counts were also increased in the RUXplus cohort one-year post-transplant (median 155 vs 58 cells/μL, p = 0.01). We did not observe any significant differences in γδT cell reconstitution. Regarding NK cells, we observed a trend toward increased counts in the RUXplus cohort beginning at three months, reaching statistical significance at six months post-transplant (median 175 vs 74 cells/μL, p = 0.03). One-year post-transplant, B cell numbers were significantly higher in the RUXplus cohort (median 193 vs 65 cells/μL, p = 0.05). Overall, these findings suggest that peri-transplant ruxolitinib is not associated with impaired T cell recovery following αbTCR-depleted transplantation.

Acute and chronic GVHD

αβTCR-depleted transplantation with peri-transplantation ruxolitinib resulted in low incidences of both aGVHD and cGVHD. aGVHD grade II-IV at 100 days post-transplantation was 50% in the RUXmin cohort and 18% in the RUXplus cohort (p = 0.2; **Figure 2A**). Incidence of aGVHD grade III-IV at 100 days post-transplantation was 30% in the RUXmin cohort and 4 % in the RUXplus cohort (p = 0.066; **Figure 2B**). The incidence of cGVHD was low in both cohorts. At two years post-transplantation, mild cGVHD occurred in 10% of patients in the RUXmin cohort and 14% in the RUXplus cohort (p = 0.3; **Figure 2C**), while moderate-to-severe cGVHD occurred in 10% and 8%, respectively (p = 0.6; **Figure 2D**).

Non-relapse mortality and relapse

Given the low incidence of GVHD observed with αβTCR–depleted transplantation and peri-transplant ruxolitinib, we evaluated its impact on non-relapse mortality and relapse. The incidence of non-relapse mortality at two years was higher in the RUXmin cohort than in the RUXplus cohort (50 vs 18%, p = 0.025; **Figure 3A**). Relapse rates were 16% in the RUXplus cohort and 10% in the RUXmin cohort (p = 0.3; **Figure 3B**). These results demonstrate that peri-transplantation ruxolitinib combined with αβTCR-depletion improves non-relapse mortality, but relapse continues to represent a major challenge.

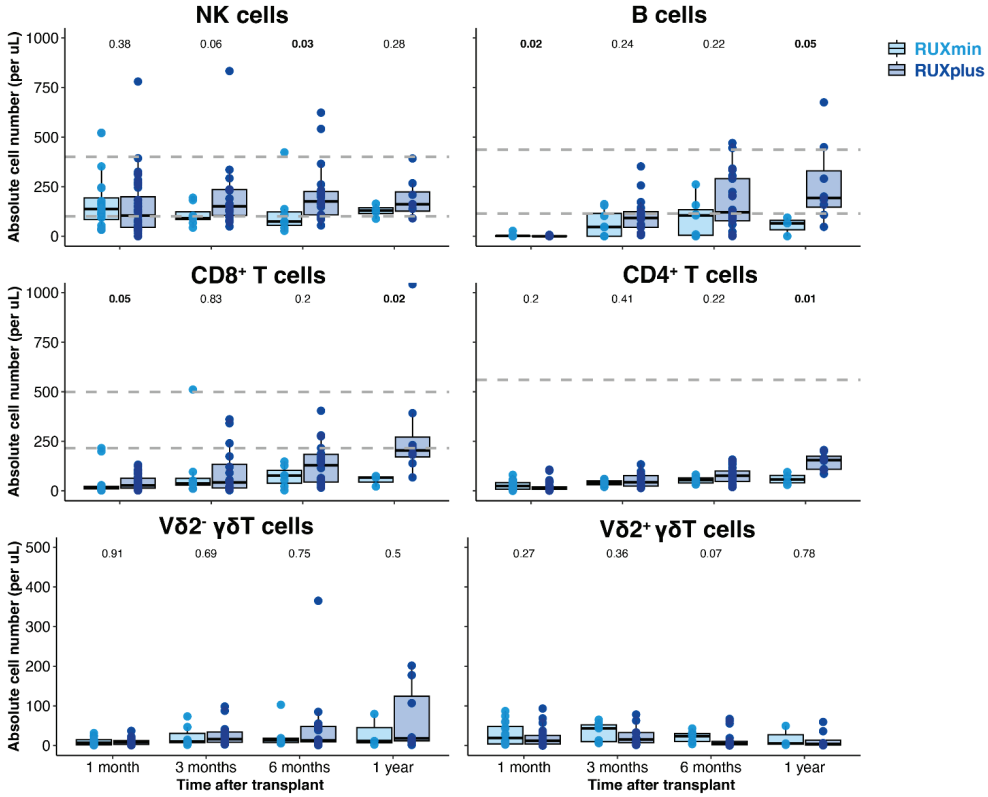


Figure 1: Impact of peri-transplant ruxolitinib on immune reconstitution. *Numerical reconstitution shown. P-values calculated using Mann-Whitney U test.*

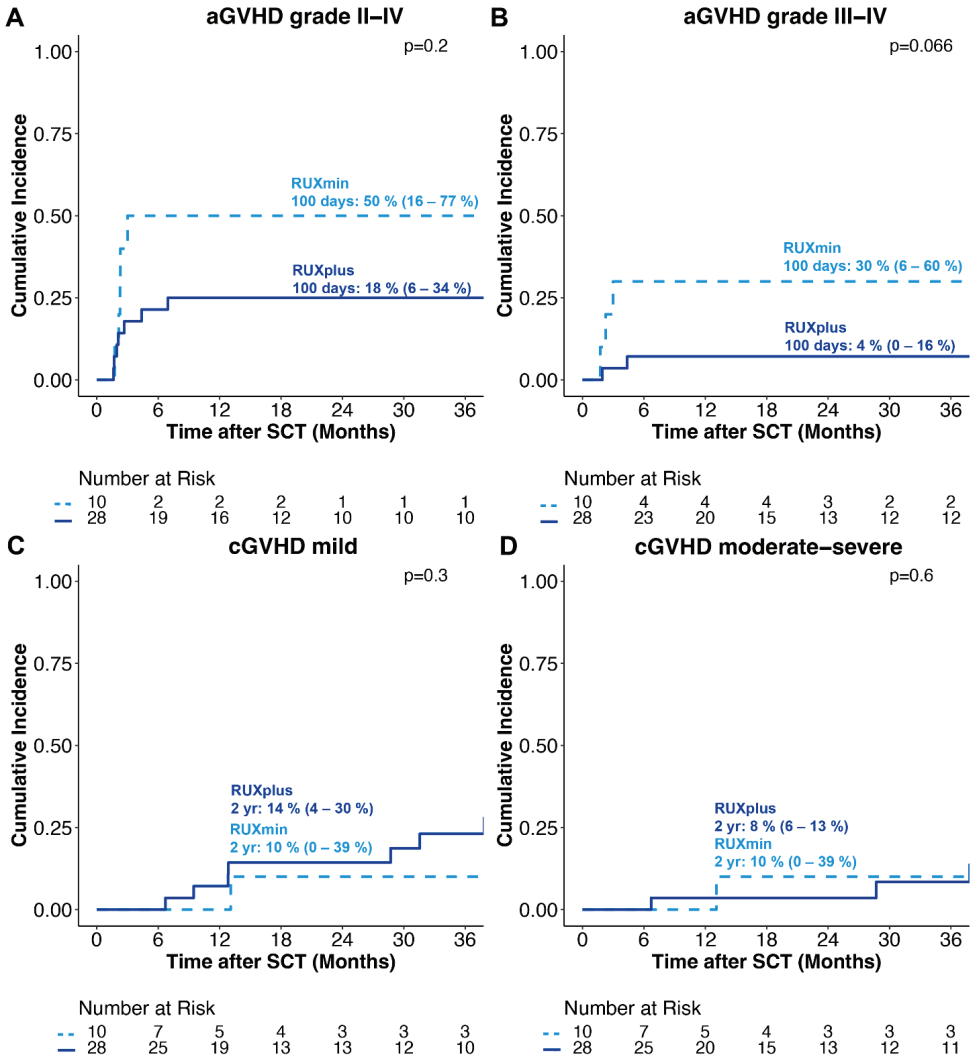


Figure 2: abT cell +/- CD19 depleted transplantation with peri-transplantation ruxolitinib results in low incidences of GVHD. *Cumulative incidence curves of A) acute GVHD grade II-IV, B) acute GVHD grade III-IV, C) mild chronic GVHD, and D) moderate-severe chronic GVHD. Cumulative incidence is defined as time to onset of GVHD, with death as competing event. P-values shown calculated using Fine and Grey's test. RUXmin n = 10, RUXplus n = 28.*

Molecular monitoring and donor lymphocyte infusions

We evaluated the follow-up of all patients who received peri-transplant ruxolitinib (**Supplementary Figure S2**). Among the six patients who experienced hematological relapse, three required a second stem cell transplantation after having received DLIs first. In 2021, we introduced ddPCR to monitor MRD, intending to reduce hematological relapse risk. For patients transplanted after 2021 (n = 15, indicated in bold in **Supplementary Figure S2**), the two-year incidence of MRD positivity was 37% (**Figure 4A**). Based on MRD

status and relapse events, we implemented a donor lymphocyte infusion (DLI) strategy, as described in the methods. This approach effectively prevented hematological relapse in all but one patient, who subsequently required a second transplant (**Figure 4**). These findings suggest that integrating MRD-guided monitoring with a tailored DLI strategy likely enhances disease control.

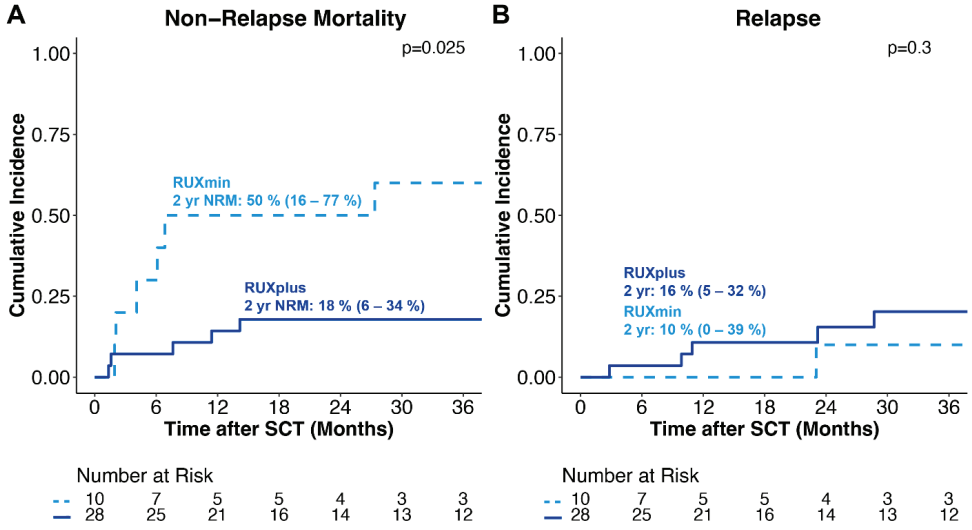


Figure 3: αβT cell +/- CD19 depleted transplantation with peri-transplantation ruxolitinib is associated with low non-relapse mortality, relapse remains a challenge. *A) Cumulative incidence curves of non-relapse mortality. Cumulative incidence is defined as time to death with relapse as competing event. B) Cumulative incidence curves of relapse. Cumulative incidence is defined as time to relapse with death as competing event. P-values shown calculated using Fine and Grey's test. RUXmin n = 10, RUXplus n = 28.*

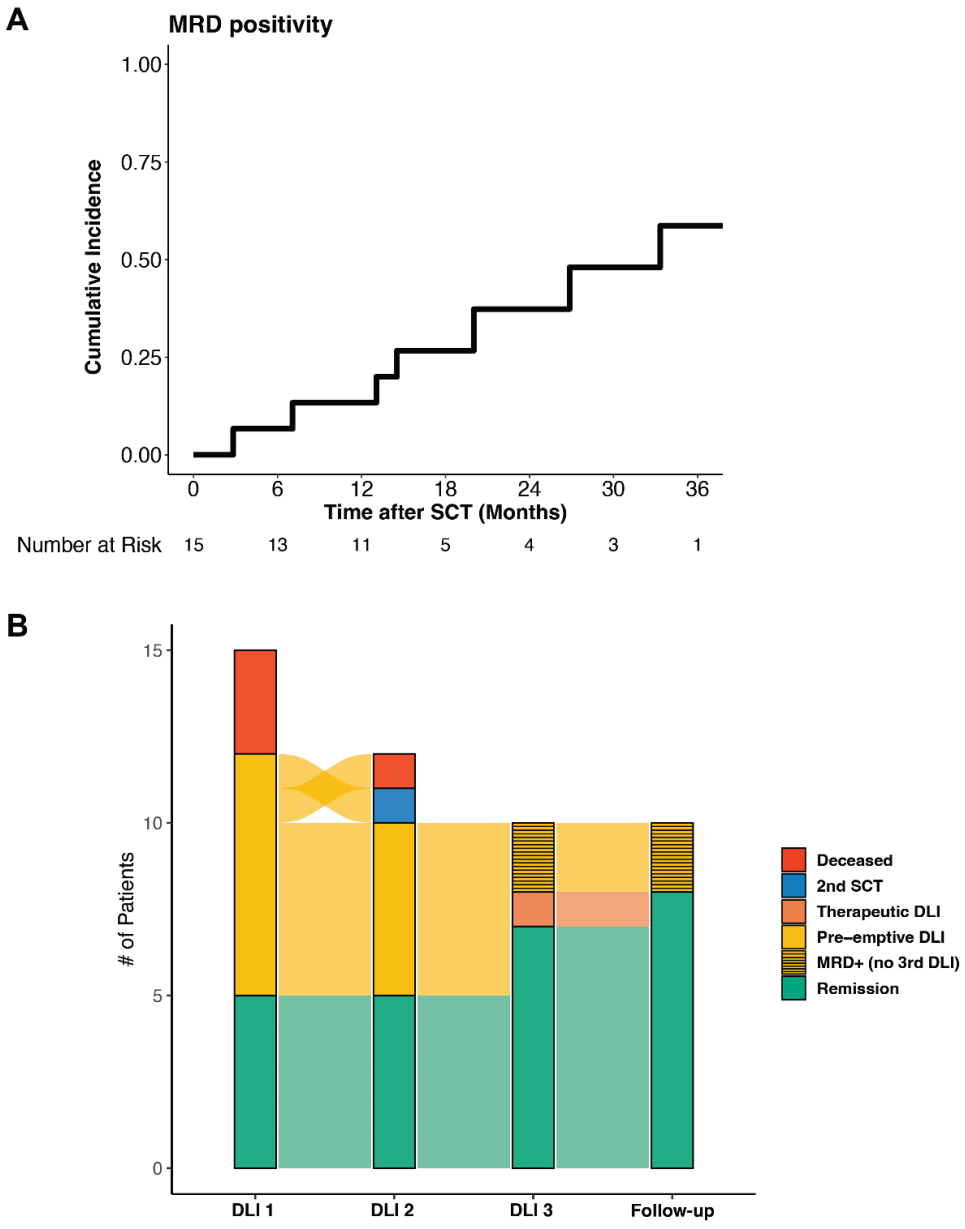


Figure 4: Donor lymphocyte infusions can successfully revert (molecular) relapse. *A) Cumulative incidence curve of MRD positivity after introduction of ddPCR. Cumulative incidence defined as time to onset of MRD positivity with relapse and death as competing events. B) Changes in remission status of patients who received peri-transplantation ruxolitinib and were monitored by digital droplet PCR (n = 15). Remission was defined as the absence of driver mutation as measured by digital droplet PCR. DLIs with dose level 1x10^5 $CD3^+$ cells/kg are not included in this plot.*

Survival

Finally, we evaluated whether the changes to our transplantation protocol improved survival outcomes. Overall survival was significantly higher in patients who received peri-transplantation ruxolitinib (82%) than in those who did not (50%) (p = 0.024; **Figure 5A**). Event-free survival was 67% in the RUXplus cohort and 40% in the RUXmin cohort (p = 0.12; **Figure 5B**). Similarly, graft-versus-host disease-free, relapse-free survival (GRFS) was 59% in the RUXplus cohort versus 20% in the RUXmin cohort (p = 0.06; **Figure 5C**). Taken together, these findings indicate an improved overall survival in patients undergoing αβTCR-depleted transplantation with peri-transplantation ruxolitinib.

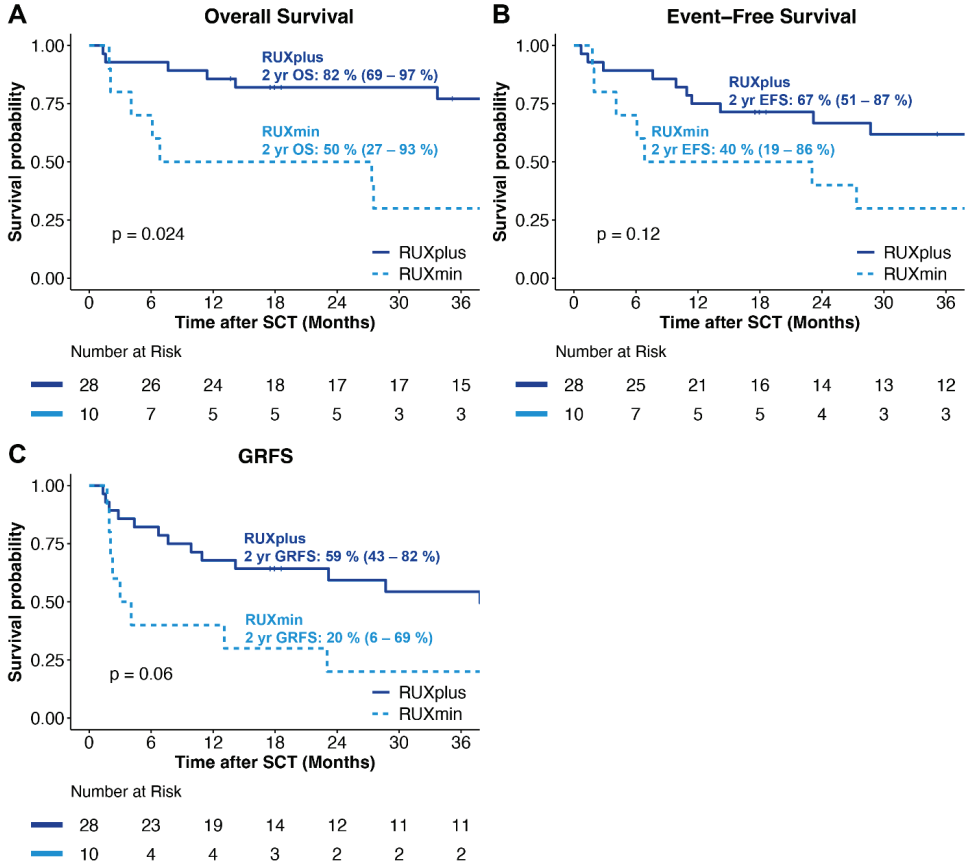


Figure 5: αβT cell +/- CD19 depleted transplantation with peri-transplantation ruxolitinib results in favourable survival outcomes. *A) Kaplan-Meier curves of overall survival, defined as time from transplantation to death from any cause, censoring at the last day of follow-up. B) Kaplan-Meier curves of event-free survival, defined as the time from transplantation to relapse, graft failure or death, and censoring on the last day of follow-up. C) Kaplan-Meier curves of GVHD-free, relapse-free survival, defined as as the time from transplantation to relapse, acute GVHD (aGVHD) grade III–IV, moderate-severe chronic GVHD (cGVHD), or death, censoring at the last day of follow-up. Log-rank test was used to determine p-values.*

DISCUSSION

In this retrospective study, we investigated whether combining ruxolitinib with αβTCR-depleted grafts after a myeloablative conditioning could improve outcomes for patients with myelofibrosis undergoing stem cell transplantation. Here, we highlight four key findings. First, our transplantation platform with peri-transplantation ruxolitinib resulted in excellent overall survival and a promising incidence of non-relapse mortality in this patient category. Second, we observed low acute and chronic GVHD incidences in patients receiving peri-transplant ruxolitinib. Third, peri-transplant ruxolitinib did not impair T cell recovery following αbTCR-depleted transplantation. Fourth, relapse was effectively controlled through (MRD) monitoring combined with donor lymphocyte infusions in a substantial number of patients.

Overall survival at two years ranged from 50% in patients who did not receive ruxolitinib to 82% in those treated with peri-transplant ruxolitinib. Notably, survival outcomes in the peri-transplant ruxolitinib cohort compared favorably with previously reported data for myelofibrosis[13,14,18,30-33]. This is despite the inclusion of an elderly population with a median age of above 60 years and the use of myeloablative conditioning, factors previously associated with increased non-relapse mortality[5-7]. The favorable overall survival we observed appeared to be largely driven by peri-transplantation ruxolitinib, which may have played a protective role in preventing non-relapse mortality. This aligns with findings by Rathje et al., who reported a favorable one-year overall survival of 97% in myelofibrosis patients treated with peri-transplant ruxolitinib[29].

We observed low incidences of both acute and chronic GVHD in our study population as compared to other large patient series on transplantation for myelofibrosis[5-7]. This partly agrees with other studies that peri-transplantation ruxolitinib reduces incidences of aGVHD in myelofibrosis patients. However, the incidence of cGVHD remained considerable in these studies[13,14,29]. For example, Ali et al. reported an incidence of cGVHD of 42% in patients who received peri-transplantation ruxolitinib[14]. In contrast, Hobbs et al. reported an incidence of moderate-severe cGVHD of 15% at 2 years when ruxolitinib was continued for a year post-transplant, suggesting that the duration and timing of ruxolitinib may be critical for cGVHD prevention[15]. Taken together, shorter peri-transplant ruxolitinib may be insufficient, and additional T cell depletion strategies may be warranted to control cGVHD[17,34,35]. Supporting this, Kunte et al. reported notably low extensive cGVHD incidence (8% at two years after transplantation) in myelofibrosis patients treated with post-transplantation cyclophosphamide[18]. Together, these results suggest that peri-transplantation ruxolitinib may reduce aGVHD, but optimizing its duration and combining it with T cell depletion strategies may be necessary to mitigate the risk of cGVHD.

Overall, immune reconstitution seemed superior in the peri-transplant ruxolitinib cohort, with higher NK cell counts at six months and increased $CD8^+$ and $CD4^+$ αβT cells at one year post-transplantation. This is partly in line with findings by Rathje et al., who also observed improved NK cell recovery in patients receiving peri-transplantation ruxolitinib [29]. However, their study did not demonstrate enhanced αβT cell reconstitution, in contrast to our results and those of Ali et al., who reported a trend toward improved αβT cell recovery[14]. Moreover, in contrast to Rathje et al.[29], we observed no effect of ruxolitinib on γδT cell recovery. This is possibly due to the use of αβTCR-depleted grafts in our platform, which may promote γδT cell recovery independently of ruxolitinib. Also, B cell recovery showed a different pattern in our cohort compared to previous findings: although initially lower in the ruxolitinib cohort, B cell counts were higher at one-year post-transplant. In contrast, Rathje et al. described a transient enhanced recovery during the first three months, but without sustained differences[29]. A possible explanation for this discrepancy is the high proportion of patients in our peri-transplant ruxolitinib cohort who received αβTCR and CD19-depleted grafts, in which, in contrast to a full graft, ruxolitinib-induced T cell suppression is less likely to confer a relative advantage in early B-cell recovery. Taken together, these comparisons highlight how graft composition and ruxolitinib dosing likely interact to shape immune reconstitution patterns following transplantation.

While non-relapse mortality improved and acute and chronic GVHD rates were promising, 16% of patients relapsed after peri-transplant ruxolitinib. Early detection of driver mutation persistence, combined with timely administration of DLIs, proved effective in managing relapse. In line with our observations, a study of 37 myelofibrosis patients showed that molecular monitoring followed by DLI effectively improved survival, with significantly better outcomes when DLIs were given for molecular rather than for hematological relapse (77% vs 32%)[30]. The importance of driver mutation clearance was further supported by a recent study of 324 myelofibrosis patients, which found that clearance of driver mutations by day 30 strongly predicted outcomes after transplantation[33]. Taken together, these results suggest that integrating early molecular monitoring with timely DLI administration can improve survival outcomes in myelofibrosis patients undergoing stem cell transplantation.

Our study has several limitations. The primary limitation is its retrospective nature and small sample size, particularly in the cohort that did not receive peri-transplantation ruxolitinib. Despite this, we observed a significant difference in overall survival between the two cohorts. Another limitation is the concurrent change in allograft engineering strategy: shortly after implementing peri-transplant ruxolitinib, we transitioned from using αβTCR depletion alone to αβTCR and CD19 depletion. Therefore, it remains possible that the improved outcomes observed in the ruxolitinib cohort were partly influenced by the addition of CD19 depletion. However, in a larger cohort of patients with various hematological malignancies that received either αβTCR depletion or αβTCR and CD19

depletion, we did not see these striking differences in overall survival and non-relapse mortality (unpublished data).

Future work should test whether peri-transplant ruxolitinib shows benefit across different T-cell-depletion platforms, including post-transplant cyclophosphamide (PTCy), and should define the optimal dose, timing, and duration of peri-transplant ruxolitinib in myelofibrosis. Given that late relapses are not uncommon[30,33], standardized MRD monitoring seems essential. Current guidelines define molecular relapse as the reappearance of the MRD marker in two consecutive peripheral blood samples[26], but thresholds vary by assay. In our analysis, MRD positivity was defined as ddPCR ≥0.1%. However, in some cases, values fluctuated around this threshold before declining again. Establishing assay-specific thresholds for MRD detection would help standardize the definition of molecular relapse and reduce the risk of misclassification, thereby reducing the risk of over- or undertreatment of patients. Together, these future studies will be critical for optimizing transplant strategies and post-transplant monitoring in myelofibrosis.

In conclusion, we showed that myeloablative conditioning, combined with an αβTCR/CD19-depleted allograft, peri-transplantation ruxolitinib, and MRD-based DLI is a promising strategy to achieve long-term GRFS in patients with myelofibrosis.

DATA AVAILABILITY STATEMENT

The data that support the findings of this study are available from the EBMT registry, but restrictions apply to the availability of these data, which were used under license for the current study, and so are not publicly available. Data are, however, available from the authors upon reasonable request and with permission of the corresponding author.

AUTHOR CONTRIBUTIONS

MdW was responsible for the conception and design of the study. MdW and JK were responsible for funding of the study. AS, FW, JD, JK and MdW contributed to data analysis and interpretation. AS, FW, JK and MdW were responsible for writing the manuscript and preparing the figures. AS and FW had full access to and verified the underlying data. AJ, CO, LvdW, AvR, LvH, RR, JK, MdW were responsible for resources (patients). AS and MdW were responsible for submission of the manuscript. FW, AS, CN, FV, IB, KW, TH, and LvdC were responsible for the collection and assembly of data. All authors were responsible for critical revision of the manuscript and approved the final version of the manuscript.

REFERENCES

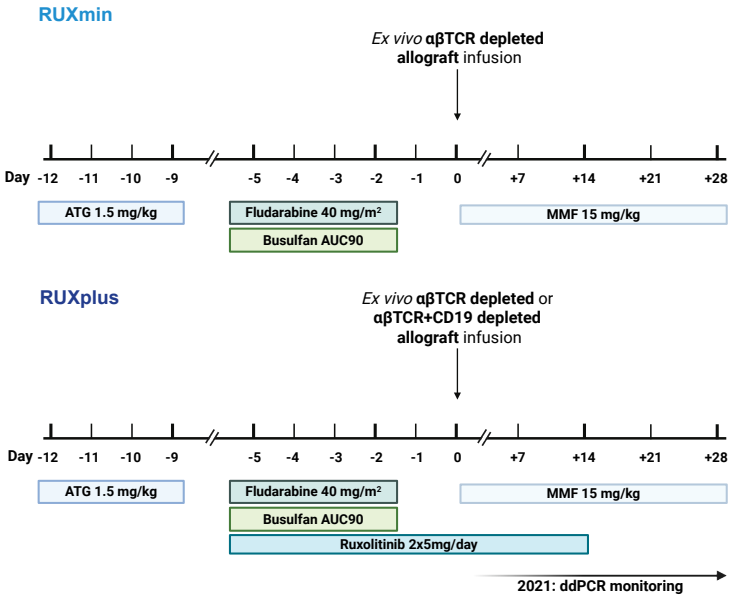
1. Tefferi A, Vardiman JW. Classification and diagnosis of myeloproliferative neoplasms: the 2008 World Health Organization criteria and point-of-care diagnostic algorithms. *Leukemia*. 2008;22(1):14-22.
2. Abdel-Wahab OI, Levine RL. Primary myelofibrosis: update on definition, pathogenesis, and treatment. *Annu Rev Med*. 2009;60:233-245.
3. Vainchenker W, Kralovics R. Genetic basis and molecular pathophysiology of classical myeloproliferative neoplasms. *Blood*. 2017;129(6):667-679.
4. Spivak JL. The chronic myeloproliferative disorders: clonality and clinical heterogeneity. *Semin Hematol*. 2004;41(2 Suppl 3):1-5.
5. McLornan D, Szydlo R, Koster L, et al. Myeloablative and Reduced-Intensity Conditioned Allogeneic Hematopoietic Stem Cell Transplantation in Myelofibrosis: A Retrospective Study by the Chronic Malignancies Working Party of the European Society for Blood and Marrow Transplantation. *Biol Blood Marrow Transplant*. 2019;25(11):2167-2171.
6. McLornan D, Eikema DJ, Czerw T, et al. Trends in allogeneic haematopoietic cell transplantation for myelofibrosis in Europe between 1995 and 2018: a CMWP of EBMT retrospective analysis. *Bone Marrow Transplant*. 2021;56(9):2160-2172.
7. Hernandez-Boluda JC, Pereira A, Kroger N, et al. Allogeneic hematopoietic cell transplantation in older myelofibrosis patients: A study of the chronic malignancies working party of EBMT and the Spanish Myelofibrosis Registry. *Am J Hematol*. 2021;96(10):1186-1194.
8. Gerds AT, Verstovsek S, Vannucchi AM, et al. Momelotinib versus danazol in symptomatic patients with anaemia and myelofibrosis previously treated with a JAK inhibitor (MOMENTUM): an updated analysis of an international, double-blind, randomised phase 3 study. *Lancet Haematol*. 2023;10(9):e735-e746.
9. Harrison C, Kiladjian JJ, Al-Ali HK, et al. JAK inhibition with ruxolitinib versus best available therapy for myelofibrosis. *N Engl J Med*. 2012;366(9):787-798.
10. Zeiser R, von Bubnoff N, Butler J, et al. Ruxolitinib for Glucocorticoid-Refractory Acute Graft-versus-Host Disease. *N Engl J Med*. 2020;382(19):1800-1810.
11. Spoerl S, Mathew NR, Bscheider M, et al. Activity of therapeutic JAK 1/2 blockade in graft-versus-host disease. *Blood*. 2014;123(24):3832-3842.
12. Parampalli Yajnanarayana S, Stubig T, Cornez I, et al. JAK1/2 inhibition impairs T cell function in vitro and in patients with myeloproliferative neoplasms. *Br J Haematol*. 2015;169(6):824-833.
13. Kroger N, Shahnaz Syed Abd Kadir S, Zabelina T, et al. Peritransplantation Ruxolitinib Prevents Acute Graft-versus-Host Disease in Patients with Myelofibrosis Undergoing Allogenic Stem Cell Transplantation. *Biol Blood Marrow Transplant*. 2018;24(10):2152-2156.
14. Ali H, Tsai NC, Synold T, et al. Peritransplantation ruxolitinib administration is safe and effective in patients with myelofibrosis: a pilot open-label study. *Blood Adv*. 2022;6(5):1444-1453.
15. Hobbs GS, Kim HT, Hao R, et al. Phase II Study of Peri- and Post-Transplant Ruxolitinib for Patients With Myelofibrosis Receiving Allogeneic Hematopoietic Cell Transplantation. *JCO Oncology Advances*. 2025(2).
16. Wall SA, Tamari R, DeFilipp Z, Hobbs GS. Optimization of allogeneic hematopoietic cell transplantation for patients with myelofibrosis treated with ruxolitinib: eligibility, best practices, and improving transplant outcomes. *Ann Hematol*. 2025;104(4):2125-2141.
17. Stuut AHG, Nijssen C, van der Wagen L, et al. Improved GVHD-free and relapse-

free survival after ex vivo alphabetaTCR and CD19 depleted allogeneic HSCT compared to T cell replete HSCT. *Bone Marrow Transplant*. 2025.

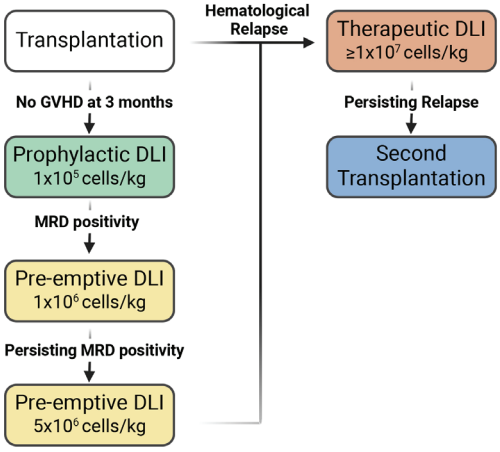
18. Kunte S, Rybicki L, Viswabandya A, et al. Allogeneic blood or marrow transplantation with haploidentical donor and post-transplantation cyclophosphamide in patients with myelofibrosis: a multicenter study. *Leukemia*. 2022;36(3):856-864.
19. Scott BL, Gooley TA, Sorror ML, et al. The Dynamic International Prognostic Scoring System for myelofibrosis predicts outcomes after hematopoietic cell transplantation. *Blood*. 2012;119(11):2657-2664.
20. Gagelmann N, Ditschkowski M, Boγδanov R, et al. Comprehensive clinical-molecular transplant scoring system for myelofibrosis undergoing stem cell transplantation. *Blood*. 2019;133(20):2233-2242.
21. Chaleff S, Otto M, Barfield RC, et al. A large-scale method for the selective depletion of alphabeta T lymphocytes from PBSC for allogeneic transplantation. *Cytotherapy*. 2007;9(8):746-754.
22. Li Pira G, Malaspina D, Girolami E, et al. Selective Depletion of alphabeta T Cells and B Cells for Human Leukocyte Antigen-Haploidentical Hematopoietic Stem Cell Transplantation. A Three-Year Follow-Up of Procedure Efficiency. *Biol Blood Marrow Transplant*. 2016;22(11):2056-2064.
23. Przepiorka D, Weisdorf D, Martin P, et al. 1994 Consensus Conference on Acute GVHD Grading. *Bone Marrow Transplant*. 1995;15(6):825-828.
24. Jagasia MH, Greinix HT, Arora M, et al. National Institutes of Health Consensus Development Project on Criteria for Clinical Trials in Chronic Graft-versus-Host Disease: I. The 2014 Diagnosis and Staging Working Group report. *Biol Blood Marrow Transplant*. 2015;21(3):389-401 e381.
25. Coccaro N, Tota G, Anelli L, Zagaria A, Specchia G, Albano F. Digital PCR: A Reliable Tool for Analyzing and Monitoring Hematologic Malignancies. *Int J Mol Sci*. 2020;21(9).
26. McLornan DP, Hernandez-Boluda JC, Czerw T, et al. Allogeneic haematopoietic cell transplantation for myelofibrosis: proposed definitions and management strategies for graft failure, poor graft function and relapse: best practice recommendations of the EBMT Chronic Malignancies Working Party. *Leukemia*. 2021;35(9):2445-2459.
27. Therneau TM. A Package for Survival Analysis in R; 2024.
28. Sjoberg DD, Fei T. tidycmprsk: Competing Risks Estimation; 2024.
29. Rathje K, Gagelmann N, Badbaran A, et al. Clinical and Immune Effects of Peri-Transplantation JAK Inhibition for Myelofibrosis. *Am J Hematol*. 2025;100(2):200-209.
30. Gagelmann N, Wolschke C, Badbaran A, et al. Donor Lymphocyte Infusion and Molecular Monitoring for Relapsed Myelofibrosis After Hematopoietic Cell Transplantation. *Hemasphere*. 2023;7(7):e921.
31. Oechsler S, Gagelmann N, Wolschke C, et al. Graft-versus-host disease and impact on relapse in myelofibrosis undergoing hematopoietic stem cell transplantation. *Bone Marrow Transplant*. 2024;59(4):550-557.
32. Robin M, Iacobelli S, Koster L, et al. Treosulfan compared to busulfan in allogeneic haematopoietic stem cell transplantation for myelofibrosis: a registry-based study from the Chronic Malignancies Working Party of the EBMT. *Bone Marrow Transplant*. 2024;59(7):928-935.
33. Gagelmann N, Quarder M, Badbaran A, et al. Clearance of Driver Mutations after Transplantation for Myelofibrosis. *N Engl J Med*. 2025;392(2):150-160.

34. de Witte MA, Janssen A, Nijssen K, et al. alphabeta T-cell graft depletion for allogeneic HSCT in adults with hematological malignancies. *Blood Adv*. 2021;5(1):240-249.
35. Bethge WA, Eyrich M, Mielke S, et al. Results of a multicenter phase I/II trial of TCRalphabeta and CD19-depleted haploidentical hematopoietic stem cell transplantation for adult and pediatric patients. *Bone Marrow Transplant*. 2022;57(3):423-430.

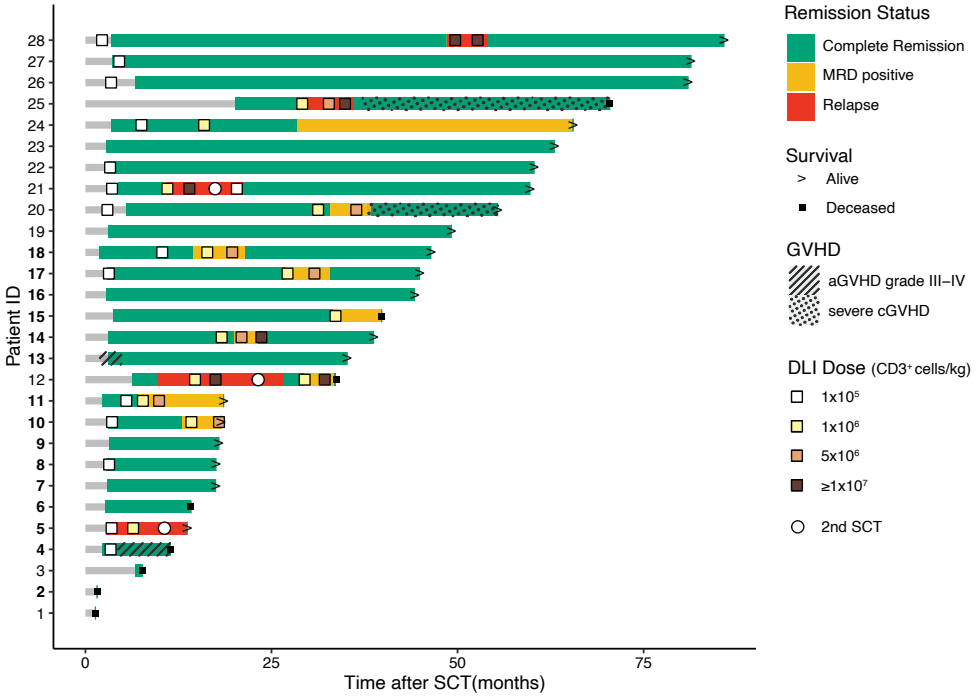
SUPPLEMENTARY FIGURES



Supplementary Figure S1: Overview of conditioning regimens.



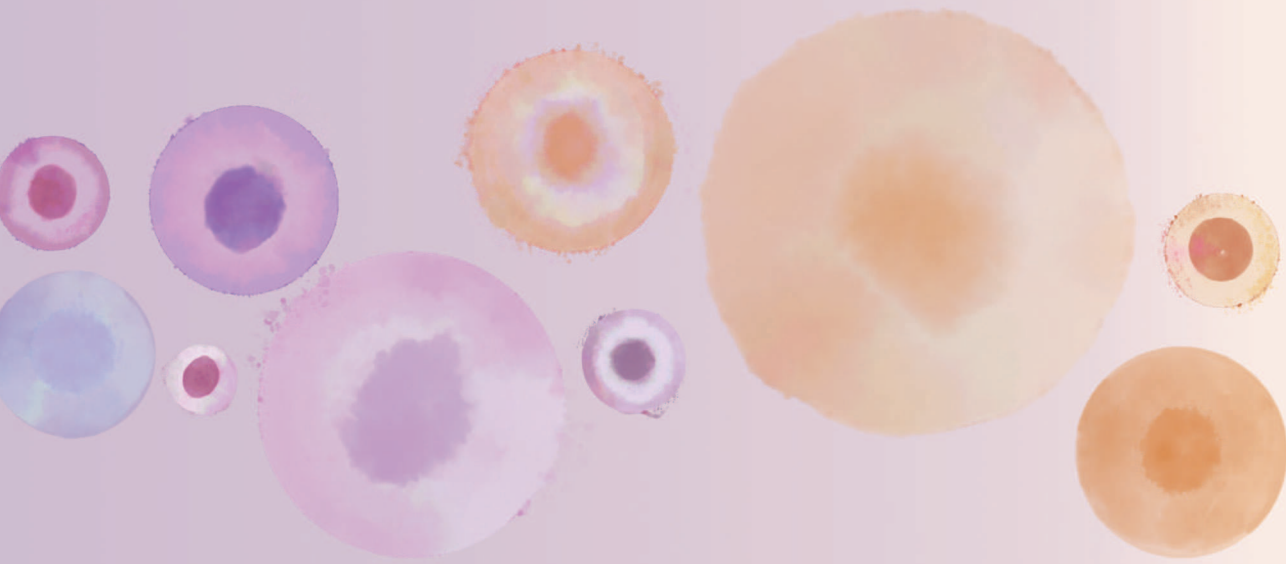
Supplementary Figure S2: Summary of donor lymphocyte infusion strategy.



Supplementary Figure S3: Follow-up of patients in RUXplus group. *Patient IDs in* **bold** *highlight patients who were monitored per protocol for minimal residual disease by ddPCR (transplanted after 2021).*

Part 2

Immune reconstitution after αβT-cell-depleted allogeneic HSCT



5

Short-Term Post-Transplant Proteomics in Myeloid Malignancies

Anniek Stuut[1], Pleun Schonewille[2], Maud van den Broek[1], Coco de Koning[1,3], Klaartje Nijssen[2], Julia Drylewicz[1], Jurgen Kuball[1,2], Stefan Nierkens[1, 3], Moniek de Witte[1, 2]

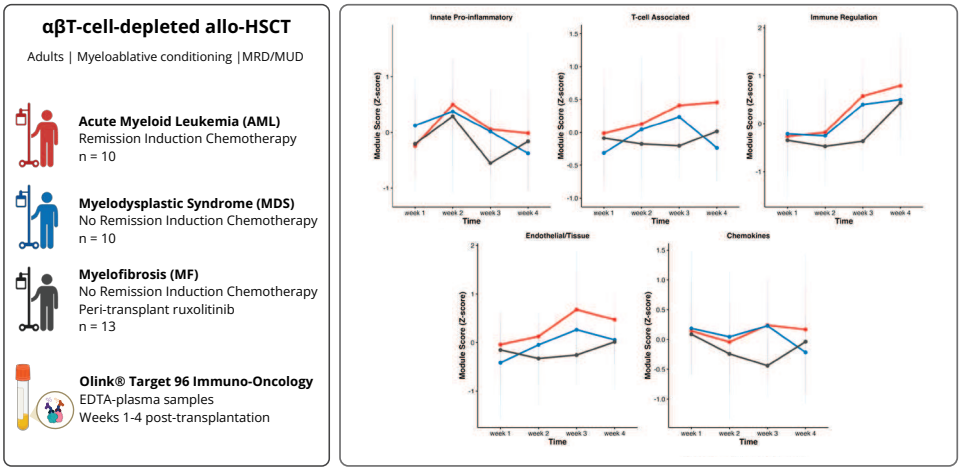
1. *Center for Translational Immunology, University Medical Center Utrecht, The Netherlands*
2. *Department of Hematology, University Medical Center Utrecht, The Netherlands*
3. *Princess Máxima Center for Pediatric Oncology, Utrecht, The Netherlands*

Manuscript in preparation

ABSTRACT

Allogeneic hematopoietic stem cell transplantation is the only curative option for several myeloid malignancies. Early immune dysregulation may contribute to disease-specific complications and non-relapse mortality, particularly in myelodysplastic syndromes (MDS) and myelofibrosis (MF). We investigated whether post-transplant immune dynamics are shaped by underlying disease biology and peri-transplant interventions by longitudinally profiling 92 immune-related plasma proteins during the first four weeks after transplantation in patients with acute myeloid leukemia (AML) (n=10), MDS (n=10), and MF (n=13). MF patients received peri-transplant ruxolitinib (day −5 to +14). Unsupervised analyses showed that time since transplantation accounted for most of the variation in protein expression, with prominent contributions from pro-inflammatory cytokines, T-cell–associated proteins, immune-regulatory markers, endothelial/tissue injury proteins, and chemokines. To facilitate interpretation, we grouped a subset of proteins into five functional modules. These five module-based trajectories were similar in AML and MDS up to week three, but diverged at week four, with lower module scores in MDS. On the other hand, MF displayed lower scores in weeks two and three, followed by an increase after week three, suggesting a transient dampening of early immune activation, potentially due to ruxolitinib. Overall, early post-transplant immune dynamics appear strongly time-driven but modulated by disease context and peri-transplant treatment, supporting multiplex protein profiling to capture disease-specific immune trajectories for subsequent correlation with clinical outcomes.

Short-Term Post-Transplant Proteomics Reveal Temporal and Disease-Specific Trajectories in Myeloid Malignancies



INTRODUCTION

Allogeneic hematopoietic stem cell transplantation (allo-HSCT) is the only curative treatment option for several myeloid malignancies. Despite improvements in transplantation techniques and supportive care, treatment-related toxicities such as graft-versus-host disease (GVHD), endothelial damage, graft failure, and infections still may result in non-relapse mortality (NRM)[1].

The risk of NRM can vary across malignancies, as shown in a recent EBMT study comparing outcomes between post-transplantation cyclophosphamide and *ex vivo* T-cell depletion in patients with acute leukemia and myelodysplastic syndromes/myeloproliferative neoplasms (MDS/MPN)[2]. In this study, the risk of NRM in patients with acute leukemia was 16-19%, whereas in patients with MDS/MPN, it was 29-30%. A potential explanation could be that leukemia patients typically receive induction therapy prior to transplantation, whereas patients with MDS and myeloproliferative neoplasms, such as myelofibrosis (MF), usually receive upfront transplantation, without prior induction therapy. We hypothesize that upfront transplantation in chronic myeloid diseases may preserve a pro-inflammatory disease state that shapes early post-transplant immune dynamics, thereby contributing to excess NRM.

In patients with MF, peri-transplant administration of the JAK1/2 inhibitor ruxolitinib has been shown to reduce the rates of GVHD and NRM[3-5]. These observations raise the hypothesis that peri-transplant ruxolitinib shapes early immune dynamics after allo-HSCT and may alter disease-specific host conditions that contribute to NRM. To explore this, we investigated early post-transplant immune-oncology profiles in a retrospective cohort of three distinct patient groups: AML, a disease with classically lower NRM; MDS, a disease with higher NRM; and MF, in which peri-transplant ruxolitinib was used as an immune-modulating intervention. All patients received the same myeloablative conditioning and an *ex vivo* αβTCR ± CD19-depleted allograft. With longitudinal proteomic profiling during the first four weeks after allo-HSCT, we aimed to characterize temporal and disease-specific immune trajectories in the early post-transplant period.

MATERIALS AND METHODS

Study participants

Adult patients with either AML, MDS, or MF treated with an *ex vivo* αβTCR +/- CD19-depleted allogeneic hematopoietic stem cell transplantation between 2018 and 2023 were included in this retrospective study. An overview of the patients included is presented in **Table 1**. Data was collected from electronic health records and the European Society for Blood and Marrow Transplantation (EBMT) database. All patients provided written informed consent to the use of their data for scientific purposes before transplantation. Informed consent was approved by the local ethics committee (METC nr 21-322) at the University Medical Center Utrecht (UMCU, the Netherlands) in accordance with JACIE guidelines and the declaration of Helsinki. Healthy controls were included through an in-house healthy donor program, approved by the UMCU ethics committee (07/025), as previously described[6].

Conditioning regimen and graft processing

All patients received a myeloablative conditioning regimen consisting of anti-thymocyte globulin (ATG) 1.5 mg/kg IV on days −12 to -9, fludarabine 40 mg/m^2 IV on days −5 to -2, and busulfan (Busilvex® AUC90 IV on days −5 to -2. Mycophenolate mofetil was administered to all patients as GVHD prophylaxis until day +28 post-transplantation. MF patients received ruxolitinib at a dose of 5mg twice daily from day -5 to day +14. Peripheral blood stem cells were collected from 9/10- or 10/10-human leukocyte antigen (HLA)- matched related or unrelated donors, in accordance with institutional donor selection guidelines. *Ex vivo* depletion was performed using the automated CliniMACS® device (Miltenyi Biotec, Bergisch Gladbach, Germany), with magnetic microbeads conjugated to anti-αβTCR and, when applicable, anti-CD19 antibodies, as previously described[7,8].

Plasma samples

EDTA-plasma samples at weeks 1, 2, 3, and 4 post-transplantation were obtained from the virology department of the University Medical Center Utrecht (UMCU). Samples were stored at -80 °C until further use. All patients provided written informed consent for the use of the samples for scientific purposes. Informed consent was obtained from participants, and the study was approved by the local ethics committee (TCBio nrs. 11-063 and 23-052). Healthy control samples were obtained through the UMCU in-house healthy donor program (07/025), as described previously[6]

Olink multiplex assay

EDTA-plasma samples were analyzed with the Olink® Target 96 Immuno-Oncology panel at the UMCU following the manufacturer's manual. EDTA-plasma samples were thawed and randomly distributed into 96-well plates. Randomization was done using the OlinkAnalyze package in R[9]. The Olink assay is based on proximity extension assay

technology[10,11]. In short, the proximity extension assay uses antibody pairs directed to specific proteins, each labeled with a unique DNA oligonucleotide. Upon binding, these DNA oligonucleotides generate unique DNA barcodes for each protein. These newly created DNA barcodes were subsequently amplified by PCR and quantified using a BioMark HD Real-Time PCR Platform (Fluidigm, South San Francisco, CA). Raw quantification cycle values were normalized and converted to normalized protein expression (NPX) units, expressed on a log2 scale, in which a one-unit increase corresponds to a two-fold increase in the measured protein concentration. The 92 measured proteins are listed in **Supplementary File 1**. The assay was performed simultaneously for all patient samples, whereas healthy control samples were measured earlier[6].

Statistical analysis

Data was analyzed using RStudio (R version 4.4.0). Baseline characteristics are reported as frequencies and percentages for categorical variables and median (interquartile range (IQR)) for continuous variables. Patient samples were distributed across two 96-well plates, resulting in two datasets. Before analysis, the datasets were merged, and batch effects were corrected using the BAMBOO method[12]. Values below the lower limit of detection (LOD) were replaced with the LOD value for each respective protein. Proteins with zero variance were excluded from subsequent analyses. For principal component analysis (PCA), patient samples were scaled and centered, and the variance explained by each component was calculated. The top 10 contributing proteins for PC1, PC2, and PC3 were identified based on absolute loading values.

Proteins were grouped into five functional modules based on biological function: (1) Innate/Pro-inflammatory Cytokines (IL-6, TNF, IL-18, IL-8), (2) T-cell Associated Cytokines (IFN-γ, GZMB, GZMA, IL-2, IL-7, IL-15, IL-10), (3) Immune Regulation (LAG-3, PD-1, PD-L1, PD-L2, CD27, CD28, TNFRSF9, TNFRSF4, CD244, KLRD1, MIC-A/B, NCR1), (4) Endothelial/Tissue (ANGPT1/2, TIE2, VEGFA, VEGFR-2, PGF, LGALS9, MMP7, MMP12, HGF, HO-1), and (5) Chemokines (CXCL9/10/11/12/13, CCL2/3/4/17/19/20/23, CX3CL1) (Supplemental table 1). Module scores were calculated as the mean scaled NPX value of all proteins within each module. Heatmaps were generated using median module scores per disease-timepoint group, with hierarchical clustering disabled to preserve temporal ordering.

For differential expression analysis, Wilcoxon rank tests were performed comparing weeks 2, 3, and 4 to week 1 for each disease group, with FDR correction for multiple testing ($q < 0.05$). Proteins with an absolute log2 fold change > 0.5 and adjusted p-value < 0.05 were considered significantly differentially expressed.

Table 1. Baseline Characteristics

	AML (n = 10)	MDS (n = 10)	MF (n = 13)
Male (%)	4 (40)	5 (50)	7 (54)
Median age, yrs (IQR)	67 (66, 70)	64 (62, 67)	63 (58, 66)
Donortype (%)			
9/10 MUD	1 (10)	1 (10)	1 (8)
10/10 MUD	6 (60)	7 (70)	8 (67)
10/10 MRD	3 (30)	2 (20)	3 (25)
Depletion (%)			
αβTCR depletion	-	-	3 (23)
αβTCR + CD19 depletion	10 (100)	10 (100)	10 (77)

IQR, inter quartile range; MUD, matched unrealted donor, MRD, matched related donor

RESULTS

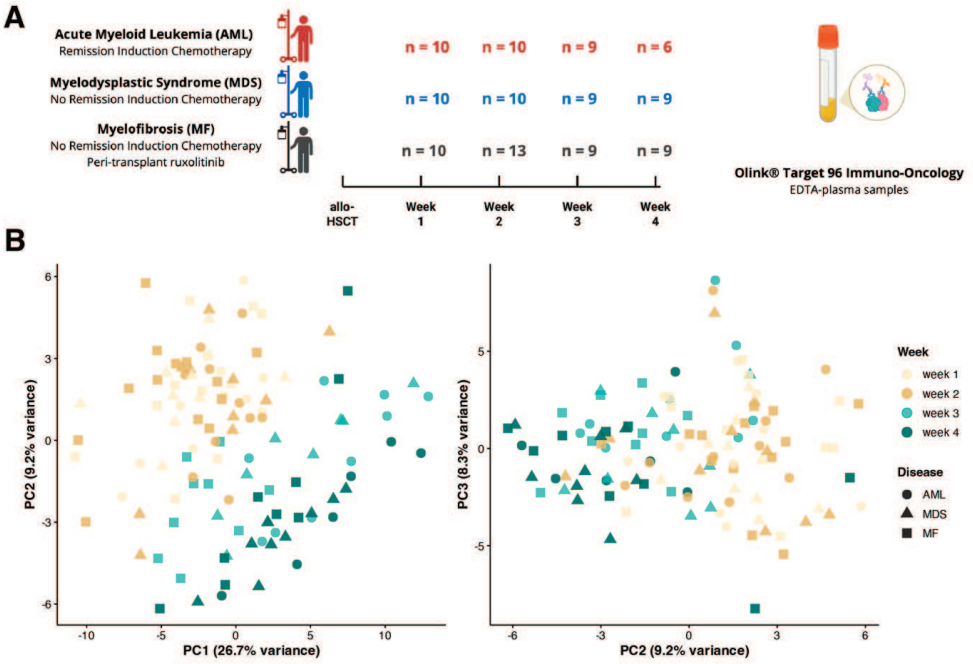


Figure 1. Overview of samples and principal component analysis. (A) *Sample overview* **(B)** *PCA was performed after batch correction. The first two components (PC1: 26.7%, PC2: 9.2%) separate samples by time after transplantation. Points are colored by time point (light sand = week 1, sand = week 2, teal = week 3, deep teal = week 4) and shaped by disease (circle = AML, triangle = MDS, square = MF).*

Patient characteristics

We included 33 patients in this analysis (**Table 1**). The indications for transplantation were AML (n = 10), MDS (n = 10), and MF (n = 13). Median age ranged from 63 years in patients with MF to 67 years in patients with AML. The majority (>60%) of patients received a graft from a 10/10 matched unrelated donor (MUD). All AML and MDS patients received an αβTCR- and CD19-depleted allograft, whereas three MF patients received an αβTCR-depleted graft. All MF patients received ruxolitinib peri-transplantation, as described in the methods. For all patients, at least two timepoints were available (**Figure 1A**).

Time drives the expression of immuno-oncology proteins

First, we explored the dataset by performing principal component analysis (PCA). PC1 and PC2 explained 26.7% and 9.2% of the variance, respectively (**Figure 1B**). Samples were separated primarily by time post-transplant, with week 1-2 samples clustering apart from week 3-4 along PC1 and PC2, whereas disease groups largely overlapped. The top 10 proteins contributing to PC1 were Granzyme B, Granzyme A, TGF-β1, ADA, Granzyme H, Caspase-8, Galectin-9, PD-L1, Fas Ligand, and CD244. The top 10 proteins contributing to PC2 were CCL2, IL-8, IL-15, CX3CL1, CCL3, IL-6, CCL20, CXCL12, IL-7, and CCL4.

We next examined which proteins were differentially expressed over time by comparing week 2, week 3, and week 4 timepoints to week 1 across all disease groups (**Supplementary Figure S1A-C**). At week 2 relative to week 1, only two proteins were significantly different in AML (1 lower and 1 higher expressed), none in MDS, whereas MF already showed six proteins with significantly lower expression. By week 3, the number of differentially expressed proteins increased markedly in AML (4 lower and 24 higher expressed) and MDS (4 lower and 21 higher expressed), while MF showed a more modest, bidirectional shift (8 lower and 5 higher expressed). At week 4, differential expression remained evident, with AML showing 3 proteins with lower expression and 11 with higher expression, MDS 6 with lower and 21 with higher expression, and MF 6 with lower and 10 with higher expression (**Supplementary Figure S1D**). Thus, although protein expression changes increased over time across groups, MF displayed a distinct profile with comparatively fewer proteins showing higher expression at week 3. Several proteins showed consistently higher expression across all three disease groups, including Granzyme A, whereas CCL2 (MCP-1) and IL-15 showed consistently lower expression over time.

Distinct disease immune trajectories

To further explore differences among patients with AML, MDS, and MF, we grouped proteins by biological function (**Supplementary Table S1**). Although differences in protein expression between AML/MDS and MF patients were minor in the first week after transplantation, they diverged in the second week (**Figure 2**). In weeks 2 and 3, proteins in all groups were less expressed in the MF group than in the AML/MDS group. Interestingly,

however, in week 4 this difference appeared to have largely disappeared. These findings suggest short-term downregulation of several proteins in patients with MF.

Disease-specific immune trajectories were also evident when examining individual proteins in these functional groups (**Figure 3**). For example, MF patients had lower expression of several proteins, including IFN-γ, granzymes, and chemokines. In contrast, we observed similar patterns across all disease groups for the pro-inflammatory cytokines IL-6 and IL-8, with values peaking in week 2 and subsequently declining to levels similar to those of healthy controls (**Supplementary Figure S2**). Overall, these data highlight both conserved post-transplant cytokine kinetics and distinct, disease-associated patterns in immune effector proteins.

DISCUSSION

In this exploratory study, we characterized early post-transplant proteomic dynamics in three myeloid malignancies. We observed that the early post-transplant period (the first 4 weeks) is characterized by dynamic, substantial changes in circulating immune-oncology-related proteins. These changes were primarily driven by the time since transplantation, with disease-associated differences emerging when proteins were grouped into functional modules.

Allogeneic stem cell transplantation substantially disrupts homeostatic mechanisms, and we found that the time after transplantation was the primary driver of variation in circulating protein levels in the post-transplant period. Interestingly, we found limited changes in most proteins between weeks 1 and 2 post-transplantation, except for a peak in IL-6 expression. Additionally, many protein levels at week 1 differed from those of healthy controls. These findings suggest that a substantial part of the proteomic shift may occur during conditioning and the immediate peri-transplant period; however, this cannot be confirmed in the absence of pre-conditioning baseline samples.

Other studies have also reported dynamic changes in inflammatory cytokines during the early post-transplant period[13,14]. More specifically, Melenhorst et al. described two cytokine storms: the first peaking when leukocyte concentrations were at their lowest, and the second coinciding with the achievement of full donor lymphocyte chimerism[14]. A similar pattern is observed in our data, with IL-6 and IL-8 levels peaking around week 2. Across studies, the timing of this peak is variable. This could be due to differences in immune reconstitution, as levels of IL-6 are inversely correlated with neutrophil numbers, and other cytokines, such as IL-15 and IL-7, are inversely correlated with absolute T cell counts[14,15]. Together, these findings suggest that early cytokine storms can develop dur-

ing leukopenia, but that their onset and magnitude can depend on pre-transplant factors such as conditioning intensity and *in vivo* and *ex vivo* T cell depletion strategies.

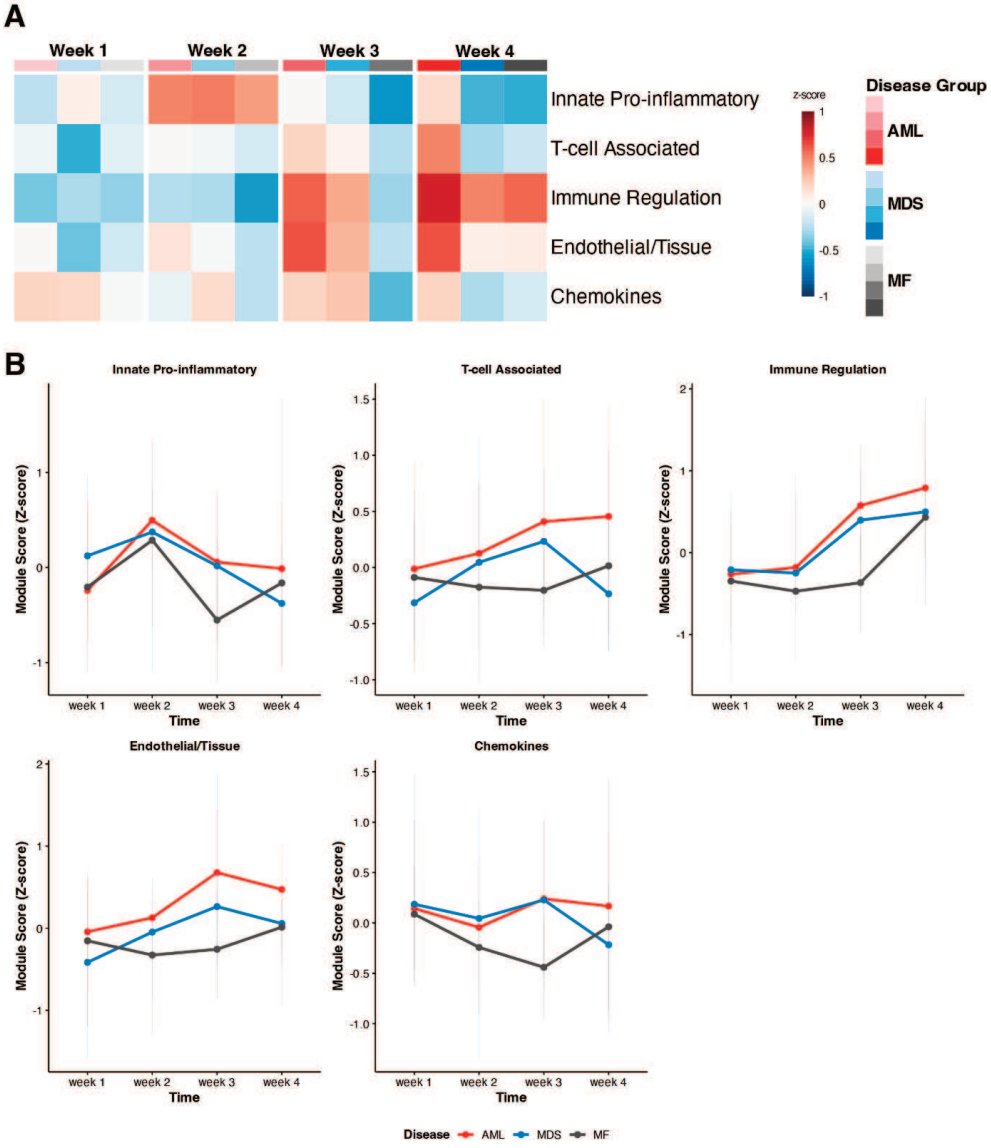


Figure 2. Temporal dynamics of protein module scores across disease groups. **(A)** *Heatmap showing median module scores per disease group and timepoint. Protein modules were defined based on functional categories: Innate Pro-inflammatory, T-cell Associated, Immune Regulation, Endothelial/Tissue, and Chemokines. Values represent Z-score normalized expression. Columns are grouped by timepoint (weeks 1–4) and colored by disease-timepoint combination (AML: red gradient; MDS: blue gradient; MF: grey gradient).* **(B)** *Module score trajectories over time. Lines with points indicate group means per disease. Colors indicate disease group (red: AML; blue: MDS; grey: MF).*

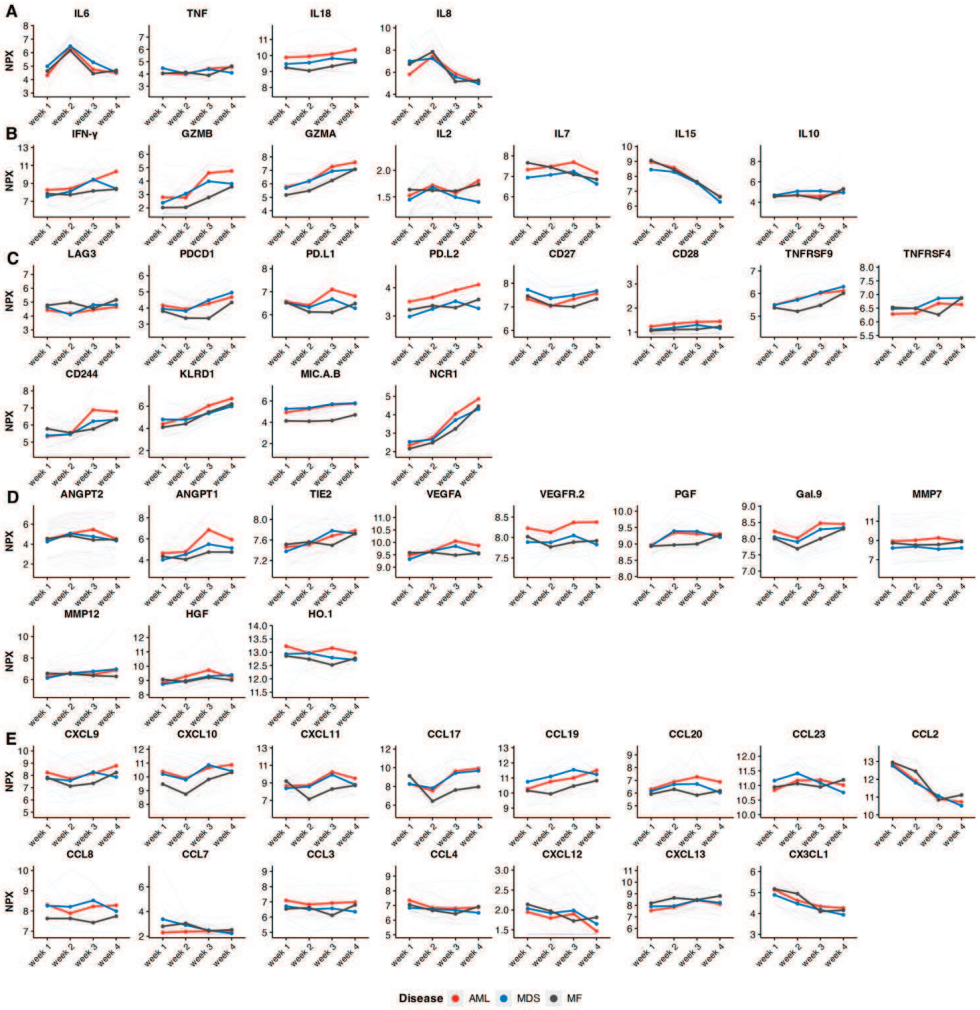


Figure 3. Disease-specific protein expression trajectories by functional module.
Individual protein trajectories across weeks 1–4 post-HSCT, organized by functional module: **(A)** *Innate Pro-inflammatory,* **(B)** *T-cell Associated,* **(C)** *Immune Regulation,* **(D)** *Endothelial/Tissue, and* **(E)** *Chemokines. Thin, transparent lines represent individual patient trajectories; thick lines with points indicate mean NPX values for each disease group. Colors indicate disease (red: AML; blue: MDS; grey: MF). NPX: Normalized Protein eXpression (log2 scale).*

Limited research has examined the effects of underlying diseases on post-transplant proteomics. Min et al. reported that the underlying disease had no significant effect on cytokine profiles[13]. A potential limitation of this study was a large heterogeneity in conditioning intensity. In contrast, we performed our study using a broader 92-plex panel that extends beyond cytokines. In addition, our cohort was treated using a uniform conditioning regimen and graft manipulation platform, reducing procedural heterogeneity. In our analysis, disease-associated differences did become apparent when proteins were grouped into biologically relevant functional modules.

The distinct protein trajectories were most striking in MF patients, where our data suggests transient alterations in early post-transplant immune dynamics relative to AML and MDS. One possible explanation for this temporary suppression is the peri-transplant use of the JAK1/2 inhibitor ruxolitinib in MF patients, which was stopped on day 14 post-transplant. Specifically, the relative downregulation of multiple protein classes during weeks 2 and 3 in MF may reflect temporary suppression of immune activation and/or cytokine signaling. This suppression appeared to be reversible, as protein expression levels at week 4 were comparable between MF and AML, arguing against a sustained defect in immune reconstitution. Consistent with our observations, previous studies have shown reduced IL-6 and IFN-γ after peri-transplant ruxolitinib[3,4,16]. Prior work has also reported decreases in regulatory T cells[16-18], which may align with the modest reduction in IL-10 we observed around week 3. As peri-transplant ruxolitinib is increasingly used in MF[5], it is notable that withdrawal has been associated with rebound inflammation (cytokine storm) and potentially increased GVHD risk[19,20]. In our cohort, we observed no evidence of a cytokine storm following ruxolitinib discontinuation, possibly due to the low ruxolitinib dose. Together, these findings suggest that the timing and reversibility of the protein-expression dip in MF may be attributable to pharmacologic effects rather than MF-intrinsic differences.

We and others have previously shown that peri-transplant ruxolitinib improves outcome by reducing GVHD and NRM[3-5]. Although this study was not powered to correlate changes in protein expression to clinical outcomes, our data may suggest that temporary immunosuppression during the peak of conditioning-induced inflammation may prevent "immune-dysregulation" after allo-HSCT, with a subsequent reduced risk of complications such as infections, GVHD, poor graft function, and endothelial damage. Apart from the sample size, another limitation of this study is that we measured only relative protein expression, which makes it more difficult to compare our findings with those of other studies. In addition, we did not have pre-transplant (pre-conditioning) plasma samples, limiting our ability to establish individual baseline levels and to directly assess how conditioning and peri-transplant treatment altered the proteomic profile relative to the pre-transplant state. On the other hand, to our knowledge, this is one of the most elaborate proteomic profiling studies in this early post-transplant period. Mapping early proteomic changes after transplantation may help identify biological processes that influence immune reconstitution and inflammation. Moreover, multiplex protein panels can be a powerful hypothesis-generating tool for capturing dynamic post-transplant processes that are difficult to assess with single biomarkers.

Future studies should include larger cohorts and integrate proteomic data with long-term clinical outcomes, including GVHD, NRM, and relapse. A key question is whether and to what extent biological events in the first four weeks after transplantation determine later outcomes. However, there are no standardized methods for measuring inflamma-

tion and immune reconstitution after transplantation. Recently, there has been increased attention to the relation between immune subsets and outcomes[21]. Moreover, studies on plasma markers have mostly focused on GVHD only[22]. We propose that systematic measurements of plasma markers, especially during the first weeks after transplantation, will allow us to link immune profiles to outcome and better understand the underlying biology of immune dysregulation, thereby helping to design early immune interventions to prevent GVHD. In conclusion, this study highlights the early post-transplantation period as a phase of profound biological change, driven primarily by time since transplantation, but modulated by disease context and possibly by peri-transplant ruxolitinib. Ultimately, insights into early plasma proteomics and their associations with outcomes may inform optimal timing, duration, and patient selection for peri-transplant interventions.

REFERENCES

1. Carreras E, Dufour C, Mohty M, Kroeger N. The EBMT handbook: hematopoietic stem cell transplantation and cellular therapies: EBMT, European Society for Blood and Marrow Transplantation ; Fondation José Carreras contre la leucémie ; Springer Open, Springer International Publishing : Imprint : Springer; 2019.
2. de Witte M, Mooyaart JE, Blaise D, et al. The 51(st) Annual Meeting of the European Society for Blood and Marrow Transplantation: Physicians - Oral Session (O008-O166). *Bone Marrow Transplant*. 2025;60(Suppl 1):19-182.
3. Kroger N, Shahnaz Syed Abd Kadir S, Zabelina T, et al. Peritransplantation Ruxolitinib Prevents Acute Graft-versus-Host Disease in Patients with Myelofibrosis Undergoing Allogenic Stem Cell Transplantation. *Biol Blood Marrow Transplant*. 2018;24(10):2152-2156.
4. Ali H, Tsai NC, Synold T, et al. Peritransplantation ruxolitinib administration is safe and effective in patients with myelofibrosis: a pilot open-label study. *Blood Adv*. 2022;6(5):1444-1453.
5. Wall SA, Tamari R, DeFilipp Z, Hobbs GS. Optimization of allogeneic hematopoietic cell transplantation for patients with myelofibrosis treated with ruxolitinib: eligibility, best practices, and improving transplant outcomes. *Ann Hematol*. 2025;104(4):2125-2141.
6. Delemarre EM, Smits HM, van Baarle D, et al. Proteomic Signatures Over Age Reveal Significant Changes From Infancy Till Late Adulthood. *Adv Biol (Weinh)*. 2026;10(1):e00455.
7. Chaleff S, Otto M, Barfield RC, et al. A large-scale method for the selective depletion of alphabeta T lymphocytes from PBSC for allogeneic transplantation. *Cytotherapy*. 2007;9(8):746-754.
8. Li Pira G, Malaspina D, Girolami E, et al. Selective Depletion of alphabeta T Cells and B Cells for Human Leukocyte Antigen-Haploidentical Hematopoietic Stem Cell Transplantation. A Three-Year Follow-Up of Procedure Efficiency. *Biol Blood Marrow Transplant*. 2016;22(11):2056-2064.
9. Nevola K, Sandin M, Guess J, et al. Olink-Analyze: Facilitate Analysis of Proteomic Data from Olink. 2025;4.4.0.
10. Lundberg M, Eriksson A, Tran B, Assarsson E, Fredriksson S. Homogeneous antibody-based proximity extension assays provide sensitive and specific detection of low-abundant proteins in human blood. *Nucleic Acids Res*. 2011;39(15):e102.
11. Assarsson E, Lundberg M, Holmquist G, et al. Homogenous 96-plex PEA immunoassay exhibiting high sensitivity, specificity, and excellent scalability. *PLoS One*. 2014;9(4):e95192.
12. Smits HM, Delemarre EM, Pandit A, et al. The BAMBOO method for correcting batch effects in high throughput proximity extension assays for proteomic studies. *Sci Rep*. 2025;15(1):1498.
13. Min CK, Lee WY, Min DJ, et al. The kinetics of circulating cytokines including IL-6, TNF-alpha, IL-8 and IL-10 following allogeneic hematopoietic stem cell transplantation. *Bone Marrow Transplant*. 2001;28(10):935-940.
14. Melenhorst JJ, Tian X, Xu D, et al. Cytopenia and leukocyte recovery shape cytokine fluctuations after myeloablative allogeneic hematopoietic stem cell transplantation. *Haematologica*. 2012;97(6):867-873.
15. Thiant S, Yakoub-Agha I, Magro L, et al. Plasma levels of IL-7 and IL-15 in the first month after myeloablative BMT are predictive biomarkers of both acute GVHD and relapse. *Bone Marrow Transplant*. 2010;45(10):1546-1552.
16. Parampalli Yajnanarayana S, Stubig T, Cornez I, et al. JAK1/2 inhibition impairs T cell function in vitro and in patients

with myeloproliferative neoplasms. *Br J Haematol*. 2015;169(6):824-833.

17. Massa M, Rosti V, Campanelli R, Fois G, Barosi G. Rapid and long-lasting decrease of T-regulatory cells in patients with myelofibrosis treated with ruxolitinib. *Leukemia*. 2014;28(2):449-451.
18. Stubig T, Alchalby H, Ditschkowski M, et al. JAK inhibition with ruxolitinib as pretreatment for allogeneic stem cell transplantation in primary or post-ET/PV myelofibrosis. *Leukemia*. 2014;28(8):1736-1738.
19. Palandri F, Tiribelli M, Breccia M, et al. Ruxolitinib rechallenge in resistant or intolerant patients with myelofibrosis: Frequency, therapeutic effects, and impact on outcome. *Cancer*. 2021;127(15):2657-2665.
20. Shanavas M, Popat U, Michaelis LC, et al. Outcomes of Allogeneic Hematopoietic Cell Transplantation in Patients with Myelofibrosis with Prior Exposure to Janus Kinase 1/2 Inhibitors. *Biol Blood Marrow Transplant*. 2016;22(3):432-440.
21. Hammoudi T, Nucera S, Troullioud Lucas AG, et al. Harmonized immune recovery monitoring after HCT: evidence and practical guidance from the Westhafen Intercontinental Group. *Blood Adv*. 2025;9(23):6141-6157.
22. Akahoshi Y, Spyrou N, Hoepting M, et al. Flares of acute graft-versus-host disease: a Mount Sinai Acute GVHD International Consortium analysis. *Blood Adv*. 2024;8(8):2047-2057.

Supplementary Table S1

Marker	Eponym	Pathway	Summary
IL6		Innate/pro-inflammatory cytokines	Pleiotropic cytokine produced by many cell types that induces acute-phase responses, B-cell maturation, and regulation of inflammation.
TNF		Innate/pro-inflammatory cytokines	Pro-inflammatory cytokine mainly secreted by macrophages that mediates systemic inflammation, fever, and apoptosis through TNF receptors.
IL18		Innate/pro-inflammatory cytokines	Pro-inflammatory cytokine involved in epithelial barrier repair, capable of stimulating IFNγ production and regulating Th1, Th2 and NK cell responses
IL8	CXCL8	Innate/pro-inflammatory cytokines	Chemokine that acts as a potent chemoattractant and activator of neutrophils at sites of inflammation.
IL10		T-cell associated cytokines	Anti-inflammatory cytokine produced by regulatory T cells and myeloid cells that suppresses pro-inflammatory cytokine synthesis and antigen presentation.
IFNγ		T-cell associated cytokines	Type II interferon secreted by activated T and NK cells that activates macrophages, upregulates MHC expression, and exerts antiviral, antimicrobial and antitumor effects.
Granzyme B		T-cell associated cytokines	Serine protease in cytotoxic granules of NK cells and cytotoxic T lymphocytes that triggers apoptosis in target cells by cleaving caspases and other substrates.
Granzyme A		T-cell associated cytokines	Serine protease in cytotoxic lymphocyte granules that induces caspase-independent cell death.
IL7		T-cell associated cytokines	Homeostatic cytokine essential for lymphocyte development and survival, particularly for B and T cell development
IL15		T-cell associated cytokines	Cytokine that supports development and survival of NK cells and T cells, sharing receptor components and functions with IL-2.
IL2		T-cell associated cytokines	Cytokine produced by activated T cells, important for proliferation of T and B cells.
LAG3		Immune Regulation	Inhibitory receptor on activated T cells and Tregs, dampens T-cell proliferation and activation, contributing to immune checkpoint control
PDCD1	PD-1	Immune Regulation	Inhibitory receptor on activated T cells, can directly inhibit T-cell activation
PDL1	CD274	Immune Regulation	Cell-surface ligand for PD-1 expressed on immune and non-immune cells, inhibits T-cell activation and cytokine production.
PDL2	PDCD1LG2	Immune Regulation	Cell-surface ligand for PD-1 mainly expressed on dendritic cells and macrophages, modulates T-cell activation and peripheral tolerance.

Supplementary Table S1 (*continued*)

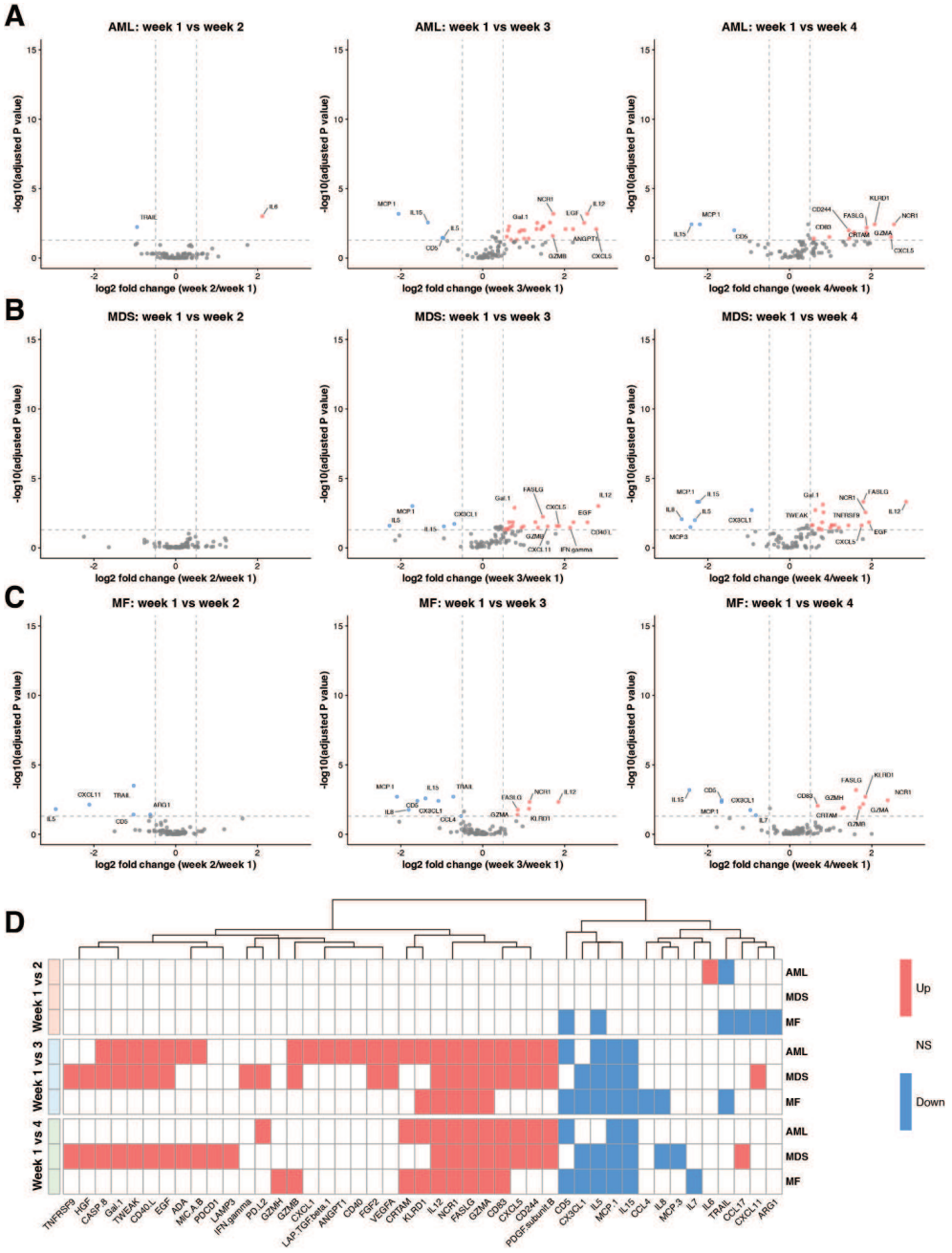
Marker	Eponym	Pathway	Summary
CD27		Immune Regulation	Co-stimulatory receptor on T, B and NK cells, required for generation and long-term maintenance of T-cell immunity
CD28		Immune Regulation	Constitutive co-stimulatory receptor on T cells that binds CD80/CD86 on antigen-presenting cells to provide essential second signals for T-cell activation.
TNFRSF9	4-1BB, CD137	Immune Regulation	Inducible co-stimulatory receptor, contributes to clonal expansion, survival and development of T cells
TNFRSF4	OX40	Immune Regulation	Co-stimulatory receptor implicated in long-term T-cell immunity
CD244	2B4	Immune Regulation	Surface receptor on NK cells and some T cells, mediates non-MHC complex restricted killing
KLRD1	CD94	Immune Regulation	Surface receptor on NK cells, pairs with NKG2 family members to recognize HLA-E and modulate NK-cell activation or inhibition.
MICAB		Immune Regulation	Stress-inducible MHC class I-related molecules expressed on damaged or transformed cells, serve as ligands for the activating receptor NKG2D on NK and T cells.
NCR1	NKp46	Immune Regulation	Natural cytotoxicity receptor, expressed mainly on NK cells, recognizes viral and tumor ligands and triggers NK-cell activation.
ANGPT2		Endothelial/Tissue Injury	Context-dependent angiopoietin that often antagonizes ANGPT1–TIE2 signaling, promoting vascular remodeling, leakage, and inflammation.
ANGPT1		Endothelial/Tissue Injury	Angiopoietin ligand that activates TIE2 on endothelial cells to stabilize blood vessels, reduce permeability, and maintain quiescent vasculature.
TIE2	TEK	Endothelial/Tissue Injury	Cell-surface receptor for ANGPT1, ANGPT2, and ANGPT4, regulates angiogenesis, endothelial survival, migration and vascular integrity.
VEGFA		Endothelial/Tissue Injury	Key vascular endothelial growth factor that stimulates endothelial proliferation, migration, and increased vascular permeability in angiogenesis.
VEGFR2	KDR	Endothelial/Tissue Injury	Principal signaling receptor for VEGFA on endothelial cells that mediates most of its angiogenic and permeability responses.
PGF		Endothelial/Tissue Injury	VEGF-family growth factor active in angiogenesis and endothelial cell growth, stimulating their proliferation and migration, binds to the receptor FLT1/VEGFR-1.
LGALS9		Endothelial/Tissue Injury	β-galactoside-binding lectin that can modulate immune and endothelial cells, including inducing apoptosis or exhaustion of T cells via receptors such as TIM-3.

Supplementary Table S1 (*continued*)

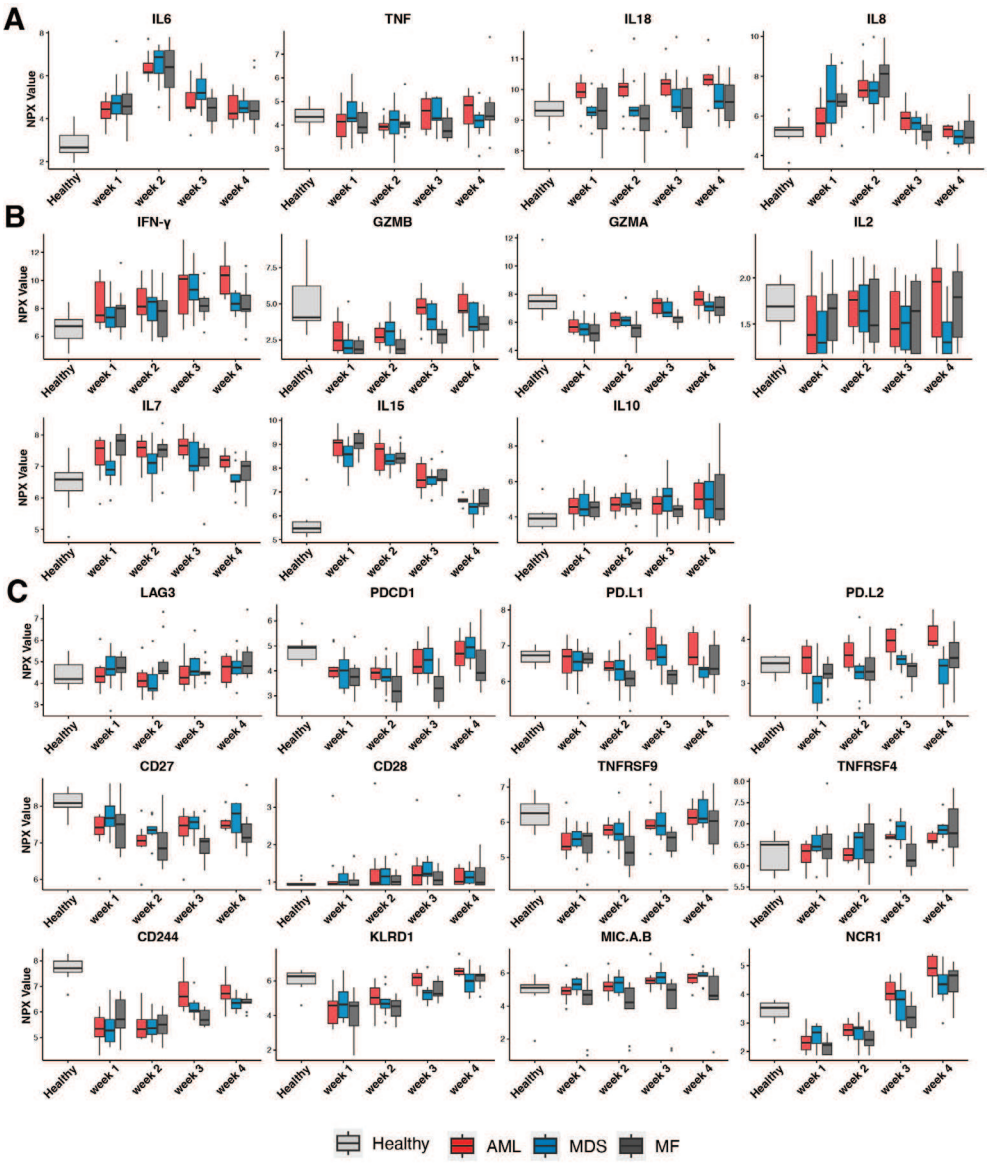
Marker	Eponym	Pathway	Summary
MMP7		Endothelial/Tissue Injury	Secreted matrix metalloproteinase that degrades components of the extracellular matrix and cell-surface proteins, contributing to tissue remodeling and injury.
MMP12		Endothelial/Tissue Injury	Macrophage elastase that degrades elastin and other matrix proteins and is implicated in inflammatory tissue destruction, especially in lung and vascular disease.
HGF		Endothelial/Tissue Injury	Pleiotropic growth factor, promotes cell proliferation, motility, and survival, driving tissue repair and angiogenesis via the MET receptor.
HO1	HMOX1	Endothelial/Tissue Injury	Stress-inducible enzyme, degrades heme to biliverdin, carbon monoxide, and free iron, providing cytoprotective, antioxidant, and anti-inflammatory effects.
CXCL9		Chemokines	IFN-γ–inducible chemokine that binds CXCR3 to recruit activated T cells and NK cells to inflamed tissues.
CXCL10		Chemokines	Chemokine induced by interferons that signals via CXCR3 to attract Th1 cells, cytotoxic T cells, NK cells, and monocytes.
CXCL11		Chemokines	High-affinity CXCR3 ligand induced by interferons that chemoattracts activated T cells and NK cells and promotes Th1-polarized responses.
CCL17		Chemokines	Binds CCR4 to attract Th2 cells and regulatory T cells to inflamed tissues and lymphoid organs.
CCL19		Chemokines	CCR7 ligand, chemotactic for T cells and B cells, guides lymphocyte homing and recirculation to lymphoid tissues
CCL20		Chemokines	CCR6 ligand that recruits immature dendritic cells, Th17 cells and certain B cells, particularly to mucosal and epithelial surfaces.
CCL23		Chemokines	Attracts resting T cells, monocytes, and neutrophils and is produced mainly by myeloid cells, signals mainly via CCR1
CCL2	MCP1	Chemokines	Recruits monocytes, memory T cells and dendritic cells to sites of tissue injury or infection.
CCL3	MIP-1α	Chemokines	Produced by monocytes and T cells, attracts multiple leukocyte subsets and binds CCR1, CCR4 and CCR5, contributing to antiviral and inflammatory response
CCL4	MIP-1β	Chemokines	Acts as a chemoattractant for NK cells, monocytes and other leukocytes
CCL7	MCP-3	Chemokines	Signals through multiple CCRs to attract monocytes, eosinophils, basophils, NK cells and activated T cells.
CCL8	MCP-2	Chemokines	Chemoattracts monocytes, lymphocytes, basophils and eosinophils through several CCRs.

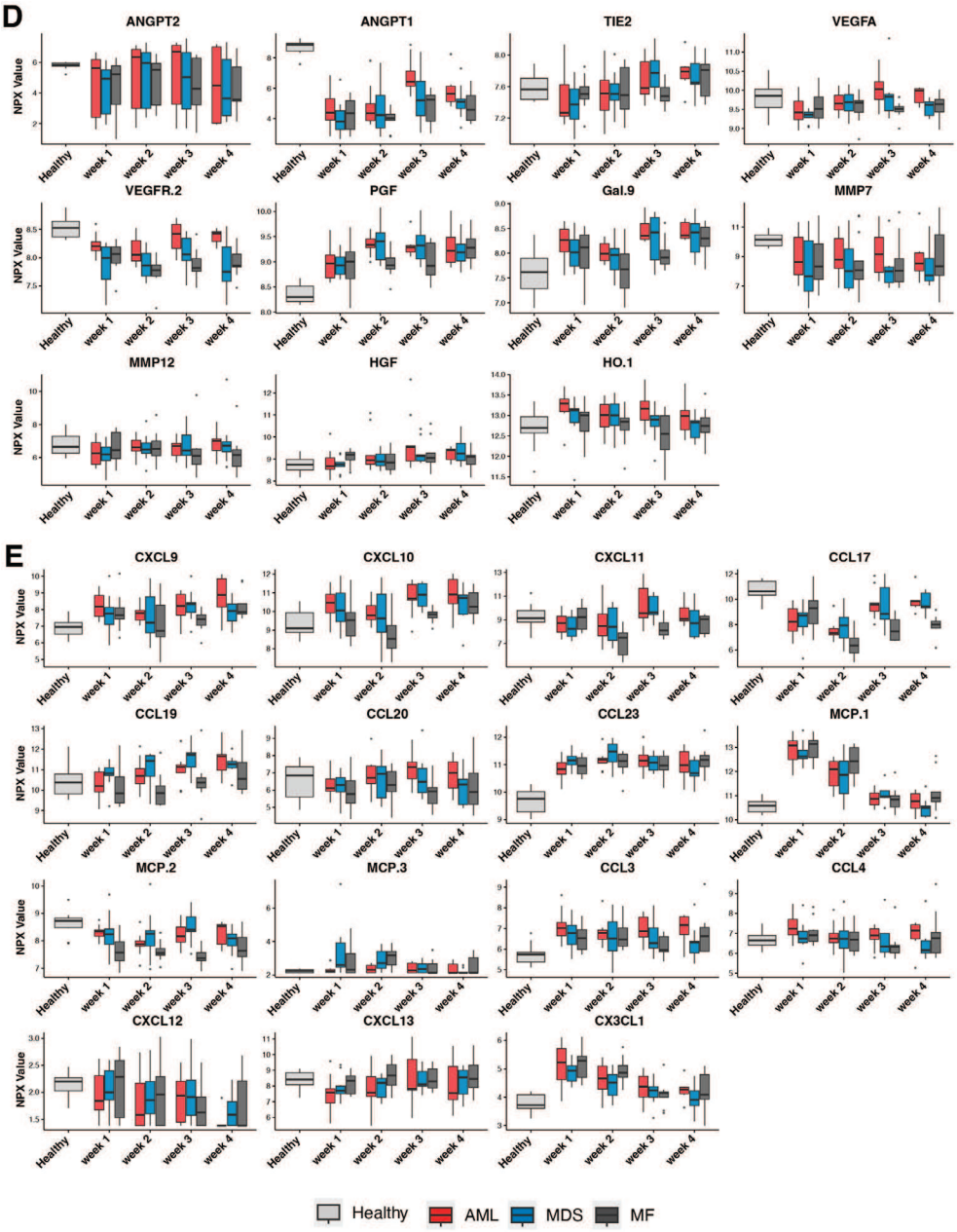
Supplementary Table S1 (*continued*)

Marker	Eponym	Pathway	Summary
CXCL12	SDF-1	Chemokines	Binds CXCR4 and CXCR7 to regulate hematopoietic stem-cell retention, organ development, and lymphocyte trafficking.
CXCL13	BCA-1	Chemokines	Attracts CXCR5-positive B cells and T follicular helper cells and organizes B-cell follicles and germinal centers.
CX3CL1		Chemokines	Atypical chemokine, binds CX3CR1 on monocytes, NK cells and cytotoxic T cells to promote adhesion to and migration along activated endothelium.

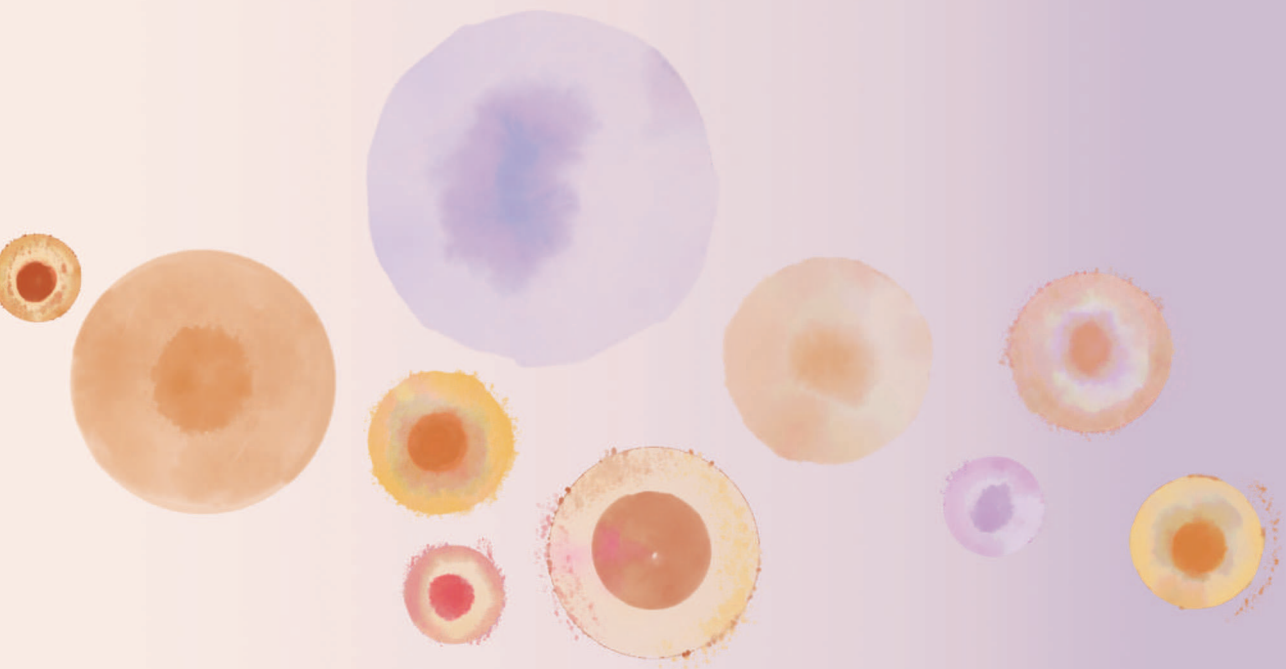


Supplementary Figure S1. Differential protein expression analysis across timepoints. *(A–C) Volcano plots showing differentially expressed proteins comparing week 1 to weeks 2, 3, and 4 in (A) AML, (B) MDS, and (C) MF patients. X-axis shows log2 fold change; y-axis shows −log10 FDR-adjusted p-value. Horizontal dashed line indicates FDR = 0.05; vertical dashed lines indicate absolute log2FC = 0.5. Red points: significantly upregulated proteins; blue points: significantly downregulated proteins; grey points: non-significant. Protein names are labeled for significant proteins. (D) Summary heatmap of protein regulation patterns across all comparisons. Red: upregulated (FDR < 0.05, log2FC > 0.5); blue: downregulated (FDR < 0.05, log2FC < −0.5); white: not significant. Columns are clustered hierarchically; rows are grouped by timepoint comparison. Statistical testing performed using Wilcoxon rank-sum test with FDR correction.*


A
IL6
TNF
IL18
IL8
B
IFN-γ
GZMB
GZMA
IL2
IL7
IL15
IL10
C
LAG3
PDCD1
PD.L1
PD.L2
CD27
CD28
TNFRSF9
TNFRSF4
CD244
KLRD1
MIC.A.B
NCR1
NPX Value
Healthy
week 1
week 2
week 3
week 4
Healthy
AML
MDS
MF



Supplementary Figure S2: Plasma protein expression levels across disease groups and time points *Boxplots showing normalized protein expression (NPX) values for individual proteins measured in plasma samples from patients with acute myeloid leukemia (AML, n = 10), myelodysplastic syndrome (MDS, n = 10), and myelofibrosis (MF, n = 13), compared to healthy controls (n =10). Each panel represents a single protein, with NPX values plotted across different time points post-transplantation (weeks) and baseline (healthy controls). Boxes represent the interquartile range (IQR), with the median indicated by the center line. Whiskers extend to 1.5× IQR, and outliers are shown as individual points. Colors indicate disease groups. Proteins are grouped by functional category.* **(A)** *Innate Pro-inflammatory,* **(B)** *T-cell Associated,* **(C)** *Immune Regulation,* **(D)** *Endothelial/Tissue, and* **(E)** *Chemokines.*



6

Platform-Imprinted Transcriptional and Clonal Remodeling of αβ and γδT Cells After Allogeneic Transplantation

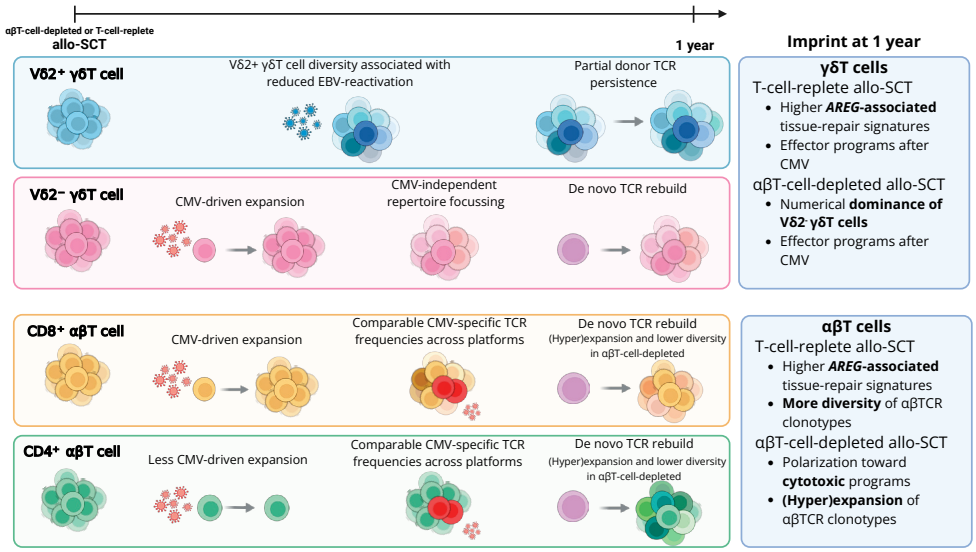
A.H.G. Stuut[1#], P. Brazda[1#], A. Janssen[1, 2#], A. Vyborova[1], E. Karaiskaki[1], F. Keramati[1], C.Nijssen[2], D.A. de Bont[1], M.J.T. Nicolasen[1], L.C.D.E. Gatti[1], T.J.A. Hutten[3], J. Yildiz[3], H.T. Spierings[3], G.C.M. Straetemans[2], D.X. Beringer[1], S. Pagliuca[4], H.G. Stunnenberg[5], Z. Sebesyten[1], J. Drylewicz[1], M.A. de Witte[1,2*], J. Kuball[1,2*]

[1]Center for Translational Immunology, University Medical Center Utrecht, Utrecht, The Netherlands
[2]Department of Hematology, University Medical Center Utrecht, Utrecht, The Netherlands
[3]Central Diagnostic Laboratory, University Medical Center Utrecht, Utrecht, The Netherlands
[4]Hematology Department, Nancy University Hospital & UMR-CNRS 7365, IMOPA, University of Lorraine, Vandoeuvre-lès-Nancy, France
[5]Princess Máxima Center for Pediatric Oncology, Utrecht, The Netherlands
[#]These authors share first authorship
*These authors share senior authorship

Revised version submitted

ABSTRACT

Immune reconstitution after allogeneic hematopoietic stem cell transplantation is influenced by graft composition and viral reactivation, but the combined long-term impact on αβ and γδT cells remains unclear. We analyzed a cohort of 213 patients receiving either αβT cell-depleted grafts (n=146; graft engineering that removes donor αβT cells) or T cell-replete grafts (n=67; containing donor T cells). Longitudinal immune phenotyping was integrated with bulk and single-cell TCR repertoire and transcriptomic profiling. CMV reactivation was associated with expansion of $CD8^+$ αβT cells across both transplant types and with numerical dominance of $V\delta2^-$ γδT cells specifically in αβT cell-depleted recipients. $V\delta2^-$ γδT cells underwent early polyclonal expansion followed by repertoire focusing, independent of CMV, whereas αβT cells remained clonally restricted. Reduced early $V\delta2^+$ γδTCR diversity was associated with EBV reactivation. Single-cell and TCR tracking analyses revealed long-term persistence of donor-derived $V\delta2^+$ γδTCRs, whereas $V\delta1^+$ γδ and αβT cell repertoires were predominantly rebuilt de novo. Despite de novo rebuilding, αβTCR repertoire diversity diverged by platform at one year: αβT cell-depleted recipients exhibited marked (hyper)expansion of αβTCR clonotypes and lower diversity than T cell-replete recipients, indicating a durable imprint of graft engineering on αβTCR-clonality. Transcriptomic profiling showed that post-transplant T cells predominantly adopted effector programs, with platform-dependent polarization toward cytotoxic signatures in αβ T cell–depleted recipients and toward *AREG*-associated tissue-repair signatures in T cell–replete recipients, consistent with wound-healing functions. In conclusion, long-term αβ and γδT cell reconstitution diverge by graft type, with viral reactivation primarily amplifying expansion rather than fundamentally reshaping repertoire structure.



INTRODUCTION

A well-balanced immune reconstitution is critical for the success of allogeneic hematopoietic stem cell transplantation (allo-HSCT), as it determines a patient's ability to control complications such as graft-versus-host disease (GVHD) and viral infections. However, immune reconstitution dynamics vary substantially across transplantation platforms, with pronounced differences between αβT cell-depleted and T cell-replete graft[1-6]. αβT-cell-depleted grafts reduce transfer of mature donor αβT cells to mitigate GVHD but may delay adaptive T cell recovery, while T-cell-replete grafts provide immediate donor T cell immunity but carry a higher risk of alloreactivity[1]. These platform-specific differences affect the timing and composition of immune subset recovery and, consequently, host responses to viral challenges such as cytomegalovirus (CMV) and Epstein–Barr virus (EBV), both of which frequently reactivate post-transplantation and remain major contributors to morbidity and mortality[7,8].

Most studies examining the interplay between immune recovery and viral reactivation have been conducted in T cell-replete settings. In this context, early reconstitution of NK cells and $CD4^+$ αβT cells has been associated with protection against CMV reactivation, but not EBV reactivation[9]. CMV reactivation has been shown to drive numerical expansion and effector differentiation of $V\delta2^-$ γδT cells and $CD8^+$ αβT cells[9-14], accompanied by clonal proliferation and reduced TCR repertoire diversity, as revealed by next-generation sequencing studies[15-19]. In contrast, EBV reactivation typically occurs in the setting of insufficient immune control. It does not promote immune recovery, which has motivated the development of EBV-specific adoptive T cell therapies to prevent post-transplant lymphoproliferative disease[20]. However, as transplantation platforms evolve, these established immune–virus relationships may no longer directly translate.

This has become increasingly relevant with the growing clinical implementation of ex vivo αβT cell-depleted grafts[21,22], which introduce fundamentally distinct immune reconstitution dynamics[1,2]. Profound delay of αβT cell recovery shifts early immune responses toward innate and unconventional lymphocyte populations, including NK and γδT cells[2,4,6,23-25]. In this αβT cell-depleted setting, viral reactivations are likely to shape immune phenotypes differently than in T cell-replete platforms. For instance, CMV reactivation in αβT cell-depleted or umbilical cord blood recipients has been associated with the expansion of memory-like $CD57^+NKG2C^+$ NK cells[26-29]. Despite these emerging observations, systematic comparative analyses across platforms and immune subsets remain limited.

To address this gap, we investigated how αβT cell–depleted versus T cell–replete transplantation platforms shape post-transplant immune reconstitution, and how CMV and EBV reactivations modulate this process. We performed longitudinal immune profiling and integrated bulk and single-cell TCR repertoire and transcriptomic analyses to charac-

terize reconstitution of both αβ and γδT cell compartments across platforms. In addition, we performed single-cell RNA sequencing on donor samples and on recipient samples one year post-transplantation from both platforms in patients with CMV reactivation to characterize phenotypic and transcriptional changes in T cell subsets. We demonstrate that the transplantation platform establishes the baseline long-term framework of post-transplant immunity. At the same time, CMV reactivation amplifies this framework by driving distinct transcriptional and functional polarization of expanding $CD8^+$ αβ and $V\delta2^-$ γδT cell subsets.

MATERIALS & METHODS

Clinical cohort

Patients with hematological malignancies who received an αβT cell-depleted stem cell transplantation at the University Medical Center Utrecht (UMCU) between 2015 and 2017 were included in this retrospective study. Conditioning consisted of anti-thymocyte globulin (ATG), fludarabine, and busulfan. αβT cell depletion was performed using anti-αβTCR antibodies and the CliniMACS system, allowing a maximum residual αβT cell dose of 5×10^5 cells/kg. Mycophenolate mofetil (MMF) was used as single GVHD prophylaxis, and pre-emptive donor lymphocyte infusion (DLI; 1×10^5 $CD3^+$ T cells/kg) was administered at three months post-transplantation in eligible patients. As a comparator group, T cell-replete transplant recipients treated at UMCU between 2011 and 2018 were included after either reduced-intensity or myeloablative conditioning with standard GVHD prophylaxis. Peripheral blood stem cells were used in both cohorts. Immune reconstitution and viral reactivations were monitored longitudinally as part of routine care, with immune subset recovery assessed by flow cytometry. CMV reactivation was defined as >250 IU/mL, and EBV reactivation as >1000 IU/mL by PCR. All patients provided written informed consent, and the study was approved by the local ethics committee (METC nr 21-322, UMCU) (see[30,31] and **Supplementary Material**).

T cell receptor repertoire sequencing and single-cell profiling

To characterize the clonal composition and transcriptional programs of αβ and γδ T cell subsets during post-transplant immune reconstitution, we combined bulk next-generation sequencing of the T cell receptor (TCR) with paired single-cell RNA sequencing (scRNA-seq) and single-cell TCR sequencing (scTCR-seq). These complementary approaches enabled quantitative assessment of repertoire diversity, clonal expansion, and functional polarization at both population and single-cell resolution. TCRβ and TCRδ repertoires were sequenced from flow-sorted $CD4^+$ αβ, $CD8^+$ αβ, and γδT cell subsets using established amplification protocols[32], followed by Illumina-based sequencing. Productive CDR3 sequences were extracted using MiXCR[33], normalized for sequencing depth, and analyzed with the immunarch package[34]. For single-cell profiling, αβ and γδT cells were

flow-sorted from PBMCs collected approximately one year post-transplantation and processed using the 10x Genomics Chromium 5′ platform with paired V(D)J enrichment, including custom γδTCR primers. scRNA-seq data were processed with Cell Ranger and analyzed in Seurat[35-38], with reference-based cell-type annotation using Azimuth[37,39]. Furthermore, we used the T CellAnnoTator (TCAT) pipeline to characterize functional programs in T cells[40]. αβTCRs were screened for CMV specificity using the scRepertoire and Trex packages[41,42], which annotate αβTCRs with epitope data from VDJdb, McPAS-TCR, IEDB, and PIRD databases[43-46]. Complete experimental protocols and detailed analytical workflows for TCR sequencing, scRNA-seq, and scTCR-seq are provided in the **Supplementary Material**.

RESULTS

CMV-driven divergence in long-term T cell recovery across transplantation platforms

To compare immune reconstitution following αβT cell-depleted- (n = 146) versus T cell-replete allo-HSCT (n = 67) (baseline characteristics in **Table 1**), we longitudinally assessed the numerical recovery of $CD8^+$ αβT cells, $CD4^+$ αβT cells, $V\delta2^+$ γδT cells, and $V\delta2^-$ γδT cells over the first three years post-transplantation. Given the known impact of CMV reactivation on post-transplant immunity[11,15], patients were stratified by CMV reactivation status. CMV reactivation occurred at 27 days (median, range 0–202) after αβT cell-depleted and 33 days (median, range 3–237) after T cell-replete transplantation. In patients without CMV reactivation, $CD4^+$ and $CD8^+$ αβT cells reconstituted more rapidly and reached higher absolute counts after T cell-replete transplantation (**Figure 1A, B**). In CMV-reactivated patients, a distinct numerical recovery pattern emerged. $CD8^+$ αβT cells expanded markedly in both transplant platforms (**Figure 1C,D; Supplementary Figure S1**). In contrast, $CD4^+$ αβT cell recovery was slow and was not augmented by CMV reactivation (**Figure 1C,D**). Across both platforms, the $V\delta2^+/V\delta2^-$ γδT cell ratio declined over time, with a sustained inversion in patients who received an αβT cell-depleted allograft and/or experienced CMV reactivation (**Supplementary Table S1**). Notably, from the earliest phase of immune reconstitution (median day 23), CMV reactivation in the αβT cell-depleted platform was associated with a sustained numerical expansion of $V\delta2^-$ γδT cells, which resulted in an inversion of the $V\delta2^+/V\delta2^-$ γδT cell ratio that persisted for up to three years (**Figure 1C; Supplementary Figure S1A**). Alongside $CD8^+$ αβT and $V\delta2^-$ γδT cells, NK cells also expanded in association with CMV reactivation. This effect was significant in the αβT cell-depleted platform ($p = 0.010$; **Supplementary Figure S1A**) and similarly observed in the T cell-replete platform (**Supplementary Figure S1B**). B cell numbers were unaffected by CMV reactivation in both platforms. Together, these data demonstrate that while CMV reactivation serves as a strong numerical amplifier of $CD8^+$

Table 1. Baseline characteristics

	Ex vivo αβT-cell depleted N = 146	T-cell-replete N = 67	p-value
Median age (IQR)	53 (43, 64)	53 (45, 62)	0.84[1]
Male, n (%)	95 (65%)	47 (70%)	0.47[2]
Median follow-up post allo-HSCT in months (IQR)	35 (6, 60)	60 (27, 100)	<0.001[1]
Year of allo-HSCT, n (%)			<0.001[2]
2011-2015	53 (36%)	55 (82%)	
2016-2022	93 (64%)	12 (18%)	
Disease, n (%)			0.22[2]
ALL	21 (14%)	8 (12%)	
AML/MDS RAEB2	48 (33%)	20 (30%)	
LYMPHOMA	20 (14%)	19 (28%)	
MDS	14 (10%)	6 (9%)	
MF	14 (10%)	6 (9%)	
MM	17 (12%)	3 (5%)	
Others	12 (8%)	5 (8%)	
Donor type, n (%)			0.057[2]
MRD 10/10	29 (20%)	20 (30%)	
MUD 10/10	90 (62%)	42 (63%)	
MMUD 9/10	27 (18%)	5 (8%)	
CMV serostatus, n (%)			0.70[2]
R-/D-	55 (38%)	20 (30%)	
R-/D+	18 (12%)	8 (12%)	
R+/D-	22 (15%)	11 (16%)	
R+/D+	51 (35%)	28 (42%)	
EBV serostatus, n (%)			0.56[2]
R-/D-	1 (1%)	2 (3%)	
R-/D+	12 (8%)	3 (5%)	
R+/D-	14 (10%)	6 (9%)	
R+/D+	111 (76%)	51 (80%)	
R+/Unknown	8 (6%)	2 (3%)	
ATG received, n (%)	146 (100%)	48 (72%)	<0.001[2]

IQR – inter quartile range; allo-HSCT – allogeneic hematopoietic stem cell transplantation; ALL – acute lymphatic leukemia; AML – acute myeloblastic leukemia; MDS – myelodysplastic syndrome; MF – myelofibrosis; MM – multiple myeloma; MRD – matched related donor; MUD – matched unrelated donor; CMV – cytomegalovirus; R – recipient; D – donor; EBV – Epstein-Barr Virus; ATG – anti-thymocyte globulin

αβT cells across transplant platforms, αβT cell depletion uniquely imprints a long-lasting inversion of the Vδ2$^+$/Vδ2$^-$ γδT cell balance.

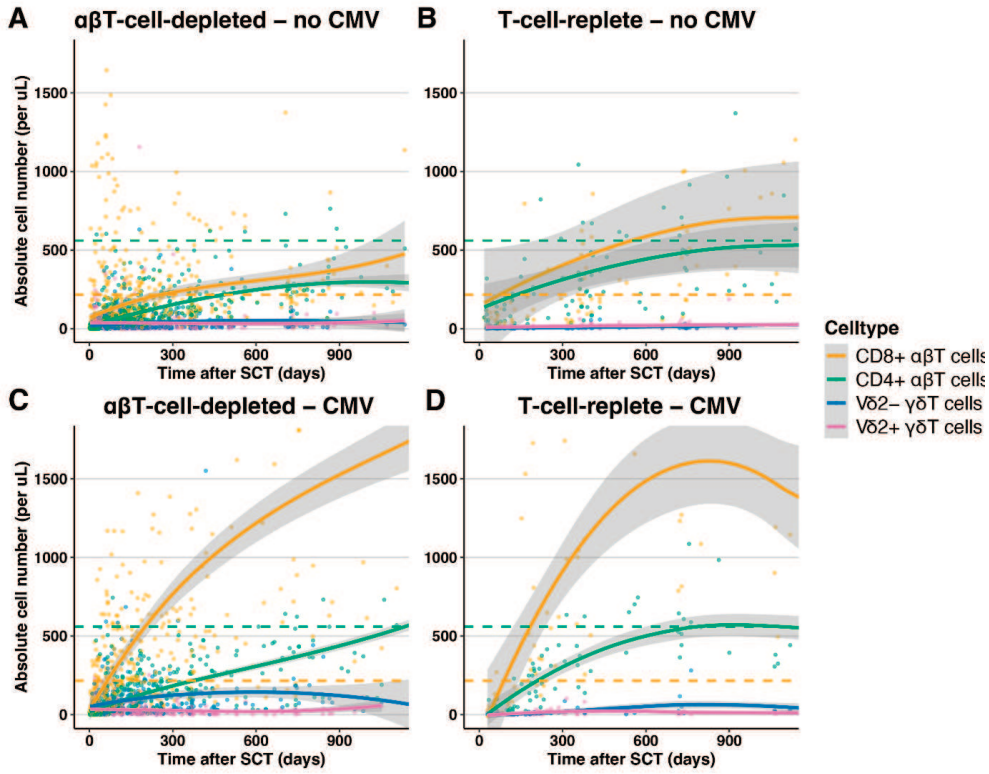


Figure 1. T cell reconstitution after αβT-cell-depleted allo-HSCT and T-cell-replete allo-SCT, stratified by CMV reactivation. *Numerical reconstitution of CD8$^+$ αβT cells (ref values 216 – 499), CD4$^+$ αβT cells (ref values 560 – 1067), Vδ2$^-$ T cells and Vδ2$^+$ T cells (ref values total γδ T cells 20-120) after αβT-cell-depleted allo-SCT or T-cell replete allo-SCT, stratified by CMV reactivation.* ***(A)*** *Patients received αβT-cell-depleted allo-SCT and did not have CMV reactivation (n=83),* ***(B)*** *patients received T-cell replete allo-SCT and did not have CMV reactivation (n=36),* ***(C)*** *patients received αβT-cell-depleted allo-SCT and had CMV reactivation (n=59), and* ***(D)*** *patients received T-cell replete allo-SCT and had CMV reactivation (n=27). All available clinical laboratory data are shown with LOESS curves (span = 1), and 95% confidence intervals are shown. Dashed line: lower limits of reference values for CD8$^+$ αβT cells (orange) and CD4+ αβT cells (green).*

γδ and αβT cell repertoires follow fundamentally distinct rebuilding rules after αβT cell-depleted transplantation

To define clonal rebuilding dynamics, we performed longitudinal bulk TCR sequencing in a subset of αβT cell-depleted transplant recipients (n = 30). Repertoire evenness was quantified using the D75 index, a repertoire diversity metric defined as the minimum number of unique clonotypes required to account for 75% of total TCR sequencing reads, with higher values indicating a more diverse, less oligoclonal repertoire. In healthy donors, Vδ2$^-$ γδT cells displayed a median D75 of 6.5, whereas Vδ2$^+$ γδT cells had a median D75 of 39.5. After transplantation, both γδT subsets exhibited markedly higher early diversity before day 100 (Vδ2$^-$ median 60.5; Vδ2$^+$ median 90), followed by a significant contraction toward donor-like values beyond day 100 (**Figure 2A-B**; Vδ2$^-$ p = 0.008,

Vδ2$^+$ p = 0.01), indicating an early polyclonal burst followed by repertoire focusing. In contrast, αβT cell repertoires remained persistently restricted. Healthy donors displayed high diversity in CD8$^+$ (median D75 221) and CD4$^+$ αβT cells (median D75 2394). Post-transplantation, CD8$^+$ and CD4$^+$ αβT cells exhibited profoundly reduced diversity before day 100 (medians 14.5 and 30.5, respectively), with only minimal diversification thereafter (**Figure 2A-B**). Notably, CD4$^+$ αβT cell diversity remained severely constrained even one year post-transplantation. These findings reveal opposing rebuilding strategies: γδT cells undergo early polyclonal expansion followed by clonal focusing, whereas αβT cells, particularly CD4$^+$, remain persistently clonally contracted.

CMV amplifies γδ and αβ numerically but does not dictate γδ repertoire focusing; EBV associates with early Vδ2$^+$ restriction

Despite the marked numerical expansion of Vδ2$^-$ γδT cells in CMV-reactivated patients (**Figure 1**), γδTCR repertoire evenness before day 100 did not differ between CMV-reactivated and non-reactivated patients (median D75 143 vs. 60; p = 1; **Figure 2C**). After day 100, Vδ2$^-$ γδTCR repertoires became increasingly oligoclonal in both groups (p = 0.008; **Figure 2A**), indicating that repertoire focusing occurred independently of CMV. EBV reactivation was associated with reduced early Vδ2$^+$ γδTCR evenness prior to day 100 (median D75 13 vs. 108; p = 0.034 **Figure 2D**), an effect that was not sustained later. This suggests that early Vδ2$^+$ repertoire restriction may represent a transient risk state for EBV reactivation. In CD8$^+$ αβT cells, CMV reactivation was associated with significantly greater repertoire focusing (median D75 6 vs. 34; p = 0.042; **Figure 2C**), consistent with dominant clonal expansion, whereas CD4$^+$ αβT cells were unaffected. EBV had no detectable effect on the αβTCR repertoire. Thus, CMV primarily acts as a numerical and clonal amplifier of CD8$^+$ αβT cells, while γδTCR repertoire focusing proceeds largely independently of viral reactivation. Additionally, Vδ2$^+$ repertoire evenness may modulate susceptibility to antiviral EBV responses.

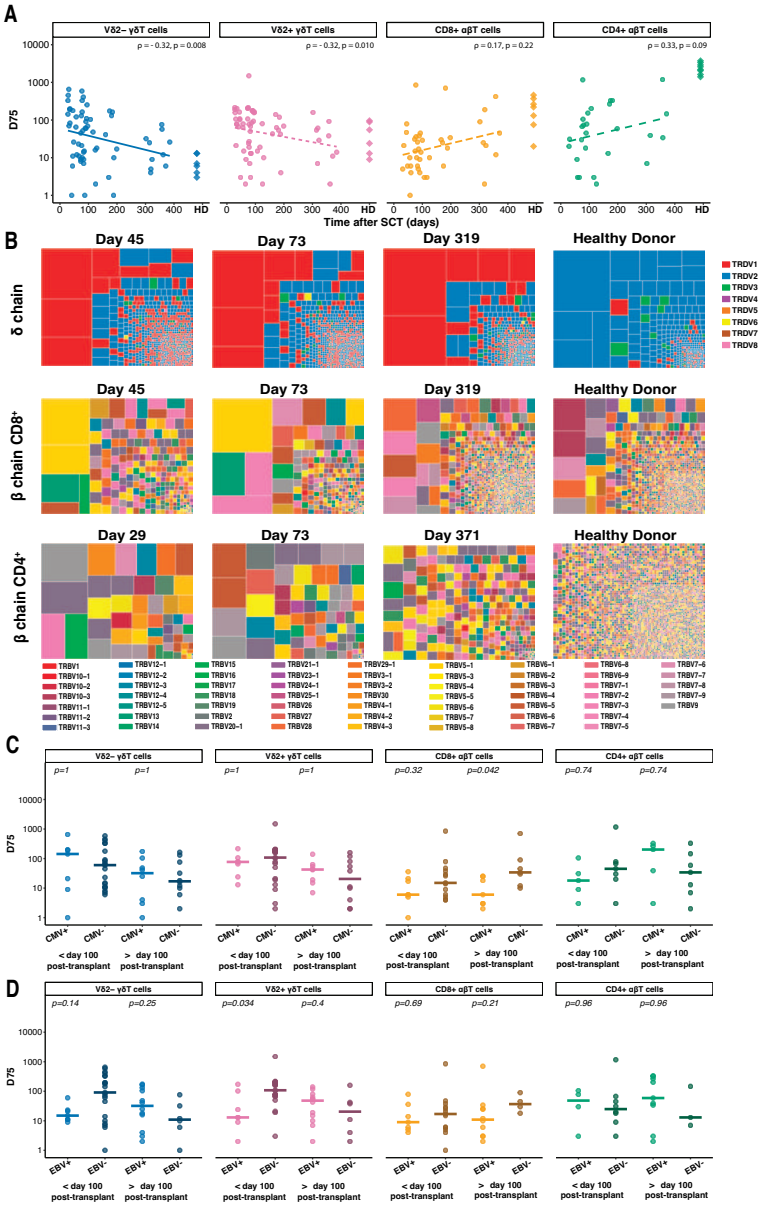


Figure 2. TRD and TRB sequencing were performed to estimate the diversity of the TCR repertoire in αβT-cell-depleted allo-SCT recipients. ***(A)*** *Evenness of TCR repertoire as estimated by unique clonotypes making up 75% of the repertoire (D75). P-values found with Spearman's correlation, ρ = Spearman's correlation coefficient. D75 of healthy donors (HD) added for comparison.* ***(B)*** *Examples of TCR repertoires of patients vs healthy references (not SCT donors). Delta chain and beta chain CD8$^+$ sequential samples from one patient. Beta-chain CD4$^+$ representative repertoires from 3 patients. D75/Evenness of TCR repertoire per group (<100 days after SCT, >100 days after SCT) stratified by* ***(C)*** *CMV reactivation and* ***(D)*** *EBV reactivation. C + D) Median shown. Vδ2$^-$ and Vδ2$^+$ TRD < 100 days after SCT n = 28 (CMV reactivation n = 7; EBV reactivation n = 7), Vδ2$^-$ and Vδ2$^+$ TRD > 100 days after SCT n = 18 (CMV reactivation n = 8, EBV reactivation n = 12), CD8$^+$ TRB <100 days after SCT n = 20 (CMV reactivation n = 7, EBV reactivation n = 7), CD8$^+$ TRB >100 days after SCT n = 14 (CMV reactivation n = 7, EBV reactivation n = 10), CD4$^+$ TRB <100 days after SCT n = 14 (CMV reactivation n = 6, EBV reactivation n = 4), CD4$^+$ TRB >100 days after SCT n = 13 (CMV reactivation n = 5, EBV reactivation n = 9). P-values found using the Wilcoxon Rank-Sum test, corrected for multiple testing per cell type and group with Holm-Bonferroni correction.*

αβTCR, but not γδTCR, clonality retains a durable imprint of graft engineering at single-cell resolution

To explore these observations at higher resolution, we performed single-cell RNA and TCR sequencing on donor samples and samples one year after transplantation (EBMT landmark[47]) in three αβT cell-depleted and three T cell-replete recipients, all of whom experienced CMV reactivation (**Supplementary Figure 2A-B**). After quality control, 95,435 cells were retained, of which 46,223 cells were annotated with a TCR α and/or β chain and 28,716 cells with a TCR γ and/or δ chain (**Supplementary Figure S2C-F**). γδT cell repertoires were not strongly influenced by transplant strategy, as they were highly patient-specific and dominated either by Vδ1$^+$ or by Vδ1$^-$Vδ2$^-$ γδT cell subsets (**Figure 3A, Supplementary Figure S3**). The proportion of single γδT cell clones was low in all patients (<25% of the repertoire). Hyperexpanded γδT cell clones (>75% of the repertoire) were observed in only two patients, one in the αβT cell-depleted (IR067) and one in the T cell-replete (TR007) group (**Figure 3A**). In contrast, the transplant strategy strongly influenced αβTCR-clonality one year after transplantation. Patients who received αβT cell-depleted transplants showed a markedly higher proportion of hyperexpanded αβT cell clones and a lower proportion of singlet clonotypes compared with T cell-replete recipients (**Figure 3B**). In donor samples, both γδTCR and αβTCR repertoires were comparatively evenly distributed and did not show corresponding skewing (**Supplementary Figure S4A–B**). These data demonstrate that αβT cell clonality, but not γδT cell clonality, retains a durable imprint of graft engineering at single-cell resolution.

Vδ2$^+$ γδTCRs retain limited donor persistence, whereas Vδ1$^+$ γδ and αβ repertoires are largely newly generated

Tracking TCRδ and TCRβ chains between donors and recipients revealed consistent low-level persistence of donor-derived Vδ2$^+$ γδTCRs, accounting for <20% of δ chains in recipients one year after transplantation (**Figure 3C,** full TCRs **Supplementary Figure 4C**). The majority (>90%) of these shared Vδ2$^+$ δ chains were private clonotypes rather than public sequences (**Supplementary Table S2**). In contrast, Vδ1$^+$ γδTCR and αβTCR overlap between donors and patients was minimal across platforms, except in rare cases where a small donor clone became hyperexpanded post-transplantation (**Figure 3C,** patient IR067). Overlap of αβTCRs between early post-transplant samples (<100 days) and one-year post-transplant samples was pronounced only after CMV reactivation, with αβTCR overlap exceeding 40% of total β chains in several patients (**Figure 3D,** patients IR048 and TR001; full TCRs **Supplementary Figure 4C**). Together, these findings indicate that Vδ2$^+$ γδT cells persist partially from the donor pool, whereas the Vδ1$^+$ γδ and αβ T cell compartments are predominantly rebuilt de novo after transplantation.

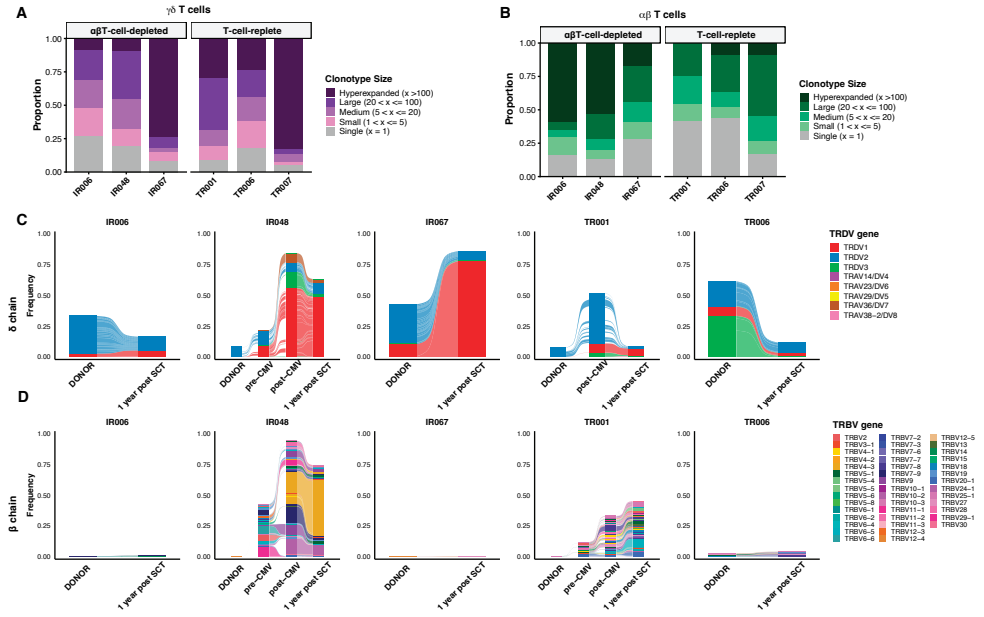


Figure 3. Overview of single-cell TCR data. *Single-cell TCR sequencing of peripheral T cells ~1 year after αβ-T cell–depleted (n = 3) or T cell–replete (n = 3) allogeneic SCT. All patients experienced CMV reactivation. Full TCR clones were grouped by size: single (1 cell), small (2–5 cells), medium (6–20 cells), large (21–100 cells) and hyperexpanded (>100 cells). The proportions for each category are shown for individual patients.* ***A)*** *γδT cells and* ***B)*** *αβT cells.* ***C-D)*** *Longitudinal analysis of shared delta chain* ***(C)*** *or beta chain* ***(D)*** *clonotypes between donors and patients (n = 5), and pre- and post-CMV samples (n=2).*

CMV-driven αβT cell expansion is only partially explained by CMV-specific clonotypes

Considering the substantial increase in CD8$^+$ αβT cell numbers in response to CMV reactivation and the expansion of αβT cell clones in αβT cell-depleted allo-HSCT patients, we assessed whether these dominant clones were predominantly CD8$^+$ or whether they could also be CD4$^+$. In our single-cell RNA sequencing dataset of samples collected 1 year post-allo-HSCT, 8,222 cells expressed either CD8A or CD8B, and 1,669 cells expressed CD4 (**Figure 4A-B**). Because all patients included in this analysis had experienced CMV reactivation, we further examined whether any αβT cell clones were CMV-specific using the Trex package[41,42]. We detected a small proportion of CMV-specific CD8$^+$ αβT cell clones in all patients, ranging from 1.8% to 10.5%, with no major differences between αβT cell-depleted and T cell-replete allo-HSCT recipients (**Figure 4B**). Fewer than 25% of these CMV-specific CD8$^+$ clones were single-cell clones, with no differences across transplantation platforms (**Figure 4C**). In contrast, >75% of CMV-specific clones within the CD4$^+$ αβT cell compartment were single-cell clones in T cell-replete recipients, whereas CMV-specific CD4$^+$ clones were more expanded in patients who received αβT cell-depleted grafts (**Figure 4D**). Interestingly, one patient exhibited a hyperexpanded CMV-specific clone, while the remaining five patients showed similar, lower proportions of CMV-specific clones

(4.4–7.2%) (**Figure 4D**). In clones annotated as non-CMV-specific, we observed patterns that closely mirrored those observed in CMV-specific clones. CD8$^+$ αβT cell clones were predominantly (hyper)expanded, except in patients IR067 and TR001 (**Figure 4E**), whereas CD4$^+$ αβT cell clones were generally smaller and displayed a higher proportion of single-cell clones in the T cell-replete transplant setting (**Figure 4F**). Together, these findings indicate that although CMV reactivation is associated with marked αβT cell expansion, the contribution of CMV-specific clonotypes remains relatively limited one year post-transplantation. Moreover, the proportional contribution of CMV-specific clones is comparable between transplant platforms, despite the CMV-driven αβT cell expansion and the reduction in unique clonotypes observed in αβT cell-depleted transplant recipients.

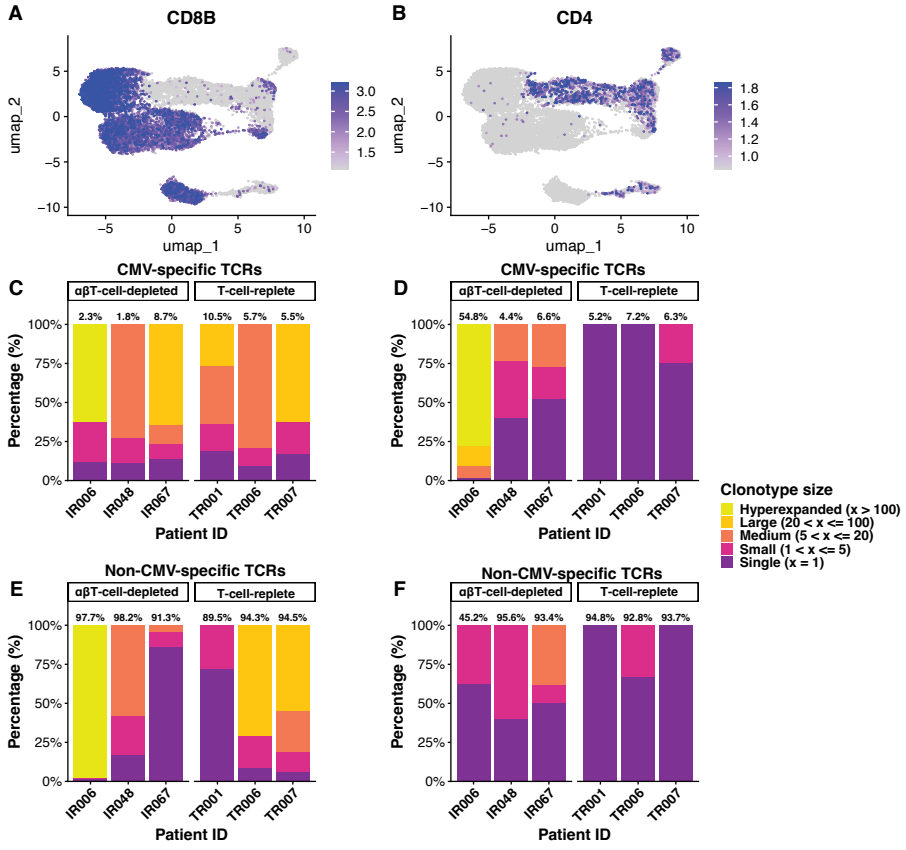


Figure 4. Single cell transcriptomic data and scTCR sequencing data of αβT cells ~1 year post αβT-cell-depleted allo-SCT (n=3) or T-cell-replete allo-SCT (n=3). ***(A)*** *and* ***(B)*** *UMAP including all patient samples showing RNA expression of CD8B (left) and CD4 (right).* ***(C-F)*** *Stacked barplot showing* ***(C)*** *and* ***(D)*** *CMV-specific clones and* ***(E)*** *and* ***(F)*** *non-CMV-specific clones as determined by the Trex package per patient in CD8$^+$ αβT cells (**C, E**) and CD4$^+$ αβT cells (**D, F**), coloured by TCR clone size. Dark blue = single (1 cell), purple = small (2–5 cells), pink = medium (6–20 cells), orange = large (21–100 cells), and yellow = hyperexpanded (>100 cells).*

Donor and patient T cells occupy distinct transcriptomic states after allo-HSCT

To assess whether patient T cells retained donor-like transcriptional features, we partitioned the scRNA-seq dataset into Vδ2$^-$ γδT cells, Vδ2$^+$ γδT cells, CD8$^+$ αβT cells, and CD4$^+$ αβT cells. Pseudo-bulk analysis showed that donors were transcriptionally more similar to one another than to patients across all subsets (**Supplementary Figures S5A–E**). TCellAnnoTator (TCAT) and Azimuth mapping placed post-transplant T cells within a standardized transcriptional reference framework[37,39,40]. Across γδT cell compartments, patient-derived Vδ2$^-$ and Vδ2$^+$ γδT cells predominantly exhibited *GZMK*$^+$ or *GZMB*$^+$ effector phenotypes (**Supplementary Figure S6A–B**). In contrast, donor αβT cells displayed greater phenotypic diversity, with higher proportions of naïve CD8$^+$ and CD4$^+$ cells, whereas patient αβT cells were consistently skewed toward effector memory phenotypes across transplantation settings (**Supplementary Figures S6C–D, S7A–B**).

To further resolve transcriptional structure beyond predefined functional states, we applied non-negative matrix factorization (NMF) at single-cell resolution to define recurrent transcriptional programs across donor and patient T cells (**Supplementary Table S3**). In γδT cells, cytotoxic effector programs increased after transplantation and CMV reactivation (MP2; **Supplementary Figure S8A**), whereas helper-like programs were highest in donors and reduced after transplantation (MP1; **Supplementary Figure S8A**). In αβT cells, NMF revealed a shift from donor-enriched naïve programs (MP1; **Supplementary Figure S8B**) toward cytotoxic effector programs (MP2; **Supplementary Figure S8B**). Together, these analyses show that long-term T cell reconstitution after allo-HSCT is characterized by transcriptional states in patients that are distinct from those of their donors across both γδ and αβ lineages.

Transplantation platform imprints durable gene-expression programs and functional states in T cells

To assess platform-specific effects on T cell transcriptional states, we performed comparative gene-expression analyses between αβT cell-depleted and T cell-replete recipients within the same subsets, identifying four sets of differentially expressed genes (DEGs) (**Supplementary File S1**). No genes were consistently downregulated in the T cell-replete setting (**Figure 5A**); however, seven genes were upregulated across all subsets (*AREG, ELL2, FKBP5, NFKBIA, NR4A2, SELL, and ZFP36*) (**Figure 5B-C**). Increased amphiregulin (*AREG*) expression suggests engagement of tissue-repair or wound-healing programs in T cell-replete recipients[48,49]. Moreover, NMF revealed higher scores of IL7R+ helper signatures in Vδ2$^+$ γδT cells of T cell-replete recipients (**Figure 6A**). Together these findings indicate qualitative functional differences between transplantation platforms.

Functional state scoring using the TCAT pipeline[40] showed higher cytotoxicity scores in Vδ2$^-$ γδT cells from T cell-replete recipients, whereas CD8$^+$ and CD4$^+$ αβT cells exhibited

higher cytotoxicity scores in αβT cell-depleted recipients (**Supplementary Figure S9**), which was confirmed by NMF (MP2; **Figure 6B**). Cytotoxicity scores were consistently higher in patient samples than in donor samples across these subsets (**Figure 6B, Supplementary Figure S10**), indicating that these states are not inherited from donor T cells. Additionally, activation and inflammatory response programs (MP5) were relatively more prominent in αβT cells of T cell-replete recipients (**Figure 6B**). Collectively, transcriptional analyses demonstrate that the transplantation platform leaves a durable imprint on reconstituting T cells, differentially balancing cytotoxic and tissue-repair–associated programs between γδ and αβT cell lineages.

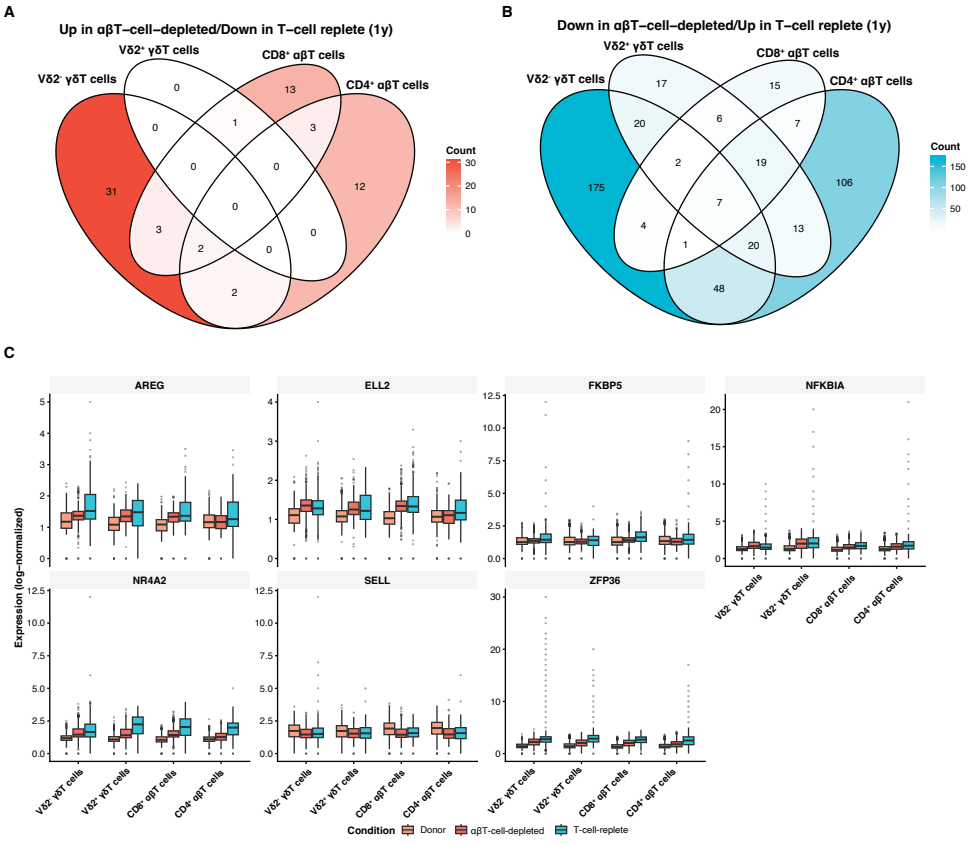


Figure 5. Differential gene expression analysis across T cell subsets at 1 year post-SCT. ***(A)*** *Venn diagram showing the overlap of significantly downregulated genes in T-cell-replete compared to αβT-cell-depleted recipients (log2FC < -1, adjusted p-value < 0.05) across the four T cell subsets* ***(A)*** *Venn diagram showing the overlap of significantly upregulated genes in T-cell-replete compared to αβT-cell-depleted recipients (log2FC > 1, adjusted p-value < 0.05) across Vδ2⁻ γδT cells, Vδ2⁺ γδT cells, CD8⁺ αβT cells, and CD4⁺ αβT cells. Numbers indicate the count of differentially expressed genes unique to or shared between cell types. Color intensity reflects the number of overlapping genes..* ***(C)*** *Expression levels of selected differentially expressed genes across cell types and conditions. Boxplots show log-normalized expression values for donor samples (orange), αβT-cell-depleted recipients (red), and T-cell-replete recipients (blue) at 1 year post-SCT.*

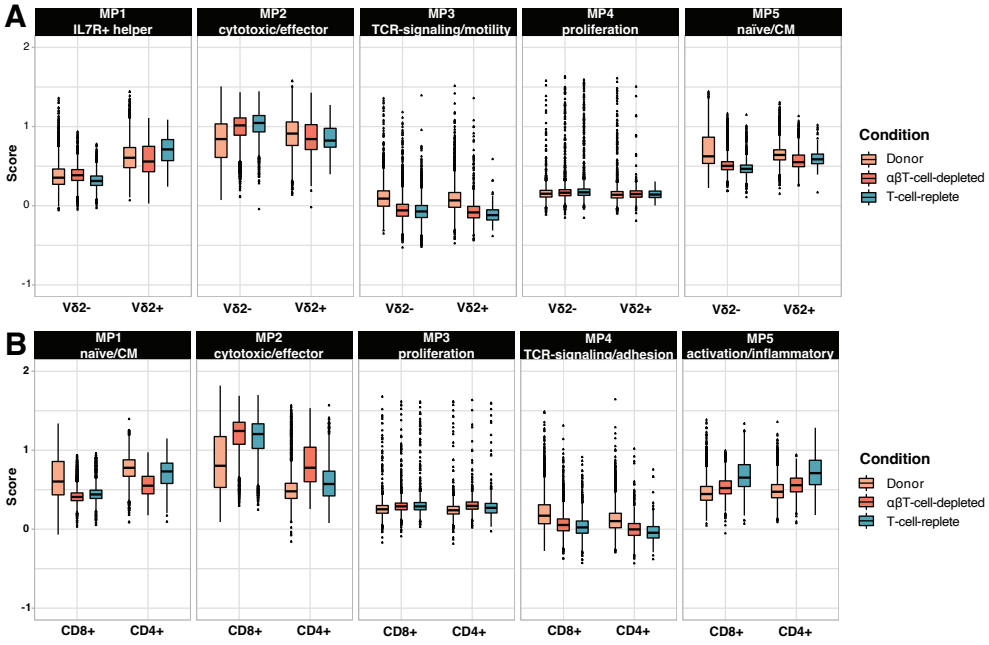


Figure 6. Platform-specific activity of T-cell NMF meta-programs. (A) *γδ T cells: Single-cell module scores of five γδ T-cell NMF meta-programs (MP1–MP5) are shown as boxplots, stratified by transplantation platform (donor, αβT-cell-depleted, and T-cell-replete) and γδT-cell subset (Vδ2$^-$ and Vδ2$^+$). MP1 represents an IL7R$^+$ helper-like γδ T-cell program (e.g., IL7R, KLRB1, RORA, IL18RAP), MP2 a cytotoxic effector program (e.g., CCL5, NKG7, PRF1, GNLY, FGFBP2), MP3 a TCR signaling and motility-associated program, MP4 a proliferation/cell-cycle program, and MP5 a naïve/central-memory-like program (e.g., TCF7, LEF1, CCR7, BACH2). Vδ2$^-$ and Vδ2$^+$ γδ T cells are shown separately.* ***(B)*** *αβ T cells: Single-cell module scores of five αβ T-cell NMF meta-programs (MP1–MP5) are shown as boxplots, stratified by transplantation platform (donor, αβT-cell-depleted, and T-cell-replete) and αβT-cell subset (CD8$^+$ and CD4$^+$). MP1 corresponds to a naïve/central-memory-like program (e.g., TCF7, LEF1, IL7R, CCR7), MP2 to a cytotoxic effector program (e.g., CCL5, NKG7, PRF1, GNLY, granzymes), MP3 to a proliferation/cell-cycle program (e.g., MKI67, PCNA), MP4 to a TCR signaling and adhesion program (e.g., FYN, PRKCH, ITGA4, STAT4), and MP5 to an activation/inflammatory response program (e.g., TNFAIP3, ZFP36, DUSP1/2, JUN/JUNB, NR4A2, CD69). CD8$^+$ and CD4$^+$ αβ T cells are shown separately. Boxplots indicate median and interquartile range, with individual points representing single cells.*

DISCUSSION

Allo-HSCT induces a profound and prolonged disruption of immune homeostasis, requiring coordinated rebuilding of both innate-like and adaptive T cell compartments under conditions of lymphopenia, inflammation, and viral exposure. Here, by integrating longitudinal immune phenotyping with bulk and single-cell TCR repertoire and transcriptomic profiling across αβ and γδT cell subsets, we delineate how graft engineering and viral reactivation jointly shape post-transplant immune architecture over multiple years. By comparing αβT cell–depleted and T cell-replete platforms, we could identify platform-imprinted, lineage-specific patterns of clonal rebuilding, cellular origin, and functional programming that persist long after transplantation.

First, we identified an association between reduced early Vδ2$^+$ γδTCR repertoire evenness and subsequent EBV reactivation within the first 100 days post-transplantation. Although correlative, this finding is biologically plausible given the known capacity of Vδ2$^+$ γδT cells to recognize EBV-transformed B cells[50] and genetic variation in BTN- and RhoB-linked regions that affect γδTCR responses[51-54]. In contrast to prior reports linking EBV reactivation to reduced γδT cell numbers[55], Vδ2$^+$ γδT cell counts in our cohort remained stable, suggesting that repertoire composition rather than absolute cell number may be the more sensitive indicator of EBV immune pressure. These data support that early γδTCR repertoire composition could serve as a potential surrogate marker of antiviral immune competence, pending prospective validation.

Second, we demonstrate a significant CMV-driven expansion of Vδ2$^-$ γδT cells in αβT cell-depleted transplant recipients, consistent with prior observations in the T cell-replete context[10,13,15,18]. Notably, in the αβT cell-depleted platform, this expansion results in a persistent inversion of the Vδ2$^+$/Vδ2$^-$ ratio and sustained dominance of effector-like Vδ2$^-$ γδT cells for up to 3 years post-transplantation. Intriguingly, narrowing of the Vδ2$^-$ γδT cell repertoire occurred even in the absence of CMV reactivation, suggesting homeostatic proliferation rather than persistent viral antigen exposure as the primary mechanism underlying repertoire focusing. This aligns with recent findings in healthy CMV-seronegative individuals[19] and challenges the paradigm of persistent antigen exposure as the sole driver of long-term modulation of the γδTCR repertoire[18].

Third, our paired donor–patient single-cell and TCR analyses revealed a strikingly limited overlap of Vδ1$^+$ and αβTCR clonotypes between donors and recipients one year after transplantation, independent of transplant platform. This finding indicates that, in contrast to partial donor persistence observed for Vδ2$^+$ γδTCRs, the Vδ1$^+$ and αβT cell compartments are largely rebuilt de novo after allo-HSCT[56-58]. The minimal donor–patient Vδ1$^+$ and αβTCR overlap further supports the notion that post-transplant Vδ1$^+$ and αβT cell immunity is not simply a passive extension of the donor repertoire but is actively reshaped by post-transplant antigenic, homeostatic, and inflammatory cues. Importantly, this does not imply equivalent rebuilding dynamics across platforms. Rather, early donor-derived αβT cells present in T cell-replete grafts may condition the post-transplant immune niche through cytokine production, antigen-presenting cell licensing, and competition for homeostatic signals, thereby facilitating more even de novo repertoire diversification despite limited long-term clonotypic persistence[59].

Fourth, recipients of αβT cell-depleted grafts displayed marked contraction of the αβTCR repertoire with increased hyperexpansion of individual clonotypes. Given that GVHD is a stochastic event, the low incidence observed in this cohort[24] likely reflects a reduced overall probability of alloreactive encounters rather than a direct relationship with baseline repertoire features. In this context, clonal hyperexpansion may primarily reflect

homeostatic filling of available immune space following profound αβT cell depletion, rather than pathogenic alloreactivity. While prior studies in T cell-replete transplantation have linked increased αβTCR diversity and post-transplant clonal hyperexpansion to GVHD risk[60-63], our data suggest that these relationships are highly platform-dependent. Importantly, the presence of early hyperexpanded clones does not preclude their further expansion in the event of GVHD; rather, it indicates that baseline clonality alone is unlikely to be mechanistically deterministic.

Fifth, despite pronounced CMV-driven expansion of $CD8^+$ αβT cells, the fraction of CMV-specific clonotypes one year post-transplantation remained relatively low across platforms, consistent with previous findings[64]. This dissociation between numerical expansion and classical CMV specificity suggests that bystander activation, cytokine-driven proliferation, and NK-like adaptive programs may substantially contribute to CMV-associated $CD8^+$ T cell expansion. The preferential expansion of cytotoxic, NK-like $CD8^+$ T cells in αβT cell-depleted recipients is consistent with emerging models of CMV-driven adaptive cytotoxic immunity that extend beyond strictly antigen-restricted responses.

Sixth, transcriptomic profiling revealed that both γδ and αβT cells in patients adopted predominantly effector-like states distinct from those of donors, with the transplantation platform exerting a durable influence on functional polarization. Across T cell subsets, transplantation platform–associated transcriptional programs were characterized by shared upregulation of activation- and stress-responsive genes, whereas they differentially redistributed cytotoxic and tissue-repair–associated states among lineages. In T cell-replete recipients, $V\delta2^-$ γδT and αβT cells showed relatively higher engagement of tissue-repair–associated programs, including *AREG* expression[48,49], whereas αβT cell-depleted recipients showed preferential skewing of $CD8^+$ αβT cells toward cytotoxic effector programs. These divergent transcriptional profiles suggest that graft engineering qualitatively reprograms effector function, potentially balancing tissue protection and cytotoxic immunity in a platform-dependent manner. Whether these programs differentially influence viral clearance, GVHD, or epithelial recovery remains to be determined.

Collectively, our data support a model in which post-transplant immune rebuilding is shaped by three interacting forces: (i) graft engineering, which imposes durable constraints on αβTCR diversity and platform-specific effector programming; (ii) viral exposure, particularly CMV, which acts as a dominant numerical amplifier of cytotoxic lineages without fully dictating long-term repertoire architecture; and (iii) intrinsic homeostatic mechanisms, which drive early polyclonal γδT cell expansion followed by progressive repertoire focusing. Crucially, these forces act on T cell lineages with fundamentally different relationships to the detectable donor repertoire. Within this framework, $V\delta2^+$ γδT cells constitute a rapidly adaptive compartment that partially persists from the donor pool, whereas $V\delta2^-$ γδ and αβT cells undergo substantial post-transplant repertoire reconstitu-

tion, characterized by the emergence of new dominant clonotypes not detectable in the graft.

These findings suggest that early post-transplant TCR repertoire composition may represent a previously underappreciated determinant of immune behavior after allo-HSCT. As post-transplant interventions such as DLIs, kinase inhibitors, and immunomodulatory therapies become increasingly integrated into standard care[65,66], baseline clonal diversity and lineage balance may critically condition both therapeutic efficacy and immune toxicity. Likewise, early restriction of γδT cell repertoires may influence antiviral control and responsiveness to emerging γδ-directed strategies[14]. These data support the incorporation of TCR repertoire monitoring into post-transplant risk-stratification frameworks[66]. Moreover, genetic variation in γδTCR ligands, such as BTN2A1, BTN3A1, and RhoB, may further condition Vδ2$^+$ γδT cell responsiveness[54].

Several limitations warrant consideration. The number of patients analyzed by single-cell RNA and TCR sequencing was small, limiting statistical power for transcriptomic and clonotype-level comparisons and precluding robust adjustment for conditioning, disease type, and GVHD prophylaxis. In addition, matched bulk and single-cell TCR sequencing was not available for all patients. Where overlap existed, concordant clonotype detection across platforms supports the robustness of the analytical approach. Larger, prospectively designed studies will be required to validate the clinical implications of these findings and to define their relevance for viral control, GVHD, and relapse across additional transplantation strategies[67].

In conclusion, post-transplant immune reconstruction is not uniform but is durably shaped by graft engineering, viral exposure, and intrinsic homeostatic forces in a lineage-specific manner. By defining distinct rebuilding rules for γδ and αβT cells at numerical, clonal, and functional levels, these findings provide a framework for understanding individual immune trajectories after allo-HSCT. As immune-directed therapies continue to expand, such insights may enable more precise alignment of post-transplant interventions with each patient's evolving immune architecture.

Acknowledgments

The authors would like to thank the Single Cell Genomics Core Facility at the Princess Máxima Center for Pediatric Oncology for technical support.

Competing Interests:

JK is shareholder of Gadeta founders. JK, ZS, and DXB are inventors on patents with γδTCR-related topics. JK, ZS, and DXB are inventors on patents with CD277-related topics.

Funding

Funding for this study was provided by KWF 13493 to MdW and JK, and by the Oncode Accelerator to JK.

Author contributions

Conceptualization: MdW, JK; Methodology: AS, PB, AJ, MdW, JK; Formal analysis: AS, PB, AJ; Unique resources: JY, HTS, HS, SP; Data collection: AJ, EK, CN, DdB, MN, LG; Investigation: all authors; Writing; original draft: AS, PB, MdW, JK; Writing; editing and revision: all authors; Supervision: ZS, MdW, JK.

REFERENCES

1. de Witte M, Daenen LGM, van der Wagen L, et al. Allogeneic Stem Cell Transplantation Platforms With Ex Vivo and In Vivo Immune Manipulations: Count and Adjust. *Hemasphere*. 2021;5(6):e580.
2. Janssen A, van Diest E, Vyborova A, et al. The Role of gammadelta T Cells as a Line of Defense in Viral Infections after Allogeneic Stem Cell Transplantation: Opportunities and Challenges. *Viruses*. 2022;14(1).
3. de Witte MA, Sarhan D, Davis Z, et al. Early Reconstitution of NK and gammadelta T Cells and Its Implication for the Design of Post-Transplant Immunotherapy. *Biol Blood Marrow Transplant*. 2018.
4. Savani BN, Mielke S, Adams S, et al. Rapid natural killer cell recovery determines outcome after T-cell-depleted HLA-identical stem cell transplantation in patients with myeloid leukemias but not with acute lymphoblastic leukemia. *Leukemia*. 2007;21(10):2145-2152.
5. Buhlmann L, Buser AS, Cantoni N, et al. Lymphocyte subset recovery and outcome after T-cell replete allogeneic hematopoietic SCT. *Bone Marrow Transplant*. 2011;46(10):1357-1362.
6. Dekker L, de Koning C, Lindemans C, Nierkens S. Reconstitution of T Cell Subsets Following Allogeneic Hematopoietic Cell Transplantation. *Cancers (Basel)*. 2020;12(7).
7. Fujimoto A, Suzuki R. Epstein-Barr Virus-Associated Post-Transplant Lymphoproliferative Disorders after Hematopoietic Stem Cell Transplantation: Pathogenesis, Risk Factors and Clinical Outcomes. *Cancers (Basel)*. 2020;12(2).
8. Teira P, Battiwalla M, Ramanathan M, et al. Early cytomegalovirus reactivation remains associated with increased transplant-related mortality in the current era: a CIBMTR analysis. *Blood*. 2016;127(20):2427-2438.
9. Drylewicz J, Schellens IM, Gaiser R, et al. Rapid reconstitution of CD4 T cells and NK cells protects against CMV-reactivation after allogeneic stem cell transplantation. *J Transl Med*. 2016;14(1):230.
10. Knight A, Madrigal AJ, Grace S, et al. The role of Vdelta2-negative gammadelta T cells during cytomegalovirus reactivation in recipients of allogeneic stem cell transplantation. *Blood*. 2010;116(12):2164-2172.
11. Prinz I, Thamm K, Port M, et al. Donor Vdelta1+ gammadelta T cells expand after allogeneic hematopoietic stem cell transplantation and show reactivity against CMV-infected cells but not against progressing B-CLL. *Exp Hematol Oncol*. 2013;2(1):14.
12. Scheper W, Van Dorp S, Kersting S, et al. γδT cells elicited by CMV reactivation after allo-SCT cross-recognize CMV and leukemia. *Leukemia*. 2013;27(6):1328-1338.
13. Khairallah C, Dechanet-Merville J, Capone M. gammadelta T Cell-Mediated Immunity to Cytomegalovirus Infection. *Front Immunol*. 2017;8:105.
14. Beringer DX, Straetemans T, Minguet S, et al. Disrupting the balance between activating and inhibitory receptors of gammadeltaT cells for effective cancer immunotherapy. *Nat Rev Cancer*. 2025;25(8):590-612.
15. Suessmuth Y, Mukherjee R, Watkins B, et al. CMV reactivation drives posttransplant T-cell reconstitution and results in defects in the underlying TCRbeta repertoire. *Blood*. 2015;125(25):3835-3850.
16. Link CS, Eugster A, Heidenreich F, et al. Abundant cytomegalovirus (CMV) reactive clonotypes in the CD8(+) T cell receptor alpha repertoire following allogeneic transplantation. *Clin Exp Immunol*. 2016;184(3):389-402.
17. Link-Rachner CS, Eugster A, Rucker-Braun E, et al. T-cell receptor-alpha reper-

toire of CD8+ T cells following allogeneic stem cell transplantation using next-generation sequencing. *Haematologica*. 2019;104(3):622-631.
18. Ravens S, Schultze-Florey C, Raha S, et al. Human gammadelta T cells are quickly reconstituted after stem-cell transplantation and show adaptive clonal expansion in response to viral infection. *Nat Immunol*. 2017;18(4):393-401.
19. Davey MS, Willcox CR, Joyce SP, et al. Clonal selection in the human Vdelta1 T cell repertoire indicates gammadelta TCR-dependent adaptive immune surveillance. *Nat Commun*. 2017;8:14760.
20. Lammoglia Cobo MF, Ritter J, Gary R, et al. Reconstitution of EBV-directed T cell immunity by adoptive transfer of peptide-stimulated T cells in a patient after allogeneic stem cell transplantation for AITL. *PLoS Pathog*. 2022;18(4):e1010206.
21. de Witte MA, Mooyaart JE, Hoogenboom JD, et al. Activity of ex vivo graft and DLI Engineering within the last decade increases, a survey from the EBMT Cellular Therapy & Immunobiology Working Party. *Bone Marrow Transplant*. 2023.
22. Nijssen K, Westinga K, Stuut A, et al. Graft engineering: how long can you wait, how low can you go, and pandemic readiness. *Bone Marrow Transplant*. 2023:1-3.
23. de Witte MA, Kuball J, Miller JS. NK Cells and gammadeltaT Cells for Relapse Protection After Allogeneic Hematopoietic Cell Transplantation (HCT). *Curr Stem Cell Rep*. 2017;3(4):301-311.
24. de Witte MA, Janssen A, Nijssen K, et al. alphabeta T-cell graft depletion for allogeneic HSCT in adults with hematological malignancies. *Blood Adv*. 2021;5(1):240-249.
25. Salzmann-Manrique E, Bremm M, Huenecke S, et al. Joint Modeling of Immune Reconstitution Post Haploidentical Stem Cell Transplantation in Pediatric Patients With Acute Leukemia Comparing CD34(+)-Selected to CD3/CD19-Depleted Grafts in a Retrospective Multicenter Study. *Front Immunol*. 2018;9:1841.
26. Foley B, Cooley S, Verneris MR, et al. Cytomegalovirus reactivation after allogeneic transplantation promotes a lasting increase in educated NKG2C+ natural killer cells with potent function. *Blood*. 2012;119(11):2665-2674.
27. Muccio L, Bertaina A, Falco M, et al. Analysis of memory-like natural killer cells in human cytomegalovirus-infected children undergoing alphabeta+T and B cell-depleted hematopoietic stem cell transplantation for hematological malignancies. *Haematologica*. 2016;101(3):371-381.
28. de Witte MA, Sarhan D, Davis Z, et al. Early Reconstitution of NK and gammadelta T Cells and Its Implication for the Design of Post-Transplant Immunotherapy. *Biol Blood Marrow Transplant*. 2018;24(6):1152-1162.
29. Cichocki F, Cooley S, Davis Z, et al. CD56dimCD57+NKG2C+ NK cell expansion is associated with reduced leukemia relapse after reduced intensity HCT. *Leukemia*. 2016;30(2):456-463.
30. Chaleff S, Otto M, Barfield RC, et al. A large-scale method for the selective depletion of alphabeta T lymphocytes from PBSC for allogeneic transplantation. *Cytotherapy*. 2007;9(8):746-754.
31. Frederik Falkenburg JH, Schmid C, Kolb HJ, Locatelli F, Kuball J. Delayed Transfer of Immune Cells or the Art of Donor Lymphocyte Infusion. In: th, Carreras E, Dufour C, Mohty M, Kroger N, eds. The EBMT Handbook: Hematopoietic Stem Cell Transplantation and Cellular Therapies. Cham (CH); 2019:443-448.
32. Mamedov IZ, Britanova OV, Zvyagin IV, et al. Preparing unbiased T-cell receptor and antibody cDNA libraries for the deep next generation sequencing profiling. *Front Immunol*. 2013;4:456.
33. Nazarov VI, Tsvetkov VO, Fiadziushchanka S, et al. immunarch: Bioinformatics

Analysis of T-Cell and B-Cell Immune Repertoires; 2023.
34. Tan L, Fichtner AS, Bruni E, et al. A fetal wave of human type 3 effector gammadelta cells with restricted TCR diversity persists into adulthood. *Sci Immunol*. 2021;6(58).
35. Stuart T, Butler A, Hoffman P, et al. Comprehensive Integration of Single-Cell Data. *Cell*. 2019;177(7):1888-1902 e1821.
36. Butler A, Hoffman P, Smibert P, Papalexi E, Satija R. Integrating single-cell transcriptomic data across different conditions, technologies, and species. *Nat Biotechnol*. 2018;36(5):411-420.
37. Hao Y, Hao S, Andersen-Nissen E, et al. Integrated analysis of multimodal single-cell data. *Cell*. 2021;184(13):3573-3587 e3529.
38. Hao Y, Stuart T, Kowalski MH, et al. Dictionary learning for integrative, multimodal and scalable single-cell analysis. *Nat Biotechnol*. 2024;42(2):293-304.
39. Gong Q, Sharma M, Kuan EL, et al. Longitudinal Multi-omic Immune Profiling Reveals Age-Related Immune Cell Dynamics in Healthy Adults. *bioRxiv*. 2024.
40. Kotliar D, Curtis M, Agnew R, et al. Reproducible single-cell annotation of programs underlying T cell subsets, activation states and functions. *Nat Methods*. 2025;22(9):1964-1980.
41. Borcherding N, Kim W, Quinn M, et al. CD4(+) T cells exhibit distinct transcriptional phenotypes in the lymph nodes and blood following mRNA vaccination in humans. *Nat Immunol*. 2024;25(9):1731-1741.
42. Borcherding N, Bormann NL, Kraus G. scRepertoire: An R-based toolkit for single-cell immune receptor analysis. *F1000Res*. 2020;9:47.
43. Shugay M, Bagaev DV, Zvyagin IV, et al. VDJdb: a curated database of T-cell receptor sequences with known antigen specificity. *Nucleic Acids Res*. 2018;46(D1):D419-D427.
44. Tickotsky N, Sagiv T, Prilusky J, Shifrut E, Friedman N. McPAS-TCR: a manually curated catalogue of pathology-associated T cell receptor sequences. *Bioinformatics*. 2017;33(18):2924-2929.
45. Vita R, Blazeska N, Marrama D, et al. The Immune Epitope Database (IEDB): 2024 update. *Nucleic Acids Res*. 2025;53(D1):D436-D443.
46. Zhang W, Wang L, Liu K, et al. PIRD: Pan Immune Repertoire Database. *Bioinformatics*. 2020;36(3):897-903.
47. Snowden JA, Saccardi R, Orchard K, et al. Benchmarking of survival outcomes following haematopoietic stem cell transplantation: A review of existing processes and the introduction of an international system from the European Society for Blood and Marrow Transplantation (EBMT) and the Joint Accreditation Committee of ISCT and EBMT (JACIE). *Bone Marrow Transplant*. 2020;55(4):681-694.
48. Gray JI, Caron DP, Wells SB, et al. Human γδ T cells in diverse tissues exhibit site-specific maturation dynamics across the life span. *Science Immunology*. 2024;9(96).
49. Harmon C, Zaborowski A, Moore H, et al. gammadelta T cell dichotomy with opposing cytotoxic and wound healing functions in human solid tumors. *Nat Cancer*. 2023;4(8):1122-1137.
50. Xiang Z, Liu Y, Zheng J, et al. Targeted activation of human Vgamma9Vdelta2-T cells controls epstein-barr virus-induced B cell lymphoproliferative disease. *Cancer Cell*. 2014;26(4):565-576.
51. Mamedov MRV, S.; Freimer, J.W.; Das Sahu, A.; Ramesh, A.; Arce, M.M.; Meringa, A.D.; Ota, M.; ChenP.M.; Hanspers, K.; Nguyen, V.Q.; Takeshima, K.A.; Pritchard, J.K; Kuball, J.; Sebestyen, Z.; Adams, E.J.; Marson, A. CRISPR screens decode cancer cell pathways that trigger γδ T cell detection. *Nature*. 2023(In print).
52. Vyborova A, Janssen A, Gatti L, et al. γ9δ2 T-Cell Expansion and Phenotypic Profile

Are Reflected in the CDR3δ Repertoire of Healthy Adults. *Frontiers in Immunology*. 2022;13.

53. Sebestyen Z, Prinz I, Dechanet-Merville J, Silva-Santos B, Kuball J. Translating gammadelta (gammadelta) T cells and their receptors into cancer cell therapies. *Nat Rev Drug Discov*. 2020;19(3):169-184.
54. Sebestyen Z, Scheper W, Vyborova A, et al. RhoB Mediates Phosphoantigen Recognition by Vgamma9Vdelta2 T Cell Receptor. *Cell Rep*. 2016;15(9):1973-1985.
55. Liu J, Bian Z, Wang X, et al. Inverse correlation of Vdelta2(+) T-cell recovery with EBV reactivation after haematopoietic stem cell transplantation. *Br J Haematol*. 2018;180(2):276-285.
56. Pagliuca S, Gurnari C, Hong S, et al. Clinical and basic implications of dynamic T cell receptor clonotyping in hematopoietic cell transplantation. *JCI Insight*. 2021;6(13).
57. Buhler S, Bettens F, Dantin C, et al. Genetic T-cell receptor diversity at 1 year following allogeneic hematopoietic stem cell transplantation. *Leukemia*. 2020;34(5):1422-1432.
58. Schafer A, Calderin Sollet Z, Herve MP, et al. NK- and T-cell repertoire is established early after allogeneic HSCT and is imprinted by CMV reactivation. *Blood Adv*. 2024;8(21):5612-5624.
59. Dai W, Dong F, Cheng T, Hao S. T Cell immune reconstitution after allo-HSCT: key factors and implications. *Blood Sci*. 2025;7(4):e00261.
60. van Heijst JW, Ceberio I, Lipuma LB, et al. Quantitative assessment of T cell repertoire recovery after hematopoietic stem cell transplantation. *Nat Med*. 2013;19(3):372-377.
61. van Bergen CA, van Luxemburg-Heijs SA, de Wreede LC, et al. Selective graft-versus-leukemia depends on magnitude and diversity of the alloreactive T cell response. *J Clin Invest*. 2017;127(2):517-529.
62. Leick M, Gittelman RM, Yusko E, et al. T Cell Clonal Dynamics Determined by High-Resolution TCR-beta Sequencing in Recipients after Allogeneic Hematopoietic Cell Transplantation. *Biol Blood Marrow Transplant*. 2020;26(9):1567-1574.
63. Goel M, Eugster A, Schetelig J, Bonifacio E, Bornhauser M, Link-Rachner CS. Potential of TCR sequencing in graft-versus-host disease. *Bone Marrow Transplant*. 2022.
64. Calderin Sollet Z, Schafer A, Ferrari-Lacraz S, et al. CMV serostatus and T-cell repertoire diversity 5 years after allogeneic hematopoietic stem cell transplantation. *Leukemia*. 2023;37(4):948-951.
65. Schonewille PvR, Anna; ten Ham, Renske MT; de Witte, Moniek; Kuball, Jürgen. Post-Transplant Cells for the Win? DLI and Adoptive Cell Therapy to Eradicate MRD *Hematology Am Soc Hematol Educ Program*. 2025.
66. Pagliuca S, Schmid C, Santoro N, et al. Donor lymphocyte infusion after allogeneic haematopoietic cell transplantation for haematological malignancies: basic considerations and best practice recommendations from the EBMT. *Lancet Haematol*. 2024;11(6):e448-e458.
67. Lapoutge A, Gaudfrin M, Raus N, et al. Hallmarks of allogeneic hematopoietic cell transplant success: A study on immune signatures and predictive features of graft versus host disease-free remission states from the SFGM-TC registry and cryostem biobank. *Blood*. 2025;146(Supplement 1):2476-2476.

SUPPLEMENTARY METHODS

Details of the Clinical Cohort

Patients with hematological malignancies who underwent αβ T-cell-depleted stem cell transplantation at the University Medical Center Utrecht between 2015 and 2017 were included in this retrospective analysis. The conditioning regimen consisted of ATG (Thymoglobulin®) 1.5 mg/kg i.v. on days −12 to −9; fludarabine 40 mg/m² i.v. on days −5 to −2; and busulfan i.v. (Busilvex®) with AUC90 on days −5 to −2. αβ T cell reduction was performed by depletion using anti-αβ T cell receptor (TCR) antibodies in combination with magnetic microbeads on the automated CliniMACS device (Miltenyi Biotec, Bergisch Gladbach, Germany), as described previously[1] and according to standard operating procedures. The maximum allowable residual αβ T-cell number was 5×10^5 cells/kg. The allograft was infused within 24 hours after depletion. Mycophenolate mofetil (MMF) was administered at 15 mg/kg three times daily (maximum 3000 mg total) for 28 days as single GVHD prophylaxis. Patients received a pre-emptive donor lymphocyte infusion (DLI; 1×10^5 $CD3^+$ T cells/kg) at three months after stem cell infusion, in accordance with guidelines for T cell depletion, provided patients were free of GVHD and not receiving immunosuppressive medication at the time of DLI.

As a comparator group, patients who underwent a T-cell-replete stem cell transplantation at UMCU between 2011 and 2018 were included. Patients received either reduced-intensity conditioning (RIC) or myeloablative conditioning (MA). RIC regimens consisted of: (i) fludarabine 30 mg/m² i.v. on days −3 to −1 with total body irradiation (TBI) 2 Gy on day 0, with or without ATG (Thymoglobulin®) 2 mg/kg i.v. on days −7 to −4; (ii) fludarabine 30 mg/m² i.v. on days −6 to −2 with melphalan 70 mg/m² i.v. on days −3 to −2, with or without ATG 2 mg/kg i.v. on days −9 to −7; or (iii) fludarabine orally 50 mg/m² on days −9 to −4 with melphalan 100 mg/m² i.v. on day −3 and alemtuzumab 15 mg on days −3 and −2. MA regimens consisted of either cyclophosphamide 60 mg/kg i.v. on days −4 to −3 with TBI 6 Gy on days −1 to 0, with or without ATG 2 mg/kg i.v. on days −8 to −5; or fludarabine 40 mg/m² i.v. on days −5 to −2 with busulfan (Busilvex®) i.v. on days −5 to −2 and ATG 1.5 mg/kg i.v. on days −9 to −6. In most regimens, MMF was administered at 15 mg/kg three times daily (maximum 3000 mg total) for 84 days, in combination with cyclosporine (2 × 1.5 mg/kg i.v. or 4.5 mg/kg p.o.) for 180 days as GVHD prophylaxis. In melphalan-containing regimens, MMF was used as single GVHD prophylaxis at the same dosage. In alemtuzumab-containing regimens, cyclosporine was used as single GVHD prophylaxis. Peripheral blood stem cells were used as the graft source in both cohorts. At regular time points after allo-HSCT, levels of B cells, T cells, and NK cells, as well as their subsets, were measured as part of routine clinical care. CMV reactivation was defined as a viral load >250 IU/mL and EBV reactivation as >1000 IU/mL, as assessed by PCR. Data regarding immune reconstitution and viral reactivations were retrieved from the hospital medical record system.

Next-generation sequencing of the T cell receptor

Frozen PBMC samples from patients and healthy donors were thawed. PBMCs were stained with the following monoclonal antibodies: anti-CD3 eFluor450 (clone OKT3, eBioscience), anti-TCRαβ APC (clone IP26, eBioscience), anti-TCRγδ PE (clone IMMU510, Beckmann Coulter), anti-CD8 PerCP-Cy5.5 (clone RPA-T8, Biolegend), and anti-CD4 FITC (clone RPA-T4, eBioscience). Next, cells were sorted (BD FACSAriaTM II cell sorter) into $CD8^+$ and $CD4^+$ αβT cell fractions (CD3pos, TCRαβpos, CD8pos or CD4pos) and γδT cell fractions (CD3pos, TCR γδpos). After sorting, total RNA was isolated using RNeasy Mini or RNeasy Micro kits (QIAGEN) according to the manufacturer's instructions, with kit selection based on input cell number (RNeasy Mini for >5×10^5 cells; RNeasy Micro for ≤5×10^5 cells).

The protocol for sequencing the variable region of the β chain of the T cell receptor (TCR) for the CD4 and CD8 fractions was adapted from Mamedov *et al.*[2]. cDNA was synthesized (SuperScriptTM II Reverse Transcriptase, Thermo Fisher Scientific) utilizing a specific primer at the 3' constant region and a universal template switch adaptor at the 5' end of the V region (Supplementary Table S4). Purified cDNA (NucleoSpin Gel and PCR Clean-UP, Macherey-Nagel) was amplified using Q5® High-Fidelity DNA polymerase (New England BioLabs, Inc.) on a T100TM Thermal Cycler (Bio-Rad). A specific nested primer located in the constant region and a step-out primer, which anneals to the switch adaptor, were used (Supplementary Table S4). The PCR product was loaded onto a 1.5% agarose gel, electrophoresed, and products between 400-600 base pairs were size-selected and purified (NucleoSpin Gel and PCR Clean-UP, Macherey-Nagel).

A multiplex PCR was used to sequence the variable region of the δ-chain TCR for the γδ fraction. First cDNA was synthesized (SuperScriptTM II Reverse Transcriptase, Thermo Fisher Scientific) and purified (NucleoSpin Gel and PCR Clean-UP, Macherey-Nagel). cDNA was amplified using using Q5® High-Fidelity DNA polymerase (New England BioLabs, Inc.) on a T100TM Thermal Cycler (Bio-Rad) and purified (NucleoSpin Gel and PCR Clean-UP, Macherey-Nagel).

Both the PCR products of the β and the δ chain were loaded on the QIAxcel (Qiagen) and the intensity of the PCR product was measured as relative fluorescent units (RFU). Based on the RFU the samples were diluted for the HTS library preparations, which were carried out using the HTSgo-LibrX kit with HTSgo-IndX indices following the manufacturer's (Gendx) recommendations. Subsequently, samples were purified using HighPrep PCR beads (GC Biotech), and HTS was performed on an Illumina MiSeq 500 (2 x 250 bp read length).

NGS data analysis

Sequences of the CDR3 region of the β and the δ chain of the TCR were extracted from the raw Illumina files using MiXCR software[3]. Only productive reads were considered, and sequences with a read count <2 were excluded from analysis. To correct for potential bias, read counts were normalized to the sample with the lowest count (8400 reads). Repertoire analyses were performed using the immunarch package (version 0.9.0) in R version 4.2.2[4].

Single-cell RNA sequencing and single-cell TCR sequencing

Frozen PBMC samples from patients collected ~1 year after SCT (range 356–463 days) were thawed. All patients had prior CMV reactivation. In addition, corresponding donor PBMC samples were available for 5 patients, and for 2 of these patients, we included paired pre- and post-CMV reactivation samples. PBMCs were stained with the following monoclonal antibodies: anti-CD3 Pacific Blue (clone UCHT1, BD), anti-TCRαβ APC (clone IP26, eBioscience), anti-TCRγδ PE-Cy7 (clone IMMU510, Beckmann Coulter), anti-Vδ1 PE (clone REA173, Miltenyi), anti-Vδ2 FITC (clone B6, Biolegend), and anti-CD8 PerCP-Cy5.5 (clone RPA-T8, Biolegend). Subsequently, they were stained with LIVE/DEAD Aqua (ThermoFisher). Next, cells were sorted (BD FACSAriaTM II cell sorter) into αβT cell fractions (alive cells, CD3pos, TCRαβpos) and γδT cell fractions (alive cells, CD3pos, TCR γδpos).

Libraries for single-cell transcriptome sequencing and scTCR-seq were prepared using the Chromium Single-Cell 5′ Library GEM-X Gel Bead and Construction Kit and Chromium Single-Cell V(D)J Enrichment Kit (v3, 10x Genomics, CA, USA). Custom primers for the capture of γδTCR transcripts were produced as described by Tan et al[5]. The scRNA-seq and scTCR-seq libraries were sequenced on the Illumina Novaseq 6000 platform.

scRNAseq expression data analysis

Raw FASTQ files from 5′ gene expression (GEX) and targeted V(D)J libraries were merged by lane for each sample and organized into multimodal inputs. Joint processing of matched GEX and V(D)J data was performed with Cell Ranger (v8.0.1) using *cellranger multi* with GRCh38 references for gene expression and V(D)J. To assign cells to their donor of origin, SNPs were called from the Cell Ranger BAM using *cellSNP*-lite[6], with a gnomAD hg38 variant panel, and genotype-based demultiplexing was performed with *Vireo*[7], assuming two donors per library; singlet, doublet, and unassigned calls were added to the Seurat metadata. Seurat (5.1.0) was used in R version 4.4.1 for dimensional reduction, cell clustering, and differential gene expression analysis[8-11]. Azimuth was used to integrate our dataset with CD8+ αβT cell, CD4+ αβT cell, and γδT cell subsets from the Human Immune Health Atlas by the Allen Institute[10,12]. Furthermore, we used the T-CellAnnoTator (TCAT) pipeline to characterize functional programs in T-cells[13].

scTCRseq data analysis

Alignment of γδTCRs was performed by using IMGT/HighV-QUEST on unfiltered FASTA outputs from CellRanger[14]. Unproductive sequences and duplicated barcodes were filtered out. scTCRseq data was added as metadata to the scRNAseq Seurat objects by matching the barcodes. We defined single clones as one cell with a unique TCR, small clones as one to five cells with the same TCR, medium clones as five to twenty cells with the same TCR, large clones as twenty to one hundred cells with the same TCR, and hyper-expanded clones as over one hundred cells with the same TCR. αβTCRs were screened for CMV specificity using the scRepertoire and Trex packages[15,16], which annotate αβ TCRs with epitope data from VDJdb, McPAS-TCR, IEDB, and PIRD databases[17-20].

Non-negative matrix factorization (NMF) analysis

NMF was performed as described earlier by Gavish et al.[21], independently for each sample to capture within-sample transcriptional heterogeneity while minimizing sensitivity to batch effects. Factorization was run across multiple ranks (k = 4–9), and for each resulting program, the top 50 genes ranked by factor loadings were retained.

To derive robust and non-redundant programs, a multi-step filtering strategy was applied. First, within-sample robustness was achieved by retaining only programs that recurred across multiple k values within the same sample, defined as≥70% overlap in their top genes. Second, across-sample robustness was imposed by requiring programs to share ≥20% of their genes with at least one program identified in another sample. Third, to remove redundancy within samples, overlapping programs were ranked by their maximal cross-sample overlap, and only the highest-ranking program was retained when overlaps exceeded 20%.

Robust programs were subsequently grouped into higher-order meta-programs using a greedy gene-overlap–based clustering approach, as previously described. Programs were iteratively clustered based on Jaccard similarity of their gene sets, and each meta-program (MP) was represented by a consensus gene signature reflecting the most frequently shared genes across its constituent programs. For both αβ and γδ T cells, this approach yielded five conserved MPs. MP activity was quantified by computing module scores at the single-cell level (via the *AddModuleScore* function of Seurat), which were then compared across donors and transplantation platforms.

Statistical analyses

Statistical analyses were performed using R (R version 4.2.2). Wilcoxon rank-sum test was used to test for differences between groups as described in figure legends. Statistical analyses were performed in R (version 4.2.0) using the nlme package. For the αβT-cell–depleted cohort, we fitted a piecewise linear mixed-effects model with a single knot at 60 days post-transplant. The model included fixed effects for time before the knot (Days1), time after the knot (Days2), CMV status, and their two interaction terms (Days1×CMV and Days2×CMV). Patient ID was entered as a grouping factor supplying random intercepts and random slopes to account for within-patient correlations over time. For the T-cell–replete cohort, we fitted a simpler linear mixed-effects model with a single slope: fixed effects were time (continuous), CMV status, and their interaction, and patient ID entered as a random intercept. We used two-sided Wald t-tests on the time × CMV interaction to evaluate effect of CMV reactivation on reconstitution rates. P-values < 0.05 were considered significant.

REFERENCES

1. de Witte MA, Janssen A, Nijssen K, et al. alphabeta T-cell graft depletion for allogeneic HSCT in adults with hematological malignancies. *Blood Adv.* 2021;5(1):240-249.
2. Mamedov IZ, Britanova OV, Zvyagin IV, et al. Preparing unbiased T-cell receptor and antibody cDNA libraries for the deep next generation sequencing profiling. *Front Immunol.* 2013;4:456.
3. Bolotin DA, Poslavsky S, Mitrophanov I, et al. MiXCR: software for comprehensive adaptive immunity profiling. *Nat Methods*. 2015;12(5):380-381.
4. Nazarov VI, Tsvetkov VO, Fiadziushchanka S, et al. immunarch: Bioinformatics Analysis of T-Cell and B-Cell Immune Repertoires; 2023.
5. Tan L, Fichtner AS, Bruni E, et al. A fetal wave of human type 3 effector gammadelta cells with restricted TCR diversity persists into adulthood. *Sci Immunol*. 2021;6(58).
6. Huang X, Huang Y. Cellsnp-lite: an efficient tool for genotyping single cells. *Bioinformatics*. 2021;37(23):4569-4571.
7. Huang Y, McCarthy DJ, Stegle O. Vireo: Bayesian demultiplexing of pooled single-cell RNA-seq data without genotype reference. *Genome Biol*. 2019;20(1):273.
8. Stuart T, Butler A, Hoffman P, et al. Comprehensive Integration of Single-Cell Data. *Cell*. 2019;177(7):1888-1902 e1821.
9. Butler A, Hoffman P, Smibert P, Papalexi E, Satija R. Integrating single-cell transcriptomic data across different conditions, technologies, and species. *Nat Biotechnol*. 2018;36(5):411-420.
10. Hao Y, Hao S, Andersen-Nissen E, et al. Integrated analysis of multimodal single-cell data. *Cell*. 2021;184(13):3573-3587 e3529.
11. Hao Y, Stuart T, Kowalski MH, et al. Dictionary learning for integrative, multimodal and scalable single-cell analysis. *Nat Biotechnol*. 2024;42(2):293-304.
12. Gong Q, Sharma M, Kuan EL, et al. Longitudinal Multi-omic Immune Profiling Reveals Age-Related Immune Cell Dynamics in Healthy Adults. *bioRxiv*. 2024.
13. Kotliar D, Curtis M, Agnew R, et al. Reproducible single-cell annotation of programs underlying T cell subsets, activation states and functions. *Nat Methods*. 2025;22(9):1964-1980.
14. Alamyar E, Duroux P, Lefranc MP, Giudicelli V. IMGT((R)) tools for the nucleotide analysis of immunoglobulin (IG) and T cell receptor (TR) V-(D)-J repertoires, polymorphisms, and IG mutations: IMGT/V-QUEST and IMGT/HighV-QUEST for NGS. *Methods Mol Biol*. 2012;882:569-604.
15. Borcherding N, Kim W, Quinn M, et al. CD4(+) T cells exhibit distinct transcriptional phenotypes in the lymph nodes and blood following mRNA vaccination in humans. *Nat Immunol*. 2024;25(9):1731-1741.
16. Borcherding N, Bormann NL, Kraus G. scRepertoire: An R-based toolkit for single-cell immune receptor analysis. *F1000Res*. 2020;9:47.
17. Shugay M, Bagaev DV, Zvyagin IV, et al. VDJdb: a curated database of T-cell receptor sequences with known antigen specificity. *Nucleic Acids Res*. 2018;46(D1):D419-D427.
18. Tickotsky N, Sagiv T, Prilusky J, Shifrut E, Friedman N. McPAS-TCR: a manually curated catalogue of pathology-associated T cell receptor sequences. *Bioinformatics*. 2017;33(18):2924-2929.
19. Vita R, Blazeska N, Marrama D, et al. The Immune Epitope Database (IEDB): 2024 update. *Nucleic Acids Res*. 2025;53(D1):D436-D443.
20. Zhang W, Wang L, Liu K, et al. PIRD: Pan Immune Repertoire Database. *Bioinformatics*. 2020;36(3):897-903.
21. Gavish A, Tyler M, Greenwald AC, et al. Hallmarks of transcriptional intratumour

heterogeneity across a thousand tumours. *Nature*. 2023;618(7965):598-606.
22. Vyborova A, Janssen A, Gatti L, et al. γ9δ2 T-Cell Expansion and Phenotypic Profile Are Reflected in the CDR3δ Repertoire of Healthy Adults. Frontiers in Immunology. 2022;13

SUPPLEMENTARY TABLES

Supplementary Table S1. Impact of CMV reactivation on the ratio of Vδ2$^+$/Vδ2$^-$ γδT cells. N indicates the total number of samples.

Platform	CMV	Ratio < day 100 (IQR)	n	Ratio > day 100 (IQR)	n
αβT-cell-depleted	No	1.80 (0.66-4.18)	239	0.61 (0.22-1.42)	260
αβT-cell-depleted	Yes	0.58 (0.25-1.66)	180	0.16 (0.07-0.39)	158
T-cell-replete	No	5.62 (5.11-9.58)	15	1.63 (0.28-5.62)	52
T-cell-replete	Yes	1.49 (0.91-11.33)	7	0.40 (0.20-2.20)	47

Supplementary Table S2. Overview of private clones shared between donor and allo-HSCT recipient

PatientID	Private shared Vδ2+ δ chains (%)
IR006	94,2
IR048	99,5
IR067	96,3
TR001	96,8
TR006	100

Definition private: not present in database with public clones [22]

Supplementary Table S3. Overview of top 50 genes per NMF program

		γδT cells					αβT cells		
MP_1	MP_2	MP_3	MP_4	MP_5	MP_1	MP_2	MP_3	MP_4	MP_5
EEF1A1	CCL5	KLF12	CDT1	ARHGAP15	TMSB10	CCL5	GAPDH	CBLB	CXCR4
IL7R	CST7	PRKCH	DUT	EEF1A1	TPT1	CST7	TUBA1B	KLF12	ZFP36L2
PHACTR2	EEF1A1	ARHGAP15	GAPDH	IFITM1	EEF1A1	GZMA	TYMS	NEAT1	EEF1A1
TPT1	GZMH	MALAT1	HMGB2	LEF1	LTB	NKG7	ACTB	RABGAP1L	TNFAIP3
CEBPD	IL32	PARP8	MCM7	LTB	TMSB4X	PFN1	DUT	UTRN	BTG1
ERN1	NKG7	RABGAP1L	PCLAF	MALAT1	LEF1	ACTB	HMGB2	ARHGAP15	JUNB
GZMK	SH3BGRL3	SKAP1	PCNA	NOSIP	MALAT1	CTSW	HMGN2	FYN	ZFP36
KLRB1	TMSB10	ZBTB20	STMN1	SELL	NOSIP	GZMH	MCM7	PRKCH	PDE4B
PLCB1	PFN1	AOAH	TUBA1B	SERINC5	PCED1B-AS1	MALAT1	PCLAF	SYNE2	DDIT4
SLC4A10	S100A4	DOCK10	TUBB	TCF7	TCF7	CD8A	STMN1	CELF2	SLC2A3
ALOX5AP	TMSB4X	DPYD	TYMS	TMSB10	B2M	EEF1A1	TUBB	IQGAP2	HLA-B
CD69	ACTB	MACF1	ACTB	TMSB4X	BACH2	EFHD2	FABP5	MACF1	JUN
DUSP1	CTSW	SYNE2	CLSPN	CCR7	CCR7	FGFBP2	H2AFZ	MALAT1	CREM
LTB	GNLY	UTRN	DEK	GAS5	MAL	HCST	HIST1H4C	P2RY8	SRGN
MALAT1	GZMA	ANKRD44	HMGN2	LDHB	PDE3B	HLA-B	MKI67	PARP8	TMSB4X
RORA	HCST	ARHGAP26	MCM5	MAL	CAMK4	PRF1	PCNA	RNF213	FTH1
TRDV2	IFITM1	CBLB	MKI67	MAML2	FOXP1	SH3BGRL3	SLC25A5	SMCHD1	CD69
B2M	CD52	CELF2	CDCA7	NELL2	IFITM1	TMSB4X	ACTG1	SYNE1	MALAT1
BTG1	IFITM2	FOXN3	CENPU	PDE3B	IL7R	CD52	CENPM	ATXN1	PABPC1
DPP4	MALAT1	FYN	H2AFZ	PIK3IP1	PRKCQ-AS1	GZMB	CENPU	FOXP1	DUSP2
MYBL1	PRF1	IQGAP2	CENPM	PRKCQ-AS1	SELL	IL32	CLSPN	MBNL1	UBC
SPOCK2	S100A6	NEAT1	COTL1	RCAN3	TXK	TMSB10	COTL1	RASA3	PTMA
ZFP36L2	TPT1	PITPNC1	DTL	RTKN2	TXNIP	B2M	HLA-DRA	RORA	HIST1H1E

Supplementary Table S3. Overview of top 50 genes per NMF program

		γδT cells					αβT cells		
MP_1	MP_2	MP_3	MP_4	MP_5	MP_1	MP_2	MP_3	MP_4	MP_5
CD28	EFHD2	RUNX1	MCM4	TESPA1	BCL2	GNLY	MCM3	RUNX1	H3F3B
FOS	TXNIP	SSH2	RRM2	TPT1	CD7	GZMM	MCM5	SIK3	TPT1
GPR65	FTL	ATXN1	SLC25A5	TXNIP	FHIT	IFITM1	PFN1	SKAP1	HIST1H1C
GZMA	PTMA	MBNL1	TK1	ACTN1	HLA-A	S100A4	RRM2	ZBTB20	YPEL5
HLA-B	CRIP1	PDE3B	ANP32B	B2M	HLA-B	TPT1	TK1	AOAH	IL7R
IL18RAP	GZMB	RASA3	DHFR	BACH2	MAML2	CD8B	CDT1	ARHGAP26	PDE4D
JUN	KLF2	RNF213	DNAJC9	BCL2	ACTB	FTL	CFL1	CEMIP2	HSPA5
NFKBIA	LY6E	SLFN12L	FABP5	CAMK4	FCMR	IFITM2	DTL	CHST11	DUSP1
S100A4	CD247	SYNE1	GINS2	CD52	FLT3LG	S100A6	H2AFV	DPYD	HIST1H1D
TRGV9	HLA-B	AHNAK	H2AFV	DGKA	TRABD2A	ABHD17A	HELLS	FOXN3	PIK3R1
TTC39C	S100A10	AKT3	HELLS	FYB1	JUNB	CD99	HIST1H1B	PDE3B	FAM177A1
AQP3	ACTG1	CHST11	HIST1H4C	GIMAP7	VIM	CFL1	MCM4	PITPNC1	KLRB1
CNN2	BTG1	DOCK2	MCM3	IL7R	FXYD5	HLA-A	NASP	STAT4	NR4A2
CXCR4	CX3CR1	FOXP1	NASP	JUNB	BTG1	HLA-C	NUSAP1	ZEB2	B2M
CXCR6	FCGR3A	LRBA	PTMA	MAP3K1	OXNAD1	ITGB2	TMSB4X	PIP4K2A	SRSF7
HIST1H1E	FGFBP2	NCALD	VIM	OXNAD1	LDHB	SYNE1	GINS2	ITGA4	PNRC1
IFNG-AS1	GAPDH	PIP4K2A	ACTG1	PCED1B-AS1	TGFBR2	ZEB2	PPIA	PTPRC	TSC22D3
IL23R	HOPX	PRKCB	FEN1	TXK	KLF2	AOAH	TMSB10	PTPRJ	KDM6B
JUNB	KLRD1	RIPOR2	HMGB1	BTG1	ABLIM1	FLNA	VIM	ARL15	EML4
MGAT4A	PLEK	RORA	HNRNPAB	FXYD5	PRKCA	GAPDH	MCM2	ANKRD44	TSPYL2
NCR3	SYNE2	SIK3	PPIA	CD27	RCAN3	KLRD1	HNRNPAB	PRKCB	DNAJB1
PBXIP1	ZEB2	SMYD3	SMC4	PRKCA	HSP90AB1	PLEK	HMGB1	HIVEP2	EZR
PDE4D	B2M	STAT4	PFN1	TMEM123	PCED1B	TXNIP	FEN1	RIPOR2	JMJD1C
SYTL2	CYBA	TNRC6B	NUSAP1	SNHG29	CD55	ACTG1	DEK	DOCK10	PARP8

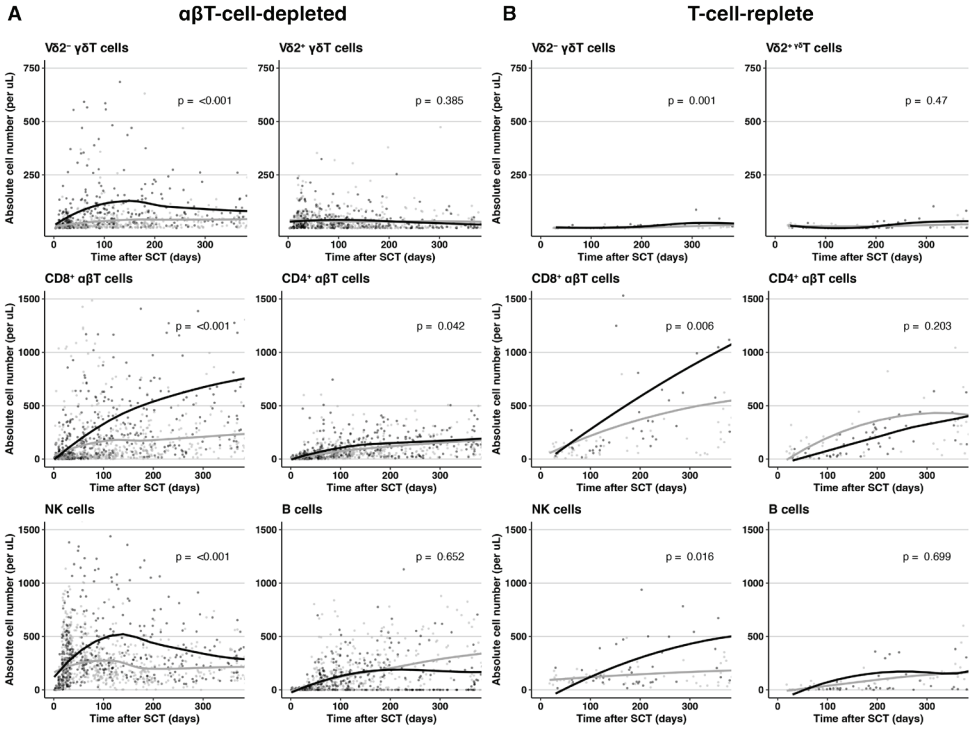
Supplementary Table S3. Overview of top 50 genes per NMF program

		γδT cells					αβT cells		
MP_1	MP_2	MP_3	MP_4	MP_5	MP_1	MP_2	MP_3	MP_4	MP_5
TC2N	H3F3B	ZEB2	SLBP	ACTB	PIK3IP1	CYBA	HSPD1	PCNX1	HLA-A
ZBTB16	DUSP2	ZFAND3	MCM6	RIPOR2	ARHGAP15	HMGB1	DNAJC9	PPP1R16B	DYNLT1
DUSP2	ZFP36L2	CNOT6L	ATAD2	ARID5B	IL6ST	HLA-DPB1	IDH2	CDK17	MAP3K2
$IL7R^+$ $KLRB1^+$ helper-/type-17–skewed, tissue-adapted γδ T	$CX3CR1^+$ $PRF1^+$ $GNLY^+$ terminal cytotoxic / NK-like effector γδ T	TCR signaling & motility	proliferation program	naive / central-memory–like γδ T	Naive / central-memory–like (stem-like) αβ T cells	Terminal cytotoxic / NK-like effector αβ T cells	proliferation program	TCR signaling & adhesion	Early activation / NF-κB–AP-1 response with negative-feedback regulators

Supplementary Table S4. Overview of primers used for next-generation sequencing of the TCR

TCR Beta	Sequences
cDNA synthese	
Switch adaptor	AAGCAGUGGTAUCAACGCAGAGUNNNNUNNNNUNNNNUCTTrGrGrGrG
PCR	
Reverse primer constant region	TGCTTCTGATGGCTCAAACAC
Forward primer adaptor	AAGCAGTGGTATCAACGCA
TCR Delta	
cDNA synthese	
Reverse primer constant region	GCAGTGGTATCAACGCAGAGTNNNNTNNNNTNNNNTTCACCAGACAAGCGACA
PCR	
Reverse primer adaptor	GCAGTGGTATCAACGCA
Forward primer Vd1	AGTGTGGCCCAGAAGGTTAC
Forward primer Vd2	TCTCTTCTGGGCAGGAGTC
Forward primer Vd3	GCACGCTGTGTGACAAAGTA
Forward primer Vd4	CAGCTTCACTGTGGCTAGG
Forward primer Vd5	GGGCATCAGTGCTGATTC
Forward primer Vd6	GCTTCAACTATGCTGGGTGAG
Forward primer Vd7	CTTCTACTGAGCTGGGTGAG
Forward primer Vd8	CTTGTGATCTCCACCTGTCTTG

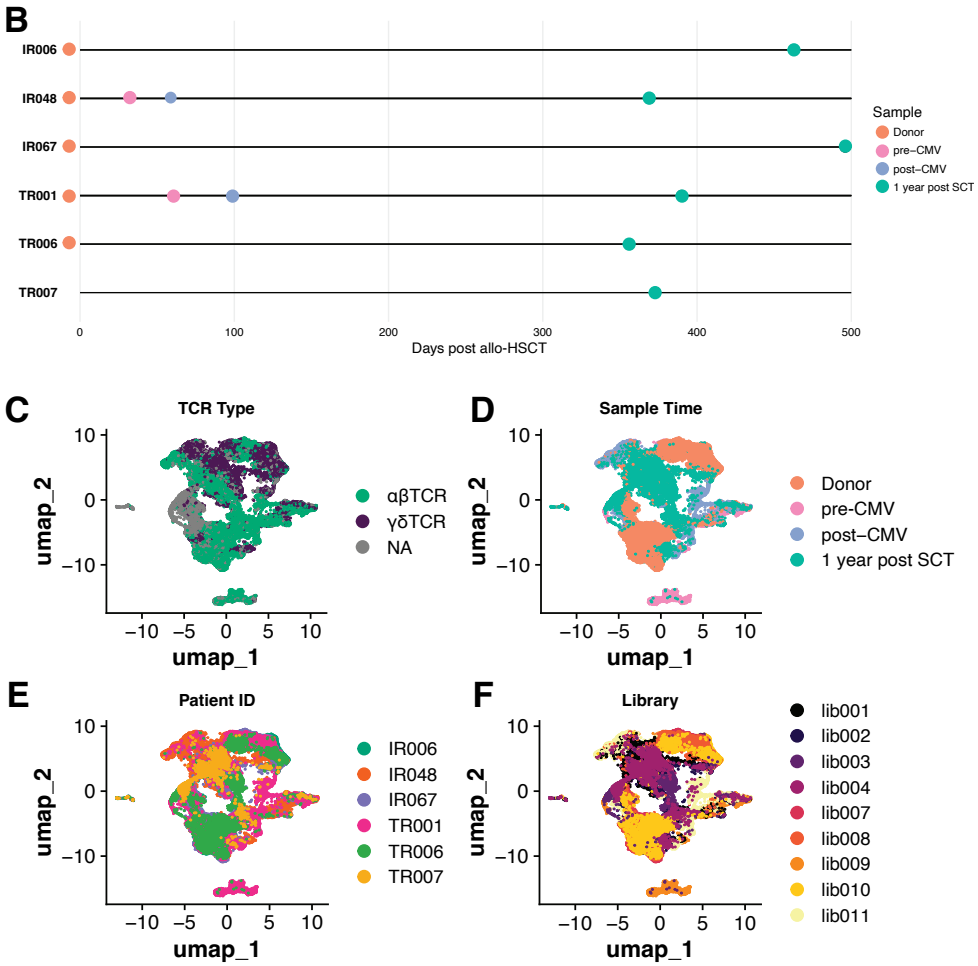
SUPPLEMENTARY FIGURES



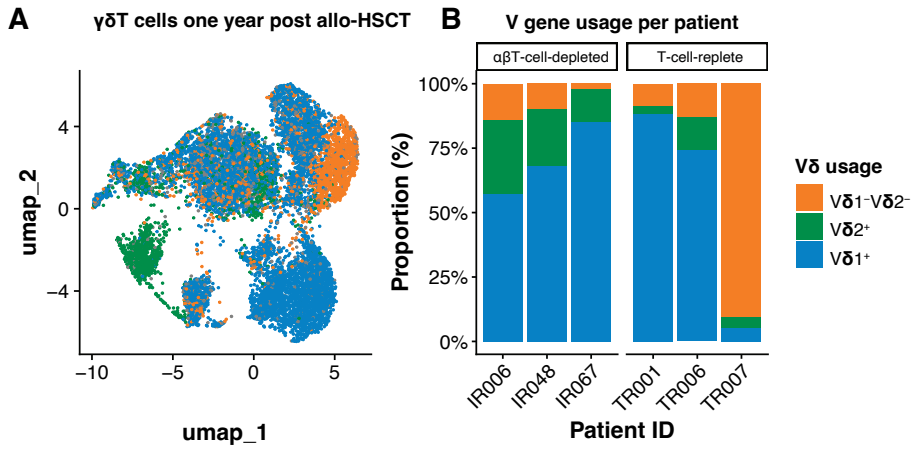
Supplementary Figure S1. Impact of CMV reactivation on immune reconstitution. ***(A)*** *Immune reconstitution of Vδ2⁻ γδT cells, Vδ2⁺ γδT cells, CD8⁺ αβT cells, CD4⁺ αβT cells, NK cells, and B cells after αβT-cell-depleted allo-SCT, stratified by CMV reactivation. Black = CMV reactivation (n=59), grey = no CMV reactivation (n=83). P-values show whether CMV had a significant impact on the slope in the first 60 days post-transplantation using a linear mixed-effects model. LOESS curves shown, span = 0.9.* ***(B)*** *Immune reconstitution of Vδ2⁻ γδT cells, Vδ2⁺ γδT cells, CD8⁺ αβT cells, CD4⁺ αβT cells, NK cells, and B cells after T-cell-replete allo-SCT, stratified by CMV reactivation. Black = CMV reactivation (n=27), grey = no CMV reactivation (n=36). P-values show whether CMV had a significant impact on the slope using a linear mixed-effects model. LOESS curves shown, span = 0.9.*

A

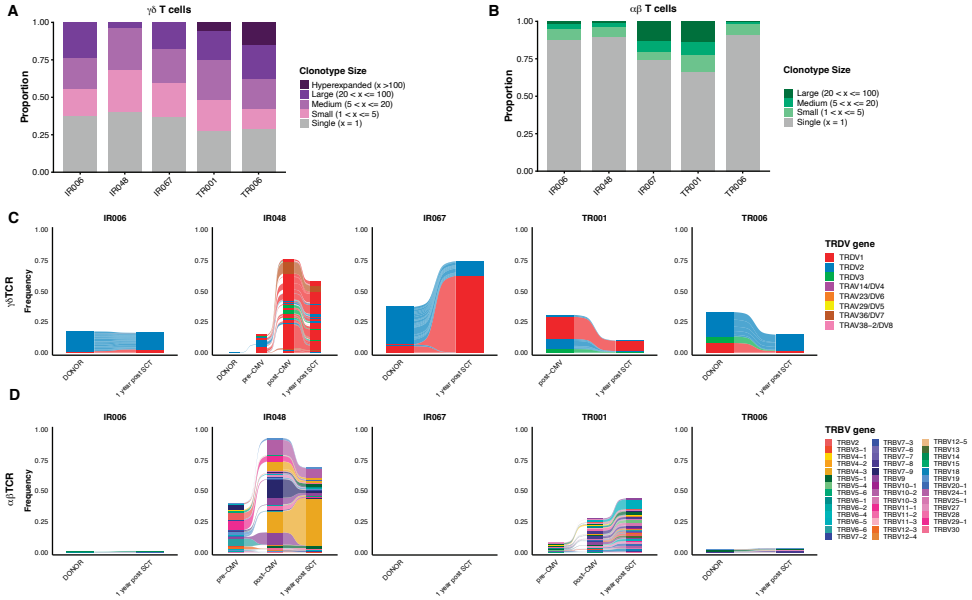
	αβTCR depleted			T cell replete		
patientID	IR006	IR048	IR067	TR001	TR006	TR007
Age	57	73	32	53	58	41
Sex	Female	Male	Female	Male	Female	Female
Disease	AML/MDS RAEB2	AML/MDS RAEB2	ALL	MDS/MPN	AML/MDS RAEB2	Lymphoma
Conditioning	MA + ATG	MA + ATG	MA + ATG	NMA + ATG	NMA	MA + ATG
Donortype	MUD 10/10	MUD 10/10	MRD 10/10	MUD 10/10	MRD 10/10	MUD 10/10
CMV serostatus	R+/D-	R+/D+	R+/D-	R+/D-	R+/D+	R+/D-



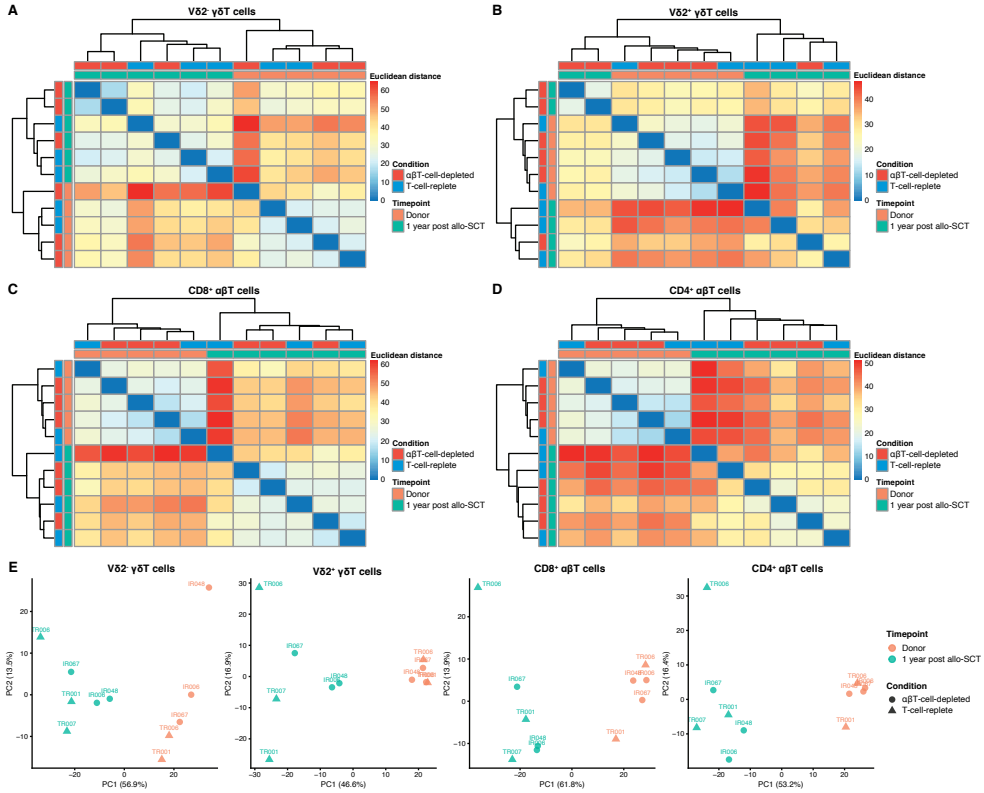
Supplementary Figure S2. Overview of patient samples used for scRNAseq and scRNAseq data. ***(A)*** *Overview of patient characteristics included for scRNA sequencing. AML = Acute Myeloid Leukemia, MDS RAEB-2 = Myelodysplastic Syndrome, Refractory Anemia with Excess Blasts type 2, ALL = Acute Lymphoblastic Leukemia, MA = myeloablative, NMA = non-myeloablative, ATG = anti-thymocyte globulin, MUD = matched unrelated donor, MRD = matched related donor, CMV = cytomegalovirus, R = recipient, D = donor.* ***(B)*** *Timeline of samples.* ***(C-F)*** *UMAPs of sequenced cells, colored by* ***C)*** *TCR,* ***D)*** *time of sampling,* ***E)*** *Patient ID, and* ***F)*** *Sequencing Library. Cells were clustered after filtering out V(D)J genes. A total of 95435 cells were retained after QC, of which 46223 were annotated with a TCR α and/or β chain, and 28716 cells were annotated with a TCR γ and/or δ chain. Cells annotated with more than one chain type were classified as doublets and excluded from downstream analysis. No batch correction was performed.*



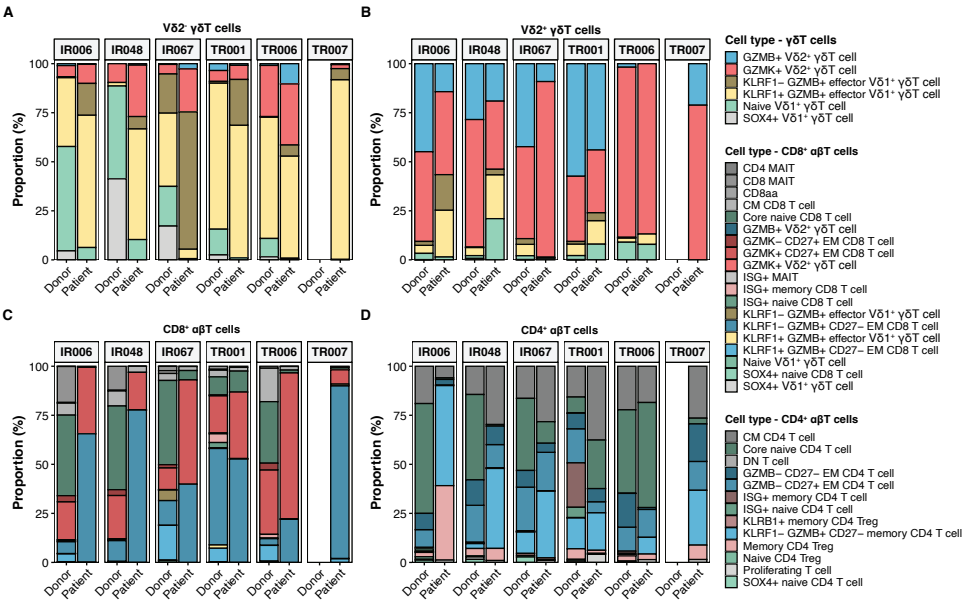
Supplementary Figure S3. Single-cell TCR sequencing analysis of V-gene usage in γδ T cells 1 year after allo-SCT. *All patients experienced CMV reactivation* ***(A)*** *UMAP of annotated γδ T cells from all patient samples, colored by V gene usage: Vδ1⁺ (blue), Vδ2⁺ (green), and Vδ1⁻Vδ2⁻ (orange). No batch correction was performed.* ***(B)*** *Stacked bar plots showing the proportion of each Vδ subset per patient.*



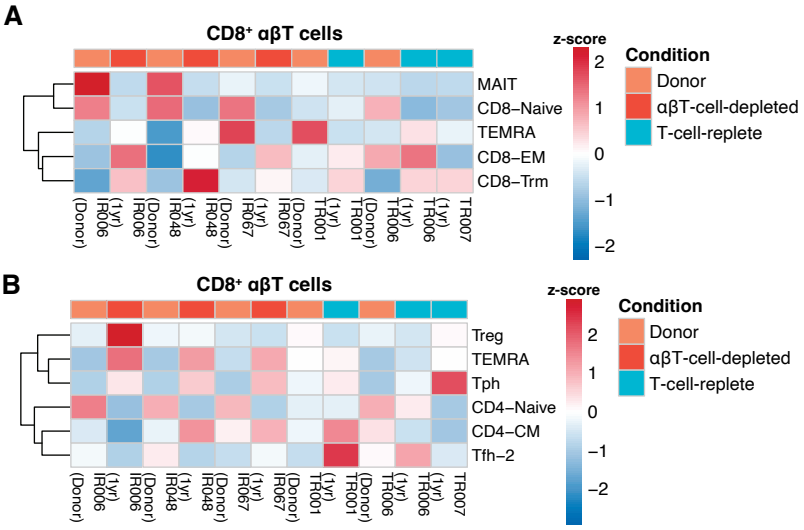
Supplementary Figure S4. Overview of single-cell TCR data. ***A-B)*** *Single-cell TCR sequencing of peripheral T cells of stem cell transplantation donors (n=5). Full TCR clones were grouped by size: single (1 cell), small (2–5 cells), medium (6–20 cells), large (21–100 cells) and hyperexpanded (>100 cells). The proportion of each category is shown for individual donors.* ***(A)*** *γδT cells and* ***(B)*** *αβT cells.* ***(C-D)*** *Longitudinal analysis of shared γδTCR* ***(C)*** *or αβTCR* ***(D)*** *clonotypes between donors and patients (n = 5), and pre- and post-CMV samples (n=2).*



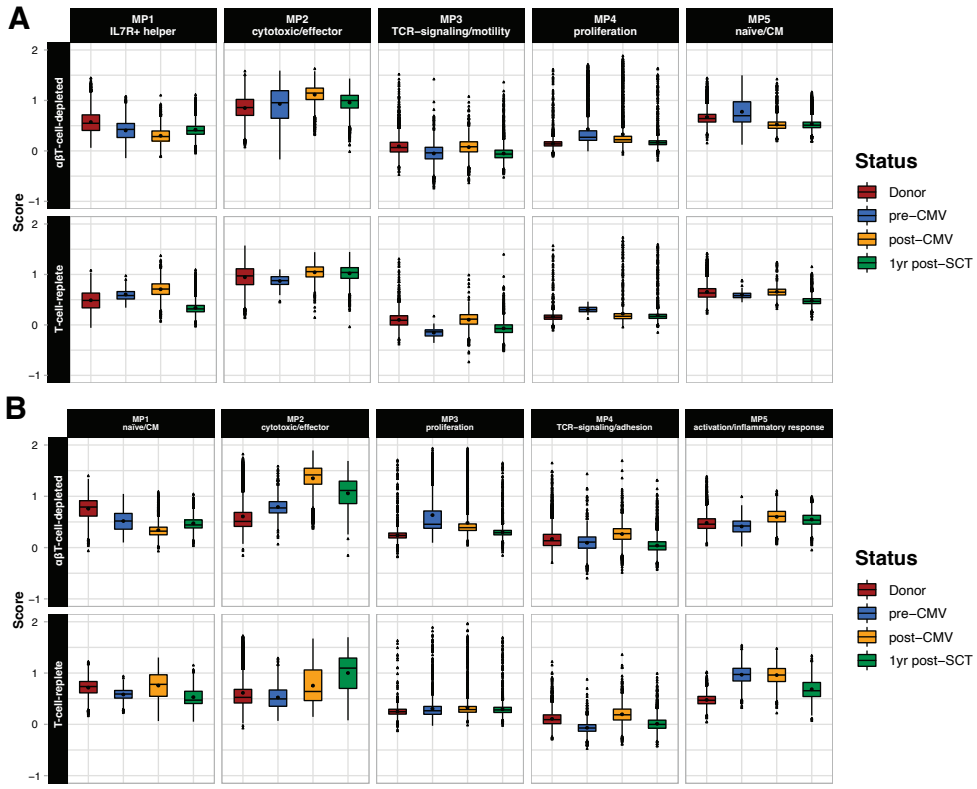
Supplementary Figure S5. Sample-to-sample Euclidean distance heatmaps and principal component analysis of four T cell subtypes comparing donor baseline and 1 year post allo-HSCT across graft types. *Distance calculations and PCA were performed using the top 1,000 most variable genes from pseudobulk-aggregated, normalized log-CPM expression values.* ***(A-D)*** *Euclidean distance heatmaps - Hierarchical clustering based on transcriptome-wide distances between samples for* ***(A)*** *Vδ2⁻ γδT cells,* ***(B)*** *Vδ2⁺ γδT cells,* ***(C)*** *CD8⁺ αβT cells, and* ***(D)*** *CD4⁺ αβT cells. Sample annotations indicate timepoint (orange: donor; teal: 1 year post-SCT) and graft condition (red: αβT-cell-depleted; blue: T-cell-replete). Dark red means the greatest transcriptional distance between samples.* ***(E)*** *Principal component analysis (PCA) plots showing the first two principal components for each T cell subset. Points are colored by time point and shaped by graft condition (circles: αβT-cell-depleted; triangles: T-cell-replete), with patient IDs labeled. The percentage of variance explained by each PC is shown on the axes.*



Supplementary Figure S6. Stacked bar plots showing the proportional distribution of T cell phenotypes in donor grafts and patient peripheral blood at one year post-SCT across six donor-patient pairs. *Cell phenotypes were annotated using Azimuth with the Allen Institute Data as a reference dataset.* ***(A)*** *Vδ2⁻ γδT cells,* ***(B)*** *Vδ2⁺ γδ T cells,* ***(C)*** *CD8⁺αβ T cells,* ***(D)*** *CD4⁺ αβT cells. Colors indicate phenotype categories, including naive, memory, effector memory, and cytotoxic (Granzyme+) subsets. Patient TR007 lacks a matched donor sample. Percentages are calculated relative to the total number of cells within each T cell subset per sample.*

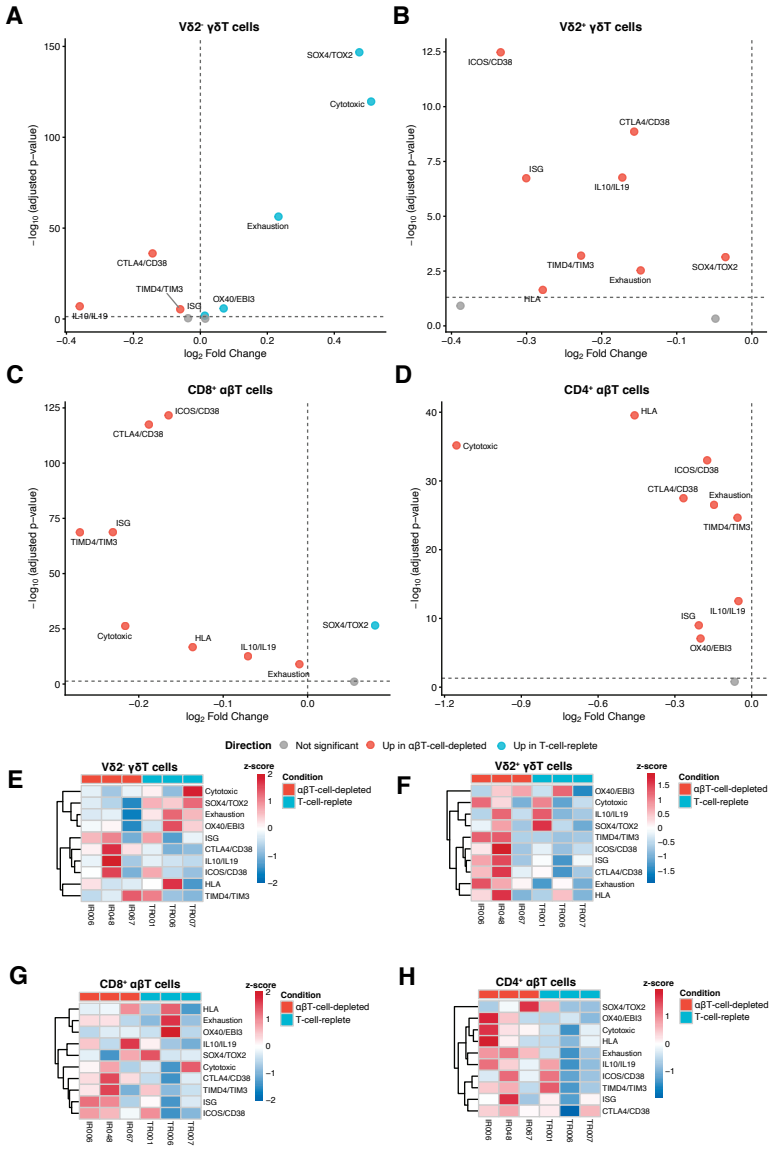


Supplementary Figure S7. Heatmaps showing average lineage scores *for* ***(A)*** *CD8⁺ αβT cells, and* ***(B)*** *CD4⁺ αβT cells. Each column represents an individual patient sample at 1 year post-SCT, grouped by transplant type (αβT-cell-depleted: IR006, IR048, IR067; T-cell-replete: TR001, TR006, TR007). Rows represent lineage programmes identified by TCAT. Values are scaled by row (z-score) to highlight relative differences across samples. Color scale: blue (low), white (medium), red (high). Hierarchical clustering of programmes is shown on the left.*

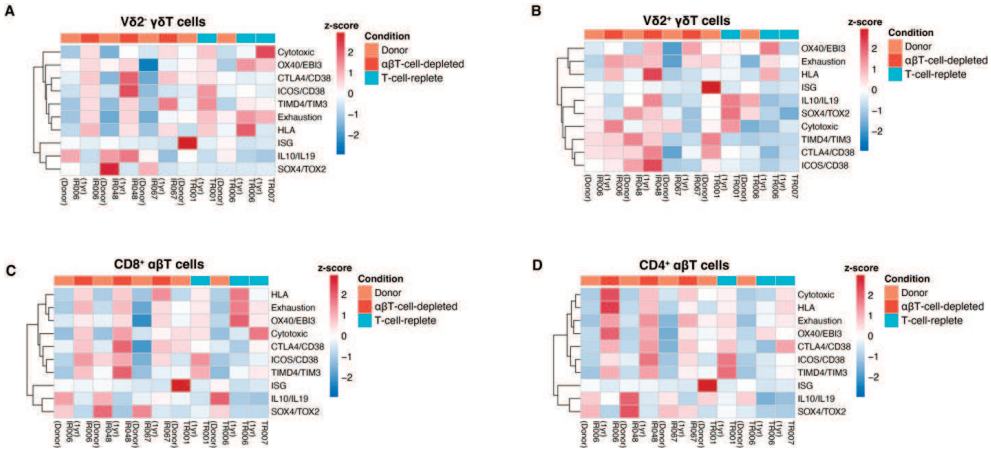


Supplementary Figure S8. NMF meta-program dynamics during T-cell reconstitution after allo-HSCT.

(A) *Single-cell module scores of five γδ T-cell NMF meta-programs (MP1–MP5) are shown as boxplots across donors and post-transplant timepoints, stratified by transplantation platform. MP1 reflects a helper-like γδ program (IL7R, KLRB1, RORA, IL18RAP); MP2 a terminal cytotoxic/NK-like γδ effector program (CCL5, NKG7, PRF1, GNLY, FGFBP2); MP3 a TCR signaling and motility-associated program; MP4 a proliferation/cell-cycle program; and MP5 a naïve/central-memory-like γδ program (TCF7, LEF1, CCR7, BACH2).* ***(B)*** *Single-cell module scores of five αβ T-cell NMF meta-programs (MP1–MP5) are shown as boxplots across donors and post-transplant timepoints, stratified by transplantation platform (stratified by patient in Supplementary Fig. S8). MP1 corresponds to a naïve/central-memory-like program (TCF7, LEF1, IL7R, CCR7); MP2 to a terminal cytotoxic effector program (CCL5, NKG7, PRF1, GNLY, granzymes); MP3 to a proliferation/cell-cycle program (MKI67, PCNA); MP4 to a signaling/adhesion program (FYN, PRKCH, ITGA4, STAT4); and MP5 to an early activation/inflammatory response program (TNFAIP3, ZFP36, DUSP1/2, JUN/JUNB, NR4A2, CD69). Full gene lists for each meta-program are provided in Supplementary Table 3. Colors indicate sampling status. Boxplots show median and interquartile range; points represent individual cells.*



Supplementary Figure S9. Differential enrichment of functional programmes ***(A-D)*** *Volcano plots showing differential enrichment of functional programmes between T-cell-replete and αβT-cell-depleted transplants for each T cell subset at 1 year post-SCT. X-axis: log2 fold change (positive values indicate higher in T-cell-replete). Y-axis: -log10(adjusted p-value). Horizontal dashed line indicates FDR < 0.05. Points are colored by direction: blue (higher in T-cell-replete), red (higher in αβT-cell-depleted), grey (not significant). Significantly different programmes (FDR < 0.05) are labeled. Statistical comparison by Wilcoxon rank-sum test with Benjamini-Hochberg correction. Heatmaps showing average functional programme scores for* ***(E)*** *Vδ2⁻ γδT cells,* ***(F)*** *Vδ2⁺ γδT cells,* ***(G)*** *CD8⁺ αβT cells, and* ***(H)*** *CD4⁺ αβT cells. Each column represents an individual patient sample at 1 year post-SCT, grouped by transplant type (αβT-cell-depleted: IR006, IR048, IR067; T-cell-replete: TR001, TR006, TR007). Rows represent individual functional programmes identified by TCAT. Values are scaled by row (z-score) to highlight relative differences across samples. Color scale: blue (low), white (medium), red (high). Hierarchical clustering of programmes is shown on the left.*



Supplementary Figure S10. *Heatmaps showing average functional programme scores for* ***(A)*** *Vδ2⁻γδT cells,* ***(B)*** *Vδ2⁺ γδT cells,* ***(C)*** *CD8⁺αβ T cells, and* ***(D)*** *CD4⁺ αβT cells. Each column represents an individual patient sample at 1 year post-SCT, grouped by transplant type (αβT-cell-depleted: IR006, IR048, IR067; T-cell-replete: TR001, TR006, TR007). Donor samples are shown for reference where available. Rows represent individual functional programmes identified by TCAT. Values are scaled by row (z-score) to highlight relative differences across samples. Color scale: blue (low), white (medium), red (high). Hierarchical clustering of programmes is shown on the left.*

Supplementary File S1. Top 50 DEGs between αβT cell-depleted and T cell-replete patients per cell type

Vδ2$^-$ γδT cells

p_val	avg_log2FC	pct.1	pct.2	p_val_adj	gene
<2,2E-308	10,2312828	0,959	0,846	<2,2E-308	ITGB2
<2,2E-308	108,294215	0,993	0,964	<2,2E-308	NKG7
<2,2E-308	240,808485	0,998	0,996	<2,2E-308	TMSB10
<2,2E-308	99,1821572	0,999	1	<2,2E-308	HLA-A
<2,2E-308	137,643957	1	1	<2,2E-308	HLA-B
3,263E-297	260,051692	0,999	0,997	5,001E-293	PFN1
2,896E-290	14,303044	0,73	0,407	4,437E-286	FGFBP2
2,715E-280	6,7722406	0,554	0,194	4,161E-276	FKBP5
1,146E-257	5,67650056	0,782	0,448	1,757E-253	DDIT4
6,126E-254	-1,8365382	0,216	0,552	9,388E-250	TC2N
6,742E-236	28,3575661	0,941	0,85	1,033E-231	ZFP36
9,112E-226	684,646938	0,999	1	1,396E-221	ACTB
1,015E-212	52,915806	0,988	0,991	1,556E-208	IFITM1
3,799E-208	288,138008	1	1	5,821E-204	B2M
3,627E-205	3,49700622	0,259	0,041	5,557E-201	AREG
3,677E-205	34,6820716	0,993	0,989	5,634E-201	EIF1
8,355E-204	-0,57248338	0,377	0,639	1,28E-199	S100A11
3,214E-200	-4,3042772	0,02	0,264	4,925E-196	KLRC1
2,006E-194	7,66954305	0,565	0,277	3,073E-190	SPON2
1,296E-181	3,13796833	0,274	0,058	1,986E-177	KIR2DL3
2,025E-178	272,179289	0,999	0,995	3,103E-174	PTMA
5,087E-168	76,8405275	0,165	0,422	7,796E-164	LTB
8,21E-167	54,3461089	0,997	0,99	1,258E-162	SH3BGRL3
1,986E-155	241,654379	1	0,999	3,043E-151	EEF1A1
5,657E-151	323,407322	0,985	0,973	8,669E-147	GAPDH
1,69E-148	17,7171866	0,984	0,949	2,589E-144	CST7
3,504E-144	105,197092	0,993	0,989	5,369E-140	CFL1
1,671E-140	5,18115774	0,896	0,748	2,561E-136	RUNX3
1,74E-138	-2,69508807	0,052	0,255	2,666E-134	ALOX5AP
1,23E-136	69,0471138	0,358	0,603	1,885E-132	LGALS1
4,392E-133	40,8916545	0,989	0,972	6,731E-129	SERF2
1,853E-132	-0,96718894	0,377	0,573	2,84E-128	GIMAP7
2,041E-131	4,19385929	0,539	0,266	3,128E-127	FCGR3A
6,741E-129	29,4977391	0,936	0,945	1,033E-124	TXNIP
4,864E-124	21,9685743	0,987	0,979	7,453E-120	CYBA

Vδ2$^-$ γδT cells (*continued*)

p_val	avg_log2FC	pct.1	pct.2	p_val_adj	gene
8,949E-124	50,1097064	0,751	0,509	1,371E-119	MT2A
1,729E-120	233,099447	0,861	0,856	2,65E-116	GNLY
7,591E-119	20,140638	0,822	0,818	1,163E-114	GZMH
2,186E-118	3,15344014	0,157	0,024	3,35E-114	BNC2
2,39E-115	22,6885336	0,808	0,9	3,663E-111	S100A10
1,114E-109	-10,4696901	0	0,131	1,707E-105	HLA-DQA2
2,6E-109	1,48381635	0,469	0,23	3,984E-105	TTC38
3,835E-107	3,81093789	0,144	0,022	5,877E-103	MYO3B
5,175E-105	58,701793	0,985	0,981	7,931E-101	CD52
2,1E-101	-1,99268497	0,079	0,251	3,2187E-97	THEMIS
8,239E-101	5,0357564	0,603	0,726	1,2626E-96	ITGA4
9,526E-101	6,08822535	0,138	0,336	1,4597E-96	IL7R
1,9899E-97	64,9184827	0,994	0,959	3,0493E-93	CCL5
3,9203E-95	1,45808239	0,571	0,333	6,0074E-91	ADGRG1

Vδ2^{+} γδT cells

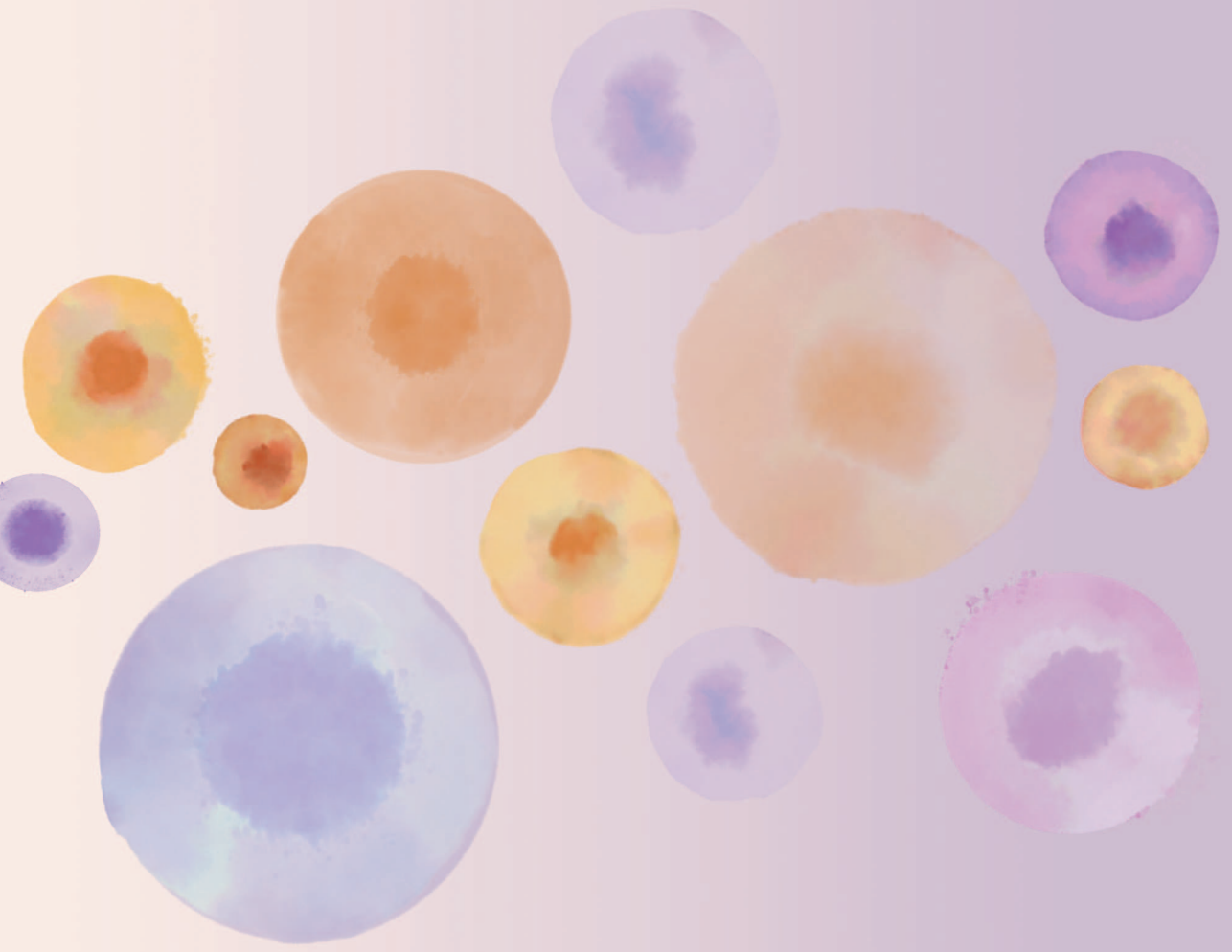
p_val	avg_log2FC	pct.1	pct.2	p_val_adj	gene
5,0256E-39	18,5269102	0,98	0,81	7,7012E-35	ZFP36
1,0567E-37	14,9882675	0,99	0,98	1,6193E-33	EIF1
7,2007E-30	75,704448	1	1	1,1034E-25	HLA-B
6,913E-29	4,18760854	0,16	0,01	1,0593E-24	NOCT
4,5308E-28	110,092026	1	1	6,9429E-24	EEF1A1
7,3944E-28	29,0054847	0,99	0,92	1,1331E-23	ZFP36L2
1,0583E-27	20,7111885	1	0,94	1,6217E-23	BTG1
5,539E-26	2,69841689	0,27	0,05	8,488E-22	AREG
1,0608E-24	2,50326439	0,28	0,05	1,6255E-20	NR4A3
7,7728E-23	2,72846915	0,18	0,02	1,1911E-18	TUBB2A
9,0711E-22	56,3983047	0,96	0,88	1,3901E-17	DUSP2
4,102E-20	16,8338998	1	0,99	6,2859E-16	PTMA
9,4073E-19	12,213805	0,99	0,98	1,4416E-14	FTH1
1,0645E-18	7,28104216	0,79	0,48	1,6312E-14	DDIT4
3,1114E-18	14,7492691	0,98	0,98	4,7679E-14	UBA52
4,7419E-18	5,7828386	0,96	0,89	7,2665E-14	JUND
9,0675E-18	40,9330087	1	1	1,3895E-13	HLA-A
1,2361E-17	2,52346741	0,17	0,03	1,8942E-13	PLK3
2,0728E-17	1,52749225	0,49	0,2	3,1764E-13	SOCS1
9,2668E-17	1,70324375	0,42	0,16	1,42E-12	SLC7A5
1,8197E-16	44,9142278	1	0,99	2,7886E-12	TMSB10
5,4414E-16	2,10001643	0,59	0,31	8,3383E-12	TUBA4A
7,9131E-16	1,70729818	0,31	0,09	1,2126E-11	ELL2
1,994E-15	14,0045412	0,94	0,82	3,0556E-11	CXCR4
7,5953E-15	1,27892617	0,63	0,35	1,1639E-10	RBM38
1,0589E-14	3,95669706	0,95	0,85	1,6226E-10	HNRNPA1
4,8442E-14	44,6421315	1	0,99	7,4233E-10	TPT1
5,0663E-14	15,1208421	1	0,98	7,7636E-10	CALM1
8,288E-13	1,27650741	0,43	0,18	1,27E-08	AUTS2
2,4876E-12	27,1877808	0,99	0,96	3,812E-08	S100A4
4,05E-12	15,1295006	0,86	0,67	6,2062E-08	DUSP1
8,1707E-12	1,52629327	0,26	0,09	1,2521E-07	KDM6B
8,3795E-12	1,48406672	0,34	0,13	1,2841E-07	IFRD1
9,6715E-12	-0,77206957	0,43	0,63	1,4821E-07	GIMAP7
1,0977E-11	6,02750993	0,96	0,9	1,6821E-07	SRGN
1,2756E-11	1,72153006	0,19	0,05	1,9548E-07	SKI
1,4554E-11	2,6675443	0,93	0,82	2,2303E-07	TGFB1
1,6764E-11	1,33149684	0,58	0,34	2,569E-07	ZNF331
1,9849E-11	-2,53607029	0,09	0,33	3,0417E-07	HLA-DRB5
2,8505E-11	1,76756942	0,1	0,02	4,3681E-07	CD8B
5,0655E-11	1,77065977	0,17	0,05	7,7624E-07	GRAMD1B
1,1951E-10	1,34540754	0,6	0,33	1,8313E-06	SELL
1,218E-10	1,23250668	0,37	0,16	1,8665E-06	MIDN
1,5424E-10	1,2550135	0,47	0,23	2,3635E-06	IDI1
1,7333E-10	1,62519044	0,23	0,07	2,6561E-06	UAP1
3,4493E-10	4,44060831	0,99	0,96	5,2857E-06	ARHGDIB
4,2793E-10	1,43833744	0,83	0,72	6,5577E-06	SRSF7
7,8355E-10	1,52049107	0,41	0,2	1,2007E-05	FKBP5
1,3601E-09	1,39256945	0,67	0,52	2,0843E-05	LDHA

CD8⁺ αβT cells

p_val	avg_log2FC	pct.1	pct.2	p_val_adj	gene
9,616E-303	1,25474205	0,93	0,75	1,474E-298	ZFP36
3,812E-221	0,73759595	0,98	0,9	5,842E-217	BTG1
2,339E-201	1,76027326	0,53	0,23	3,584E-197	FKBP5
1,718E-188	-1,32998313	0,4	0,67	2,633E-184	S100A11
1,092E-185	-1,3570331	0,37	0,64	1,673E-181	GIMAP7
1,754E-172	1,97212717	0,38	0,12	2,688E-168	PDE4D
1,703E-163	0,98166841	0,76	0,46	2,609E-159	DDIT4
1,99E-163	3,6710703	0,19	0,02	3,049E-159	NR4A3
1,028E-157	-1,37297044	0,36	0,61	1,576E-153	HLA-DRB5
2,648E-150	1,37917834	0,55	0,29	4,057E-146	RBM38
7,653E-142	0,52179967	1	0,98	1,173E-137	EIF1
1,564E-137	-0,91023742	0,57	0,75	2,396E-133	ITGA4
4,5E-137	1,76426056	0,34	0,12	6,896E-133	SOCS1
2,357E-128	1,39605336	0,65	0,43	3,613E-124	TUBA4A
1,701E-123	1,99856817	0,26	0,07	2,606E-119	SLC7A5
4,275E-113	1,55263626	0,31	0,11	6,552E-109	SELL
7,457E-113	1,72771051	0,4	0,19	1,143E-108	ZNF331
5,33E-111	-0,26029951	1	1	8,168E-107	HLA-C
1,037E-110	1,62166227	0,36	0,15	1,589E-106	PIM3
9,534E-109	1,13650925	0,54	0,31	1,461E-104	NFKBIA
1,047E-104	-0,82710061	0,57	0,74	1,605E-100	GNLY
5,084E-100	1,46793588	0,41	0,21	7,7909E-96	FAM177A1
9,623E-100	-0,57066131	0,77	0,89	1,4747E-95	GZMA
1,076E-99	1,94699186	0,22	0,06	1,6482E-95	ELL2
6,059E-99	1,95062165	0,22	0,07	9,2846E-95	SKIL
2,0168E-92	-1,1495255	0,29	0,49	3,0905E-88	GIMAP4
3,2516E-89	1,02258901	0,61	0,42	4,9827E-85	SRSF2
1,8985E-88	1,02912572	0,64	0,45	2,9092E-84	LDHA
9,3278E-88	1,58421803	0,28	0,11	1,4294E-83	AUTS2
1,2515E-85	0,61424482	0,86	0,68	1,9178E-81	DUSP2
2,0333E-85	0,47811765	0,95	0,89	3,1159E-81	ZFP36L2
2,6715E-83	-0,29824577	0,99	1	4,0938E-79	IL32
8,2427E-82	-8,8162652	0	0,12	1,2631E-77	HLA-DQA2
1,4843E-81	-1,59025612	0,15	0,33	2,2746E-77	CX3CR1
9,9434E-81	0,82409488	0,65	0,46	1,5237E-76	LEPROTL1
1,5004E-80	3,2891439	0,11	0,02	2,2993E-76	AREG
4,2889E-80	-0,51337695	0,87	0,92	6,5722E-76	CRIP1
1,7578E-78	-0,79390948	0,48	0,66	2,6937E-74	LGALS1
2,4446E-76	1,53159842	0,32	0,16	3,7461E-72	CREM
1,0705E-75	2,37238584	0,14	0,03	1,6404E-71	PLK3
2,5393E-75	1,90526791	0,23	0,09	3,8913E-71	IFRD1
4,1668E-75	0,66800358	0,79	0,65	6,3851E-71	PABPC1
7,1151E-75	-1,2856212	0,2	0,38	1,0903E-70	PATL2
3,9504E-74	-1,41473766	0,16	0,33	6,0535E-70	GIMAP5
6,8594E-74	1,34360253	0,34	0,17	1,0511E-69	IDI1
9,1517E-74	1,54218229	0,27	0,11	1,4024E-69	JMJD6
2,5026E-73	1,90871955	0,42	0,27	3,835E-69	NR4A2
2,8846E-72	-0,4371758	0,87	0,91	4,4204E-68	EMP3
4,4578E-72	0,61708834	0,79	0,65	6,8311E-68	TNFAIP3

CD4⁺ αβT cells

p_val	avg_log2FC	pct.1	pct.2	p_val_adj	gene
1,6485E-66	21,836239	1	0,99	2,5261E-62	EIF1
4,482E-64	7,62075084	0,99	0,91	6,8682E-60	SARAF
2,0139E-63	31,1645341	0,99	0,95	3,086E-59	BTG1
1,0229E-53	3,60688672	0,29	0,04	1,5675E-49	AREG
9,4712E-51	31,0387281	0,99	0,91	1,4514E-46	ZFP36L2
1,119E-50	5,74581002	0,83	0,48	1,7147E-46	DDIT4
1,948E-50	2,50901114	0,45	0,13	2,9851E-46	BACH2
3,9329E-50	2,44124967	0,45	0,13	6,0267E-46	CCR7
1,0168E-44	245,636023	1	1	1,5582E-40	EEF1A1
2,8129E-42	2,41459139	0,37	0,1	4,3105E-38	CSRNP1
2,556E-40	11,8084294	0,93	0,83	3,9168E-36	PABPC1
1,4186E-39	2,39955978	0,26	0,05	2,1739E-35	SKIL
4,8127E-39	3,33058046	0,2	0,02	7,375E-35	NR4A3
1,1001E-37	2,51749673	0,85	0,66	1,6858E-33	LEPROTL1
1,5206E-37	4,19553847	0,18	0,02	2,3302E-33	CDKN1A
4,2661E-37	-0,77850733	0,16	0,48	6,5373E-33	HLA-DRB5
8,6345E-34	112,261504	1	1	1,3231E-29	TPT1
2,4345E-33	1,8305531	0,43	0,17	3,7306E-29	ARRDC2
2,7469E-33	1,3834725	0,62	0,33	4,2093E-29	RBM38
8,2599E-33	2,12965706	0,52	0,28	1,2657E-28	ZNF331
8,8747E-33	2,2233596	0,35	0,11	1,36E-28	SNX9
3,1081E-32	1,65161958	0,55	0,28	4,7628E-28	FAM177A1
2,0609E-31	10,0164641	0,94	0,82	3,1581E-27	TSC22D3
5,1559E-31	70,995337	0,91	1	7,9009E-27	IL32
2,9563E-30	8,69476714	0,85	0,7	4,5303E-26	CXCR4
1,5936E-29	3,89073957	0,14	0,01	2,442E-25	LYPD3
3,2273E-29	2,45834543	0,25	0,07	4,9456E-25	ELL2
3,2435E-29	1,39700769	0,64	0,36	4,9704E-25	PIK3IP1
1,4929E-28	14,0251314	1	0,98	2,2878E-24	EEF1D
2,6739E-28	13,3851341	0,82	0,72	4,0974E-24	ZFP36
5,3148E-28	20,97013	0,81	0,56	8,1444E-24	NFKBIA
2,3574E-27	31,6582524	0,24	0,57	3,6125E-23	NKG7
3,3935E-27	30,1962121	1	0,99	5,2002E-23	FTH1
9,3156E-27	2,21060598	0,38	0,15	1,4275E-22	FHIT
1,4219E-26	4,48787317	0,1	0	2,179E-22	PMEPA1
4,153E-26	12,6103814	0,82	0,92	6,3641E-22	IFITM2
1,1673E-25	2,14640561	0,48	0,28	1,7887E-21	NR4A2
1,0146E-24	11,6730347	0,96	0,89	1,5548E-20	HNRNPA1
2,276E-24	0,66530725	0,18	0,44	3,4877E-20	PRF1
3,2863E-24	5,72759951	0,88	0,71	5,0359E-20	TNFAIP3
3,5453E-24	2,41924541	0,2	0,05	5,4328E-20	NELL2
4,9093E-24	77,440235	1	1	7,5231E-20	PTMA
7,4005E-24	1,50836986	0,44	0,21	1,1341E-19	IDI1
1,3133E-23	11,7173893	0,58	0,81	2,0125E-19	S100A11
2,3915E-23	2,64837113	0,14	0,02	3,6647E-19	ADTRP
3,9487E-23	-3,01459155	0,06	0,28	6,0509E-19	CISH
5,0535E-23	7,0203945	0,94	0,88	7,744E-19	NPM1
7,5533E-23	1,63982282	0,44	0,21	1,1575E-18	PER1
8,8003E-23	3,92971576	0,11	0,01	1,3486E-18	NR4A1



7

Summarising Discussion

DISCUSSION

Since the discovery of allogeneic haematopoietic stem cell transplantation in 1957, our knowledge of immunology has greatly increased[1-3]. This has resulted in significant improvements in outcomes after allogeneic haematopoietic stem cell transplantation (allo-HSCT) and in its widespread application. However, balancing graft-versus-host-disease (GVHD) and graft-versus-leukaemia (GVL) effects, along with other toxicities, remains a challenge. In this thesis, we aimed to investigate how *ex vivo* T-cell-depleted allo-HSCT shapes the balance between GVHD and GVL, and immune recovery, across different disease contexts.

Clinical performance of αβT-cell-depleted allo-HSCT

GVHD is mediated by activated αβT cells[4]. Therefore, recent studies have focused on *ex vivo* or *in vivo* T-cell depletion to reduce GVHD after allo-HSCT[5]. In **chapter 2**, we compared patient outcomes after *ex vivo* αβT-cell- and $CD19^+$ cell-depleted allo-HSCT with two historical T-cell-replete cohorts from our centre. We observed a significant reduction in extensive chronic GVHD and a corresponding improvement in GVHD-free, relapse-free survival, supporting the concept that graft engineering can improve long-term morbidity after allo-HSCT. This clinical benefit, however, was accompanied by increased cytomegalovirus (CMV) reactivation among CMV-seropositive individuals. This risk profile is likely to evolve with letermovir prophylaxis, which may alter both CMV incidence and downstream immune-reconstitution trajectories[6,7]. Finally, non-relapse mortality was not increased despite the use of myeloablative conditioning in the αβT-cell- and $CD19^+$ cell-depleted allo-HSCT cohort.

Comparison to other allo-HSCT platforms

To place these findings in context, it is essential to consider how graft engineering compares with other GVHD-prevention strategies in routine practice. Our results align with previous reports on αβT-cell- and $CD19^+$ cell-depleted allo-HSCT[8,9.] *Ex vivo* depletion, or graft engineering, is likely the most sophisticated method for T cell depletion, and its use has increased in Europe over the last decade[10]. However, *in vivo* methods such as anti-thymocyte globulin (ATG) and post-transplant cyclophosphamide (PT-Cy) have also been proposed and are widely used[5,11-15]. Evidence comparing ATG and PT-Cy is mixed across retrospective cohorts and has not shown consistent superiority in prospective randomised trials, suggesting context dependence[16-22].

A limitation of these studies is that ATG is treated as a binary variable, whereas its effect depends on dosage and infusion timing. When ATG is administered early, before transplantation, it affects host T cells, likely facilitating engraftment and affecting host immunity and antigen presentation. On the other hand, when ATG is administered shortly before transplantation, it can affect graft cells, potentially reducing engraftment[5].

Moreover, active ATG exposure is often not measured, and both over- and underexposure can negatively impact patient outcomes[23-26].

Because the mechanisms differ, comparing *in vivo* and *ex vivo* depletion methods is difficult, especially given that studies employ different inclusion criteria and that comparative prospective trials are lacking. Retrospective studies in children have found that T-cell-depleted allo-HSCT is associated with higher overall survival in inborn errors of immunity [11,27] and lower GVHD after a second transplant for malignancies[28]. Moreover, preliminary evidence from an EBMT registry study suggests that the incidence of GVHD is lower after αβT-cell-depleted allo-HSCT than after PT-Cy[29].

Overall, αβT-cell- and $CD19^+$ cell-depleted allo-HSCT appears to shift the post-transplant risk profile toward lower rates of chronic GVHD and improved GRFS. However, comparisons with alternative platforms are largely non-randomised and susceptible to centre- and time-related confounding. Prospective evaluations with harmonised supportive care will be essential to define which patient groups benefit most from this platform. Additionally, real-world feasibility will determine where this platform can be implemented.

Practical considerations of graft engineering: costs

One major hurdle in implementing graft engineering strategies is the upfront cost of the procedure. The cost of an engineered haplo-identical graft has been estimated at $28 963, compared with $27 297 for matched unrelated donor grafts, suggesting that an engineered unrelated donor graft is likely more expensive[30]. However, graft price alone is an incomplete metric: over a lifetime, average per-patient medical costs of allo-HSCT have been estimated at $942,373- $1,247,917, with 37-53% attributable to chronic GVHD treatment[31]. In line with this, the average annual cost of chronic GVHD has been estimated at $291,357, and emerging therapies may further increase these costs[32,33]. Chronic GVHD also drives substantial societal costs, as approximately 25% of patients are unable to return to the workforce due to permanent disability[34]. Therefore, the relevant question is not whether graft engineering is more expensive upfront, but whether it reduces the total cost of care, given that chronic GVHD drives substantial long-term medical and societal costs, whereas relapse-directed interventions such as donor lymphocyte infusions are typically less costly[35] These considerations are likely to vary by healthcare system and centre expertise. In this context, cryopreservation and streamlined graft processing may be key implementation tools that determine whether engineered grafts can be scaled beyond highly specialised centres.

Practical implementation of graft engineering: feasibility of cryopreservation and graft characteristics

Graft engineering is resource-intensive, and broad application depends not only on clinical outcomes but also on logistical robustness. Cryopreservation of engineered grafts could increase scheduling flexibility and allow centralised manufacturing models. Moreover, the COVID-19 pandemic demonstrated that cryopreservation can be essential for sustaining transplant programmes during global crises[36]. In **chapter 3**, we retrospectively analysed outcomes in patients who received cryopreserved grafts. We found that freezing the allograft did not significantly affect patient outcomes.

Historically, cryopreservation of grafts has been limited by concerns about the potential to damage mononuclear cells and the increased risk of transfusion reactions associated with DMSO[37]. Early retrospective studies reported slightly delayed neutrophil and platelet recovery and inconsistent findings regarding the risk of GVHD[37-41]. One study found an impact on non-relapse mortality and overall survival; however, reasons for cryopreservation were not routinely collected, and in a subset, cryopreservation was due to a change in patient condition[42]. In $CD34^+$ selected and PT-Cy allo-HSCT settings, no differences in outcomes were reported between patients receiving cryopreserved and fresh grafts[43,44]. Moreover, several studies conducted during the COVID-19 pandemic reported no differences in outcomes[45,46].

Although several studies did not report differences in outcomes between cryopreserved and fresh grafts, cryopreservation was associated with a loss of $CD34^+$ cells in several studies[38,45,46]. Consistent with these observations, we observed a 65% recovery of $CD34^+$ cells (**chapter 3**), resulting in lower median $CD34^+$ cells/kg in frozen allografts than in fresh allografts. These lower $CD34^+$ cell counts (<4x10^6/kg) did not affect patient outcomes in our cohort. Prior studies have reported that low doses of $CD34^+$ cells are associated with delayed engraftment and increased relapse[47-49]. In contrast, very high doses have been associated with poorer survival and GVHD in some analyses[50,51]. Although these associations are derived mainly from T-cell-replete settings, they underscore the importance of monitoring post-thaw $CD34^+$ yield and ensuring adequate dosing.

Thus, planned cryopreservation did not affect primary outcomes in our cohort, supporting its role as a pragmatic tool to improve logistics and broaden access to graft engineering. Nevertheless, the reduction in post-cryopreservation $CD34^+$ recovery indicates that freezing can lower the effective infused dose. Future studies should therefore combine clinical endpoints with post-thaw graft characterisation and dose-response analyses to define optimal $CD34^+$ targets in T-cell-depleted settings. Moreover, this optimal $CD34^+$ target may be disease-dependent, and T-cell-depleted platforms may require disease-specific optimisation.

Disease-specific optimisation: αβT-cell-depleted allo-HSCT with peri-transplant ruxolitinib in myelofibrosis

Allo-HSCT is the only curative option for myelofibrosis patients, but it has historically been associated with a high non-relapse mortality (NRM), especially in patients over 50 receiving myeloablative conditioning[52,53]. Additionally, JAK inhibitors, such as ruxolitinib, have transformed the symptomatic management of myelofibrosis, but they are not curative[54]. Moreover, ruxolitinib has been introduced as a treatment for steroid-refractory GVHD[55]. Together, these findings led to the introduction of 'peri-transplant' ruxolitinib, i.e., the inclusion of ruxolitinib in the conditioning regimen and its continuation post-transplant. In **chapter 4**, we retrospectively analysed two cohorts of patients who all received myeloablative conditioning with a αβT cell-depleted allograft. One of the cohorts received peri-transplant ruxolitinib, while the other did not. We found that overall survival was significantly improved in the cohort that received peri-transplant ruxolitinib, as non-relapse mortality was significantly decreased in this cohort.

The overall survival rate of 84% at 2 years in the peri-transplant ruxolitinib group compared favourably with that reported in other studies of allo-HSCT in myelofibrosis[53,56-62]. Moreover, recent studies using peri-transplant ruxolitinib in patients with myelofibrosis have shown similar favourable outcomes[63-67]. However, in a T-cell-replete setting, chronic GVHD persisted despite a short course of peri-transplant ruxolitinib[64]. In contrast, longer peri-transplant ruxolitinib duration or PT-Cy was associated with a lower incidence of chronic GVHD[65-67]. This is in line with the lower rate of chronic GVHD we reported in our cohort. Together, these results suggest that peri-transplantation ruxolitinib may reduce acute GVHD; however, optimizing its duration and combining it with T-cell depletion strategies may be necessary to mitigate chronic GVHD risk more effectively.

Disease control and immune intervention after αβT-cell-depleted allo-HSCT in myelofibrosis

A reduction of GVHD in myelofibrosis patients may be associated with an increased risk of relapse[59]. Relapse can occur relatively late after allo-HSCT in myelofibrosis, providing time to implement strategies, such as donor lymphocyte infusions (DLI). Thanks to new techniques such as digital PCR[68], we can effectively track driver mutations in myelofibrosis. Recent studies have highlighted the importance of clearing these driver mutations and treating molecular relapse with DLI before it evolves into haematological relapse[58,61]. However, the question remains when to administer these DLIs and at what dose[35]. To guide these post-transplant interventions and refine disease-specific strategies, we need a better understanding of immune recovery and how it is shaped by platform, disease, medication, and viral reactivation.

Monitoring immune recovery after αβT-cell-depleted allo-HSCT

Short-term immune-related proteomics after allo-HSCT

One way to examine immune recovery after allo-HSCT is through proteomics. In **chapter 5**, we used the Olink immuno-oncology assay to analyse immune-related proteins during the first 4 weeks after allo-HSCT. We found distinct temporal changes, with disease-specific trajectories. Due to the small sample size, we were unable to correlate these findings with patient outcomes.

In recent years, extensive research has focused on identifying biomarkers of early complications after allo-HSCT, resulting in long lists of potential biomarkers[69-75]. Of these, the MAGIC biomarker panel, including ST2 and REG3α appears to be the most promising in predicting non-relapse mortality due to GVHD[76,77]. However, with the implementation of new allo-HSCT platforms, such as αβT-cell depletion, and more disease-specific modulations, such as peri-transplant ruxolitinib, it would be beneficial to study how these factors influence potential biomarkers. For example, high baseline IL-6 has been linked to acute GVHD and worse overall survival in a PT-Cy allo-HSCT setting[69]. Moreover, ruxolitinib has been associated with reduced levels of IL-6 and IFN-γ, both in a peri-transplant and a non-transplant setting, in myelofibrosis[56,64,78]. Notably, we observed a marked increase in IL-6 in week two after transplantation, followed by a subsequent decrease, in all three disease settings. This is consistent with previous studies reporting IL-6 peaks during the leukopenic phase[79,80].

However, we also observed high inter-individual variability. This inter-individual variability will remain a challenge, complicating biomarker discovery, and may require larger, harmonised cohorts with longitudinal sampling. Moreover, the clinical value of biomarker monitoring depends on actionability: biomarkers are most useful when they inform interventions that can meaningfully alter outcomes rather than merely predict them. Finally, interpreting biomarker dynamics benefits from cellular and repertoire-level context, which we examined in **chapter 6**.

Innate/adaptive T-cell reconstitution and TCR repertoire dynamics

To optimise post-transplant immune intervention strategies, we need to understand the details of immune reconstitution. In **chapter 6**, we studied immune reconstitution after αβT-cell-depleted allo-HSCT versus T-cell-replete allo-HSCT, focusing on CMV reactivation, the TCR repertoire, and transcriptomics. CMV reactivation was associated with an expansion of $CD8^+$ αβT cells and $V\delta2^{neg}$ γδT cells in both allo-HSCT settings. Moreover, $V\delta2^{neg}$ γδT cells underwent early polyclonal expansion. This was followed by oligoclonal expansion, largely independent of CMV reactivation, in the T-cell-depleted allo-HSCT setting. Single-cell TCR sequencing at 1 year post-transplant revealed marked hyperexpansion of the αβTCR clones in αβT-cell-depleted allo-HSCT recipients, whereas the γδTCR

repertoire showed greater inter-patient variability. Finally, we found platform-dependent effector profiles in patient T cells. Together, these findings suggest CMV reactivation is a dominant driver of T cell reconstitution, with platform-specific imprinting on top.

In line with our findings, other studies have shown that CMV reactivation is a significant driver of immune reconstitution post-transplantation, expanding $V2^{neg}$ γδT and $CD8^{+}$ αβT cells in T-cell-replete allo-HSCT settings[81-86]. Additionally, although CMV reactivation imprints the T cell repertoire early after allo-HSCT, the effects can be long-lasting[87,88]. Consistent with this, our one-year transcriptomic analyses showed that patient T cells were predominantly effector cells compared to donor T cells across both platforms, suggesting ongoing activation that may be partly driven by CMV reactivation. However, we did not detect a high proportion of CMV-specific clonotypes one year after allo-HSCT. The question remains whether the process of "memory inflation", i.e., expansion of CMV-specific effector T cell clones, is harmful or beneficial. CMV reactivation is associated with a reduced risk of relapse in some allo-HSCT settings[89]. Still, it may depend on disease stage, conditioning type, and the use of *in vivo* depletion methods, such as ATG[89-91]. Moreover, this beneficial effect may be T cell subset-specific, as CMV-induced γδT cells can cross-react with leukemic blasts[92]. In this context, hyper-expansion of specific clones may be less concerning for γδT cells than for αβT cells, as γδT cell responses are often characterised by rapid, oligoclonal expansions that can represent physiological reconstitution rather than pathological skewing[93,94].

While CMV reactivation emerged as a dominant driver of $CD8^{+}$ αβT-cell and $V\delta2^{neg}$ γδT-cell expansion, new therapies might modulate this effect. For example, letermovir has recently been approved for CMV prophylaxis[6]. Letermovir may delay CMV-specific cellular reconstitution, likely due to reduced CMV antigen exposure[7]. This may lead to reduced 'memory inflation', yielding a more diverse post-transplant TCR landscape. At the same time, suppressing CMV-driven immune activation could influence downstream outcomes in uncertain directions. While it may reduce immune exhaustion, it could also diminish context-dependent CMV-associated protection against relapse reported in some settings[89]. This highlights the need to integrate prophylaxis status into immune-monitoring studies and to test whether CMV prevention modifies not only infection endpoints but also GVL and long-term immune fitness.

Besides CMV reactivation, graft engineering can also shape both the immediate and later repertoires. This effect of graft engineering is highlighted by differences in αβTCR clonality between recipients of αβT-cell-depleted allo-HSCT and T-cell-replete allo-HSCT one year after allo-HSCT. While some studies have found that reduced TCR repertoire diversity is associated with increased risk of GVHD, others have not[85,95-102]. Together with our findings, these studies suggest that graft engineering strategies may substantially influence this relationship. Additionally, we found that graft engineering affected patients'

transcriptomic profiles. Specifically, we found increased *AREG* expression in T cells from patients treated with a T-cell-replete allo-HSCT. Recently, *AREG* has been associated with a repair T-cell phenotype in solid tumours and tissue[103,104]. These findings suggest that the allo-HSCT platform may impact later phenotypes of cells. To interpret these platform effects, it is also essential to consider the origin of the post-transplant repertoire: whether it persists from graft clones or is *de novo* generated.

We found limited overlap in Vδ2^{neg} TCR and TCR repertoires between donors and patients one year after allo-HSCT, with some Vδ2^{pos} TCR overlap in both the αβT-cell-depleted and T-cell-replete allo-HSCT groups. While an early study using CDR3 spectratyping found that the γδTCR repertoire was donor-dependent; later studies using TCR sequencing techniques found limited patient-donor overlap[86,105,106]. This was also true for αβTCR repertoires, although early reconstitution in the T-cell-replete setting was driven by rapidly expanding (small) clones from the graft[87,101,107]. These findings suggest a substantial role for *de novo* generation, even in older patients, in whom thymic regeneration was thought to be limited[108].

Taken together, our data reinforce the notion that immune reconstitution after allo-HSCT is jointly shaped by the allo-HSCT platform and viral reactivation (in particular CMV), resulting in distinct patterns of T-cell expansion and repertoire evolution. However, our conclusions are limited by sampling primarily from peripheral blood and by cohort size. Integrating repertoire analysis with functional readouts and clinical decision points (e.g., CMV management or DLI timing) will be crucial to translate immune monitoring into improved outcomes.

FUTURE DIRECTIONS

In conclusion, *ex vivo* T-cell-depleted allo-HSCT is associated with low GVHD incidence; however, some patient groups may require specific adjustments to ensure optimal performance of this platform. To this end, we need a better understanding of immune reconstitution, as multiple factors shape it after allo-HSCT, including graft engineering, viral reactivation, underlying disease, peri-transplant medication, and conditioning regimens.

Several considerations are essential for future studies. Comparative analyses should account for differences in conditioning intensity and *in vivo* immune suppression exposure (e.g., ATG timing), and use harmonised endpoints. Moreover, immune profiling studies require larger, longitudinal, ideally prospectively sampled, cohorts to address inter-individual variability. Finally, expanding beyond peripheral blood to bone marrow and tissue compartments may be necessary to link immune reconstitution to clinically relevant processes such as GVL and organ-specific GVHD. To this end, newer tools, such as

spatial transcriptomics, may be of interest, as they may provide insight into the clonality of the TCR repertoire at specific locations.

Additionally, with the rise of cellular therapies such as chimeric antigen receptor (CAR) T cells[109], the treatment landscape for haematological malignancies continues to evolve. Rather than replacing allo-HSCT, these approaches may function alongside it, for example, as a bridge to transplantation or, potentially, as an immunomodulatory strategy[110,111]. This evolution further underscores the importance of optimising allo-HSCT platforms to minimise GVHD while preserving immune recovery, and it raises practical questions regarding costs and access to care.

Finally, while identifying new treatment options and outcome biomarkers remains essential, we should not overlook immediately actionable improvements in care. In a field with multiple transplant approaches, early and transparent communication about expected benefits, risks, and uncertainty is a core part of quality care. This is particularly important for GVHD, where unmet needs in information, communication, and support are repeatedly reported by patients and caregivers[112]. Thus, efforts to optimise the GVHD–GVL balance should go hand in hand with strengthening shared decision-making and expectation management, even if platform choice may be limited by centre expertise.

REFERENCES

1. Thomas ED, Lochte HL, Jr., Lu WC, Ferrebee JW. Intravenous infusion of bone marrow in patients receiving radiation and chemotherapy. *N Engl J Med*. 1957;257(11):491-496.
2. Chabannon C, Kuball J, Bondanza A, et al. Hematopoietic stem cell transplantation in its 60s: A platform for cellular therapies. *Sci Transl Med*. 2018;10(436).
3. Granot N, Storb R. History of hematopoietic cell transplantation: challenges and progress. *Haematologica*. 2020;105(12):2716-2729.
4. Zeiser R, Blazar BR. Acute Graft-versus-Host Disease - Biologic Process, Prevention, and Therapy. *N Engl J Med*. 2017;377(22):2167-2179.
5. de Witte M, Daenen LGM, van der Wagen L, et al. Allogeneic Stem Cell Transplantation Platforms With Ex Vivo and In Vivo Immune Manipulations: Count and Adjust. *Hemasphere*. 2021;5(6):e580.
6. Marty FM, Ljungman P, Chemaly RF, et al. Letermovir Prophylaxis for Cytomegalovirus in Hematopoietic-Cell Transplantation. *N Engl J Med*. 2017;377(25):2433-2444.
7. Zamora D, Duke ER, Xie H, et al. Cytomegalovirus-specific T-cell reconstitution following letermovir prophylaxis after hematopoietic cell transplantation. *Blood*. 2021;138(1):34-43.
8. Leahy AB, Li Y, Talano JA, et al. Unrelated donor alpha/beta T cell- and B cell-depleted HSCT for the treatment of pediatric acute leukemia. *Blood Adv*. 2022;6(4):1175-1185.
9. Bethge WA, Eyrich M, Mielke S, et al. Results of a multicenter phase I/II trial of TCRalphabeta and CD19-depleted haploidentical hematopoietic stem cell transplantation for adult and pediatric patients. *Bone Marrow Transplant*. 2022;57(3):423-430.
10. de Witte MA, Mooyaart JE, Hoogenboom JD, et al. Activity of ex vivo graft and DLI Engineering within the last decade increases, a survey from the EBMT Cellular Therapy & Immunobiology Working Party. *Bone Marrow Transplant*. 2023.
11. Morales E, Pulsipher MA. A better approach to mismatched HSCT than PTCY? *Blood*. 2024;144(5):474-476.
12. Luznik L, O'Donnell PV, Symons HJ, et al. HLA-haploidentical bone marrow transplantation for hematologic malignancies using nonmyeloablative conditioning and high-dose, posttransplantation cyclophosphamide. *Biol Blood Marrow Transplant*. 2008;14(6):641-650.
13. Munchel A, Kesserwan C, Symons HJ, et al. Nonmyeloablative, HLA-haploidentical bone marrow transplantation with high dose, post-transplantation cyclophosphamide. *Pediatr Rep*. 2011;3 Suppl 2(Suppl 2):e15.
14. Pulsipher MA. Haplo is the new black. *Blood*. 2014;124(5):675-676.
15. Fierro-Pineda JC, Tsai HL, Blackford A, et al. Prospective PTCTC trial of myeloablative haplo-BMT with posttransplant cyclophosphamide for pediatric acute leukemias. *Blood Adv*. 2023;7(18):5639-5648.
16. Ruggeri A, Sun Y, Labopin M, et al. Post-transplant cyclophosphamide versus anti-thymocyte globulin as graft-versus-host disease prophylaxis in haploidentical transplant. *Haematologica*. 2017;102(2):401-410.
17. Battipaglia G, Labopin M, Kroger N, et al. Posttransplant cyclophosphamide vs antithymocyte globulin in HLA-mismatched unrelated donor transplantation. *Blood*. 2019;134(11):892-899.
18. Battipaglia G, Labopin M, Hamladji RM, et al. Post-transplantation cyclophosphamide versus antithymocyte globulin in patients with acute myeloid leukemia undergoing allogeneic stem cell transplantation from HLA-identical sibling donors: A retrospective analysis

from the Acute Leukemia Working Party of the European Society for Blood and Marrow Transplantation. *Cancer*. 2021;127(2):209-218.

19. Brissot E, Labopin M, Moiseev I, et al. Post-transplant cyclophosphamide versus antithymocyte globulin in patients with acute myeloid leukemia in first complete remission undergoing allogeneic stem cell transplantation from 10/10 HLA-matched unrelated donors. *J Hematol Oncol*. 2020;13(1):87.
20. Brissot E, Labopin M, Labussiere H, et al. Post-transplant cyclophosphamide versus anti-thymocyte globulin after reduced intensity peripheral blood allogeneic cell transplantation in recipients of matched sibling or 10/10 HLA matched unrelated donors: final analysis of a randomized, open-label, multicenter, phase 2 trial. *Blood Cancer J*. 2024;14(1):31.
21. Penack O, Abouqateb M, Peczynski C, et al. GVHD prophylaxis in matched related stem cell transplantation: Why post-transplant cyclophosphamide can be recommended a study by the EBMT transplant complications working party. *Leukemia*. 2025;39(6):1503-1511.
22. Penack O, Abouqateb M, Peczynski C, et al. ATG or post-transplant cyclophosphamide to prevent GVHD in matched unrelated stem cell transplantation? *Leukemia*. 2024;38(5):1156-1163.
23. Admiraal R, Boelens JJ. Anti-thymocyte globulin for GVHD: one dose does not fit all. *Lancet Haematol*. 2020;7(7):e505.
24. Admiraal R, Nierkens S, Bierings MB, et al. Improved survival with model-based dosing of antithymocyte globulin in pediatric hematopoietic cell transplantation. *Blood Adv*. 2025;9(9):2344-2353.
25. Admiraal R, Nierkens S, Bierings MB, et al. Individualised dosing of anti-thymocyte globulin in paediatric unrelated allogeneic haematopoietic stem-cell transplantation (PARACHUTE): a single-arm, phase 2 clinical trial. *Lancet Haematol*. 2022;9(2):e111-e120.
26. Admiraal R, Nierkens S, de Witte MA, et al. Association between anti-thymocyte globulin exposure and survival outcomes in adult unrelated haemopoietic cell transplantation: a multicentre, retrospective, pharmacodynamic cohort analysis. *Lancet Haematol*. 2017;4(4):e183-e191.
27. Lum SH, Albert MH, Gilbert P, et al. Outcomes of HLA-mismatched HSCT with TCRalphabeta/CD19 depletion or post-HSCT cyclophosphamide for inborn errors of immunity. *Blood*. 2024.
28. Masetti R, Leardini D, Gottardi F, et al. Outcomes of children with haematological malignancies given second haploidentical haematopoietic stem cell transplantation with either TCRalphabeta/CD19 depletion or post-transplant cyclophosphamide. *Br J Haematol*. 2025;207(3):929-937.
29. de Witte M, Mooyaart JE, Blaise D, et al. The 51(st) Annual Meeting of the European Society for Blood and Marrow Transplantation: Physicians - Oral Session (O008-O166). *Bone Marrow Transplant*. 2025;60(Suppl 1):19-182.
30. van Sambeek B, Flattery M, Mitchell R, De Abreu Lourenco R. Comparing the cost of preparing matched unrelated donor and TCR alpha(+) beta(+) /CD19(+) depleted donor material for pediatric hematopoietic stem cell transplants in Australia. *Pediatr Transplant*. 2018;22(7):e13279.
31. Maziarz RT, Devine S, Garrison LP, et al. Estimating the Lifetime Medical Cost Burden of an Allogeneic Hematopoietic Cell Transplantation Patient. *Transplant Cell Ther*. 2023;29(10):637 e631-637 e639.
32. Bachier CR, Aggarwal SK, Hennegan K, et al. Epidemiology and Treatment of Chronic Graft-versus-Host Disease Post-Allogeneic Hematopoietic Cell Transplantation: A US Claims Analysis. *Transplant Cell Ther*. 2021;27(6):504 e501-504 e506.
33. Yalniz FF, Murad MH, Lee SJ, et al. Steroid Refractory Chronic Graft-Versus-Host Disease: Cost-Effectiveness

Analysis. *Biol Blood Marrow Transplant*. 2018;24(9):1920-1927.
34. Jones CA, Fernandez LP, Weimersheimer P, et al. Estimating the Burden of Cost in Chronic Graft-versus-Host Disease: A Human Capital Approach. *J Health Econ Outcomes Res*. 2017;4(2):113-118.
35. Schonewille P, van Rhenen A, Ham RMT, de Witte M, Kuball J. Posttransplant cells for the win? DLI and adoptive cell therapy to eradicate MRD. *Hematology Am Soc Hematol Educ Program*. 2025;2025(1):537-546.
36. Ljungman P, Mikulska M, de la Camara R, et al. The challenge of COVID-19 and hematopoietic cell transplantation; EBMT recommendations for management of hematopoietic cell transplant recipients, their donors, and patients undergoing CAR T-cell therapy. *Bone Marrow Transplant*. 2020;55(11):2071-2076.
37. Frey NV, Lazarus HM, Goldstein SC. Has allogeneic stem cell cryopreservation been given the 'cold shoulder'? An analysis of the pros and cons of using frozen versus fresh stem cell products in allogeneic stem cell transplantation. *Bone Marrow Transplant*. 2006;38(6):399-405.
38. Kim DH, Jamal N, Saragosa R, et al. Similar outcomes of cryopreserved allogeneic peripheral stem cell transplants (PBSCT) compared to fresh allografts. *Biol Blood Marrow Transplant*. 2007;13(10):1233-1243.
39. Medd P, Nagra S, Hollyman D, Craddock C, Malladi R. Cryopreservation of allogeneic PBSC from related and unrelated donors is associated with delayed platelet engraftment but has no impact on survival. *Bone Marrow Transplant*. 2013;48(2):243-248.
40. Parody R, Caballero D, Marquez-Malaver FJ, et al. To freeze or not to freeze peripheral blood stem cells prior to allogeneic transplantation from matched related donors. *Eur J Haematol*. 2013;91(5):448-455.
41. Dholaria B, Malki MMA, Artz A, Savani BN. Securing the graft during pandemic: are we ready for cryopreservation for all? *Biol Blood Marrow Transplant*. 2020;26(7):e145-e146.
42. Hsu JW, Farhadfar N, Murthy H, et al. The Effect of Donor Graft Cryopreservation on Allogeneic Hematopoietic Cell Transplantation Outcomes: A Center for International Blood and Marrow Transplant Research Analysis. Implications during the COVID-19 Pandemic. *Transplant Cell Ther*. 2021;27(6):507-516.
43. Jacob RP, Flynn J, Devlin SM, et al. Universal Engraftment after Allogeneic Hematopoietic Cell Transplantation Using Cryopreserved CD34-Selected Grafts. *Transplant Cell Ther*. 2021;27(8):697 e691-697 e695.
44. Hamadani M, Zhang MJ, Tang XY, et al. Graft Cryopreservation Does Not Impact Overall Survival after Allogeneic Hematopoietic Cell Transplantation Using Post-Transplantation Cyclophosphamide for Graft-versus-Host Disease Prophylaxis. *Biol Blood Marrow Transplant*. 2020;26(7):1312-1317.
45. Facchin G, Savignano C, Battista ML, et al. Impact of Cryopreservation of Peripheral Blood Stem Cells (PBSC) in Transplantation from Matched Unrelated Donor (MUD). *J Clin Med*. 2022;11(14).
46. Laroye C, Thilly N, Gauthier M, et al. A French single-center experience on allogeneic stem cell transplant cryopreservation during severe acute respiratory syndrome coronavirus 2 pandemic. *Cytotherapy*. 2023;25(8):877-884.
47. Yamamoto C, Ogawa H, Fukuda T, et al. Impact of a Low CD34(+) Cell Dose on Allogeneic Peripheral Blood Stem Cell Transplantation. *Biol Blood Marrow Transplant*. 2018;24(4):708-716.
48. Remberger M, Gronvold B, Ali M, et al. The CD34(+) Cell Dose Matters in Hematopoietic Stem Cell Transplantation with Peripheral Blood Stem Cells from Sibling Donors. *Clin Hematol Int*. 2020;2(2):74-81.

49. Nakaya Y, Nakamae H, Harada N, et al. Effect of graft cell dose on second transplantation from a haploidentical donor with post-transplantation cyclophosphamide for relapsed/refractory acute leukemia. *Bone Marrow Transplant*. 2023;58(8):947-949.
50. Remberger M, Torlen J, Ringden O, et al. Effect of Total Nucleated and CD34(+) Cell Dose on Outcome after Allogeneic Hematopoietic Stem Cell Transplantation. *Biol Blood Marrow Transplant*. 2015;21(5):889-893.
51. Gauntner TD, Brunstein CG, Cao Q, et al. Association of CD34 Cell Dose with 5-Year Overall Survival after Peripheral Blood Allogeneic Hematopoietic Cell Transplantation in Adults with Hematologic Malignancies. *Transplant Cell Ther*. 2022;28(2):88-95.
52. McLornan D, Eikema DJ, Czerw T, et al. Trends in allogeneic haematopoietic cell transplantation for myelofibrosis in Europe between 1995 and 2018: a CMWP of EBMT retrospective analysis. *Bone Marrow Transplant*. 2021;56(9):2160-2172.
53. McLornan D, Szydlo R, Koster L, et al. Myeloablative and Reduced-Intensity Conditioned Allogeneic Hematopoietic Stem Cell Transplantation in Myelofibrosis: A Retrospective Study by the Chronic Malignancies Working Party of the European Society for Blood and Marrow Transplantation. *Biol Blood Marrow Transplant*. 2019;25(11):2167-2171.
54. Harrison C, Kiladjian JJ, Al-Ali HK, et al. JAK inhibition with ruxolitinib versus best available therapy for myelofibrosis. *N Engl J Med*. 2012;366(9):787-798.
55. Spoerl S, Mathew NR, Bscheider M, et al. Activity of therapeutic JAK 1/2 blockade in graft-versus-host disease. *Blood*. 2014;123(24):3832-3842.
56. Kroger N, Shahnaz Syed Abd Kadir S, Zabelina T, et al. Peritransplantation Ruxolitinib Prevents Acute Graft-versus-Host Disease in Patients with Myelofibrosis Undergoing Allogenic Stem Cell Transplantation. *Biol Blood Marrow Transplant*. 2018;24(10):2152-2156.
57. Hernandez-Boluda JC, Pereira A, Kroger N, et al. Allogeneic hematopoietic cell transplantation in older myelofibrosis patients: A study of the chronic malignancies working party of EBMT and the Spanish Myelofibrosis Registry. *Am J Hematol*. 2021;96(10):1186-1194.
58. Gagelmann N, Wolschke C, Badbaran A, et al. Donor Lymphocyte Infusion and Molecular Monitoring for Relapsed Myelofibrosis After Hematopoietic Cell Transplantation. *Hemasphere*. 2023;7(7):e921.
59. Oechsler S, Gagelmann N, Wolschke C, et al. Graft-versus-host disease and impact on relapse in myelofibrosis undergoing hematopoietic stem cell transplantation. *Bone Marrow Transplant*. 2024;59(4):550-557.
60. Robin M, Iacobelli S, Koster L, et al. Treosulfan compared to busulfan in allogeneic haematopoietic stem cell transplantation for myelofibrosis: a registry-based study from the Chronic Malignancies Working Party of the EBMT. *Bone Marrow Transplant*. 2024;59(7):928-935.
61. Gagelmann N, Quarder M, Badbaran A, et al. Clearance of Driver Mutations after Transplantation for Myelofibrosis. *N Engl J Med*. 2025;392(2):150-160.
62. Hernandez-Boluda JC, Sheth V, Iacobelli S, et al. Impact of Donor Type on Outcomes After Allogeneic Hematopoietic Cell Transplantation in Myelofibrosis: A Study on Behalf of the Chronic Malignancies Working Party of the EBMT. *Am J Hematol*. 2025.
63. Rathje K, Gagelmann N, Badbaran A, et al. Clinical and Immune Effects of Peri-Transplantation JAK Inhibition for Myelofibrosis. *Am J Hematol*. 2025;100(2):200-209.
64. Ali H, Tsai NC, Synold T, et al. Peritransplantation ruxolitinib administration is safe and effective in patients with

myelofibrosis: a pilot open-label study. *Blood Adv*. 2022;6(5):1444-1453.

65. Hobbs GS, Kim HT, Hao R, et al. Phase II Study of Peri- and Post-Transplant Ruxolitinib for Patients With Myelofibrosis Receiving Allogeneic Hematopoietic Cell Transplantation. *JCO Oncology Advances*. 2025(2).

67. Wall SA, Tamari R, DeFilipp Z, Hobbs GS. Optimization of allogeneic hematopoietic cell transplantation for patients with myelofibrosis treated with ruxolitinib: eligibility, best practices, and improving transplant outcomes. *Ann Hematol*. 2025;104(4):2125-2141.

67. Kunte S, Rybicki L, Viswabandya A, et al. Allogeneic blood or marrow transplantation with haploidentical donor and post-transplantation cyclophosphamide in patients with myelofibrosis: a multicenter study. *Leukemia*. 2022;36(3):856-864.

68. Coccaro N, Tota G, Anelli L, Zagaria A, Specchia G, Albano F. Digital PCR: A Reliable Tool for Analyzing and Monitoring Hematologic Malignancies. *Int J Mol Sci*. 2020;21(9).

69. Greco R, Lorentino F, Nitti R, et al. Interleukin-6 as Biomarker for Acute GvHD and Survival After Allogeneic Transplant With Post-transplant Cyclophosphamide. *Front Immunol*. 2019;10:2319.

70. Solan L, Kwon M, Carbonell D, et al. ST2 and REG3alpha as Predictive Biomarkers After Haploidentical Stem Cell Transplantation Using Post-transplantation High-Dose Cyclophosphamide. *Front Immunol*. 2019;10:2338.

71. Srinagesh HK, Ferrara JLM. MAGIC biomarkers of acute graft-versus-host disease: Biology and clinical application. *Best Pract Res Clin Haematol*. 2019;32(4):101111.

72. Pedraza A, Salas MQ, Rodriguez-Lobato LG, et al. Easix Score Correlates With Endothelial Dysfunction Biomarkers and Predicts Risk of Acute Graft-Versus-Host Disease After Allogeneic Transplantation. *Transplant Cell Ther*. 2024;30(2):187 e181-187 e112.

73. Shao Y-L, Yang J, Li X, et al. A Pragmatic Monitoring Model for Non-Relapse Mortality Risk Based on Machine Learning in Patients Undergoing Allogeneic Hematopoietic Stem-Cell Transplantation. *Blood*. 2024;144(Supplement 1):3573-3573.

74. Chen C, Qiu K, Chen J, et al. Increased Co-Expression of PD-L1 and CTLA-4 Predicts Poor Overall Survival in Patients with Acute Myeloid Leukemia Following Allogeneic Hematopoietic Stem Cell Transplantation. *Immunotargets Ther*. 2025;14:25-33.

75. Huang K, Yang M, Huang J, et al. Soluble ST2 as a Predictive Biomarker for Acute Graft-Versus-Host Disease Post -Allogeneic Stem Cell Transplantation. *Clin Transplant*. 2025;39(3):e70108.

76. Hotta M, Satake A, Yoshimura H, et al. Elevation of Early Plasma Biomarkers in Patients with Clinical Risk Factors Predicts Increased Nonrelapse Mortality after Allogeneic Hematopoietic Stem Cell Transplantation. *Transplant Cell Ther*. 2021;27(8):660 e661-660 e668.

77. Balakrishnan B, Kulkarni UP, Pai AA, et al. Biomarkers for early complications post hematopoietic cell transplantation: Insights and challenges. *Front Immunol*. 2023;14:1100306.

78. Parampalli Yajnanarayana S, Stubig T, Cornez I, et al. JAK1/2 inhibition impairs T cell function in vitro and in patients with myeloproliferative neoplasms. *Br J Haematol*. 2015;169(6):824-833.

79. Min CK, Lee WY, Min DJ, et al. The kinetics of circulating cytokines including IL-6, TNF-alpha, IL-8 and IL-10 following allogeneic hematopoietic stem cell transplantation. *Bone Marrow Transplant*. 2001;28(10):935-940.

80. Melenhorst JJ, Tian X, Xu D, et al. Cytopenia and leukocyte recovery shape cytokine fluctuations after myeloablative allogeneic hematopoietic stem

cell transplantation. *Haematologica*. 2012;97(6):867-873.

81. Knight A, Madrigal AJ, Grace S, et al. The role of Vdelta2-negative gammadelta T cells during cytomegalovirus reactivation in recipients of allogeneic stem cell transplantation. *Blood*. 2010;116(12):2164-2172.
82. Khairallah C, Dechanet-Merville J, Capone M. gammadelta T Cell-Mediated Immunity to Cytomegalovirus Infection. *Front Immunol*. 2017;8:105.
83. Suessmuth Y, Mukherjee R, Watkins B, et al. CMV reactivation drives posttransplant T-cell reconstitution and results in defects in the underlying TCRbeta repertoire. *Blood*. 2015;125(25):3835-3850.
84. Link CS, Eugster A, Heidenreich F, et al. Abundant cytomegalovirus (CMV) reactive clonotypes in the CD8(+) T cell receptor alpha repertoire following allogeneic transplantation. *Clin Exp Immunol*. 2016;184(3):389-402.
85. Link-Rachner CS, Eugster A, Rucker-Braun E, et al. T-cell receptor-alpha repertoire of CD8+ T cells following allogeneic stem cell transplantation using next-generation sequencing. *Haematologica*. 2019;104(3):622-631.
86. Ravens S, Schultze-Florey C, Raha S, et al. Human gammadelta T cells are quickly reconstituted after stem-cell transplantation and show adaptive clonal expansion in response to viral infection. *Nat Immunol*. 2017;18(4):393-401.
87. Schafer A, Calderin Sollet Z, Herve MP, et al. NK- and T-cell repertoire is established early after allogeneic HSCT and is imprinted by CMV reactivation. *Blood Adv*. 2024;8(21):5612-5624.
88. Calderin Sollet Z, Schafer A, Ferrari-Lacraz S, et al. CMV serostatus and T-cell repertoire diversity 5 years after allogeneic hematopoietic stem cell transplantation. *Leukemia*. 2023;37(4):948-951.
89. Litjens NHR, van der Wagen L, Kuball J, Kwekkeboom J. Potential Beneficial Effects of Cytomegalovirus Infection after Transplantation. *Front Immunol*. 2018;9:389.
90. Busca A, Passera R, Pini M, et al. The use of ATG abrogates the antileukemic effect of cytomegalovirus reactivation in patients with acute myeloid leukemia receiving grafts from unrelated donors. *Am J Hematol*. 2015;90(6):E117-121.
91. Turki AT, Tsachakis-Muck N, Leserer S, et al. Impact of CMV reactivation on relapse of acute myeloid leukemia after HCT is dependent on disease stage and ATG. *Blood Adv*. 2022;6(1):28-36.
92. Scheper W, Van Dorp S, Kersting S, et al. γδT cells elicited by CMV reactivation after allo-SCT cross-recognize CMV and leukemia. *Leukemia*. 2013;27(6):1328-1338.
93. Davey MS, Willcox CR, Joyce SP, et al. Clonal selection in the human Vdelta1 T cell repertoire indicates gammadelta TCR-dependent adaptive immune surveillance. *Nat Commun*. 2017;8:14760.
94. Davey MS, Willcox CR, Baker AT, Hunter S, Willcox BE. Recasting Human Vdelta1 Lymphocytes in an Adaptive Role. *Trends Immunol*. 2018;39(6):446-459.
95. van Heijst JW, Ceberio I, Lipuma LB, et al. Quantitative assessment of T cell repertoire recovery after hematopoietic stem cell transplantation. *Nat Med*. 2013;19(3):372-377.
96. Yew PY, Alachkar H, Yamaguchi R, et al. Quantitative characterization of T-cell repertoire in allogeneic hematopoietic stem cell transplant recipients. *Bone Marrow Transplant*. 2015;50(9):1227-1234.
97. Gkazi AS, Margetts BK, Attenborough T, et al. Clinical T Cell Receptor Repertoire Deep Sequencing and Analysis: An Application to Monitor Immune Reconstitution Following Cord Blood Transplantation. *Front Immunol*. 2018;9:2547.
98. van Bergen CA, van Luxemburg-Heijs SA, de Wreede LC, et al. Selective graft-versus-leukemia depends on magnitude and diversity of the alloreactive T cell

response. *J Clin Invest*. 2017;127(2):517-529.
99. Koyama D, Murata M, Hanajiri R, et al. Quantitative Assessment of T Cell Clonotypes in Human Acute Graft-versus-Host Disease Tissues. *Biol Blood Marrow Transplant*. 2019;25(3):417-423.
100. Leick M, Gittelman RM, Yusko E, et al. T Cell Clonal Dynamics Determined by High-Resolution TCR-beta Sequencing in Recipients after Allogeneic Hematopoietic Cell Transplantation. *Biol Blood Marrow Transplant*. 2020;26(9):1567-1574.
101. Buhler S, Bettens F, Dantin C, et al. Genetic T-cell receptor diversity at 1 year following allogeneic hematopoietic stem cell transplantation. *Leukemia*. 2020;34(5):1422-1432.
102. Goel M, Eugster A, Schetelig J, Bonifacio E, Bornhauser M, Link-Rachner CS. Potential of TCR sequencing in graft-versus-host disease. *Bone Marrow Transplant*. 2022.
103. Harmon C, Zaborowski A, Moore H, et al. gammadelta T cell dichotomy with opposing cytotoxic and wound healing functions in human solid tumors. *Nat Cancer*. 2023;4(8):1122-1137.
104. Gray JI, Caron DP, Wells SB, et al. Human γδ T cells in diverse tissues exhibit site-specific maturation dynamics across the life span. *Science Immunology*. 2024;9(96).
105. Hirokawa M, Horiuchi T, Kawabata Y, Kitabayashi A, Miura AB. Reconstitution of gammadelta T cell repertoire diversity after human allogeneic hematopoietic cell transplantation and the role of peripheral expansion of mature T cell population in the graft. *Bone Marrow Transplant*. 2000;26(2):177-185.
106. Alagrafi F, Stikvoort A, Gaballa A, et al. gammadelta T cell characterisation in the long term after haematopoietic stem cell transplantation and its impact on CMV control and cGVHD severity. *Clin Transl Immunology*. 2025;14(3):e70027.
107. Zvyagin IV, Mamedov IZ, Tatarinova OV, et al. Tracking T-cell immune reconstitution after TCRalphabeta/CD19-depleted hematopoietic cells transplantation in children. *Leukemia*. 2017;31(5):1145-1153.
108. Dudakov JA, van den Brink MRM. Burning Down the House: Thymic Repair and Regeneration After Acute Damage. *Immunol Rev*. 2025;332(1):e70050.
109. Bashor CJ, Hilton IB, Bandukwala H, Smith DM, Veiseh O. Engineering the next generation of cell-based therapeutics. *Nat Rev Drug Discov*. 2022;21(9):655-675.
110. Meyer E, Salhotra A, Gandhi A, et al. Orca-T versus allogeneic hematopoietic stem cell transplantation (PRECISION-T): a multicenter, randomized phase 3 trial. *Blood*. 2025.
111. Goldsmith SR, Ghobadi A, Dipersio JF, Hill B, Shadman M, Jain T. Chimeric Antigen Receptor T Cell Therapy versus Hematopoietic Stem Cell Transplantation: An Evolving Perspective. *Transplant Cell Ther*. 2022;28(11):727-736.
112. Schoemans H, Stienissen E, Goris K, et al. Ask, do not tell: consulting a patient advisory board to understand unmet needs of patients with GVHD in Europe. *Lancet Haematol*. 2025;12(3):e214-e223.



8

Appendices

NEDERLANDSE SAMENVATTING

Een allogene hematopoëtische stamceltransplantatie (hierna: allogene stamceltransplantatie) biedt voor veel patiënten met hematologische maligniteiten de beste, en soms zelfs de enige, kans op genezing. Allogene stamceltransplantatie kan leiden tot ziektecontrole en genezing doordat het donorafweersysteem achtergebleven maligne cellen kan herkennen en elimineren. Daartegenover staat dat stamceltransplantatie ernstige, soms dodelijke complicaties kan veroorzaken, met name infecties en graft-versus-host-ziekte (GVHD). Bij GVHD reageert het donorafweersysteem op gezonde weefsels van de patient, wat kan leiden tot aanzienlijke morbiditeit en sterfte. Een belangrijke infectieuze complicatie na stamceltransplantatie is reactivatie van het cytomegalovirus (CMV). CMV-reactivatie is klinisch relevant (o.a. door het risico op CMV-ziekte en een intensievere antivirale behandeling), maar beïnvloedt daarnaast ook de samenstelling en het fenotype van het herstellende T-celcompartiment. CMV-reactivatie is bovendien niet uitsluitend nadelig: CMV-geïnduceerde immuunactivatie kan in sommige gevallen ook samengaan met versterkte antitumorimmuniteit, bijvoorbeeld door activatie of expansie van T-cellen met antitumorreactiviteit. Een van de grootste uitdagingen bij het verbeteren van de uitkomsten na stamceltransplantatie is het verminderen van complicaties zonder dat dit gepaard gaat met een verhoogd risico op terugkeer van de ziekte. Om deze balans beter te kunnen beïnvloeden, is een beter begrip nodig van het herstel en de dynamiek van het afweersysteem na de transplantatie.

T-cellen spelen een sleutelrol zowel bij het ontstaan van GVHD als bij het elimineren van maligne cellen (graft-versus-leukemie-effect). Elke T-cel brengt een T-celreceptor (TCR) tot expressie, waarmee een specifiek antigeen wordt herkend. T-cellen kunnen worden onderverdeeld in verschillende subsets, onder andere op basis van het type TCR. De meeste T-cellen in het perifere bloed zijn αβT-cellen met een TCR bestaande uit een α- en een β-keten. Deze αβT-cellen worden verder onderverdeeld in $CD4^+$ (helper) en $CD8^+$ (cytotoxische) αβT-cellen. Daarnaast zijn γδT-cellen relevant, met een TCR bestaande uit γ- en een δ-keten. γδT-cellen keren vaak relatief vroeg terug na stamceltransplantatie en kunnen bijdragen aan antivirale en antitumorreacties. In het UMC Utrecht worden αβT-cellen *ex vivo* uit het transplantaat verwijderd voor toediening, waardoor γδT-cellen mogelijk een relatief belangrijkere rol spelen vroeg na stamceltransplantatie. Binnen de γδT-cellen wordt vaak onderscheid gemaakt tussen $Vδ2^+$ γδT-cellen (meestal Vγ9Vδ2; relatief 'semi-invariant') en $Vδ2^-$ γδT-cellen (heterogener en vaker patiëntspecifiek), subsets die verschillen in repertoirediversiteit en functie. Virale reactivaties, met name CMV, kunnen een sterke selectiedruk uitoefenen op zowel αβ- als γδT-cellen en leiden tot expansie van specifieke (effector)klonen, met gevolgen voor TCR-diversiteit en immuunfunctie. In dit proefschrift staat het transplantatieplatform waarbij αβT-cellen *ex vivo* worden verwijderd centraal: het eerste deel beschrijft klinische uitkomsten na stamceltransplantatie en het tweede deel richt zich op het herstel van het afweersysteem.

Deel 1: Klinische uitkomsten na allogene stamceltransplantatie

In **hoofdstuk 2** beschrijven we de resultaten van een retrospectieve studie waarin stamceltransplantatie met αβT-celdepletie wordt vergeleken met twee historische cohorten die een niet-gedepleteerd transplantaat ontvingen. Na een stamceltransplantatie met αβT-celdepletie zagen we een lage incidentie van zowel acute als chronische GVHD. Tegelijkertijd zagen we bij CMV-seropositieve patiënten vaker CMV-reactivatie. De lagere incidentie van (met name chronische) GVHD resulteerde in een verbetering van de graft-versus-hostziektevrije, recidiefvrije overleving (GRFS).

In **hoofdstuk 3** hebben we retrospectief onderzocht of cryopreservatie (invriezen) van het transplantaat invloed heeft op de klinische uitkomsten. Dit is met name relevant wanneer logistieke omstandigheden de beschikbaarheid van een vers transplantaat kunnen beperken, bijvoorbeeld tijdens grootschalige crises zoals een pandemie. In onze analyse had cryopreservatie geen aantoonbaar effect op de overleving of op het optreden van GVHD. We zagen wel een lagere $CD34^+$-stamcelopbrengst in het transplantaat, zonder dat dit leidde tot significante verschillen in overleving of GVHD.

Hoofdstuk 4 richt zich op de uitkomsten na stamceltransplantatie bij myelofibrose, een beenmergaandoening die vaak gepaard gaat met verhoogde inflammatie en constitutionele symptomen. Patiënten met myelofibrose worden regelmatig behandeld met ruxolitinib, een JAK-remmer, om hun symptomen te verlichten. De behandeling met ruxolitinib is echter niet curatief, terwijl allogene stamceltransplantatie wel tot genezing kan leiden. In onze cohorten waren de transplantatie-uitkomsten bij myelofibrose ongunstiger dan bij acute leukemie, met name door het verhoogde risico op GVHD. We onderzochten of de toediening van ruxolitinib tijdens de conditionering en in de eerste twee weken na stamceltransplantatie de uitkomsten bij myelofibrose verbetert. Patiënten die peritransplant ruxolitinib ontvingen, hadden minder GVHD en een lagere niet-recidief gerelateerde sterfte (non-relapse mortality), wat gepaard ging met een significante verbetering in de overleving.

Deel 2: Immuun herstel na stamceltransplantatie

Het tweede deel van dit proefschrift richt zich op het herstel van het afweersysteem na allogene stamceltransplantatie. In **hoofdstuk 5** onderzochten we immuunherstel door 92 eiwitten in het bloed te meten die geassocieerd zijn met immuunprocessen en oncologie. We includeerden drie patiëntgroepen met verschillende klinische risicoprofielen na transplantatie: (1) acute myeloïde leukemie (AML), (2) myelodysplastisch syndroom (MDS) en (3) myelofibrose. Alle patiënten ondergingen αβT-celgedepleteerde stamceltransplantatie. Daarnaast ontvingen de myelofibrosepatiënten peritransplant ruxolitinib, zoals beschreven in **hoofdstuk 4**. We analyseerden deze eiwitten in de eerste 4 weken na de transplantatie. In deze periode werden duidelijke, tijdsafhankelijke veranderingen waargenomen in meerdere eiwitten, met name gerelateerd aan inflammatie

en T-celgerelateerde processen. We zagen met name dat de relatieve concentratie van verschillende eiwitten lager was in het bloed van patiënten met myelofibrose tijdens de periode dat zij ruxolitinib kregen.

In **hoofdstuk 6** onderzochten we het herstel van T-cellen na allogene stamceltransplantatie binnen twee transplantatieplatforms: αβT-celgedepleteerde en niet-gedepleteerde stamceltransplantatie. Hiervoor combineerden we immunofenotypering met next-generation sequencing (NGS) van de TCR en single-cell RNA/TCR-sequencing. CMV-reactivatie was geassocieerd met expansie van zowel $CD8^+$ αβT-cellen als $V\delta2^-$ γδT-cellen. In het αβT-celgedepleteerde platform ging dit gepaard met een langdurige numerieke dominantie van $V\delta2^-$ γδT-cellen ten opzichte van $V\delta2^+$ γδT-cellen. Daarnaast werd de diversiteit van het $V\delta2^-$ γδTCR-repertoire na αβT-celdepletie niet duidelijk beïnvloed door CMV-reactivatie, terwijl het αβTCR-repertoire binnen $CD8^+$ T-cellen minder divers was.

Met single-cell RNA/TCR-sequencing konden we bovendien per individuele cel zowel genexpressie (mRNA) als de TCR karakteriseren. Door zowel patiënt- als donorcellen te analyseren, onderzochten we in welke mate TCR-klonen uit de donor terug te vinden waren in de patiënt. Eén jaar na transplantatie zagen we beperkte overlap tussen het TCR-repertoire van donor en patiënt, met uitzondering van $V\delta2^-$ γδT-cellen. Verder vertoonden T-cellen van patiënten na CMV-reactivatie een ander genexpressieprofiel dan donor-T-cellen, passend bij een meer geactiveerd en cytotoxisch fenotype. Ten slotte vonden we verschillen tussen beide platformen: na αβT-celdepletie was de TCR-diversiteit lager dan na een niet-gedepleteerd transplantaat, terwijl in de niet-gedepleteerde groep relatief meer T-cellen aanwezig waren met een transcriptieprofiel dat past bij herstel- en reparatieprocessen.

CONCLUSIE

Dit proefschrift beschrijft hoe transplantatieplatform, transplantaatbewerking en peri-transplantmedicatie samenhangen met klinische uitkomsten na allogene stamceltransplantatie. Daarnaast tonen immunologische analyses dat virale reactivatie en transplantatieplatformkeuze het herstel van T-cellen en de ontwikkeling van het TCR-repertoire mede bepalen. Deze inzichten kunnen bijdragen aan verdere optimalisatie en personalisatie van transplantatiestrategieën

ACKNOWLEDGEMENTS/DANKWOORD

Dit proefschrift had niet tot stand kunnen komen zonder de bijdrage en steun van velen, die ik hier graag wil bedanken. In het bijzonder wil ik allereerst de patiënten en stamceldonoren danken, zonder wie dit onderzoek niet mogelijk was geweest.

Moniek, dank voor de kansen die ik van jou heb gekregen, van mijn eerste onderzoeksproject voor mijn master tot (voorbij) mijn PhD. Ik was al enthousiast over stamceltransplantatieonderzoek vanaf het moment dat ik erover las, maar door jouw colleges werd dit alleen maar verder aangewakkerd. Je hebt enorm veel passie voor onderzoek, met als ultiem doel de uitkomsten voor patiënten te verbeteren. Ik heb veel respect voor hoe je altijd vol enthousiaste ideeën zit, waar ik misschien niet altijd even enthousiast op reageer als jij had gehoopt (bij het MF-project ruimschoots gecompenseerd door Flores J). Heel veel dank voor de goede gesprekken over de volgende stap(pen) in mijn carrière en voor de superleuke afsluiting van mijn PhD in Madrid.

Jürgen, thank you for giving me the opportunity to do my PhD in your lab. You are very passionate about everything science-related, from γδT-cells to CAR-T cells and from CRC to allo-HSCT, which has led to your involvement in too many committees to count. This makes you one of the busiest people I know, but you also remain approachable, which is a great skill. One of the highlights of my PhD was skiing with you in Canada and talking about non-science-related stuff, like the concerts you enjoy going to with your daughter (who would've guessed you are a Swiftie?).

Zsolt, thanks for your input and guidance, especially on the student projects. Also, many thanks for hosting the BBQs in your beautiful garden and for the great time in Lisbon.

Julia, I am very happy and grateful that you agreed to have regular meetings with me to think along with my projects. You always gave constructive feedback that I could use to move forward. It was also always a lot of fun to hear about your travels and see the pictures, and I really appreciate that I could always chat with you about anything that came up during my PhD. Even after you moved to GSK, you still made the time to meet me, which I'm grateful for.

Ik wil ook graag mijn beoordelingscommissie bedanken: **prof. dr. Helen Leavis**, **prof. dr. José Borghans**, **prof. dr. Monique Minnema, prof. dr. Mirjam Heemskerk** en **dr. Stefan Nierkens**. Dank voor het lezen en beoordelen van mijn proefschrift, ik kijk uit naar de discussie.

Jeannette en Karijn, dank voor het plaatsnemen in mijn begeleidingscommissie en voor de adviezen.

Dennis, bedankt voor het me wegwijs maken in het lab toen ik als student in de Kuball-groep stage kwam lopen. Daarnaast heel veel dank voor alle adviezen en voor jouw nuchtere kijk op de wetenschap. Je gaf me regelmatig het zetje om maar gewoon een experiment te doen als ik het te lang aan het overdenken was. Dank voor je oprechte interesse en je kritische blik.

Trudy, dank dat ik tijdens de COVID-periode toch een labstage bij jou mocht doen, hoewel ik geen I&I-student was. We hebben elkaar tijdens mijn PhD niet veel gesproken, maar de afsluiting van mijn PhD, met het feestje in Madrid, was zeker een hoogtepunt.

My fellow members of the **Kuball group**, there have been quite many over the years, so bear with me! **Pleun**, Q5 blijkt helaas wel wat ver, maar ik ben heel blij dat je daar helemaal je plekje hebt gevonden. Dank voor je scherpe statistische kijk op onderzoek en ik hoop dat we nog vaak kunnen sparren over logistische regressie (on steroids?!). **Dorine**, naast je PhD ook altijd bezig met een of meerdere sportieve doelen (hockey, (halve) marathon, Hyrox??). Ik vind het knap hoe je alle ballen hooghoudt, probeer jezelf er ook aan te herinneren dat een PhD een marathon is, geen sprint! Dank nogmaals voor het sorten nadat je net uit Canada geland was. Pleun en Dorine, allebei heel veel dank voor de superleuke tijd in Madrid! **Laia,** you are one of the kindest people I know. Thanks for always being cheerful and nice, and for the great time skiing and enjoying hot springs in Canada! **Caro,** thank you for the good chats during a rough patch in my PhD and for generally being a supernice person! Although we haven't worked together much, it's always fun to bump into you and have a chat. **Jairo**, mede Sunshine roomie. Het moment dat ik het kantoor verliet, heb je mijn plekje overgenomen, zorg er goed voor! Dank voor alle koffiemomentjes/therapiesessies ;). **Sascha**, meestal als je het kantoor binnenkwam, was je op zoek naar Jairo, maar gelukkig bleef je ook wel eens hangen voor een praatje. Je positieve energie is heel fijn om in de groep te hebben! **AJ**, mede racket-sportliefhebber! Bedankt voor de potjes padel en tennis en alle gezelligheid. Ik durf niet tegen je te badmintonnen, want dan word ik sowieso ingemaakt. **Patricia,** thanks for all the Spanish food recommendations whenever I went on holiday to Spain (which was every year), and thanks for the great meal in Madrid! Your place there looks amazing. I wish you all the best. **Sabine**, dank voor je eerlijkheid en de goede gesprekken, fijn dat je in het CTI bent gebleven! **Astrid,** thanks for your genuine interest, the really fun time in Lisbon, and the office chats, it was great sharing the sunshine room with you! **Caterina,** thanks for the random coffee breaks, and thank you a lot for co-supervising, for your input, and for continuing the TCR project! **Annet,** heel veel dank voor het me helpen opstarten in het lab toen ik nog niet eens wist hoe ik een celkweek moest doen, ik hoop dat we elkaar nog tegenkomen in je nieuwe rol! **Tineke,** volgens mij heb ik elke keer dat ik met je praatte

iets nieuws geleerd over hoe ik iets beter kon doen in het lab ;) Bij jou kon ik altijd terecht als ik niet wist hoe ik iets moest doen of waar iets stond, of gewoon voor een praatje. Dank voor alle adviezen. Geniet van je pensioen! **Peter,** thanks for performing all the scRNAseq experiments together and for being patient while I shared my plans and backup plans (and backup backup plans?). Chapter 6 would have looked very different without your input! **Farid,** thanks for the nice discussions about how to analyse scRNAseq data and for helping me if I had any noob questions about the HPC! **Yiteng,** ik vind je presentaties en analyses van de imaging data echt heel vet en inspirerend! **Esmee,** het was superfijn om jou in het kantoor te hebben, heel veel dank dat ik altijd bij jou terecht kon om te praten over van alles, of soms om gewoon even kattenfoto's uit te wisselen ;). Heel veel plezier in Friesland! **Mara,** jouw organisatietalent kwam volledig tot uiting bij het organiseren van de vele borrels en I&I-evenementen, met als hoogtepunt het tripje naar de Efteling (en natuurlijk je PhD-feest)! **Naomi en Jiali,** dank voor de gezellige etentjes en borrels en de mede-organisatie van het Kuball-uitje ;). **Konstantinos, Inez, Lucrezia, and Angelo,** thanks for the social drinks and chats. **Eva, Ganesh, Lisanne, Aiko, Anil, Romy, Steven, Floor, Oliver and Camiel** we did not work very closely together and/or our time in the group didn't overlap much, but thanks for the chats in the lab (although I wasn't there much) and at the coffee machine/Kuball meetings J Thanks as well to my students: **Liza,** your project(s) were quite challenging, so things were not always easy, but you stayed persistent and kept thinking along. It was great to see you grow! **Maud**, ik denk dat ons gezamenlijke hoogtepunt van je stage ons tripje naar Parijs was! Heel leuk dat je begonnen bent als PhD-student in de groep. Helaas wel net op de eerste dag dat ik weg was, maar we komen elkaar vast tegen!

Mijn lieve paranimfen, Emma en Flores. **Emma,** wat heb ik geluk gehad dat jij net een jaartje voor mij bent begonnen met je PhD en daarna bent gebleven als PostDoc. We hebben allebei best wat meegemaakt de afgelopen jaren, met veel hoogtepunten, maar helaas ook dieptepunten. Wat fijn dat ik voor allebei bij jou terecht kon en kan, je staat altijd klaar met een luisterend oor. Ik ben heel blij dat jij op deze dag naast me staat en misschien komt dat gedeelde paper er ook nog wel ooit ;) **Flores,** ook bij jou kon ik altijd terecht voor wat broodnodige motivatie of opbeurende woorden. Ik ken weinig mensen die zo enthousiast zijn als jij, over geneeskunde, hematologie, fietsen, noem maar op. Dank voor de leuke samenwerking op het myelofibrosetuk en natuurlijk voor de onvergetelijke opera-ervaring in Milaan.

To all my wonderful **CTI (AZU)** colleagues and **I&I PhD** students, thank you for the past years! It was great working with all of you. **Eugenia/Eugie/Eus,** grazie mille for motivating me to keep up my Italian Duolingo, for all the teas and chats, and for all the pasta dates. Your Merlino content is top-notch, and I'm very happy to be a subscriber. Thanks for taking me on some of your many side quests, and for being a great conference/retreat buddy (except the time you got food poisoning ;)) Forza Roma! **Alex,** thanks for the ten-

nis matches (even though you can beat me left-handed), and for all the fun borrels and dinners! And of course, thank you for the amazing bike rides; it's still a miracle the Elfstedentocht actually made it out of the group chat! **Thomas,** met jou kan ik altijd praten over sport in het algemeen (en fietsen in het bijzonder), maar ook over de staat van de wetenschap, heel fijn! Bedankt voor het vertrouwen dat ik je Australian Open Scorito mocht mede invullen, ik hoop dat we de volgende Grand Slam nog meer succes hebben ;) **Léon,** bedankt voor de kennismaking met de wereld van zone 2 en trainingsschema's, alhoewel ik me er nooit aan houd. Heel veel succes met de volgende stappen in je carrière. **Iria,** your general knowledge is amazing. Thank you for all the help with Emma's PhD video and all the insights into the Spanish royal family; we should really do a pub quiz sometime soon! **Joost, Ida, Ben, Corine, Bibian, Noa, Tosca, Elsemieke, Jan, Niels, Mick, Caitlyn, and Joyce,** thank you all for the lovely chats both in the lab/offices and at social events!

Sunshine roomies: **Mitchell,** dank voor je uitgebreide Formule 1-analyses en je spelletjesadviezen en natuurlijk onze poging Salmari/a te maken. **Bas en Annelisa,** jullie waren al (bijna) klaar toen ik begon, maar het was fijn om jullie advies als (afrondende) PhD-studenten te horen!

Anke, dank voor het wegwijs maken in R en in jouw data, en dank voor het vertrouwen dat ik jouw project mocht overnemen. Ook al ging het lang niet altijd zo snel als we wilden/hoopten, is het uiteindelijk toch ingediend! ;)

Eric en Jef, dank voor de samenwerking op verschillende (sequencing) projecten!

Klaartje, Iris en Frances, dank voor alle zorg en tijd die jullie steken in het bijhouden van de databases en heel veel dank voor het altijd meedenken over mijn projecten! Ik vond het heel fijn met jullie samen te werken.

Hannah, Coco, Stefan, and Caroline, thank you for all the nice allo-HSCT discussions, and input/help on the OLINK-project.

Mirjam, heel veel dank dat ik de kans heb gekregen om aan de slag te gaan als Postdoc in jouw groep. Ik vind het inspirerend om te zien hoe jij je groep leidt en ik heb heel veel zin in dit komende jaar! **Konradin, Evelyn, Margit, Iris, Nienke, Patrycja, Brigit, Nina, Maarten, and Micah,** thank you a lot for the warm welcome! I'm very excited to work together with you.

Daarnaast zijn er natuurlijk mensen die niet direct betrokken zijn geweest bij dit proefschrift, maar aan wie ik de afgelopen jaren wel veel heb gehad.

Lieve **Summies/Diner Idee**, dank voor alle etentjes, weekendjes weg en de adviezen die jullie me de afgelopen jaren hebben gegeven. Ik ben supertrots op wat jullie allemaal hebben bereikt! **Rianne,** van eindeloos CS/CE overhoren naar de coronatijd in Apeldoorn, en nu in opleiding als anesthesioloog! Je laat je niet snel uit het veld slaan en ik ga je sowieso bellen als ik weer terug de kliniek in ga om mijn kennis bij te spijkeren. **Mirthe,** jouw PhD-project was niet altijd een groot feest, maar alsnog heb je een prachtig (en enorm!) boekje geproduceerd! Het was heel fijn om even m'n hart te kunnen luchten bij jou en wat herkenning op te zoeken. **Caro,** jij hebt een enorm talent om elke situatie vanuit verschillende perspectieven te belichten zonder veroordelend te zijn, wat ik de afgelopen jaren erg heb gewaardeerd. Dank voor de uitgebreide uitleg over hoe een PDF werkt en het begrip voor de Zotero/Obsidian hype ;) **Jonne,** het was altijd leuk om te horen over je (verre en minder verre) reizen, buitenlandse congressen en plannen. Dit zal de komende tijd zeker zo blijven, heel veel succes met de opleiding internationale gezondheidszorg!

Mijn tennisteam: **de Returners** aka **de Topspinners 2**: **Léon, Justin, Niels, Cézanne, Jara en Bente**. Dank voor alle gezellige wedstrijddagen/trainingen/vrije potjes en borrels in de zon (of in de regen en kou). Net als een PhD gaat tennis gepaard met (mentale) hoogte- en dieptepunten, heel veel dank voor jullie support zowel op als buiten de baan. En onthoud: tennis is leuk!!!

Appendix A: dank voor alle etentjes en andere evenementen (o.a. verjaardagen, bruiloften, oud en nieuw). Fijn dat jullie iedereen zo vanzelfsprekend opnemen in de groep en dat ik altijd op jullie kan rekenen als ik ergens (pittig en/of exotisch) wil eten, aangezien Léon de pittige keuken niet aan kan.

Lieve **Nien,** sinds de Rome-reis van het Hondsrug zijn we elkaar nooit uit het oog verloren en dat vind ik superfijn! Ik ben heel trots op wat je bereikt hebt (en hoop stiekem nog steeds dat we in de toekomst samen kunnen werken). Heel veel dank voor alle leuke activiteiten van de afgelopen jaren, zoals het verrassende donkere doolhof (wat was ik blij dat we elkaar daar na 5 seconden al tegenkwamen!).

Erik en Antoinette, heel veel dank voor alle gezelligheid en goede gesprekken, en de support tijdens moeilijkere tijden. Ik vind het superfijn dat we altijd op jullie kunnen rekenen. Ook nogmaals heel veel dank voor de fijne week op Lanzarote, zonder jullie was het waarschijnlijk een stuk zwaarder geweest om dit proefschrift af te ronden. Op zo'n mooie locatie schrijven was echt een cadeautje! **Seline en Paul**, ook veel dank voor de gezelligheid, met name tijdens verjaardagen en feestdagen. Sinterklaas en kerst worden in de familie Wijker érg serieus genomen, dank voor het mooie introductie-gedicht zodat ik meteen alle tradities en bijnamen snapte ;)

Kirsten en Anne, het is altijd fijn om naar jullie mooie plek in Drenthe te komen. Het is niet naast de deur, dus we zien elkaar misschien niet zo vaak, maar de momenten dat we samen zijn, zijn des te meer waardevol. Met **Lieke** hebben we nu natuurlijk een extra reden om langs te komen, en aangezien jullie haar als initialen L.A.B. hebben gegeven schept dit natuurlijk wel verwachtingen voor haar toekomst ;) **Kirsten,** ik ben supertrots op wat je de afgelopen jaren allemaal hebt bereikt. De combinatie van een opleiding tot verpleegkundig specialist, meer dan fulltime werken, paarden én een sociaal leven lijkt me niet altijd makkelijk. Hopelijk kunnen we snel weer een keer naar de sauna, want dit was de afgelopen jaren een fijne bron van ontspanning.

Papa en mama, heel veel dank voor alle steun en alle kansen die jullie me al mijn hele leven hebben gegeven. Ook al was het onderwerp van mijn proefschrift niet altijd makkelijk uit te leggen, jullie steunden me altijd bij de keuzes die ik heb gemaakt. **Papa,** dank dat je me altijd hebt laten zien en weten dat er meer is dan Valthermond en me het vertrouwen en de kansen hebt gegeven om mijn vleugels uit te slaan. **Mama,** hoewel jij er misschien wat meer moeite mee had als ik (weer) naar het buitenland vertrok, liet je me toch altijd gaan. Ik heb dit alleen kunnen doen omdat ik het vertrouwen had dat ik altijd weer terug kon keren, en daar ben ik heel dankbaar voor.

Ten slotte, lieve **Léon**, vanaf het moment dat we elkaar in 2017 tegenkwamen op de tennisbaan… waren we elkaar al snel vergeten. Gelukkig hebben we elkaar uiteindelijk toch gevonden op de racefiets, want ik weet niet hoe ik de afgelopen jaren zonder jou zou zijn doorgekomen. Bij jou kom ik thuis en kan ik compleet mezelf zijn. Het leven met jou is nooit saai, van spontane etentjes, tripjes naar het strand, en vakanties in het grote niets tot vergeten karaokesessies. Je laat me relativeren en laat me zien wat er echt belangrijk is in het leven, en je bent een van de meest zorgzame personen die ik ken. Dit uit zich ook in de goede zorgen voor (meneer) Sjoerd de poes, die hierdoor volledig tot zijn recht kan komen als emotional support kitty (als hij er zin in heeft). Ik houd van je en kijk uit naar onze toekomst.

LIST OF PUBLICATIONS

In this thesis

K. Nijssen[*], K. Westinga[*], **A. Stuut**[*], A. Janssen, A. van Rhenen, L. van der Wagen, L. G. M. Daenen, R. Oostvogels, M. A. de Witte[#], J. Kuball[#]. Graft Engineering: How Long Can You Wait, How Low Can You Go, and Pandemic Readiness. *Bone Marrow Transplant* 58, no. 7 (Jul 2023): 820-22. https://dx.doi.org/10.1038/s41409-023-01976-8.

A.H.G. Stuut[*], C. Nijssen[*], L. van der Wagen, A. van Rhenen, L. G. M. Daenen, A. Janssen, F. A. Verheij, I. Brinkman, F. M. Verduyn Lunel, H. Koene, R. Fijnheer, H. J. Prins, K. Westinga, J. Drylewicz, J. Kuball[#], M. A. de Witte[#]. Improved GVHD-Free and Relapse-Free Survival after Ex Vivo αβTCR and CD19 Depleted Allogeneic HSCT Compared to T Cell Replete HSCT. *Bone Marrow Transplant* 60, no. 5 (May 2025): 673-81. https://dx.doi.org/10.1038/s41409-025-02538-w.

Other publications

J.J.H. de Winter, B.M. Ibrahimov, F A. Verheij, I.D. Brinkman, **A.H.G. Stuut**, P. Schonewille, M.W. Heijstek, A. van Rhenen, L.E. van der Wagen, L.G.M. Daenen, A. Janssen, T.J.A. Hutten, J. Kuball, H.L. Leavis, M.A. de Witte. αβT/CD19-Depleted Allogeneic Stem Cell Transplantation in Adults with Inborn Errors of Immunity. *J Clin Immunol* 46, no. 1 (Feb 3 2026): 21. https://dx.doi.org/10.1007/s10875-025-01978-9.

Submitted

A.H.G. Stuut[*], P. Brazda[*], A. Janssen[*], A. Vyborova, E. Karaiskaki, F. Keramati, C. Nijssen,D.A. de Bont, M.J.T. Nicolasen, L.C.D.E. Gatti, T.J.A. Hutten, J. Yildiz, H.T. Spierings, G.C.M. Straetemans, D.X. Beringer, S. Pagliuca, H.G. Stunnenberg, Z. Sebesyten, J. Drylewicz, M.A. de Witte[#], and J. Kuball[#]. Platform-Imprinted Transcriptional and Clonal Remodeling of αβ and γδt Cells after Allogeneic Transplantation. *bioRxiv* (2026): 2026.02.09.704768. https://dx.doi.org/10.64898/2026.02.09.704768.

A.H.G. Stuut[*], F.G. Weverling[*], A. Janssen, F.A. Verheij, I.D. Brinkman, C. Nijssen, P. Schonewille, C. Oudbier, A. van Rhenen, L. van der Wagen, L.G.M. Daenen, R. Raymakers, K. Westinga, T. Hutten, L. van de Corput, J. Drylewicz, J. Kuball[#], M.A. de Witte[#]. Peri-transplant Ruxolitinib Enhances Survival in Myelofibrosis Patients Undergoing αβTCR and CD19-depleted Stem Cell Transplantation

*Authors share first authorship
Authors share senior authorship

CURRICULUM VITAE

Anniek Henderika Geertruida Stuut was born on the 6th of September 1995 in Stadskanaal, the Netherlands. She completed her secondary education at Hondsrug College in Emmen in 2014. Before finishing secondary school, she spent an academic year on exchange at Christ the King Sixth Form in Southport, UK. In 2014, she moved to London, UK, to study Biomedical Sciences at University College London (UCL). In 2017, she graduated from UCL with First Class Honours, ranking in the top 10% of the class.

After graduating, Anniek moved to Utrecht to pursue a research-focused graduate-entry medical degree through the Selective Utrecht Medical Master (SUMMA) programme at Utrecht University. As part of this program, she wrote a literature review on reduced intensity conditioning before allogeneic haematopoietic stem cell transplantation (allo-HSCT) under the supervision of dr. Moniek de Witte. In the final year of the programme, she performed a scientific internship in the group of prof. dr. Jürgen Kuball at the Center for Translational Immunology (CTI), under the supervision of dr. Trudy Straetemans, investigating γδTCR-based engineered T-cell therapies. Moreover, she completed her senior clinical rotation on the Medical Oncology ward at University Medical Centre Utrecht (UMC Utrecht) and her elective clinical rotation at the Helen Dowling Institute, a centre specialising in psychological care for people with cancer.

After graduating from SUMMA in 2022, Anniek started her PhD in the group of prof. dr. Jürgen Kuball, under the supervision of dr. Moniek de Witte. Her research focused on outcomes and immune reconstitution after αβT-cell-depleted allo-HSCT, with particular attention to γδT-cell reconstitution and CMV reactivation. In 2026, she was awarded a Best Young Abstract Award at the EBMT annual conference in Madrid. Currently, Anniek is working as a postdoctoral researcher in the group of dr. Mirjam Belderbos, where she investigates long-term post-transplant haematopoiesis and mixed chimerism.

